DIVERSITY, FUNCTIONAL MORPHOLOGY, AND EVOLUTION OF THE JAW APPARATUS IN ORNITHISCHIAN DINOSAURS

by
Ali Nabavizadeh

A dissertation submitted to Johns Hopkins University in conformity with the requirements for the degree of Doctor of Philosophy

Baltimore, Maryland
July, 2014

Abstract

Ornithischian dinosaurs have considerable morphological diversity in jaw structure throughout the clade implying great diversity in craniomandibular musculoskeletal function. This study explores evolutionary comparative osteological and inferred muscular anatomy as well as mechanical advantage of jaw apparatuses in genera throughout Ornithischia. Craniomandibular anatomy is described in detail highlighting functional adaptations for feeding in each subclade and a qualitative test of existing and newly proposed jaw mechanisms for various taxa. Functional characters examined include: symphyseal predentary-dentary joint (including its mobility), tooth row, coronoid process, craniomandibular joint, and general craniomandibular shape. This study also uses criteria from previous jaw muscle studies, as well as more in-depth case-by-case analyses, to reconstruct and measure vector angles of jaw adductor musculature in a large diversity of ornithischian taxa spanning all subclades. Mandibular mechanical advantages among genera within ornithischian subclades as well as between these subclades were calculated using 2D lever arm methods. Such lever arm mechanics estimate relative adductor muscle force for one side of the mandible independently, indicating the effect of jaw shape and muscle angle difference on relative bite forces throughout the jaw. Notable trends include a transition from a more evenly distributed bite force throughout the jaw in basal ornithopods and marginocephalians to a strong caudal bite force in the derived hadrosaurids and ceratopsids convergently. A relatively low bite force is also shown among thyreophorans. Perturbation analyses, constructing hypothetical jaw morphologies with coronoid processes removed as well as the jaw joint

raised to the level of the tooth row, were also performed to explore effects of jaw morphologies on the mandibular mechanical advantages for each taxon. In all taxa, both the coronoid process and lowered jaw joint increase moment arm length therefore increasing mechanical advantage of the jaw apparatus. More basal taxa tend to show more use of a lowered jaw joint while the derived hadrosaurids and ceratopsids, especially, show much more use of an elevated coronoid process, as is expected. Evolutionary trends in musculoskeletal anatomy and mandibular mechanical advantages across ornithischian taxa show that these dinosaurs evolved more complex feeding apparatuses within different clades as well as morphological convergences between clades.

Dissertation Advisor: Dr. David B. Weishampel, Johns Hopkins University

Committee Members: Dr. Peter Dodson, University of Pennsylvania

Dr. Catherine A. Forster, George Washington University

Dr. Jonathan M. G. Perry, Johns Hopkins University

Acknowledgements

First and foremost, I thank my esteemed graduate mentor, D. Weishampel, for his endless knowledgeable input, his daily ever-helpful discussion, his uplifting encouragement, his gracious support (both personal and financial), and, of course, for reading this dissertation. If it weren't for him, I would not be anywhere near where I am right now, and for that I am eternally grateful to him. I am lucky to have worked with him as my mentor and friend. I would also like to express my greatest gratitude to J. Perry, P. Dodson, and C. Forster for their graciousness in agreeing to read through this very long and tedious document. I also thank P. Dodson for his mentorship as well, as he has always been optimistic of my work and has helped me progress through so much.

I thank the following people for access to museum specimens: M. Carrano and M. Brett-Surman (USNM); A. Henrici (CMNH); C. Mehling (AMNH); F. Therrien (TMP); L. Martin, D. Burnham, and D. Miao (KUVP); K. Seymour, D. Evans, and N. Campione (ROM); S. Chapman and P. Barrett (BMNH); A. Folie, P. Godefroit, and P. Lauters (IRSNB). I am also especially thankful to F. Varriale, K. Poole, and H. Feng-Liu for providing wonderful photographs of many ornithischian specimens from museums around the world. I thank L. Witmer and P. Lauters for providing CT data of many ornithischian specimens, which allowed me to take an even deeper look into their intricate morphology.

I thank L. Martin for advising me as an undergraduate and for initially sparking the question of the origins of the predentary bone in ornithischians that has continued on as my PhD dissertation project. I also thank P. Dodson, D. Evans, C. Forster, J. Mallon,

and K. Poole for many helpful and stimulating discussions that were incredibly beneficial for my project.

An enormous thank you to the faculty (V. DeLeon, K. Rose, C. Ruff, J. Perry, M. Teaford, and D. Weishampel) and concurrent students (K. Jones, C. Sartin, H. Ahrens, L. Burgess, N. Squyres, R. Frigot, H. Kristjanson, E. Powell, K. Zelazny, M. Holmes, R. Higgins, F. Gould, H. Garvin, E. Garofalo, M. Chollet) of the Center for Functional Anatomy and Evolution at the Johns Hopkins University School of Medicine for their encouragement and support. I am greatly indebted to A. Daniel, who was an incredibly enormous help in so many ways to make sure I was on the right track. I would also especially like to thank my lab-mate, R. Frigot, for her invaluable help with biomechanical discussions. I also would like to extend my utmost gratitude to my cohort-mate, K. Jones, with whom I was lucky enough to share the past five years of grueling graduate work and whose endless research advice has taught me so much throughout the years.

I am also tremendously thankful to the faculty (G. Lees, T. Phelps, D. Rini, J. Fairman), staff (D. Balch), and students of the Art as Applied to Medicine Department at the Johns Hopkins School of Medicine. I have learned so much about scientific illustration from each and every one of them and I feel extremely lucky to have been able to work with such talented and kind people who made my stay at Hopkins all the more enjoyable every day. I would especially like to also thank E. Cook for helping with animations of a hadrosaur and ankylosaur skull that were used in various conference presentations.

I thank my very good friends N. Boire, V. Atukorale, E. Basafa, and A. Falk for

always being incredibly supportive throughout my stay here and for always reminding me that I do have a life outside of graduate school. I also would like to thank all of the members of the CentriFugues a cappella group. The CentriFugues were my biggest creative outlet from work. Singing with all of them never failed to lift my spirits and I am so grateful to have been able to rehearse and perform alongside them throughout the past 3 years.

I thank coffee shops, especially the Bun Shop, Daily Grind, and Starbucks, for being my go-to places for writing this dissertation and for being my ways out of having to work in my actual workplace most of the time.

I am grateful to the NSF Graduate Fellowship Program for having helped support my research and stay here in Baltimore. It was truly an honor to be chosen for this incredible fellowship.

And, of course, last but most surely not least, I would like to thank my parents, Shohreh and Vahid, and my little brother, Omid, for their endless support, encouragement, and love throughout my PhD. Words cannot express how thankful and lucky I feel for having such a wonderful family in my life. I love you guys. Always.

Table of Contents

List of Tables

List of Figures

Chapter 1: Introduction

ORNITHISCHIA

Ornithischia was the dominant herbivorous clade of Dinosauria. It is a stem-based clade defined as including all dinosaurs more closely related to *Triceratops* than *Tyrannosaurus*. Ornithischia is split into Heterodontosauridae and Genasauria, the latter being a node-based clade consisting of the most recent common ancestor of *Ankylosaurus* and *Triceratops* and all of its descendants (Butler et al., 2008). Diversification of Ornithischia persisted for about 140 million years, until the end of the Mesozoic Era, and contained organisms that ranged from small to truly gigantic (Weishampel, 2004). These encompassed most herbivorous dinosaurs, including the armored ankylosaurs and plated stegosaurs (members of Thyreophora), the dome-headed pachycephalosaurs and horned ceratopsians (members of Marginocephalia), the Ornithopoda, as well as more basal members such as the small Heterodontosauridae (Butler et al., 2008). A phylogeny of Ornithischia (and its association with Saurischia) is given in Figure 1.1 with all integrated less inclusive clades to illustrate the relationships of all ornithischian groups.

FIGURE 1.1. Phylogenetic relationships of Ornithischia according to Butler et al. (2008).

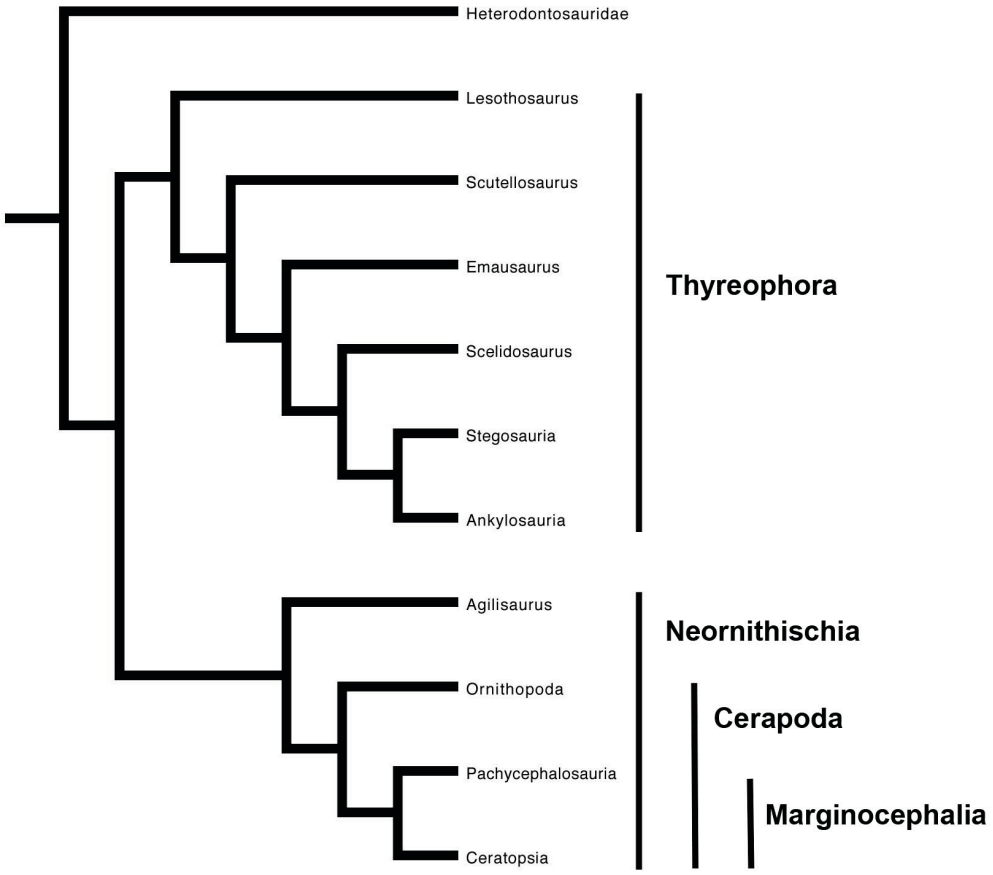

The following is a list of the major diagnostic traits of ornithischians: an opisthopubic (caudally-oriented pubis) pelvis, a biramal pubis, a roughened and edentulous tip of the snout, a shallow, broad ventral sheet of bone in the premaxillae with caudodorsally oriented processes, a palpebral bone across each orbit, relatively reduced antorbital fenestra, subtriangular maxillary and dentary tooth crowns with denticulate mesial and distal sides, cheek teeth with triangular lower crowns, at least five sacral vertebrae, loss of gastralia, ossified epaxial tendons at least above the sacral region and

many times farther along the vertebral column, a restriction of the pubic symphysis to the distal ends of the pubic shaft, a puboischial symphysis, and loss of phalanges for pedal digit V (Sereno, 1986; Weishampel, 2004).

Many of the aforementioned characters served important adaptive functional purposes. Previous studies (Ostrom, 1961; Ostrom, 1964; Ostrom, 1966; Weishampel, 1984; Crompton and Attridge, 1986; Rybczynski and Vickaryous, 2001; Bell et al., 2009; Holliday, 2009; Sereno et al., 2009; Tanoue et al., 2009; Norman et al., 2011; Cuthbertson et al., 2012; Sereno, 2012; etc.) have addressed musculoskeletal functions in this clade; specifically, ornithischians have considerable morphological diversity in jaw structure, especially between less inclusive clades, but also among species within a given clade. Important jaw characteristics that unite many ornithischians include an elevated coronoid region of the mandible, a jaw joint set ventral to level of maxillary tooth row, a buccal emargination with medially inset tooth rows (thought by some to be a possible indication of muscular cheeks [Galton, 1973; however, see Papp and Witmer, 1998]), and lastly, the presence of a neomorphic bone known as the predentary (Sereno, 1986; Weishampel, 2004).

The predentary is a single ossified mandibular element found in all Ornithischia (Weishampel, 2004). Located rostrally at the midline of the mandibular symphysis and articulating with both dentaries, it occludes with the premaxilla (as well as the rostral bone in ceratopsians dorsally and was likely covered by a rhamphotheca, a keratinous bill similar to that of a modern bird or turtle (Morris, 1970). In many cases, there are numerous foramina on the rostral surface, indicating neurovasculature to the keratinous sheath. It has been universally accepted that the predentary was part of a plant-gathering

beak used in nipping for acquiring vegetation (Morris, 1970). Its absence in fossil and extant herbivorous mammals and many other fossil herbivores (including sauropodomorphs), however, indicates that the significance of this element in jaw mechanisms of ornithischians is yet to be fully understood, especially in association with the rest of the jaw, which has a plethora of other morphologies also impacting jaw mechanics in these animals.

This dissertation is an in-depth analysis of the large diversity in osteological, myological, and arthrological morphologies in ornithischian musculoskeletal jaw anatomy. I seek to elucidate the functional and evolutionary significance of the predentary, coronoid process, and jaw joint morphologies as well as many other characteristics, such as dentition and tooth row morphology, jaw structure as a whole, and comparative muscular anatomy. I also perform a quantitative analysis of mechanical advantages of important jaw structures to convey evolutionary trends and convergences in ornithischian jaw mechanics.

DINOSAUR JAW MECHANICS

Understanding the functional implications of each bone, joint, and muscle type in extant vertebrate jaw function is crucial in elucidating craniomandibular function in extinct taxa with similar traits (Ostrom, 1961; 1964; 1966; Weishampel, 1984; Holliday and Witmer, 2007; Holliday and Witmer, 2008). Various osteological, arthrological, and

myological complexities of each feeding system relating to function in vertebrates include mechanics of general lower jaw elevation and depression, many forms of cranial kinesis (specific movements of individual cranial elements aiding in feeding), and intramandibular kinesis (specific movements at the mandibular symphysis and other areas possible joints within the mandible). The morphological characteristics in dinosaur jaw structures account for much of dinosaur taxonomic and phenotypic diversity. Among genera, most known feeding preferences are hypothesized to be represented within Dinosauria, such as carnivory, piscivory, insectivory, and herbivory. With modern vertebrate analogues, researchers have made predictions as to the various diets of each clade (see below). These predictions have been made by observation of dental morphology, general craniomandibular morphology, as well as many postcranial characters correlating with certain functions in feeding behavior, such as in axial, appendicular, and digit morphology. Many approaches that have been applied to studies in jaw mechanics of extant as well as extinct, non-dinosaurian taxa have also been applied to dinosaurs, such as lever arm mechanics, dental microwear and mesowear, beam modeling, computer modeling, and Finite Element Analysis (FEA) (see descriptions below and in Chapter 2 for references). These studies have all contributed to the elucidation of jaw movements and relative bite forces of dinosaurs to help us better understand the variety of feeding strategies among them and to clue us in to their ecological role.

Jaw muscle anatomy and orientation is a key in determining jaw function, as it is a large part of what determines exactly how and in what direction the jaws could move. Jaw musculature in crocodilians and birds is well known (Lakjer, 1926; Hofer, 1950;

Starck and Barnikol, 1954; Iordansky, 1964; Schumacher, 1973; Busbey, 1980; Holliday and Witmer, 2007) and this knowledge has aided interpretation of dinosaur jaw musculature (Holliday, 2009) as crocodilians and birds are the closest living relatives of dinosaurs (Benton, 1985). Herbivorous lepidosaurs have also been suggested to have similar musculature to select herbivorous dinosaurs, although they are more distantly related phylogenetically (Barrett, 2000).

Dinosaur jaw musculature has been interpreted through numerous observations of muscle scars on skulls and jaws in a variety of taxa (Haas, 1955; Ostrom, 1961; Ostrom, 1964; Haas, 1963; Haas 1969; Galton, 1974; Weishampel, 1984; Holliday, 2009; Norman et al., 2011; Sereno, 2012). As the focus of this research is within the dinosaurian clade Ornithischia, a brief overview of studies in feeding mechanics in its sister clade, Saurischia, including both Theropoda and Sauropodomorpha, is given below to give a comprehensive view of dinosaurian feeding as a whole and to portray how feeding mechanisms have evolved in Ornithischia compared to Saurischia. A full account of previous studies in ornithischian jaw mechanics is given in Chapter 2 (see Fig. 1.1 for phylogenetic relationships within Dinosauria).

Theropoda

A clade within Dinosauria that has been given a significant amount of attention as far as quantitative analysis of cranial mechanics and bite force in feeding is the Theropoda, a majority of which represented by all of the predatory dinosaurs known to have existed (see descriptions below for references). The fascination for this group lies in the role of certain members as "top predators". There is general interest of how much

force it would have taken the top predators of their era to bite, kill, and dismember their prey, many of which were large herbivorous dinosaurs (see Erickson et al., 1996; Meers, 2002; Bates and Falkingham, 2012). A common method used for estimating bite performance in the past decade has been Finite Element Analysis (FEA) because it gives researchers a chance to visualize the stresses that would occur throughout the skull and mandible once specific forces are applied to various parts of the jaw. This method ultimately provides insight into why the cranial elements are shaped the way they are and their evolutionary importance to the success of the clade and the feeding habits of theropods, such as *Tyrannosaurus*, *Allosaurus*, *Carnotaurus*, *Deinonychus*, and spinosaurids (Rayfield et al., 2001; Rayfield, 2004; 2005a; 2005b; Rayfield et al., 2007; Mazzetta et al., 2009). Researchers have also gone beyond cranial mechanics and have focused on mechanics of cervical spines of theropods as well, as cervical spines are hypothesized to have played a major role in head striking to capture prey (Snively and Russell, 2007; Snively et al., 2013). The combination of cranial and cervical mechanics ultimately gives a much more complete understanding of predatory behavior in these animals and the successful acquisition of prey.

Although most theropod dinosaurs were carnivorous, a few clades within Theropoda are thought to have been either omnivorous or herbivorous (Zanno and Makovicky, 2011). Oviraptorsaurs have been reconstructed as herbivores or omnivores due to the presence of gastroliths in the abdomen (Ji et al., 1998) and general jaw morphology and mechanics (Smith, 1992). *Troodon* dentition has been found to share morphometric traits with herbivorous reptiles, mostly in denticle morphology (Holtz et al., 1998). Ornithomimosaurs had an ostrich-like Bauplan; in particular they were edentulous

and instead of teeth probably had a keratinous rhamphotheca (beak) and a gastric mill, indicating a more herbivorous or omnivorous lifestyle (Barrett, 2005). Lastly, therizinosaurs had long necks, small heads, and extremely large claws on their forelimbs and are thought to also have been more herbivorous or possibly omnivorous mainly because of their leaf-shaped teeth and body form (Zanno et al., 2009). Recent studies of the therizinosaur *Erlikosaurus* (Lautenschlager, 2013; Lautenschlager et al., 2013) used computer modeling and muscle reconstruction to infer bite force, indicating that it likely had a relatively low bite force, favoring an herbivorous lifestyle and mainly using its jaws in plant cropping and stripping leaves from trees. It should also be noted that many avian species that evolved from Maniraptora likely also became herbivorous based on morphology and, sometimes, the presence of gastric mills with seeds in the abdomen. These herbivores include *Jeholornis*, *Sapeornis*, *Yanornis*, as well as possibly *Confuciusornis* (Zanno and Makovicky, 2011); however, these are all predecessors of, and morphologically similar to, modern day birds which have themselves had extensive study in their feeding mechanics and habits (Bock, 1964; Zusi, 1984; Hoese and Westneat, 1996; Bout and Zweers, 2001).

Sauropodomorpha

Sauropodomorpha is the only other major dinosaurian herbivorous clade that coexisted with ornithischian dinosaurs (Galton and Upchurch, 2004; Upchurch et al., 2004). They were large-bodied animals with long necks, small heads, columnar legs, and long, massive tails. The evolution of sauropodomorphs has been subject to a great deal of study because of its tremendous taxonomic and phenotypic diversity. It consists of a

paraphyletic group of basal sauropodomorphs, commonly referred to as "prosauropods", and is capped by an extensive monophyletic clade of sauropods (Galton and Upchurch, 2004; Upchurch et al., 2004; Yates, 2010). Below is a brief account of the evolution of each group as well as studies in their jaw mechanisms.

Basal Sauropodomorpha, or "Prosauropoda"—Basal sauropodomorphs, or "prosauropods" are a paraphyletic group of small to medium-sized sauropodomorphs, such as *Anchisaurus*, *Massospondylus*, *Thecodontosaurus*, *Yunnanosaurus*, and one of the largest members, *Plateosaurus.* They are characterized by possessing a small head, long neck, large trunk, and long tail. They mostly had longer hindlimbs than forelimbs with movable, sharp claws and have been interpreted as facultative bipeds. Basal sauropodomorphs contain what is said to be a mix of herbivores, likely such as *Plateosaurus*, and omnivores, likely such as *Anchisaurus* and *Massospondylus*. Cooper (1981) suggested a more carnivorous lifestyle for some prosauropods, especially *Massospondylus*, based on the morphology of the masticatory apparatus resembling that of a carnivore. Galton (1985) rejected this notion, stating that prosauropods were strict herbivores.

The homodont dentition of basal sauropodomorphs has been likened to that of iguanas, with a leaf shape and sharp, denticulate serrations around the crown ridge at a 45º angle to the cutting edge (Galton, 1985; Barrett, 2000). In addition to tooth shape, Galton (1985) suggested that prosauropods were herbivorous based on the offset craniomandibular articulation ventral to the tooth row that created a better mechanical advantage for bite force, which would have provided more force at an even distribution for grinding vegetation. Galton (1985) also suggested prosauropods were herbivorous

based on their precise dental occlusion, the presence of gastric mills and the fact that they had an exceptionally long neck with a proportionately small head inefficient for a carnivorous lifestyle. Barrett (2000) pointed out, however, that in many prosauropod genera the offset jaw articulation, coronoid eminence, and precise occlusion are not well developed and suggested that prosauropods represented a spectrum of omnivorous (i.e., *Anchisaurus* and *Massospondylus*) and herbivorous (i.e., *Plateosaurus*) taxa that evolutionarily ultimately led to the strictly herbivorous nature of the derived sauropod dinosaurs. Fairman et al. (2013) performed a comparative study with dissection of iguanian lizard jaw musculature. In this study, comparisons of jaw muscle orientation in iguanians and basal sauropodomorph skull structure showed differences between *Plateosaurus* and *Anchisaurus* in adductor chamber morphology. *Plateosaurus* resembled the herbivorous *Iguana* while *Anchisaurus* resembled the omnivorous *Sceloporus*, agreeing with Barrett's (2000) hypothesis of a spectrum of feeding habits.

Sauropoda—Sauropods were the largest of all dinosaurs and by far the largest terrestrial herbivores to have ever existed. Like prosauropods, they possess relatively small heads, long necks, long tails, and large trunks, although all to a much higher degree. Unlike most prosauropods, they are strictly quadrupedal and possess four columnar, elephantine legs and are predominately much larger in size. Their enormous stature and anatomical uniqueness have been subject to many debates concerning functional and physiological anomalies in this highly diverse clade (Klein et al., 2011). It is commonly accepted that they had a strictly herbivorous lifestyle and their feeding mechanisms depended on both the way the jaws functioned as well as the height and degree to which they could move and hold their elongate necks to reach various levels of trees and brush.

It is clear that neck flexibility and movement varied among different groups (i.e., brachiosaurids and camarasaurids holding their necks at mid-height to vertical (higher browsing) versus diplodocids holding their necks more horizontal [although, this has also been subject to debate], etc.) and even between species of sauropods (Upchurch and Barrett, 2000). Generally, however, it is rather clear that the most cervical flexibility occurred near the base of the cranium (except in some taxa that may have had stiff head and necks), with the least amount of flexibility occurring about mid-length down the neck. The cervical vertebrae near the proximal base of the neck had centra that were dorsoventrally compressed and zygopophyses that were transversely widened which allowed a good range of vertical bending (Upchurch and Barrett, 2000). All of this aided in both direct orientation of the head to specific heights of a tree with vegetation as well as rotation of the head for reaching more precise targets.

Although a great deal of study in sauropod feeding mechanics has focused on the role of the neck and its flexibility, the craniomandibular complex is also crucial to understanding their paleoecology. Sauropods likely did not chew; however, a diverse array of cropping, puncturing, slicing, and shearing was used in a variety of ways in many different genera as modes of oral processing with the possibility of gastric mills dealing with the remaining unprocessed foodstuffs.

Mandibular mechanics and tooth morphology in sauropods are of great interest because of the apparently large diversity of feeding styles between various sauropod taxa. Calvo (1994) analyzed tooth structures in four major sauropod clades. Each tooth morphology presents a different function. The following is a review of the four major clades that Calvo (1994) examined:

Diplodocids possessed an elongate, moderately curved, peg-like dentition. Their skulls were rather subtriangular in lateral view with the lower jaw more u-shaped in dorsal view and shorter than the cranium itself. The mandibular symphysis was inclined caudodorsally, as was the quadrate. The jaw joint was also inclined, allowing a propalinally (fore-aft) sliding quadrate-articular jaw joint. Some horizontal "slicing" was also likely, as shown by the precise tooth-tooth occlusion.

Camarasaurids possessed an interlocking, spoon-shaped dentition that formed a cutting edge for cropping and slightly functionally processing vegetation. Their skulls were shorter rostrocaudally and high, subquadrangular in lateral view. Their dentaries were robust and v-shaped in dorsal view. Dental wear shows scratches that are parallel to the labiolingual angle. They likely had a propalinal jaw action as well as a transverse chewing movement of the lower jaw during feeding, as White (1958) suggested.

Brachiosaurids possessed a cone-chisel-like dentition, with the crown wider than the root, but less so than in camarasaurids. Their teeth did not interlock and were bent lingually and implanted perpendicular to the alveolar margin, as seen in titanosaurids. Brachiosaurid skulls were rostrocaudally elongate, high, and trapezoidal in shape in lateral view. Their lower jaws were v-shaped in dorsal view with a slightly caudoventrally inclined mandibular symphysis. Dental wear shows high angled wear surfaces, indicating that they likely had an orthal (dorsoventral), isognathous, high angle shearing and slicing in a "cut-and-crop" mechanism.

Titanosaurids possessed a long, thin, chisel-like dentition with straight axes ending in a slightly lingually bent apex. Their skulls were rostrocaudally elongate and high, much like brachiosaurids; however, they possessed a u-shaped lower jaw (in dorsal

view) much like diplodocids. Their tooth wear angles were also high and sharp, in line with the tooth axis, also indicating an orthal, isognathous jaw action used to shear vegetation in a "cut and crop" mechanism.

Barrett and Upchurch (1994) offered further explanation as to why propaliny was advantageous for *Diplodocus*, stating that it permitted wider gape for stripping foliage off of high branches. Transverse movement was also possible, but it was not supported by tooth wear studies. The expanded mandibular symphysis in diplodocids likely added extra strength in the dentulous portion of the jaw, as their teeth are restricted to the rostral portion of the jaw (Barrett and Upchurch, 1994; Upchurch and Barrett, 2000). Young et al. (2012) conducted an FEA of a *Diplodocus* skull and found that it is not necessarily designed for high bite forces. Bark stripping (suggested by Holland [1924] and Bakker [1986]) was rejected due to the presence of too much stress in the skull with this jaw movement. The act of stripping smaller branches and precision biting was supported, however, due to the presence of less stress and strain induced on the skull. The peak stresses were seen in the premaxillary-maxillary lateral plates, dissipating stresses inflicting throughout the jaw while feeding (Young et al., 2012). These lateral plates, found in most sauropods, are ridges found on the labial side of the premaxillary, maxillary, and dentary dentition, protecting the basal third of each tooth labially, most prominent in the rostral region and decreasing in height toward the caudal end of the jaw (Upchurch and Barrett, 2000).

The coronoid eminence for insertion of major jaw adductor musculature is of moderate height in the majority of sauropods, except in *Camarasaurus*, in which it is rather high (Galton, 1986). The quadrate-mandibular jaw joint is approximately in line

with the maxillary tooth row in many Middle Jurassic sauropods, such as cetiosaurids, and some Late Jurassic sauropods, such as diplodocids; however, the jaw joint migrated ventral to the maxillary tooth row in other Late Jurassic sauropods, such as camarasaurids and brachiosaurids, representing an efficient cropping mechanism similar to that of prosauropods (Galton, 1986). Upchurch and Barrett (2000) reviewed sauropod jaw mechanisms and analyzed craniomandibular material to explain the evolution of the array of feeding mechanisms (orthal cropping, propaliny, chewing, etc.) in many sauropod clades. For the most part, most of their analyses seemed to be consistent with Calvo's (1994) predictions. Fiorillo (1998), using detailed dental microwear studies, found some overlap in diet between young *Camarasaurus* and adult *Diplodocus*, and that as *Camarasaurus* grew larger, its feeding habits changed. Lastly, Whitlock (2011), also with dental microwear studies, found that diplodocoids with differently shaped snouts had diverse mechanisms as well, with square-snouted diplodocoids, such as *Apatosaurus* and *Diplodocus*, being ground-height browsers (showing more scratches in dental microwear) on herbaceous plants and round-snouted diplodocoids, such as *Dicraeosaurus*, being more mid-height browsers on brittle, woody foliage (showing more pits in dental microwear). This further exemplifies the diversity of feeding mechanisms and preferences of closely related sauropod dinosaurs.

Ornithischian Jaw Mechanisms

Past ornithischian jaw mechanism studies have involved morphological observations, dental micro- and mesowear, lever arm mechanics, and bite force estimates using computer modeling and FEA, and a few of these studies have integrated ideas of

how the predentary bone might have had an impact on the overall feeding mechanisms of these animals. These ideas may provide substantial insight as to the overall significance of the predentary. Comprehensive historical accounts of studies in mechanisms in all ornithischian dinosaur groups are given in Chapter 2, starting with the most basal ornithischian clade, Heterodontosauridae, and continuing with the genasaurian Thyreophora, Ornithopoda, and, finally, Marginocephalia.

Chapter 2: A Review of Ornithischian Jaw Mechanisms

The following is a historical account of studies in jaw mechanisms of the ornithischian clades Heterodontosauridae, Thyreophora, Ornithopoda, and Marginocephalia.

HETERODONTOSAURID JAW MECHANISMS

As the most basal major clade known within Ornithischia, it is to be expected that the Heterodontosauridae would include taxa with a primitive, strictly orthal (dorsoventral) feeding cycle and isognathous jaw spacing due to its simplicity in such a small animal. However, despite their basal status, some heterodontosaurids, such as *Heterodontosaurus* (Fig. 2.1), exhibited a much more complex apparatus in which an orthal action is merely just one aspect. The heterodontosaurid skull itself is likely akinetic and similar in overall shape to most small, bipedal, and herbivorous basal Ornithopoda, a clade in which heterodontosaurids were originally placed phylogenetically until recently (e.g., Butler et al., 2008). Their uniqueness comes mainly from their namesake heterodont dentition: small, peg-like premaxillary teeth, large caniniform teeth on both the upper and lower jaws, and a set of worn, more distal, "hypsodont" dentition on the maxilla and dentary that, together, form one oblique, continuous occlusal surface on each tooth row angled labially in the dentary teeth and lingually in the maxillary teeth. These distal teeth

might have acted somewhat like mammalian molariform teeth during chewing (Norman et al., 2011). Additionally, a characteristic of heterodontosaurid jaws is the kinetic nature of the mandibular elements relative to one another, with the predentary and dentaries acting as separate entities with presumably highly mobile joints between them (Weishampel, 1984; Crompton and Attridge, 1986; Norman et al., 2011; Sereno, 2012).

FIGURE 2.1. *Heterodontosaurus* head reconstruction.

Thulborn (1971; 1974; 1978) suggested that, due to the continuous occlusal surface in the distal dentition, a propalinal (mesiodistally-oriented) jaw action was used by *Heterodontosaurus*. The dentition would have constantly worn away in a mesiodistally planar surface, a mechanism that was also supported by Barrett (1998). Hopson (1980), however, suggested a different jaw mechanism based on the mammal-like nature of the dentition, with an orthal power stroke coupled with transverse

movement of the entire mandible against the maxilla. Later, Weishampel (1984) also investigated the skull of *Heterodontosaurus* and was the first to interpret the potentially mobile nature of its mandibular elements into a hypothesis regarding their mechanism. He described a spheroidal (ball-in-cup) joint between the predentary and each dentary, with the rostral end of the dentary as being ball-shaped and the articular surface of the predentary being rather concave and cup-shaped. Weishampel proposed a jaw mechanism involving orthal adduction of the mandible coupled with long-axis rotation of each of the dentaries separately against the predentary. This was the first suggestion of intramandibular kinesis for heterodontosaurids and it set the stage for a significant number of subsequent arguments regarding this concept of predentary-dentary joint mobility, which could explain the functional purpose of the origin of the predentary bone itself in Ornithischia, given the basal positioning of Heterodontosauridae.

Crompton and Attridge (1986) reexamined Weishampel's (1984) arguments and, while they agree with the predentary-dentary joint in *Heterodontosaurus* being spheroidal, they rejected long-axis rotation of the dentaries as a possibility. Arguments against long-axis rotation include a) the planar nature of the wear facets on the dentition becoming labiolingually wider toward the more distal dentition and b) the transversely-expanded morphology of the mandibular glenoid at the quadrate-glenoid jaw joint. Instead, they proposed an orthal mechanism coupled with an "inverse wishboning" of the mandible in which each mandibular corpus would independently shift medially simultaneously on both sides of the jaw against the predentary. Crompton and Attridge's (1986) mechanism takes both of the above arguments against Weishampel's (1984) mechanism into account.

Further analysis by Porro (2007), using FEA force and stress analysis, and

Norman et al. (2011), using morphological analysis, also proposed a jaw action for *Heterodontosaurus* similar to (although slightly modified from) that suggested by Crompton and Attridge (1986). Norman et al. (2011) proposed a slight palinal motion along with orthal action and inverse wishboning. They pointed out that any lateral excursion or long axis rotation of the mandibular corpora would have been restricted due to the tight fit between the caniniform teeth, the medial walls of the diastema, and the elongate nature of the pterygoid flange and ventral jugal process. These form an aperture that would have directing jaw closure in a specific orientation. Norman et al. (2011) also demonstrated that the predentary-dentary joint was not spheroidal but was, in fact, more morphologically complex in nature. This joint might have inhibited long-axis rotation but would not have precluded any type of wishboning jaw action. They suggested that heterodontosaurids were likely able to chew tough vegetation and, possibly, even the flesh of small prey.

Sereno (2012), in a separate analysis, rejected the ability of muscle tissue slicing in heterodontosaurids due to the outward angled nature of their caniniform dentition being unsuitable for effective puncturing of soft tissue. He also made the observation that the predentary-dentary joint in heterodontosaurids is more saddle-shaped, rather than spheroidal, and also stated that constraints shown by Norman et al. (2011) are not significant due to the skull being so small in nature. With these criteria, Sereno (2012) suggested that long axis rotation of the individual mandibular corpora might have been permitted after all, resurrecting Weishampel's (1984) original hypothesis, although through slightly different morphological observations. He observed low angle wear facets on the premaxillary teeth and this suggested to him that medial inverse wishboning might

have occurred as well. He used the quadrate-articular jaw joint to further support these ideas about jaw motions, stating that this joint is actually a well-fitted rotary joint with the lateral condyle of the quadrate being offset ventral to the medial condyle that provided a curved articular suface for long-axis rotation.

More recently, Butler et al. (2012) reexamined heterodontosaurid jaw mechanics, in light of a new heterodontosaurid, *Fruitadens*, and concluded that the earlier *Heterodontosaurus* was able to occlude all of its teeth simultaneously whereas later taxa, such as *Tianyulong*, used more of a scissor-like jaw closing mechanism. They also suggested, with the support of morphology and lever arm mechanics, that later surviving heterodontosaurids, including *Fruitadens*, were adapted to a puncture crushing jaw mechanism with more rapid biting and larger gape angles. This is in contrast with the earlier *Heterodontosaurus*, which was better suited for stronger jaw adduction with smaller gape angles.

THYREOPHORAN JAW MECHANISMS

Basal Thyreophora

The evolution of jaw mechanisms in ornithischians seems to follow a trend of starting with (at least) an orthal component in the most basal members followed by the evolution of various other jaw actions in various subsequent clades. *Lesothosaurus*, among the most basal thyreophorans (Butler et al., 2008), has been universally accepted

to have implemented a primarily orthal component to their mechanism. Various hypotheses of orthal, isognathous slicing or shearing (Thulborn, 1971; Galton, 1986) and orthal pulping (Weishampel and Norman, 1989) have been suggested for *Lesothosaurus*. Its quadrate-glenoid jaw joint is offset ventral to the level of the maxillary tooth row, with a transversely broad ventral condyle of the quadrate (Thulborn, 1974; Galton, 1978; Cooper, 1985). According to Thulborn (1971), Weishampel (1984), and Crompton and Attridge (1986), the dentition of *Lesothosaurus* exhibits two oblique wear facets, both on the mesial and distal sides of the occlusal surfaces, labially on the dentary teeth and lingually on the maxillary teeth, indicating an alternating, interlocking occlusion typical of many cases of orthal biting. Sereno (1991) rejected this observation on the basis of another specimen, stating that the wear is irregular on different teeth. He also indicated, similarly to Crompton and Attridge (1986), that *Lesothosaurus* possesses a loose, ball-and-socket articulation at the predentary-dentary junction, suggesting a slightly mobile joint, as predicted in *Heterodontosaurus* (Weishampel, 1984; Crompton and Attridge, 1986). This would imply an orthal cropping mechanism with bilateral long-axis rotation of the dentaries against the predentary, although not to the extent seen in *Heterodontosaurus* (Crompton and Attridge, 1986; Sereno, 1991; Norman et al., 2011; Sereno, 2012). This, along with what is seen in other basal ornithischians such as *Heterodontosaurus*, might shed some light on the original function of the predentary at its origin at the base of Ornithischia.

Scelidosaurus, another basal thyreophoran, has been suggested to have had a primarily orthal jaw action, although not quite like that of the orthal slicing or orthal pulping mechanism of *Lesothosaurus* (Barrett, 2001). Through qualitative observations

of dental micro- and mesowear, Barrett (2001) observed signs of, direct tooth-tooth contact between the maxillary and dentary tooth rows, with the lingual surface of the maxillary dentition occluding with the labial surface of the dentary teeth, rather than an alternating occlusion as seen in *Lesothosaurus* (see above). The maxillary dentition exhibits small, apical wear facets and the dentary tooth counterparts generally exhibit large, bowlike facets. Additionally, the tooth rows are also medially bowed. All of these attributes suggest an orthal puncturing or crushing jaw mechanism, much like what is seen in a mortar and pestle action (Barrett, 2001). Other basal thyreophorans observed by Barrett (2001) include *Emausaurus*, which he suggests to have implemented a puncture mechanism similar to that inferred for *Scelidosaurus* (despite the slightly broader skull in *Emausaurus* and near absence of a medially bowed dentition), and *Scutellosaurus*, which he likened to the orthal slicing mechanism of *Lesothosaurus* based on the apparent presence of double wear facets.

Stegosauria

Stegosaurs had unusually small heads for the size of their bodies. At roughly 44 centimeters, the length of the skull in *Stegosaurus* (Fig. 2.2) hardly reached 5% of its total body length. Because most stegosaurs usually did not possess a long neck that would aid in reaching plant material that was higher off the ground (except for the anomalous *Miragaia*, which unusually possessed 17 cervical vertebrae), they were likely browsers on low-growing vegetation. With their elongate, narrow snouts, akinetic skulls, spade-shaped, denticulate teeth (similar to that of ankylosaurs, basal ornithopods, and basal marginocephalians), and pointed beaks with a predentary shaped much like that of

the basal thyreophoran *Lesothosaurus*, stegosaurs are thought to have simply used an orthal slicing mechanism (Weishampel and Norman, 1989). This is seen in dental mesowear studies as well (Barrett, 2001). More basal forms, such as *Huayangosaurus*, possessed slightly broader muzzles with maxillary tooth rows lacking any diastema.

FIGURE 2.2. *Stegosaurus* head reconstruction.

Throughout stegosaur evolution, however, the rostral dentition in the premaxillae became reduced and eventually was lost in more derived stegosaurs, such as *Stegosaurus*. The dentition of the lower jaw in stegosaurs became reduced toward the rostral end as well. A well-developed medially inset tooth row, or buccal emargination, can be seen in *Huayangosaurus* and *Paranthodon*, but it is much more reduced in the derived *Kentrosaurus* and *Stegosaurus*. In the latter taxa, with the reduction of the tooth series,

there was development of a dorsally projecting eminence, or dorsal lamina, in the coronoid region that became more prominent, hiding the dentary dentition laterally at the caudal end and projecting along the lateral edge of the tooth row. This could have acted as a functional, bony "cheek" or a mode of keeping vegetation in the oral cavity. A dorsally projecting ridge along the medial side of the tooth row rostral to the dentition served as a cropping mechanism acting as a continuation of the dentition from its caudal end (Berman and McIntosh, 1986; Czerkas, 1999; Barrett, 2001).

According to Barrett (2001), the quadrate-articular jaw joint in stegosaurs is offset ventral to the level of the maxillary tooth row, as in most ornithischian dinosaurs, indicating a more or less simultaneous occlusion of all teeth and an herbivorous lifestyle. The glenoid fossa is gently curved at its edges and is itself slightly concave. The rostrocaudal length of the glenoid fossa is about the same as the rostrocaudal length of the ventral condyles of the quadrate, which generally would not have permitted much propalinal movements, further supporting the hypothesis of an orthal power stroke in stegosaurs.

Unfortunately, stegosaur skulls are, like many basal ornithischians, rare and the only partial to relatively complete skulls found of more derived stegosaurian taxa (not including *Huayangosaurus*) belong to *Kentrosaurus*, *Paranthodon* (a maxilla), *Tuojiangosaurus*, and *Stegosaurus*, with *Stegosaurus* being the only derived form known from complete lower jaw material. The availability of stegosaur dentition is also limited, making it difficult to analyze true wear direction in stegosaurs. Computer modeling and FEA on digitally reconstructed 3D models of *Stegosaurus* teeth suggested that the denticulate, homodont dentition of stegosaurs was likely best suited for stress dissipation

from biting objects no bigger than small branches (Reichel, 2010).

Ankylosauria

Ankylosaurs, like stegosaurs, also possessed small heads for their body size (about 5% total body length); however, ankylosaurs had a much more broadened skulls of various shapes and sizes. The skulls of nodosaurids, particularly *Edmontonia* (Fig. 2.3), *Silvisaurus*, and *Gastonia*, were triangular in dorsal view and came to more of a point rostrally, a morphology likely adapted for more selective feeding. Alternatively, ankylosaurids, such as *Euoplocephalus* and *Ankylosaurus*, had skulls that are much squarer and had broad snouts, likely adapted for more generalized feeding behavior (Coombs, 1978). Ankylosaur skulls are generally dorsoventrally compressed. Fusion of many intracranial elements along with fusion of plates of dermal bone surrounding the skull would have prevented any form of cranial kinesis from occurring during feeding.

FIGURE 2.3. *Edmontonia* head reconstruction.

The lower jaws in ankylosaurs are relatively short rostrocaudally. They possess a low coronoid process and a large buccal emargination, which in such taxa as *Panoplosaurus* and *Edmontonia* is surmounted by an elliptical dermal ossification likely indicating the presence of soft tissue in this region (possibly functioning as a "cheek" helping keep vegetation inside the oral cavity). The predentary is transversely elongate, with no sign of a tight synarthrosis with the dentaries, and possessing only one small ventral process barely jutting beneath the ventral aspect of the dentaries in articulation. The quadrate-glenoid jaw joint is ventrally offset from the level of the maxillary tooth row, as in most ornithischians. The mandibular glenoid is variable in shape. According to Barrett (2001), in forms such as *Sauropelta* and *Panoplosaurus*, the glenoid fossa is shortened rostrocaudally and bounded by heightened ridges, just large enough to fit the ventral cotylus of the quadrate snugly as a hinge joint. However, in *Euoplocephalus* the glenoid is more rostrocaudally lengthened with no clear ridge that indicates boundary constraints of the quadrate and instead implies a more freely mobile joint (Barrett, 2001; Rybczynski and Vickaryous, 2001). .

The dentary tooth row in many ankylosaurs forms a bizarrely large, sigmoidal curve in lateral view while at the same time bowing medially in dorsal view, with the maxillary tooth row likewise bowing medially in ventral view (Barrett, 2001). Premaxillary teeth are known to be present in the nodosaurids *Silvisaurus*, *Pawpawsaurus*, and *Sauropelta*, but are absent in most ankylosaurids (Barrett, 2001; Carpenter, 2001). The teeth in ankylosaurs look similar to the spade-shaped, denticulate dentition seen in stegosaurs, except in ankylosaurs the denticles are much more pronounced and are sharper. Many ankylosaur jaws are found toothless, or nearly so

(Barrett, 2001; Rybczynski and Vickaryous, 2001), with few ankylosaur teeth that are actually known and found as isolated elements. Variable wear facets have been described from this small sample, some with high-angle mesial and distal wear facets (similar to *Lesothosaurus* [see above], although this is rare in ankylosaurs) and others with large, planar wear facets covering the entire crown (similar to *Scelidosaurus* [see above]) or just at the apex (Barrett, 2001; Rybczynski and Vickaryous, 2001).

Ankylosaur jaw mechanisms have been studied for a long time. Nopsca (1928) suggested the possibility that ankylosaurs were insectivorous, based on the weak nature of their jaws. Now, it is generally accepted that they were, in fact, herbivorous (Haas, 1969; Coombs, 1971; Galton, 1986; Weishampel and Norman, 1989; Barrett, 2001; Rybczynski and Vickaryous, 2001). Russell (1940) and Haas (1969) described possible movements of jaws in ankylosaurs, suggesting that the lower jaw must have adducted lateral to the maxillary tooth row. Haas (1969) indicated that the jaw musculature was far too weak for any type of powerful bite force and suggested that ankylosaurs likely fed on soft vegetation. Macrowear and qualitative studies of different bone and joint morphologies have previously suggested an orthal component in jaw mechanisms of many ankylosaurs (Galton, 1986; Weishampel and Norman, 1989), with a possibility of a puncture crushing mechanism in some, similar to that in *Scelidosaurus* (Barrett, 2001). It should be noted, however, that recent studies (Barrett, 2001) suggest that interlocking tooth occlusion (like that seen in *Lesothosaurus*) was not possible in ankylosaurs (Barrett, 2001).

Coombs (1971) suggested that, although dental microwear seemed to suggest otherwise, a strictly orthal jaw mechanism was unlikely due to craniomandibular

morphology as well as size and orientation of the inferred jaw adductor musculature. Instead, he suggested that there was a propalinal movement of the jaw during occlusion that coincided with an orthal movement during the power stroke. Moderate transverse motion of the jaw was also suggested due to the unusual shape of the tooth row (Coombs, 1971). Coombs and Maryańska (1990) described wear facets in ankylosaur teeth that indicated a propalinal component, further validating this inference.

Most recently, an analysis of the craniomandibular complex of the ankylosaurid *Euoplocephalus titus* by Rybczynski and Vickaryous (2001) has suggested palinal motion coupled with a medial "pivoting" of each mandibular corpus against the quadrate at the jaw joint on either side during the power stroke (also suggested by Coombs [1971]). Evidence for this motion lies in the rostrocaudally and somewhat transversely widened, slightly concave expansions of the glenoid articular surfaces, providing a large range of movement. Rybczynski and Vickaryous (2001) described two regions of quadratic stability at the jaw joint that are at an angle relative to one another, one slightly elevated rostrolateral region and one transversely expanded caudomedial region (which is at more of an oblique angle relative to the long axis of the tooth row). This jaw mechanism was also characterized by a highly mobile predentary-dentary and dentary-dentary symphyseal joint because of the peculiar morphology and absence of a firm, clasping junction between the predentary and dentary. It should be noted, however, that the likelihood of any sort of rotation of the mandibular corpora around their long axes was precluded in this study, although a clear explanation was not given as to why this might be the case (Rybczynski and Vickaryous, 2001). Conversely, Nabavizadeh (2011) presented a jaw mechanism for ankylosaurs involving simultaneous palinal jaw motion

coupled with long-axis rotation of the mandibular corpora. These assertions were based on the extreme curvature of the tooth row as well as indeterminate articulation at the predentary-dentary joint and expanded jaw joint morphology. Ösi et al. (2014) examined dentary morphology in the nodosaurid *Hungarosaurus* and also proposed long-axis rotation of the mandibular corpora, mainly due to the curved nature of the tooth row and more extensive tooth wear analysis, although there was no predentary in their sample.

ORNITHOPOD JAW MECHANISMS

The evolution of ornithopod jaw mechanisms has been subject to investigation for over a century, with in-depth analyses of craniomandibular structure, intracranial and intramandibular joint morphology, and dental microwear (Marsh, 1893; Nopcsa, 1900; Versluys, 1910, 1912, 1923; Lambe, 1920; Kripp, 1933; Lull and Wright, 1942; Ostrom, 1961; Thulborn, 1971; Galton, 1974; Hopson, 1980; Sues, 1980; Weishampel, 1984; Norman, 1984; Norman and Weishampel, 1985; Rybczynski et al., 2008; Williams et al., 2009; Bell et al., 2009). Ornithopod skulls, mandibles, and dentition are of such unique morphology that there is no modern analogue with which to compare them exactly. With the herbivorous nature of dental morphology in Ornithopoda, including flat occlusal surfaces used for oral processing, they have been likened to modern large ungulates. Yet there are numerous differences in their jaw morphologies that complicate this analogy. These include in placement of the craniomandibular joint, jaw curvature, muscular attachment sites, dental morphology, and morphology of the mandibular symphysis.

Consequently, researchers proposed novel mechanisms that are unrecognized in modern herbivores based on morphological properties of distinctive traits.

FIGURE 2.4. *Parasaurolophus* (hadrosaurid) head reconstruction.

A wide variety of jaw mechanisms involving various kinds of cranial kinesis have been hypothesized for ornithopods (Fig. 2.4). Marsh (1893) and Nopcsa (1900) suggested that the quadrate bone, articulating with the glenoid of the lower jaw ventrally, moved against the squamosal dorsally in a rostrocaudal motion. Nopcsa (1900), Versluys (1923), and Kripp (1933) observed the potential for each side of the lower jaw to rotate around its long axis, much like that suggested for heterodontosaurids, *Lesothosaurus*, and others (see above). Ostrom (1961) rejected long-axis rotation of each mandibular corpus and suggested instead a propalinal action of the jaws across the large, flat occlusal surface in

hadrosaurs. Transverse (mediolateral) chewing mechanisms have also been hypothesized for more basal members of Ornithopoda, such as *Hypsilophodon* (Galton, 1974) and *Zephyrosaurus* (Sues, 1980), in accordance with the morphology of their dentition.

For over two decades, the most accepted mechanism proposed for most ornithopods has been pleurokinesis (Weishampel, 1984; Norman, 1984; Norman and Weishampel, 1985; see Fig. 2.5), a complicated chewing style using a unique form of cranial kinesis involving many different cranial elements in motion with each other at various joints (Weishampel, 1984, Fig 2.1). The cranial joint movements involved in pleurokinesis are summarized as follows:

The ventral end of the quadrate moves caudolaterally, with its dorsal end rocking in its cotylus with the squamosal. The mandible moves with the quadrate, although only slight movement is necessary. This movement is associated with mobility at the basipterygoid-pterygoid junction. The pterygoid must move with the quadrate, which means it in turn must move against the basipterygoid process of the braincase as well. The pterygoid-quadrate joint is immobile because it is broad and squamous with many ridges. There is likely mobility at the palatine-pterygoid joint as well, as it is a thin junction. The quadratojugal is mobile against the quadrate, bearing a relatively slim contact with it, especially in non-hadrosaurian ornithopods, such as in *Iguanodon* where it meets the dorsal and ventral half of the embayment on the rostral side of the quadrate, but not inside. In hadrosauroids, the quadratojugal sits inside an expanded embayment. The quadratojugal–jugal junction is a broadly scarfed joint where the jugal overlaps the quadratojugal laterally, but it is likely immobile.

The jugal-maxilla joint was immobile as well and both elements would have acted as one unit. The maxilla-premaxilla joint, however, is highly mobile. In all hadrosaurines, as well as in non-lambeosaurine iguanodontians, there are two premaxillary processes contacting the dorsal margin of the maxilla, forming a joint between the premaxilla and the maxilla. Alternatively, lambeosaurines have a broad maxillary shelf in this region with which the premaxillae articulate. The jugal-lacrimal joint is continuous with the maxilla-premaxilla joint. Just rostral to the orbit, the lacrimal forms a buttress and that contacts the jugal wraps around it at the rostral orbital margin, making the jugal-lacrimal contact mobile. This causes the ventral half of the orbit to rotate laterally with maxilla at occlusion. The postorbital-jugal joint is thin, delicate, and highly mobile as well, as the two bones are butted against each other and, sometimes, overlap, with the dorsal process of the jugal resting caudal to the ventral process of the postorbital.

FIGURE 2.5. Pleurokinesis. A, oblique view of *Parasaurolophus* with arrows showing lateral movement of maxillae; B, coronal cross-section (illustration based on Lambe, 1920) of hadrosaur maxillae (on top) and dentaries (on bottom) before pleurokinetic power stroke with arrows showing movement (on left) and after power stroke (on right).

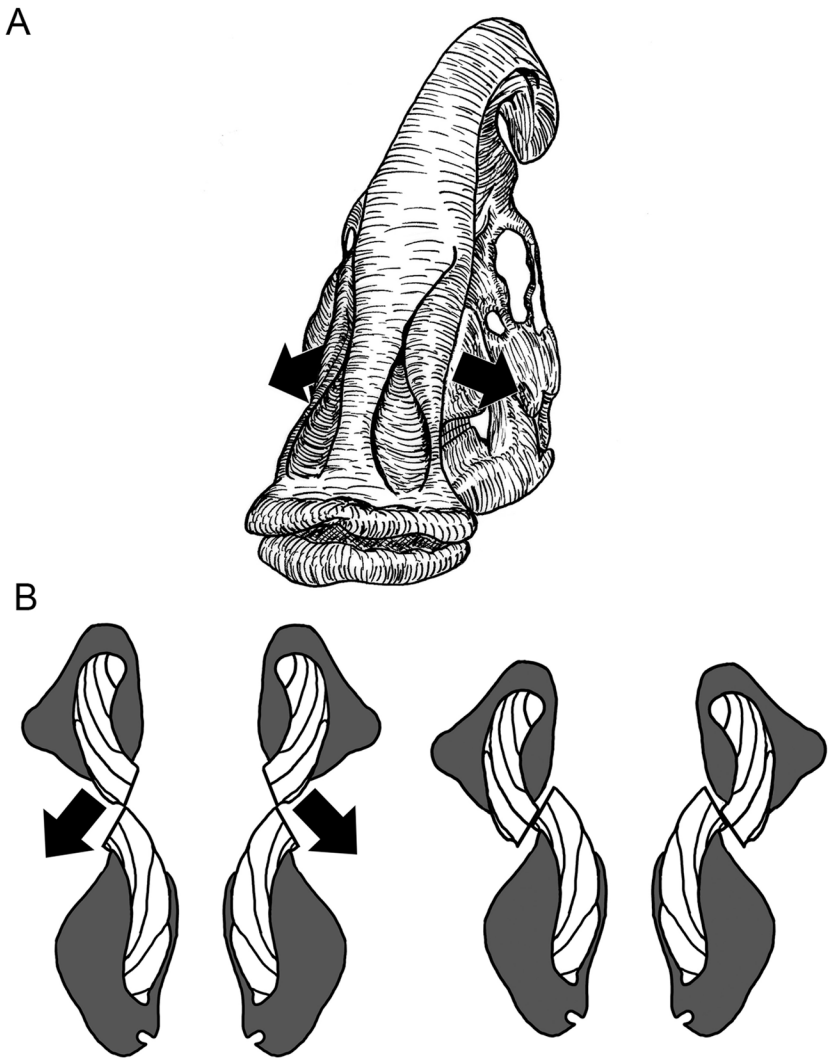

All of these movements of elements, starting with the quadrate moving against the squamosal, create a domino effect between all of these kinetic cranial elements that ultimately causes the maxillae to be pushed and rotate laterally as the lower dentition comes into occlusion with the upper dentition. This mechanism accounts for their unusual transverse tooth wear patterns, contradicting Ostrom's (1961) propalinal (fore-aft) jaw mechanism hypothesis. Recent microwear analysis of the hadrosaurid *Edmontosaurus*

quantified these transverse tooth wear patterns with statistical analysis of orientation of tooth wear on the occlusal surfaces and found support for the pleurokinetic model (Williams et al. 2009). In addition, this analysis showed signs of some propalinal jaw action in addition to transverse tooth wear.

Pleurokinesis has recently been challenged with further re-examination of hadrosaur skulls as well as computer modeling of pleurokinesis (Holliday and Witmer, 2008; Rybczynski et al., 2008; Bell et al., 2009; Cuthbertson et al., 2012). These counter-studies indicated the presence of secondary movements that must occur at various intracranial joints for the primary movements of pleurokinesis to occur and also that there are substantial endocranial spatial constraints as well as increased separation of cranial elements in response to these movements.

Although challenges to pleurokinesis have been put forward, some alternatives do not account for the concern of the transverse dental microwear, as it is such an unusual wear pattern in teeth with occlusal surfaces angled buccally on each side of the mandible, such as in the more derived hadrosaurs. Because neither solely propalinal nor orthal chewing explains this orientation of tooth wear and the angle at which teeth occlude does not allow the entire jaw to chew transversely, there is likely another aspect of the jaw mechanism that is not well understood. Cuthbertson et al. (2012) used 3D animation to test long axis rotation of the mandibular corpora and found it to be a plausible mechanism, resurrecting the original observations of Nopcsa (1900), Versluys (1923), and Kripp (1933). Since ornithopod taxa (and ornithischians as a whole) do not fuse both dentaries together rostrally, the midline, rostrally-placed predentary with which they both articulate may have assisted in a jaw mechanism involving intramandibular kinesis at the

symphysis, as suggested by Holliday and Witmer (2008), Bell et al. (2009), and Cuthbertson et al. (2012) in the derived hadrosauroids, although more basal ornithopods have yet to be studied with regards to the predentary-dentary joint.

MARGINOCEPHALIAN JAW MECHANISMS

Pachycephalosauria

Pachycephalosaur (Fig. 2.6) jaw mechanisms have not been studied in great detail, mainly due to scarcity of craniodental material with which to infer feeding styles. Gilmore (1924) described the teeth in *Stegoceras*, which, like most pachycephalosaurs, were spade-shaped, laterally compressed, and had denticulations directed toward the apex of each tooth, which was rather sharp and curved distally. Most pachycephalosaurs possessed a larger caniniform tooth. Pachycephalosaurs had teeth in the premaxilla, the maxilla, as well as the dentary, and Gilmore (1924) suggested that they (specifically *Stegoceras*) fed on soft vegetation. Maryańska and Osmólska (1974) indicated differences in dental wear and tooth size in *Homalocephale*, *Prenocephale*, and *Tylocephale*, suggesting that each pachycephalosaur, although possessing similar looking teeth, had its own particular feeding habit.

FIGURE 2.6. *Pachycephalosaurus* head reconstruction.

Sues and Galton (1987) inferred that pachycephalosaurs, specifically *Stegoceras*, had strictly orthal jaw action, possessing a simple hinge joint at the quadrate-mandibular junction. This morphology of this hinge joint prevented palinal action, a rostral convergence of the upper and lower tooth rows, and double wear facets on the maxillary and dentary teeth that implied shearing. They also suggested a potential slight long-axis rotation of the mandibular rami at the symphysis, implying movement of the dentaries within the predentary (although a predentary is yet unknown among pachycephalosaurs). Lastly, Varriale (2011) verified the orthal jaw action hypothesis in pachycephalosaurs proposed by Sues and Galton (1987) with analyses of dental microwear orientation using

scanning electron microscopy. These studies further indicated primarily vertical jaw movement between occluding teeth.

Ceratopsia

Ceratopsian jaw mechanisms have been studied to a much greater and more rigorous degree than most other ornithischian clades. With their massive skulls decorated with large horns, and spikes decorating their broad frills, they are further characterized by their pointed, nearly parrot-like beaks made up of the predentary occluding dorsally with an element unique to ceratopsians called the rostral bone, which articulates with the paired premaxillae.

Observations of occlusal surface morphology in ceratopsian dentition, especially the well-developed dental battery of more derived ceratopsids, have played a major role in inferring ceratopsian jaw occlusion and power stroke. Hatcher (1907) suggested ceratopsians (mostly ceratopsids) had an slicing orthal power stroke, with the combined sharp serrations from the apices of the teeth acting much like a pair of scissors producing a direct dorsoventral cut. This suggested mechanism was based on the observation that the occlusal surfaces of ceratopsid dentition are oriented in the vertical plane, with the buccal occlusal surface of the dentary teeth brushing across the lingual occlusal surface of the maxillary dentition.

FIGURE 2.7. *Triceratops* head reconstruction.

This hypothesis of an orthal power stroke in ceratopsids has stood the test of time for over one hundred years (Hatcher, 1907; Lull, 1933; Tait and Brown, 1928 [suggesting feeding on succulent plant material rather than fibrous]; Ostrom, 1964; Ostrom 1966; Weishampel and Norman, 1989; Dodson, 1996; Tanoue et al., 2009). Lull (1908) briefly mentioned the presence of a propalinal (mesiodistally-oriented) power stroke also in *Triceratops* (Fig. 2.7), but this is inconsistent with his observation of a solely orthal power stroke in a *Triceratops* specimen years later (Lull, 1933). Tait and Brown (1928)

further stated that, with their fused rostral cervical vertebrae, ceratopsids were able to carry their massive heads with more support and rotate them around a rostrocaudal axis. This allowed them to possibly tip the head on its side to strip vegetation in a more efficient and effective manner. Ostrom (1964; 1966) agreed with most preceding works on ceratopsian jaw mechanisms: any motion other than an orthal slicing power stroke would have been precluded by restrictions from the morphology of the quadrate-glenoid articulation (with the exception of possible slight propalinal movement).

One major contribution that Ostrom (1964; 1966) made to the study of ceratopsian jaw mechanics (and dinosaur jaw mechanics in general) was his use of lever arm mechanics in determining bite force throughout the jaw. Because the true mass of jaw adductor musculature is unknown in these fossilized specimens, adductor musculature was given a uniform value of 100 units of exerted muscle force. Most vertebrate jaws can be modeled as third-class levers, where the force being exerted by the adductor musculature onto the coronoid process is located between the quadrate-glenoid joint, or fulcrum, and the teeth that bear the force of the actual bite itself. Most derived ceratopsian jaws, however, can be thought of as second-class levers when looking at the distal dentition because the tooth row extends medial and caudal to the coronoid process. This caused the force of the jaw adductor musculature to be transferred rostral to the bite point (in the distal dentition), thereby producing a much greater mechanical advantage (at roughly a 300% increase in the distal dentition of *Triceratops*). However, this increase in caudal mechanical advantage causes a significant decrease in bite force in the mesial-most dentition (roughly 28-36% what would be expected), hence the restriction of the dentition to the distal aspect of the jaws with a large diastema mesially.

Ostrom (1966) described a phylogenetic trend toward increasing mechanical advantage and relative bite force in four evolutionarily successive taxa providing evidence of a gradation in effectiveness in chewing fibrous plant material, likely including palms and cycads. He further went on to incorrectly describe the jaw adductor musculature (specifically the m. adductor mandibulae externus muscle group) in ceratopsids as being extremely large, powerful, and having originated at the caudal extent of the frill and expanded across its dorsal surface and ultimately inserting onto the lower jaw. He used this inference as another adaptation producing great bite force at the caudal extent of the tooth row; as such a large muscle mass would produce an enormous, likely unnecessary amount of force for each bite. Dodson (1996) disagreed with Ostrom, however, in saying that the jaw adductor musculature likely did not stretch the entire span of the frill for various reasons, such as interspecific variability in frill size and shape, lack of smooth texture indicative of muscle at the caudal edge of the frill, ontogenetic inconsistencies regarding proportion of frill to jaw size, and vulnerability of this important muscle being attached to such a thin sheet of bone if the jaw musculature spanned the entire frill. Also, lengthening of the adductor musculature might increase velocity of contraction, however it would have no effect on the actual bite force. Dodson (1996) suggested that the main jaw adductor musculature instead likely only originated at the rostrodorsal edge of the frill within the upper temporal fenestrae, just caudodorsal to the supratemporal region and rostral to the large fenestrae of the frill in most ceratopsians.

One ceratopsian taxon that has been given individual attention in the literature is *Psittacosaurus*, a small, frill-less, horn-less basal ceratopsian. A variety of conflicting jaw mechanisms have been proposed as having occurred in *Psittacosaurus* feeding,

including propalinal movement (Sereno, 1987; Norman and Weishampel, 1991) as well as a possibility of an anisognathous unilateral bite (Norman and Weishampel, 1991), as opposed to isognathy found in most reptiles. More recently, Sereno et al. (2009) examined dental microwear in *Psittacosaurus gobiensis* and suggested a new jaw action he coined "clinolineal", an isognathous motion combining an orthal and propalinal component together, forming an inclined arc of dental microwear. This inference correlates well with the way the tooth rows diverge distally relative to one another throughout the jaw. These findings were further verified by Varriale (2011) in quantified dental microwear studies that indicated a similar jaw action in most psittacosaurs as well as chaoyangsaurids.

Tanoue et al. (2009) used 2D as well as 3D lever-arm mechanics to further infer the evolution of bite force throughout Ceratopsia. This study is presently the only application of Greaves' (1978) 3D bite-force model, which provides an understanding of the transfer of muscle forces through the mandibular symphysis that, in most ceratopsians, is functionally more or less fused because of the tight synarthrosis of the predentary-dentary contacts. Tanoue et al. (2009) found that, in psittacosaurids, there is more leverage at the mesial dentition and predentary compared to that of other basal ceratopsians, implying a more mesially-placed bite force (although, even though it has more leverage, it does not necessarily mean it is where the animal bites). They also found that the jaws of basal neoceratopsians could be classified as a second-class lever for bites on the more distal teeth, indicating the potential for a much higher distal bite force than input force. This transition to a second class lever in distal dentition indicates a gradual tendency toward a distal bite point in ever more-derived ceratopsians, ending with the

most-derived ceratopsids as the most exaggerated example of a more powerful distal bite force. Additionally, Tanoue et al. (2009) used the Greaves (1978) method to find that the medial position of the teeth in a medially curved tooth row in basal ceratopsians might have permitted a greater mechanical advantage than seen in a hypothetical straight tooth row, further displaying an evolutionary propensity in ceratopsians toward greater mechanical advantage in the masticatory system.

Bell et al. (2009) used FEA on the jaw of the ceratopsid *Centrosaurus* to elucidate the types of forces that could have been transmitted through the jaw during chewing. They found that the mandibular corpus of *Centrosaurus* had no resistance to torsional stresses in the mandibular corpus and was better able to transmit forces associated with an orthal, isognathous, shearing power stroke. However, they did not preclude a hypothesis suggesting a propalinal component in chewing (by Varriale, [2004]; this hypothesis was based on dental microwear showing a propalinal component in chewing should not be precluded).

Varriale (2011) quantitatively analyzed the dental microwear of most species of ceratopsians representing all internal subclades and documented the progression of orientations in jaw movements to test different previous hypotheses of ceratopsian jaw mechanisms. His analyses show that more orientations of jaw movements occur in derived clades than were previously hypothesized. He described an evolutionary, step-wise transformation in jaw movements throughout marginocephalian evolution, starting with an orthal power stroke in pachycephalosaurs and *Yinlong*, a clinolineal power stroke in Chaoyangsauridae and Psittacosauridae (representing an intermediate between orthal and palinal microwear), a palinal jaw motion in non-ceratopsid neoceratopsians (first

seen in *Liaoceratops*), and finally a complex orthopalinal power stroke (mix of orthal shearing and palinal movements) in Ceratopsoidea. Although he made many observations regarding the qualitative morphology of the jaws themselves and related them to the dental microwear, Varriale (2011) noted that more morphological studies are required to help decipher ornithischian jaw mechanics.

FIGURE 2.8. *Pentaceratops* reconstruction.

Chapter 3: Questions and Methodology

QUESTIONS / HYPOTHESES

Throughout this dissertation, I will evaluate the diversity of jaw structures and feeding mechanisms in ornithischian dinosaurs. Osteological, arthrological, and inferred muscular morphology are used to qualitatively as well as quantitatively evaluate existing and new hypotheses of jaw mechanisms in various clades. In particular, this work will ask the following general questions, with integrated hypotheses:

A. Are there distinct evolutionary trends in craniomandibular osteological, arthrological, and myological morphology and jaw mechanisms in various ornithischian clades?
    - H1: Jaw morphologies within Ornithischia consist of mosaic traits demonstrating convergent evolution across clades, with certain traits being represented in multiple clades for functional purposes. Character states of a set of traits will not segregate within clades. Such traits are as follows:
        - Distinct predentary morphologies.
        - Predentary-dentary and craniomandibular joint morphologies relative to mobility.
        - Orientation of contractile vectors of jaw musculature.
        - Ventral and medial curvature of the symphysis (symphyseal process).

- Curved tooth rows (vs. straight tooth rows).
- A diastema (the edentulous region near the rostral portion of the lower jaw mesial to the tooth row).
- Coronoid process size and shape.
- Craniomandibular joint lower than level of tooth row.

B. Does the osteological and myological craniomandibular anatomy of various ornithischian dinosaurs, assuming it can be identified, have an effect on the mechanical advantage of the different jaw mechanisms and bite forces?

- H2: Orientation of jaw musculature in ornithischian dinosaurs corroborates previous hypotheses of jaw mechanisms for different species and also supports findings incorporated with mobility at the symphysis in relevant taxa.
- H3: The distinct coronoid process in ornithischians, independently heightened in derived hadrosaurs and ceratopsians, increases the moment arm of force by the adductor jaw musculature. It also moves the line of action of the musculature caudally for better mechanical advantage at the bite points.
- H4: A lowered jaw joint relative to the tooth row gives a greater mechanical advantage to jaw adductor musculature as it creates a larger moment arm perpendicular to the muscle vector.

METHODS: MORPHOLOGICAL EXAMINATION AND DESCRIPTION

Material

All observed specimens were photographed in lateral, dorsal, rostral, caudal, and ventral views using a D-SLR camera, with a scale bar in the field of view. Careful attention was given to positioning of specimens in images to reduce error in lever arm analyses; however, some degree of error in camera placement is inevitable due to both the size and shape of the skull (skewing perception and leading to parallax), taphonomic distortion in most specimens, as well as many specimens being on display (sometimes behind glass) in exhibits during data collection, making it difficult to set up the camera for proper positioning. Lists of specimens observed personally are given in Chapters 4-7 with their corresponding less-inclusive ornithischian clade.

Institutional Abbreviations—AMNH, American Museum of Natural History, New York, New York, USA; **BMNH**, British Museum of Natural History, London, United Kingdom; **CEUM,** College of Eastern Utah Prehistoric Museum, Price, Utah, USA; **CMNH**, Carnegie Museum of Natural History, Pittsburgh, Pennsylvania, USA; **DMNH**, Denver Museum of Natural History, Denver, Colorado, USA; **GI SPS**, Geological Institute Section of Paleontology and Stratigraphy, Academy of Sciences of the Mongolian People's Republic, Ulan Bator, Mongolia; **IGCAGS**, Institute of Geology, Chinese Academy of Geological Sciences, Beijing, China; **IRSNB**, Institut Royal des Sciences Naturelles de Belgique, Brussels, Belgium; **IVPP**, Institute of Vertebrate Paleontology and Paleoanthropology, Beijing, China; **JLUM**, Jilin University Museum;

KUVP, University of Kansas Museum of Natural History, Lawrence, Kansas, USA; **MOR**, Museum of the Rockies, Bozeman, Montana, USA; **MSM**, Mesa Southwest Museum, Mesa, Arizona, USA; **MUCPv**, Museo de Geologia y Paleontologia de la Universidad Nacional del Comahue, Paleontologia de Vertebrados, Comahue, Argentina; **NCSM**, North Carolina Museum of Natural Sciences, Raleigh, North Carolina, USA; **NMC**, Canadian Museum of Nature, Ottawa, Ontario, Canada; **NMMNH**, New Mexico Museum of Natural History, Albuquerque, New Mexico, USA; **OMNH**, Sam Noble Oklahoma Museum of Natural History, Norman, Oklahoma, USA; **PVPH**, Museo Carmen Funes, Paleontologia de Vertebrados Plaza Huincu, Neuquen, Argentina; **ROM**, Royal Ontario Museum, Toronto, Ontario, Canada; **SAM-PK**, Iziko South African Museum, Cape Town, South Africa; **SDSM**, South Dakota School of Mines and Technology, Rapid City, South Dakota, USA; **TCMI**, The Children's Museum of Indianapolis, Indianapolis, Indiana, USA; **TMP**, Royal Tyrrell Museum of Palaeontology, Drumheller, Alberta, Canada**; UALVP**, University of Alberta, Laboratory of Vertebrate Paleontology, Edmonton, Alberta, Canada; **UCMP**, University of California Museum of Paleontology, Berkeley, California, USA; **UMNH**, Utah Museum of Natural History, Salt Lake City, Utah, USA; **USNM**, National Museum of Natural History (Smithsonian), Washington DC, USA; **YPM**, Yale Peabody Museum of Natural History, New Haven, Connecticut, USA; **ZDM**, Zigong Dinosaur Museum, Zigong, China; **ZPAL**, Zoological Institute of Paleobiology, Warsaw, Poland.

Osteology

Previous methods used for investigating bone, joint, and musculature of extinct and extant herbivorous species, both reptilian and mammalian, were used to gain a better understanding of mandibular musculoskeletal evolution and function in ornithischian dinosaurs by comparative means (e.g., Greaves, 1978; Weishampel, 1984; Holliday and Witmer, 2008; Holliday, 2009). In this study, predentaries, dentaries, and postdentary elements as well as their associations with the cranium representing genera spanning all ornithischian subclades are examined. Many specimens, representing genera within each clade of Ornithischia, contain relatively complete craniomandibular material. It is important to note, however, that many of these genera are only known from certain craniomandibular elements and are not complete. For this reason, elements are sometimes combined from different specimens (within the same genus) in genera that have much of the skull known from individual bones to gain a better understanding of overall skull structure in each respective genus for the purposes of morphological examination (explained below). As the purpose of this study is to outline jaw mechanisms in ornithischians mainly using mandibular elements, rather than to challenge any hypotheses of cranial kinesis (e.g., pleurokinesis in ornithopods) as in Holliday and Witmer (2008), Rybczynski et al. (2008), Bell et al. (2009), and Cuthbertson et al. (2012), intracranial joint morphologies were not pertinent for investigation, although further investigation of these models remains necessary.

Morphology of the elements themselves, as well as their placement and joint surface morphology between each articulated element was examined (following Weishampel [1984] and Holliday and Witmer [2008]). Special attention was given to

aspects of the skull and jaw that relate to its function in feeding. The predentary-dentary, dentary-dentary, and quadrate-articular (or craniomandibular) jaw joint morphology (i.e., curvature and broadness) were all used to qualitatively assess any type of mobility that could have potentially occurred at these joints (following Weishampel [1984] for interpretation of joint types). General morphology in the shape of the mandibular elements themselves, such as rostral curvature of the dentary from horizontal, shape of the coronoid process (height above tooth row and rostrocaudal breadth at dorsal tip), mediolateral curvature of the tooth row, and morphology of predentary processes as well as associations with the premaxilla, maxilla, and quadrate of the cranium were also examined with a focus on functional interpretation. Taphonomically distorted portions of craniomandibular material were considered and regions of each specimen with taphonomic distortion are, for the most part, excluded from this study. Also, previous dental micro- and macrowear studies, as well as personal observations of tooth wear, aided in focusing attention to morphologies that would allow specific masticatory movements shown by direction of tooth wear and occlusal style.

Myology

Jaw muscle anatomy reconstruction has long been utilized for inferences in the paleobiology of dinosaur feeding mechanisms (Haas, 1955; Ostrom, 1961; Ostrom, 1964; Haas, 1963; Haas 1969; Galton, 1974; Weishampel, 1984; Holliday, 2009; Norman et al., 2011; Sereno, 2012). Previous studies in dinosaur jaw musculature have used extant phylogenetic bracketing (EPB) methods (Witmer, 1995) to compare anatomical landmarks at which muscles would originate and insert (Ostrom, 1961; Weishampel,

1984; Holliday, 2009; Norman et al., 2011; etc.). These studies have been qualitative, with generalized descriptions of where muscles likely attached in life, either inferred from muscle scars or by comparison with extant archosaurs (e.g., crocodilians and birds) and lepidosaurs (e.g., lizards). The current study uses criteria used in previous studies in dinosaur jaw muscle anatomy (Weishampel, 1984; Holliday, 2009), as well as more in-depth case-by-case analyses, of a large diversity of ornithischian dinosaur taxa spanning all subclades to assess the evolutionary trends in craniomandibular muscular arrangement. The muscles interpreted are as follows: m. depressor mandibulae (mDM), m. adductor mandibulae posterior (mAMP), m. adductor mandibulae externus (mAME; consisting of superficialis [mAMES], medialis[mAMEM], and profundus [mAMEP]), m. pseudotemporalis (mPST; many times consisting of superficialis and profundus), m. pterygoideus ventralis (mPTV), and m. pterygoideus dorsalis (mPTD). Understanding these muscles specifically will help gain a better understanding of jaw movements and orientations, as they are the main muscles acting on the lower jaw.

Muscle scarring consists of either a very smooth depression in bone, indicating large muscle bundles attaching, or striations on bone indicative of more tendinous attachments. In many cases, however, no clear indication of muscular attachment sites is visible on bone in the craniomandibular region, especially in the fossil record; so, many of the attachments are estimated by EPB standards primarily indicated by Holliday (2009). This compares dinosaur jaw muscle anatomy with knowledge of attachment sites in closely related taxa. An extant alligator head as well as the head of an extant pigeon were also dissected for personal observations of muscular attachment and a further understanding the arrangement of these muscles relative to one another.

From these observations of muscle attachments in various taxa, the angle of orientation of both the m. adductor mandibulae externus muscle complex as well as the m. adductor mandibulae posterior were measured in ImageJ© (Abramoff et al., 2004) from lateral-view skull photographs of 54 genera spanning all subclades within Ornithischia. Muscles which are measured include mAMES (angle from coronoid base to middle of supratemporal bar origin), mAMEM (angle from mid-height of coronoid to caudal aspect of supratemporal bar), mAMEP (angle from coronoid apex to caudal aspect of supratemporal bar), and mAMP (estimated as the angle from ventral aspect of dentary at the rostrocaudal level of the coronoid apex to mid-height of quadrate bone). This gives a comprehensive view of the evolutionary trends in the arrangement of the main musculature involved with feeding mechanisms. For further description of photograph usage as well as sources of error involved with this kind of analysis, see below.

METHODS: TWO-DIMENSIONAL LEVER ARM ANALYSES

Bite Force Estimates in 2D

Another aspect of interpreting jaw mechanisms is measuring relative bite force (RBF) as it portrays differences in mechanical advantage of osteological and myological morphologies among genera. Relative bite forces have been measured in many modern reptilian and mammalian taxa with use of both two-dimensional lever arm mechanics (Davis, 1955; Sinclair & Alexander, 1987). These two-dimensional methods for assessing lever arm mechanics have been applied to extinct vertebrates (Olson, 1961; Hopson,

1950; DeMar & Barghusen, 1972); more specifically they have been applied to the hadrosaur *Corythosaurus* (Ostrom, 1961) and to a select few ceratopsians (Ostrom 1964; 1966; Tanoue et al., 2009) among ornithischian dinosaurs.

In this study, relative bite forces (RBFs) in 54 genera of ornithischians spanning all subclades are compared (rather than just a few genera within a given subclade as has been previously done) using the 2D lever arm method of Ostrom (1964; 1966). It should be noted that, for the purposes of this study, only one specimen (or published illustration in the case of *Camptosaurus*) was analyzed per genus, since for over half of the genera examined there is only have one skull specimen decently preserved well enough for this analysis. Mallon and Anderson (*in press*) performed a 2D lever arm study on jaws of Dinosaur Provincial Park ornithischian taxa, with multiple specimens of each genus. Their study showed no significant difference in RBF values within a given genus. Given this conclusion, one specimen per genus was considered sufficient for this study; even when multiple specimens were available, I chose the best specimen to represent the genus.

The 2D lever arm method estimates relative adductor muscle force for one side of the jaw (Fig. 3.1). Input lever, or moment arm, is the perpendicular distance from the jaw joint to the line of action of the m. adductor mandibulae externus musculature. As in Ostrom (1966), moment arm is calculated by the following equation:

$$m = \sin(\theta + \delta)d$$

Here, m = moment arm length of the input force applied, θ represents the angle of the applied force vector and lever axis relative to the horizontal plane, δ is the angle

between the diagonal distance (*d*) from the dorsal apex of the coronoid process (or eminence) and the center of the glenoid, or jaw joint.

The output lever length is the distance from the jaw joint to the bite point (the predentary, rostral tooth, middle tooth, and caudal tooth are all tested as separate bite points). A muscle mass unit of 1 is applied to all specimens, as there are no data for muscle masses in ornithischian dinosaurs. Therefore, muscle leverages (here named "relative bite forces") are represented by the simple equation: input lever / output lever.

FIGURE 3.1. *Heterodontosaurus* skull showing input lever (green line) and the four output levers (red lines) described in the text. The muscle input vector (blue line) is also shown to illustrate its association with the levers in the analysis.

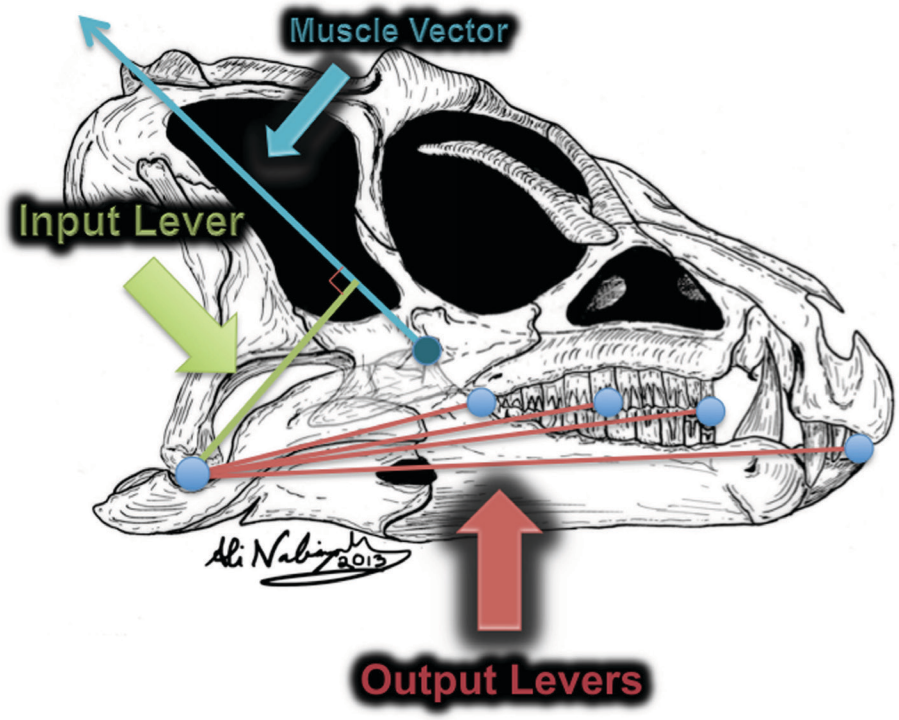

Using lateral views, and with the help of the software ImageJ© 1.45l (Abramoff et al., 2004), measurements were made as seen in Figure 3.1, using scale bars in the images to calibrate the lengths measured. The above equation (input lever / output lever) is a unit-less ratio (Mallon and Anderson, *in press*) and therefore, although measurements were made with ImageJ and are not precise, it is only the comparisons made within the image that matter most for the purposes of this study. For images without a scale bar, measurements were either taken from published data or an arbitrary set measurement within the image itself in ImageJ because it is only the ratio of lever lengths that are necessary. Because all muscle masses were reduced to a unit of 1 (as in Ostrom, 1964; 1966; Tanoue et al., 2009), this study is purely intended for comparisons of shape and morphology and discounts any effect of size, as muscle mass or cross-sectional area is other the determining factor for size comparisons and actual bite force. Mallon and Anderson (*in press*) found that ontogenetic change does not have a significant effect on jaw leverage for the most part (although it does leave some room for error), so skulls of various age groups were combined in this study for overall comparative purposes. Again, a number of sources of error are involved with this kind of analysis and they are mentioned below.

Tanoue et al. (2009) used the 3D Greaves (1978) model to estimate relative bite forces of a select few ceratopsian taxa. This mainly helped gain an understanding of how a curved tooth row creates a more advantageous effect on increasing leverage at certain bite points and also took into consideration forces that are transferred through the symphysis. Although this method could have been used in the current study, the majority of the specimens used have an unfused mandibular symphysis, with predentary acting as

yet another separate element diminishing any muscle force transfer (except in ceratopsians, in which the mandible is secondarily fused), and therefore the current study only focuses on relative bite forces on each side of the jaw separately. The effect of three-dimensional orientation of musculature in multiple planes is also an important factor to consider. However, due to difficulty of assessing exact muscle angles without recourse to 3D measurements, the effect of muscle angle in the coronal and dorsal plane was disregarded in this study.

Statistical MANOVA analyses were then performed on the leverages of the entire tooth rows in each subclade. Comparisons were done both within as well as among subclades to elucidate statistically significant differences between groups of ornithischian dinosaurs. Although, given the incredibly small sample of one specimen per genus that is used, these statistics are not robust. The purpose of doing these statistics is purely just to indicate broad-scale evolutionary trends in drastic changes from genus-to-genus, as well as clade-to-clade, giving a better understanding of both evolutionary differences and evolutionary convergences between various subclades. Results can be seen in Chapters 4-8 with their corresponding group.

In order to easily visualize transitions in RBFs between (or among) taxa, RBF values of each tooth position were optimized onto a phylogeny in the program MESQUITE and entered as continuous data. This creates a color-coded phylogenetic tree, with cooler colors (such as blue and purple) indicating relatively lower bite forces and warmer colors (such as red, yellow, and orange) indicating relatively higher bite forces. This visualization is shown in Chapters 5 – 8 and gives a better understanding of the

multiple transitions from lower to higher RBFs and vice versa, depending on the lineage that is observed.

Perturbation Analyses

A brief perturbation analysis (Otten, 1983; 1985) was performed on the data generated by this study. In this perturbation analysis, hypothetical jaw morphologies were created to test mechanical advantages of particular morphological elements in relevant taxa, such as the existence versus non-existence of a coronoid eminence or process and the lowering of the craniomandibular jaw joint beneath the level of the tooth row versus it being at level with the tooth row. The hypothetical elimination of the coronoid process was performed by carefully placing a dot directly beneath the apex of the coronoid process at the level of the tooth row and then redoing the 2D lever arm analyses mentioned above. Conversely, the hypothetical raising of the craniomandibular jaw joint to the level of the tooth row is performed by carefully placing a dot directly above the glenoid at the level of the tooth row and then, again, redoing the 2D lever arm analyses mentioned above. These analyses will further tests hypotheses 3 and 4 asserted for Question 2 above. Perturbation analyses help explore the degree of advantage each trait has in terms of leverage in a particular individual's jaw. It also compares between taxa showing the evolutionary importance of one trait compared to the other across all clades, (see Discussion [Chapter 8]).

SOURCES OF ERROR

Lateral view photographs were taken with careful consideration of error in perspective as well as using the side of the skull with the least amount of taphonomic distortion or reconstruction; however, many instances occur where taphonomic distortion and reconstruction are prevalent, causing some degree of error. For skull specimens that do not have the cranium and mandible articulating, a lateral view photograph of the mandible was digitally transposed onto a lateral view photograph of the cranium using Adobe Photoshop©, matching up scale bars to make a best fit. This is also a large source of error due to slight changes in perspective of the scale bar and elements between photographs; depending on how precisely lateral of the skull the picture was taken. Another source of error is that few specimens (e.g., *Parksosaurus* and *Ouranosaurus*) are analyzed for lever arm study based on reconstructions in publications, as they are disassembled or missing elements in life. All of these sources of error are inevitable; but, for the purposes of this study, which consists of many genera but only a sample of one individual per genus, the large differences between the genera and the overall morphologies are variable enough that it does not hinder the overall results substantially.

Another source of error includes estimating placement of the apex of the coronoid process in many species in which it is hidden behind the jugal in lateral view (e.g., hadrosaurids). The coronoid tip was estimated based on roundness of the coronoid as it extends dorsally disappearing behind the glenoid, as done by Mallon and Anderson (*in press*). In ankylosaurs, the origin of the mAME was estimated with observations of CT imaging of *Euoplocephalus*, since its supratemporal fenestra is closed off externally by

osteoderms that are fused superficially to them. Also, the ankylosaur jaw joint is hindered from view laterally by the caudoventral extension of the osteoderm projecting from the jugal, so its jaw joint position was estimated by means of observations of the specimen itself. I also superpositioned the lower jaw on top of the skull in Adobe Photoshop© in line with dentition to see where it would align caudally. In ceratopsids, the origin of adductor musculature at times needed to be estimated as well, although their supratemporal fenestra is still visible in dorsal view. As the caudal dentition of ceratopsids and hadrosaurids extends medial and caudal to the coronoid process and is hindered in lateral view, the caudal bite point, as a general rule, was assumed to be the caudal margin of the coronoid process in line with the tooth row, as done by Mallon and Anderson (*in press*).

Chapter 4: Heterodontosaurid Craniomandibular Anatomy

Mandibular morphology in Heterodontosauridae (Fig. 4.1), the basal-most clade within Ornithischia (Butler et al., 2008; see Fig. 1.1 in Chapter 1), is discussed in depth below with emphasis on functional interpretation (see Table 4.1 for specimens examined). Unless otherwise stated, osteological descriptions are based primarily on material from *Heterodontosaurus*, due to its completeness relative to other heterodontosaurid genera. As some of the postdentary elements do not show as much functional significance, only a brief discussion of each postdentary element of the mandible is given below to illustrate the general shape of this region. Cranial elements with direct contact to the mandible (i.e., the premaxilla, maxilla, and quadrate) provide functional implications in heterodontosaurid jaw mechanisms and are also described for further completeness. Cranial elements holding significance with regards to the jaw adductor musculature are described as needed in the Jaw Musculature section. See Norman et al. (2011) and Sereno (2012) for more detailed descriptions.

FIGURE 4.1. Phylogenetic relationships of genera within Heterodontosauridae compiled of Pol et al. (2011) and Sereno (2012) with a unresolved relationship of *Pisanosaurus*.

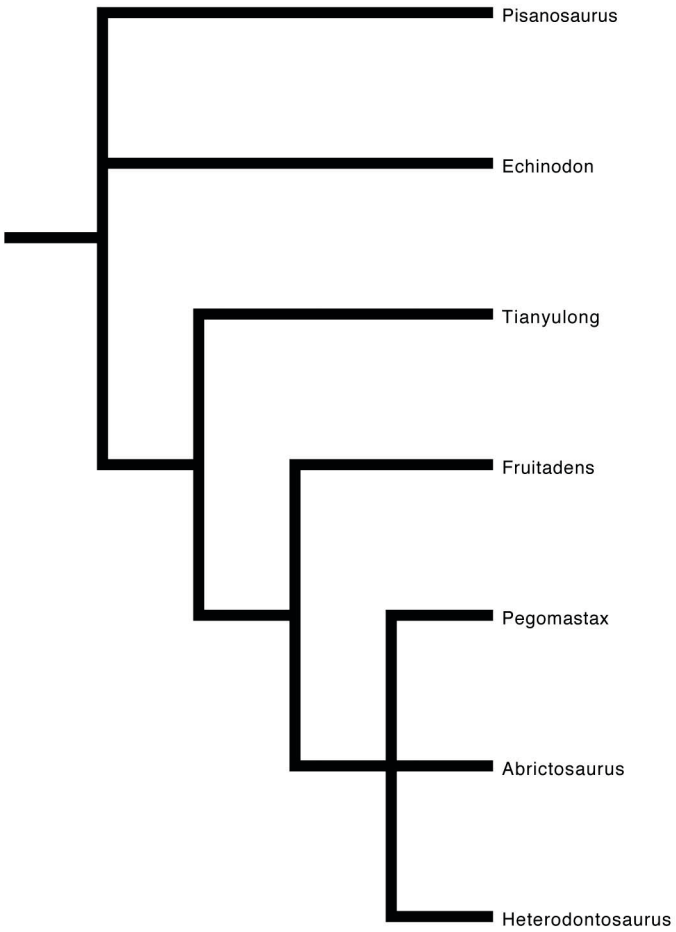

TABLE 4.1. Heterodontosaurid specimens examined in this study. (Note: SAM-PK-K132 was examined from detailed photographs courtesy of Karen Poole and are used in this study with permission.)

Taxon	Specimen	Elements
Abrictosaurus	BMNH B54	Partial jaw (with predentary) and skull
Heterodontosaurus	BMNH R8179 – Holo. Cast	Complete jaw and skull

	BMNH R14161	R. dentary
	SAM-PK-K1332	Most of jaw (with predentary) and skull

OSTEOLOGICAL DESCRIPTION

FIGURE 4.2. *Heterodontosaurus* skull reconstruction based on multiple specimens. Left lateral view. Scale bar = 1 cm.

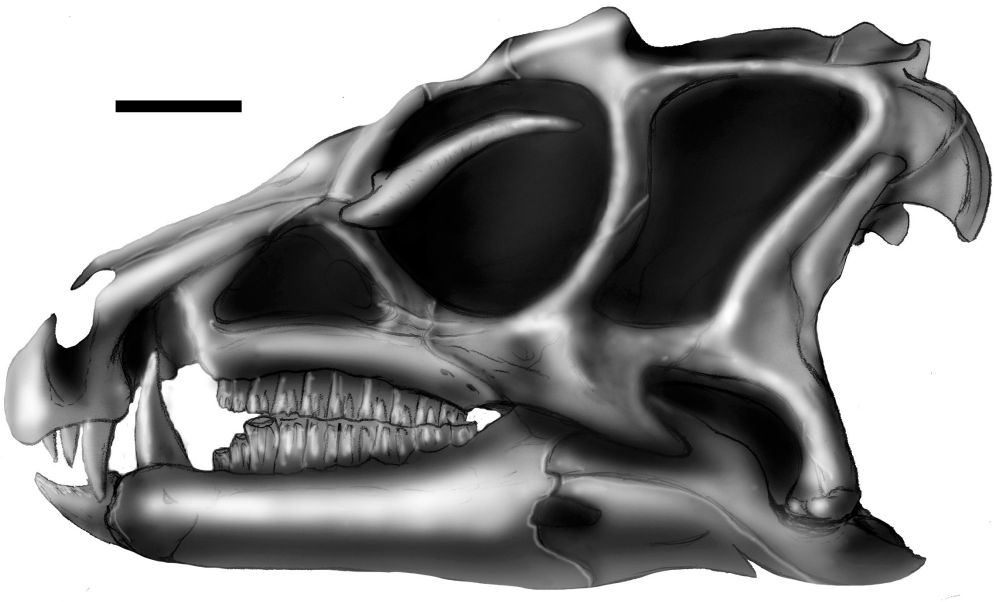

Cranium (Fig. 4.2; 4.3)

As they are small-bodied animals, heterodontosaurid skulls generally do not exceed more than 10-11cm in length. Their crania are roughly triangular in lateral and dorsal view, as in many small-bodied, bipedal, herbivorous ornithischian dinosaurs. A distinct midline sagittal crest extends from just behind the orbits to the caudal edge of the skull roof. In ventral view, the rostral extent of the slender palate comes to a point medially. Heterodontosaurids have large, circular orbits and, just caudal to them on either side, obliquely angled, roughly quadrangular infratemporal fenestrae that are wider dorsally than ventrally. The antorbital fenestra is prominent and triangular. Dorsally, the orbit is overlapped laterally by the caudodorsally-oriented palpebral bone, which arises from the lacrimal. The jugal is triangular and tapers caudoventrally relative to the ventral surface of the skull and there is a dorsally-arched margin between the jugal and quadrate. The nasal is elongate and rounded dorsally. The paroccipital processes are robust and angled laterally with respect to the occiput in caudal view.

FIGURE 4.3. *Heterodontosaurus* cranium (generalized). Abbreviations: aof, antorbital fenestra; f, frontal; itf, infratemporal fenestra; la, lacrimal; j, jugal; m, maxilla; n, nasal; or, orbit; p, palpebral; pa, parietal; pf, prefrontal; pm, premaxilla; po, postorbital; pop, paroccipital process; pt, pterygoid; q, quadrate; qj, quadratojugal; sq, squamosal; stf, supratemporal fenestra. Scale bar = 1 cm.

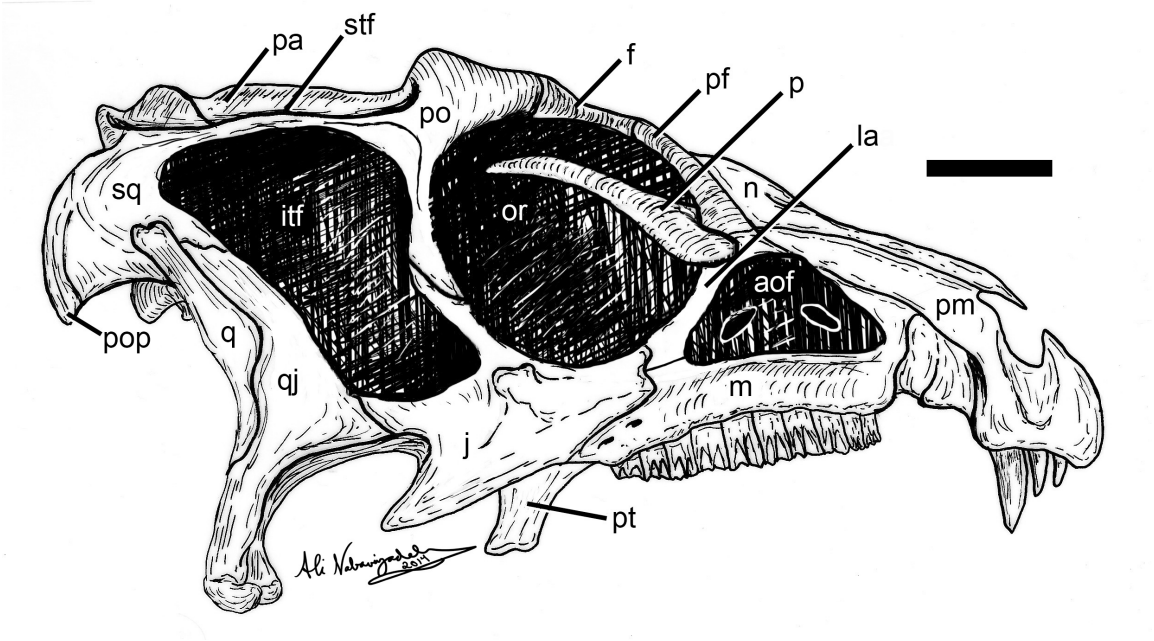

Premaxilla—The premaxilla is dorsoventrally deep and bears three teeth (see Dentition section below). These teeth are located on the caudal half of the premaxilla. The edentulous rostral half of the premaxilla remains toothless and likely occluded with the lateral surface of the keratinous rhamphotheca of the predentary. The premaxilla is ventrally offset relative to the maxilla sutured immediately caudal to it and possesses a caudomedial process that joins with its counterpart between the maxillae. A caudodorsally-oriented, long, and thin dorsal process extends between the nasal and the maxilla reaching the tip of the lacrimal. This process and the aforementioned caudomedial process together make up the snout. The ventral rim of the toothless rostral end of the premaxilla is thicker and roughened, with implications of being concealed within a keratinous rhamphotheca. The lateral rim of the premaxilla outside the premaxillary teeth is bulged and convex lateral to the alveoli. A well defined, concave embayment lies just caudal to the third (caniniform) premaxillary tooth (that is, continued.

This fossa is formed equally by the premaxilla and maxilla) which and receives the large, dorsally-oriented caniniform tooth of the dentary rests against during occlusion (Fig. 4.4). Ventrally, the premaxillary palatal roof is mediolaterally thin and arched slightly dorsally.

FIGURE 4.4. Embayment between premaxilla and maxilla for dentary caniniform tooth in *Heterodontosaurus* (SAM-PK-K1332). Abbreviations: em, embayment; m, maxilla; pm, premaxilla. (*Photo courtesy of Karen Poole*.)

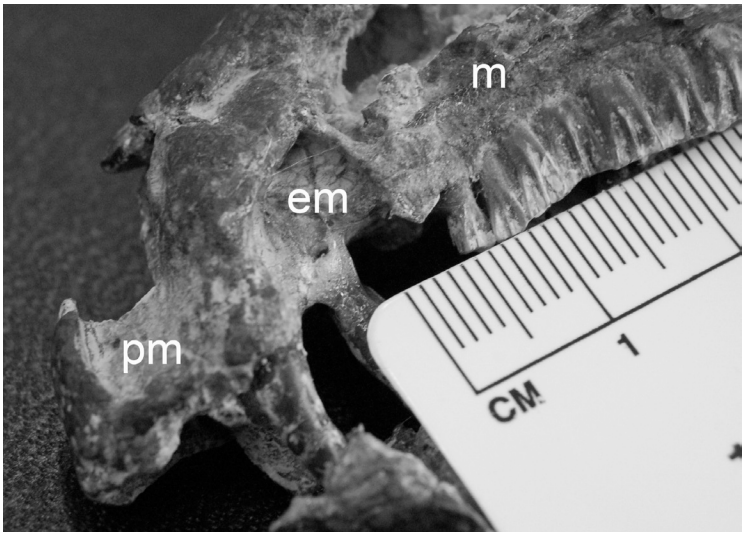

Maxilla—The maxilla is bordered by the premaxilla rostrally and dorsally, the palatine and vomer medially, the ectopterygoid caudally, and the lacrimal and jugal caudodorsally. In lateral view, the maxilla is flat and triangular with a flat lateral surface, and a rostromedially-oriented process, joining with its counterpart that joins the contralateral maxilla and fused vomers medially. The maxilla is slightly transversely expanded at its tooth-bearing ventral edge where approximately 10-12 alveoli are present in *Heterodontosaurus*. A series of small foramina are seen just dorsal to the dentition on

the medial and lateral sides. A medial shelf is formed by the maxilla as well, but it does not contact its counterpart in ventral view, although they contact the vomers rostromedially. The maxilla forms the caudal portion of the embayment continued from the premaxilla for the lower caniniform dentary tooth to shroud it during occlusion of the cheek teeth (Fig. 4.4). It also forms the rostrodorsal and ventral portions of the triangular external antorbital fenestra. The antorbital fenestra extends medially into the jugal and is, in lateral view, perforated internally by two foramina, one rostral and one caudal. These represent the modified internal antorbital fenestra. The bony lateral edge of the maxillary tooth row is extended laterally, forming a prominent buccal shelf with its tooth row consequently situated in a medially-inset, emarginated positioning (see Fig. 4.9 below), with the dentition oriented ventrally and bowed laterally. This emargination is not nearly as pronounced in *Abrictosaurus* (BMNH B54), however. See Dentition section below for description of heterodontosaurid dental morphology.

Quadrate—The quadrate is a slightly laterally twisted, columnar, and rostrally-bowed element, with its caudodorsally-oriented, rounded dorsal head securely forming a ball-and socket articulation with the ventral cotylus of the squamosal. At mid-shaft, the quadrate is rostrally bowed. Its body is expanded on its rostral side with a paper-thin sheet of bone extending rostrally from its rostromedial margin, thus forming the pterygoid wing that overlaps the lateral surface of the quadratic wing of the pterygoid. The quadratojugal joins with the rostrolateral ridge of the columnar quadratic body and overlaps the lateral side of much of the ventral half of the quadrate, except for the ventral head. As the quadrate body extends further ventrally, it is then bowed back caudally and then rostrally again at the ventral head in a sigmoidal curve. The ventral head of the

quadrate (Fig. 4.5) extends further ventrally than the level of the maxillary tooth row, resulting in a ventrally offset jaw articulation, except in *Tianyulong* in which jaw articulation is uniquely just above the level of the tooth row (Zheng et al., 2009; Sereno, 2012). Two spheroidal condyles form the mediolaterally expanded ventral head of the quadrate with a flatter rostromedial condyle and a more ventrally offset, larger, and more rounded caudolateral condyle. Both condyles, which are at a roughly 30 to 40 degree angle to the horizontal plane relative to one another in caudal view, articulate with the concave glenoid of the mandible (Sereno, 2012).

FIGURE 4.5. Ventral head of quadrate of *Heterodontosaurus* showing two condyles in caudal view.

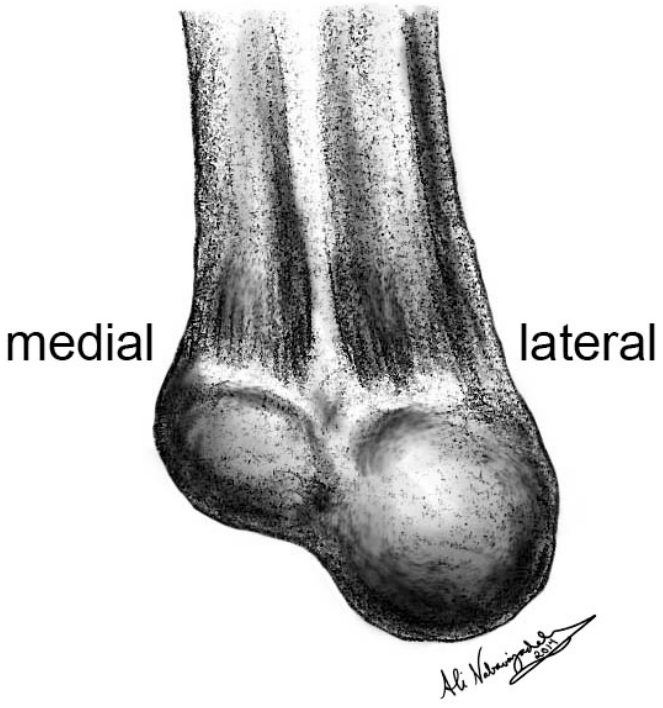

Predentary

The predentary (Fig. 4.6; 4.7; 4.8; 4.9) is a small, unpaired, midline element placed medially at the forward tip, articulating with the rostral end of each dentary. It is triangular in both lateral and dorsal views. In dorsal view, the internal portion of the predentary is shovel-like and comes to a dorsally ascending, pointed tip at its rostral midline. The dorsal, outer edge that contacts the premaxilla during occlusion is gently beveled medially at its medial ridge. The outer surface of the predentary is covered with small pits and rugosities, suggesting that in life the predentary was covered by a keratinous rhamphotheca that contacted that of the premaxilla. The length of the dorsal edge of the predentary is a roughly longer than its dorsoventral depth, except in *Pegomastax*, where the predentary is actually deeper than it is long (Fig. 4.6).

FIGURE 4.6. Heterodontosaurid predentaries in lateral view (rostral end to the right). A, *Heterodontosaurus*; B, *Pegomastax*. Scale bar = .5 cm.

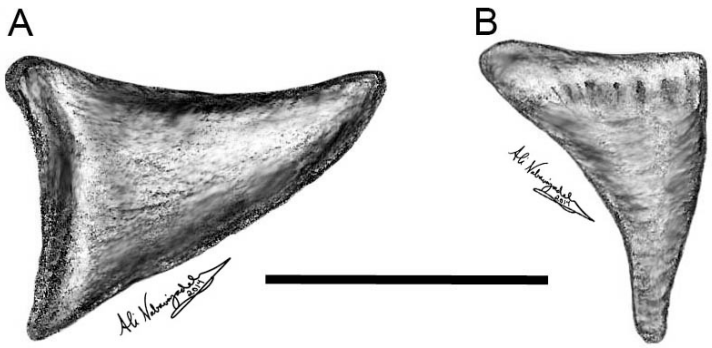

A short caudolaterally-projecting process on the lateral end of the predentary overlaps the dorsal and lateral surfaces of the dentaries (Fig. 4.7). A single, ventral

median process cradles the ventral surface of the dentaries. The caudolateral processes as well as the ventral median process together create a cradling effect that stabilized where the dentaries are stabilized within the bounds of these processes, although not to the point of immobility.

FIGURE 4.7. Dorsal view of the predentary-dentary articulation at the symphysis in *Heterodontosaurus*. Abbreviations: d, dentary; p, predentary. (Based on Sereno, 2012.)

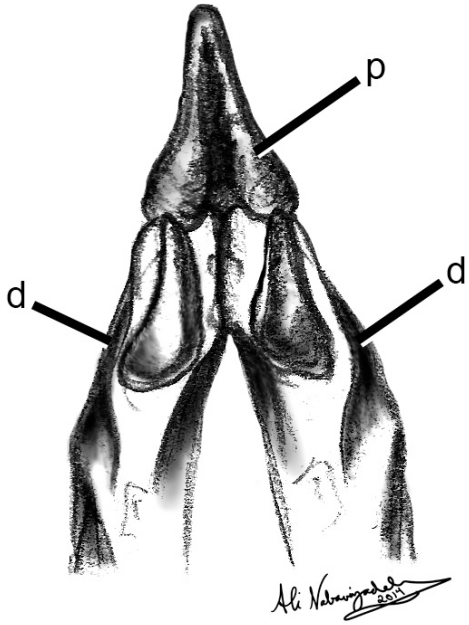

As stated by Norman et al. (2011) and Sereno (2012), in caudal view, the broad surface of the predentary that articulates with the rostral ends of the dentaries is sinuous and saddle-shaped, rather than spheroidal as stated by Weishampel (1984) and Crompton and Attridge (1986), creating an uneven articulation with each dentary with no clear indication of a tight suturing with the dentaries. The absence of a completely tightly

sutured junction suggests that some degree of mobility may have been permitted. Whether this movement was permitted by a fibrocartilagenous, ligamentous, or even synovial joint, however, is unclear. Sereno (2012) argued, however, that the constraints on wishboning indicated by Norman et al. (2011) are not significant due to the small size of the animal.

Dentary

The dentary (Fig. 4.8; 4.9; 4.10) is the largest element in the heterodontosaurid mandible. It articulates with the predentary and the opposite dentary rostrally, the splenial medially and the surangular, angular, coronoid, and prearticular caudally. In lateral view, the dentary is elongate and gradually becomes taller at its caudal end, although it maintains a straight ventral margin.

Tianyulong is an exception to this with a straight dentary ramus that is not deepened caudally but is in fact parallel throughout its length along the toothrow (Zheng et al., 2009; Sereno, 2012). The lateral surface is significantly emarginated lateral to the dentition, forming a low ridge. This ridge is curved ventrally and caudally ascends dorsally as it reaches the coronoid eminence (Fig. 4.9).

FIGURE 4.8. *Heterodontosaurus* mandibular ramus (generalized). A, lateral view; B, medial view. Abbreviations: a, angular; ar, articular; c, coronoid; d, dentary; p, predentary; pa, prearticular; sa, surangular; sp, splenial. Scale bar = 1 cm.

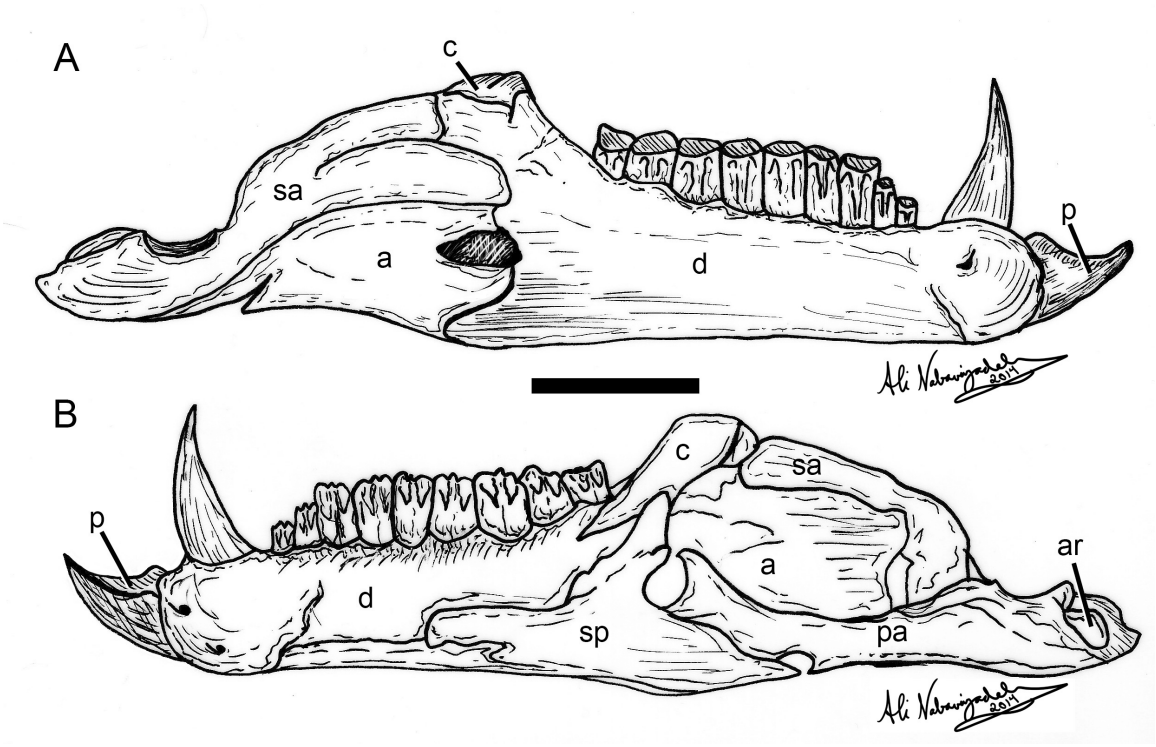

FIGURE 4.9. *Heterodontosaurus* skull specimen (SAM-PK-K1332) exhibiting buccal emargination of dentary and maxilla. Abbreviations: d, dentary; dem, dentary emargination; m, maxilla; mem, maxillary emargination; p, predentary. (*Photo courtesy of Karen Poole.*)

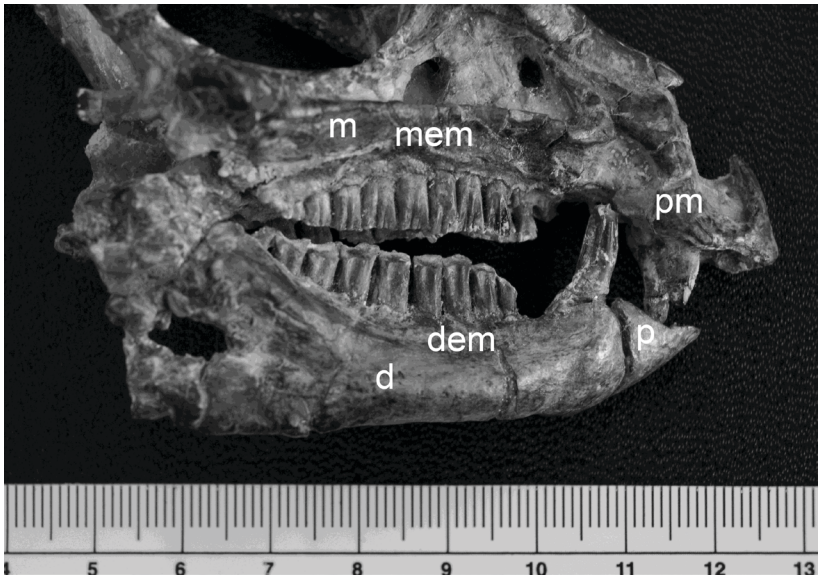

The rostral-most region of the dentary is dorsoventrally expanded, but ends in a somewhat rounded rostral edge that contacts its counterpart medially and the predentary rostrally and laterally at the symphysis. The articulated predentary and paired dentaries together create a V-shaped rostral end of the lower jaw in dorsal view, as the dentaries are at an acute angle relative to one another. The dentary is slightly rugose at its rostral margin where it contacts its counterpart, suggesting remodeling induced by forces from movement against its counterpart in life. One large foramen on the lateral surface of the rostral tip of the dentaries supplied neurovasculature (mental artery and nerve) rostrally to the predentary. Another distinctive foramen, placed caudoventral to the aforementioned foramen just caudal to the predentary-dentary articulation, likely acted as an additional foramen for the mental n. and a. to supply the predentary and the skin of the more rostral surface of the dentaries themselves.

FIGURE 4.10. Dorsal view of *Heterodontosaurus* right jaw ramus (BMNH 14161) showing medial curvature of the tooth row. (Top of image is medial, symphysis to the right). Scale bar = 1 cm.

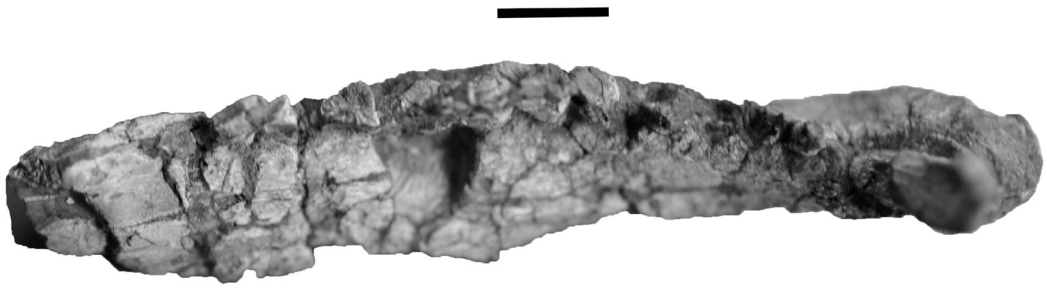

The dorsal ridge of the dentary that bears alveoli is slightly medially bowed (Fig. 4.10). The tooth row of each dentary is oriented at an acute angle relative to its mandibular counterpart, with the distal tooth of each dentary being the farthest away from its contralateral counterpart than the middle or mesial tooth. In *Heterodontosaurus*, there are roughly 10-12 tooth positions, with one larger caniniform tooth rostral to these alveoli, all of which are described below. In the more basal *Pisanosaurus*, there are a total of 15 teeth in the dentary (Bonaparte, 1976; Sereno, 2012), showing a decrease in tooth number in heterodontosaurid relatives while maintaining a more distal chewing locus. See Dentition section below for description of heterodontosaurid dental morphology.

The rostral portion of the coronoid eminence is constructed by the dentary extending dorsally just caudal to and in line with the dentition. The dentary tooth row terminates rostral to the coronoid process. The remainder of the coronoid eminence is formed by the coronoid bone, coming to a point at the apex of the coronoid eminence, and by the surangular, which gradually descends caudally at a shallower angle than the rostral dentary portion**.** In caudal view, the large mandibular canal (Meckel's groove) runs from immediately ventral to the caudal surface of the coronoid process to the ventromedial aspect of the dentary body ventral to the dentition. Caudally, it is continuous with the adductor fossa where some of the jaw musculature is housed. The mandibular canal houses the mandibular branch of the trigeminal nerve (V3), which innervates the dentition (as seen in extant crocodilians) as well as eventually the skin around the mandible and the keratinous rhamphotheca around the predentary. The caudal aspect of the dentary articulates with the coronoid, surangular, angular, and prearticular.

The caudal margin these elements as well as the splenial together open to form the caudal boundaries of the mandibular canal.

Coronoid

The coronoid (Fig. 4.8) is a sheet of bone that forms the apex of the coronoid eminence extending just caudal to the dentary and followed by the descent of the dorsal margin of the surangular. The dorsal-most aspect of the coronoid is rugose, indicative of adductor muscular insertion. It is overlapped by the dentary and splenial rostrolaterally. It has a ledge that forms the rostrodorsal aspect of the mandibular fossa in medial view.

Splenial

The splenial (Fig. 4.8) is a thin, sheet-like bone that covers the ventromedial aspect of the dentary and caudal portion of the mandibular canal before it abruptly becomes much thinner as it extends rostrally, although it does not reach the symphysis. The caudal portion of the splenial bifurcates, articulating with the coronoid dorsally and the angular and prearticular ventrally.

Angular

The angular (Fig. 4.8) is an elongate, narrow, and laterally compressed bone that lies ventral to the mandibular groove and is located on the medial surface of the dentary rostroventrally. Laterally, there is an external mandibular fenestra between the angular and dentary. The angular articulates with the surangular caudodorsally, creating the

ventromedial edge of the caudal portion of the mandibular corpus. The angular also forms the floor of adductor chamber and it articulates with the splenial rostrally and the articular caudodorsally at its outer surface. It braces the articular glenoid ventrally and, along with the surangular and prearticular, helps support the outer edges of the articular for sturdy articulation with the quadrate at the glenoid.

Surangular

The surangular (Fig. 4.8) is a tortuous element that forms the caudodorsal margin of the mandible and the continuation of the coronoid eminence caudal to the dentary and coronoid bone. It has a thickened dorsal margin rostral to the jaw joint, contacting the dentary and coronoid rostrally. It forms the lateral margin of the adductor fossa for the jaw adductor musculature as well as the dorsolateral boundary of the mandibular canal. The ventral portion of the mandible contacts the dentary at a suture ventral to the coronoid eminence but just dorsal to the small external mandibular fenestra by the dentary and angular. Medially, the surangular curves to contact the prearticular rostral to the articular and forms the ventrolateral lip of the mandibular glenoid as well as the lateral aspect of the retroarticular process caudal to the glenoid.

Prearticular

The prearticular (Fig. 4.8) is a gracile element adding to the caudomedial portion of the mandible and contacting. Its rostral end contacts the splenial as it extends rostrally. This element forms the floor of the adductor fossa in medial view where it meets the surangular rostral to the articular glenoid. It envelops the articular medially and extends

caudally to form the ventromedial aspect of the retroarticular process caudal to the glenoid.

Articular

The articular (Fig. 4.8; 4.11) is roughly diamond-shaped in dorsal view and held in place by the surangular laterally, the angular ventrally, and prearticular medially. It forms a slightly concave and rostrocaudally- as well as mediolaterally-expanded glenoid for articulation with the bicondylar distal head of the quadrate (Fig. 4.11). The rostrocaudal expansion is slightly greater than the rostrocaudal breadth of the articulating quadratic condyles, which suggests possible rostrocaudal movements of the lower jaw to have occurred in life. There is a median ridge running rostrocaudally along the dorsal surface of the glenoid, separating the articulations of each ventral quadratic condyle. There are also faintly dorsally raised ridges around the edges of the entire glenoid created by the articular medially and surangular laterally so as to create the outer boundaries of the glenoid. In dorsal view, the transverse expansion of the articular glenoid has a rostromedial to a caudolateral orientation due to the positioning of the two quadratic condyles with which they articulate. At occlusion, the entire glenoid is slanted laterally so as to allow the caniniform dentary tooth to ultimately be oriented dorsally. As stated before, the jaw articulation is usually ventrally offset from the level of the tooth row, in heterodontosaurids except in *Tianyulong*, whose jaw articulation is uniquely just above the level of the tooth row (Zheng et al., 2009; Sereno, 2012).

FIGURE 4.11. Craniomandibular joint of *Heterodontosaurus*, showing quadrate articulation with articular surface of the mandible (right lateral view, right articulation). Abbreviations: ar, articular surface; q, quadrate.

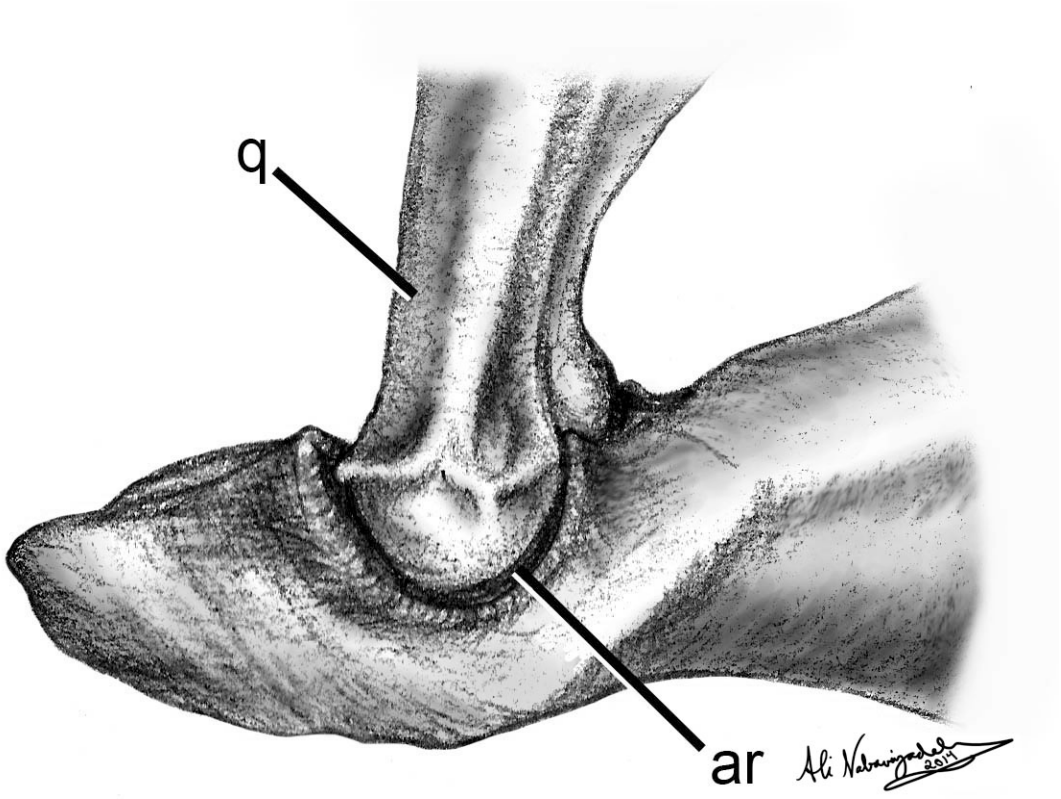

Dentition

The premaxilla bears three conical, shallowly caudally recurved, and mediolaterally-compressed teeth on either side (two in *Tianyulong* [Zheng et al., 2009]), each successively larger in size caudally with the third being largest and caniniform in shape (Fig. 4.12). The caniniform tooth is reduced in size in *Abrictosaurus* (BMNH B54) and is located in the maxilla in *Echinodon* (Sereno, 2012).

FIGURE 4.12. Right premaxillary dentition in *Heterodontosaurus*, increasing in size from rostral to caudal (right to left in image).

The maxillary dentition is tightly packed and roughly level and flush ventrally in lateral view as well as slightly medially bowed. Each tooth crown is columnar and gradually mesiodistally expanded at the distal end relative to the narrower alveolar end (Fig. 4.13). A single median ridge extends dorsoventrally in lateral view on the enamel crown, forming a pointed occlusal edge with two enamel-filled depressions on either side of it mesially and distally. The first four teeth also have an additional small ridge mesial and distal to the prominent median ridge. The mesial-most teeth are more mediolaterally compressed, forming a thinner cutting occlusal edge, for shearing vegetation, whereas the more distal teeth are thicker and form a broader, flatter, butterfly-shaped occlusal surface, likely for purposes of crushing vegetation with more surface area.

FIGURE 4.13. Right maxillary tooth (first tooth position) in *Heterodontosaurus*.

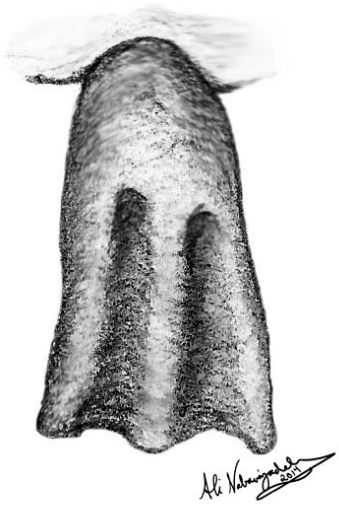

The dentary possesses one large, conical, caniniform tooth (Fig. 4.14) that, during occlusion, rests in the embayment formed at the premaxilla-maxilla suture diastema described above (Fig. 4.4). This tooth, slightly recurved distally at its apex, sits in an alveolus that is raised relative to the rest of the cheek dentition distal to it. In *Abrictosaurus*, this caniniform tooth is relatively much smaller, which, along with the much-reduced premaxillary caniniform, suggests a reduction or elimination of caniniform use in general for this taxon (Sereno, 2012).

FIGURE 4.14. Right caniniform tooth in *Heterodontosaurus* dentary.

A short diastema extends between the caniniform tooth and the rest of the dentition. The dentary tooth row is tightly packed and gradually raised dorsally as the height of the dentary rises in lateral view. The entire tooth row is also slightly bowed so that its dorsal occlusal surface is uneven and is oriented 35 to 40 degrees to the horizontal plane (Weishampel, 1984), although certain portions of the tooth row are more even with each other than others. The medial surface of each tooth resembles the lateral surface of the maxillary teeth (Fig. 4.15), with a median ridge running dorsoventrally along the enamel crown. The mesial and distal dentary cheek teeth together form a planar occlusal surface; however, the middle teeth form more of a cupped, step-like wear facet. This likely indicates more crushing or grinding action at this part of the lower jaw (pers. obs.).

FIGURE 4.15. Middle dentary cheek tooth of *Heterodontosaurus* in medial view, showing planar wear facet.

Pisanosaurus is an exception as it has more spatulate teeth with the tooth row forming an uneven occlusal plane (Sereno, 1991). *Fruitadens*, a Late Jurassic heterodontosaurid (Butler et al., 2012), has a more spade-shaped dentary tooth morphology with denticles and a pointed apex, which differs from that seen in most other heterodontosaurids (see Fig. 4.16).

FIGURE 4.16. *Fruitadens* dentary tooth (based on Butler et al., 2012; Sereno, 2012).

JAW MUSCULATURE

Organization of the jaw musculature in heterodontosaurids has been inferred through studies of presumed muscle scarring as well as extant phylogenetic bracketing methodology (Norman et al., 2011; Sereno, 2012). These descriptions were used as a baseline for inferring the morphology and usage of jaw musculature.

M. depressor mandibulae

M. depressor mandibulae (mDM; Fig. 4.17) was likely the primary muscle acting to lower and thereby open the jaw. When compared to crocodilians, it is likely that this muscle originated on the enlarged, angled paroccipital process of the exoccipital on the caudal-most aspect of the cranium (Norman et al., 2011). Rugosities on the lateral surface of this process are a convincing indication of such an attachment. The muscle inserted ventrally onto the dorsal aspect of the retroarticular process. Raised ridges around the dorsal surface of the retroarticular processes demarcate the outer boundaries of this insertion.

M. adductor mandibulae posterior

The palinal motion of the jaw mechanism was likely produced by the enlarged m. adductor mandibulae posterior (mAMP; Fig. 4.17). This muscle originated on the rostral, dorsoventrally-oriented, and deeply-creviced surface of the quadrate body. It stretched rostroventrally, inserting onto the thickened floor of the mandibular fossa on the inner caudal aspect of the caudal dentary. This would make for a direct line of action for the

muscle to contract and pull the jaw caudally to strip the vegetation against the dentition in that direction. As it is typically a large-bodied muscle, it likely produced considerable force in the caudal direction and made for substantial bite force. See Table 4.2 for muscle fiber orientations.

TABLE 4.2. Heterodontosaurid mAMP muscle vector angle.

Genus	Spec. #	mAMP(°)
Heterodontosaurus	SAM-PK-K337	39.43

M. pseudotemporalis

M. pseudotemporalis (mPST; Fig. 4.17) likely originated at the rostral-most section of the supratemporal fenestra as well as the rostral portion of the sagittal crest. It extended rostroventrally to insert on the dorsal tip of the coronoid eminence (likely through a tendinous sheet) and this orientation would also help in pulling the jaw closed when contracted. According to Norman et al. (2011), it additionally might have had an insertion inside of the mandibular canal underneath the dentary teeth.

FIGURE 4.17. *Heterodontosaurus* skull in left lateral view showing reconstructed jaw musculature. From left to right: mPST, mAMP, and mDM. See Fig. 4.2 for scale bar.

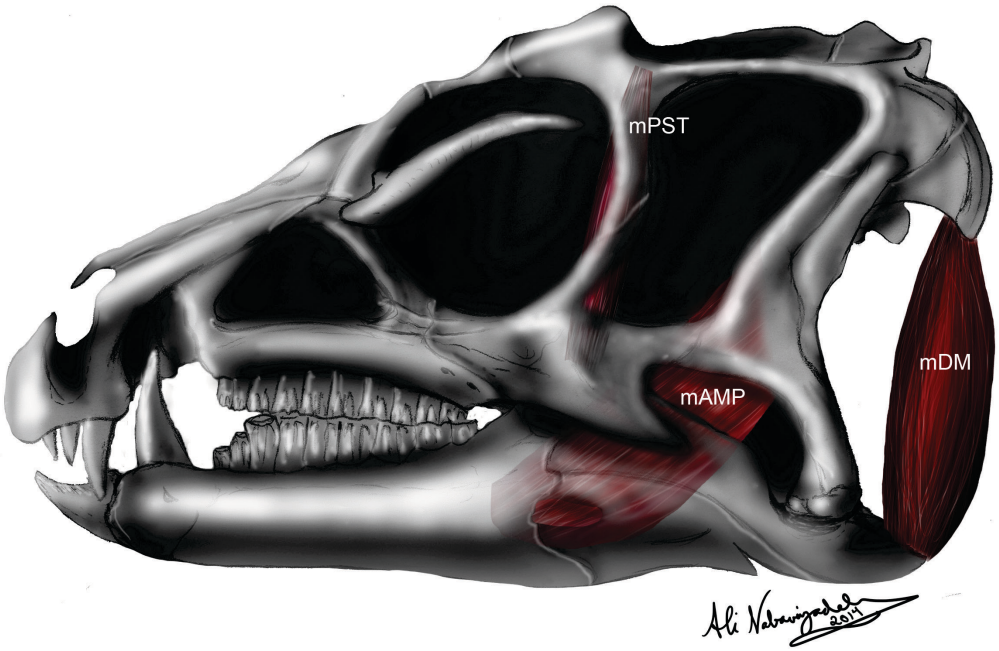

M. adductor mandibulae externus

The primary group of muscles likely acting to raises the jaw to occlusion is the adductor mandibulae externus (mAME) muscle group (Fig. 4.18) that all). This group originated on the internal surface of the squamosal (see below for specific origins of each muscle body) and in the temporal region, and together functioned as one large fan of muscle, except for m. adductor mandibulae externus ventralis, which is described below. See Table 4.3 for muscle fiber orientations. These muscle descriptions are based on observations in both crocodilians and birds (Holliday and Witmer, 2007; Holliday, 2009).

M. adductor mandibulae externus superficialis—M. adductor mandibulae externus superficialis (mAMES) likely originated within the bounds of a curved depression on the ventrolateral surface of the temporal bar on the lateral surface of the

squamosal. The temporal bar extends caudally along the lateral surface of the squamosal near the paroccipital processes and bounds the dorsal aspect of the infratemporal fenestra. Additionally, it extends rostroventrally part way down the lateral margin of the postorbital bar, creating the rostral margin of a wide fan-like origin for this muscle. MAMES then expanded along the more lateral portion of the dorsal aspect of the surangular and probably the more caudal portion of the coronoid eminence, its insertion marked by ridged textures with defined demarcations of muscle boundaries. This muscle also likely expanded onto the lateral aspect of the coronoid eminence, inserting onto the slightly-embayed lateral aspect of the angular.

M. adductor mandibulae externus medialis—M. adductor mandibulae externus medialis (mAMEM) likely originated on the medial surface of the squamosal position of the upper temporal bar just dorsal to the infratemporal fenestra, sheathing the lateral aspect, and ultimately rostral portion, of the supratemporal fenestra in superior view. It likely extended rostroventrally to insert onto the smooth medial aspect of the dorsal ridge along the surangular portion of the coronoid eminence.

M. adductor mandibulae externus profundus—M. adductor mandibulae externus profundus (mAMEP) likely originated on the medial wall of the supratemporal fenestra and caudal portion of the sagittal crest in dorsal view, with a possible additional portion blending with the rostral insertion of m. adductor mandibulae externus medialis on the dorsal rim of the surangular. This muscle is inferred to have inserted at the caudodorsal apex of the coronoid eminence, where there is rugosity on the coronoid bone.

M. adductor mandibulae externus ventralis—M. adductor mandibulae externus ventralis (mAMEV; not figured) is included in reconstructions by Sereno (2012) in which

heterodontosaurid jaws were compared to that of a parrot's jaw. This study indicates a muscle originating at the ventral edge of the caudoventrally-oriented process of the jugal (on the cranium), wrapping around the lower jaw laterally and inserting onto the ventral edge of the angular. A similar reconstruction was made for *Psittacosaurus* as well in Sereno et al. (2009). Other authors, however, have not yet confirmed whether this muscle truly existed in ornithischians. Confirmation of the existence of this muscle requires further examination of muscle scars on multiple specimens as well as closer observations of osteological correlates.

TABLE 4.3. Heterodontosaurid mAME muscle vector angles.

Genus	**Spec. #**	**mAMEP(°) (Coronoid Apex)**	**mAMEM(°) (Coronoid Mid-height)**	**mAMES(°) (Coronoid Base)**
Heterodontosaurus	SAM-PK-K337	51.28	69.64	80.62

FIGURE 4.18. *Heterodontosaurus* skull in left lateral view showing the m. adductor mandibulae externus muscle complex. Abbreviations: mAMEP, m. adductor mandibulae externus profundus; mAMES, m. adductor mandibulae externus superficialis. MAMEM (m. adductor mandibulae externus medialis) is not visible as it is between the previous two muscles. See Fig. 4.2 for scale bar.

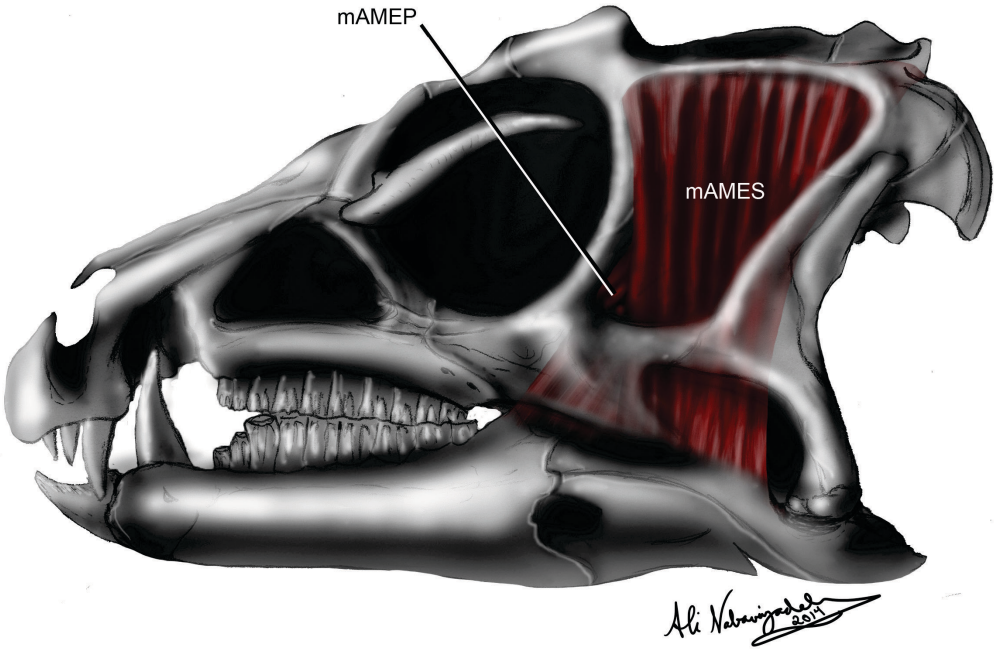

M. pterygoideus ventralis

M. pterygoideus ventralis (mPTV; Fig. 4.19) originated on the pronounced caudomedial surface of the pterygoid, with a portion originating in a concavity on its ventral surface shelf. There may have also been areas along the medial surface of the maxilla and pterygoid-quadrate flange that would have accommodated origins of various muscle fibers. This muscle would have extended caudoventrally, wrapping around the lateral aspect of the mandible and inserting onto the lateral side of the retroarticular process. Its action plausibly contributed to the medial movement or restriction of the mandibular corpus on which it is attached, depending on which side of the jaw is being used in mastication, depending on what direction the mandible is moving at a given point

in the chewing cycle. There is also likely a subtler proal and vertical component for the function of this muscle as well, although to a weaker to extent due to its orientation.

FIGURE 4.19. *Heterodontosaurus* skull in left lateral view highlighting m. pterygoideus ventralis. See Fig. 4.2 for scale bar.

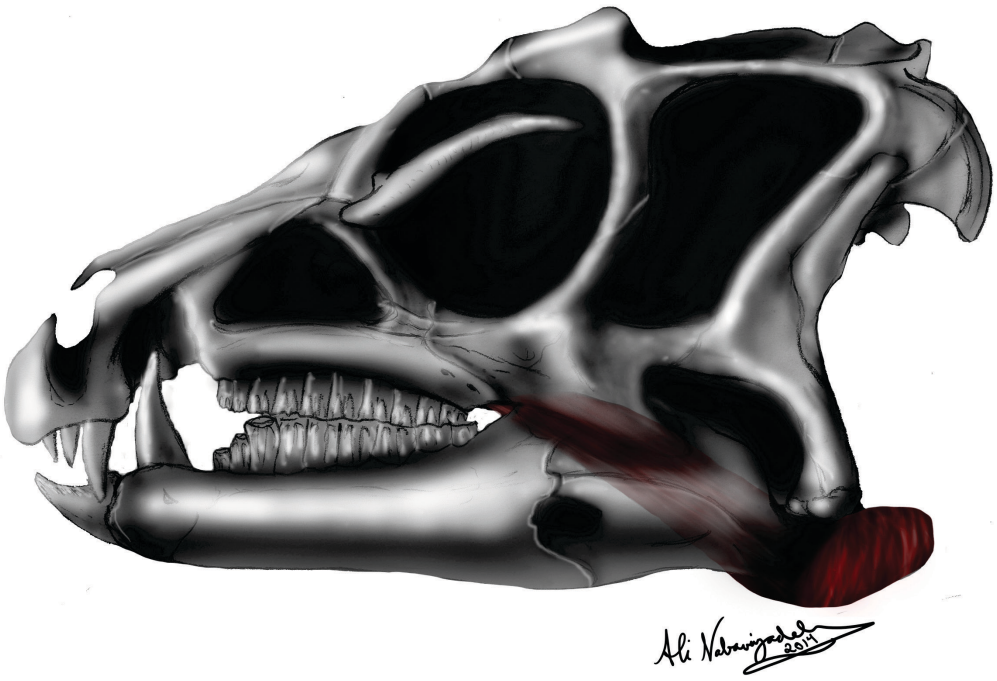

M. pterygoideus dorsalis

M. pterygoideus dorsalis (mPTD; Fig. 4.20) originated on a rostrocaudally-elongate, depressed region on the dorsal aspect of the pterygoid bone flange and ectopterygoid bone. It extended caudoventrally around the medial aspect of its respective mandibular corpus. The insertion was likely on the medial aspect retroarticular process

on the surface of the prearticular ventral to the glenoid. Its action, along with m. pterygoideus ventralis, probably contributed to the medial movement, restriction, or stabiliation of the mandibular corpus on which is attached, depending on which side of the jaw is being used in mastication.

FIGURE 4.20. *Heterodontosaurus* skull in left lateral view highlighting m. pterygoideus dorsalis. See Fig. 4.2 for scale bar.

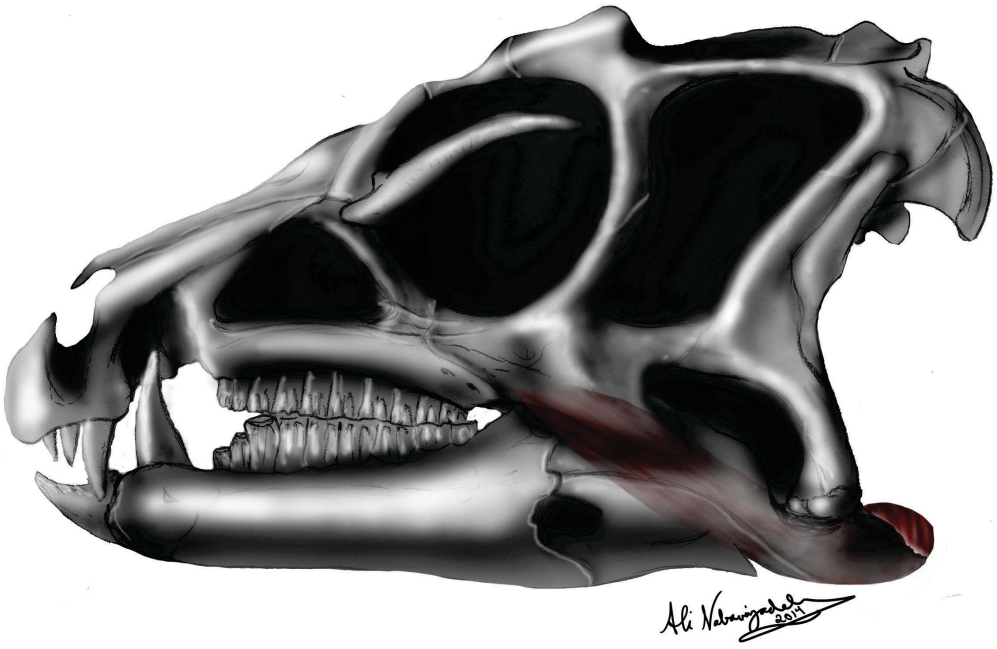

2D LEVER ARM ANALYSES

2D lever arm analysis of relative bite force (RBF) was done on one *Heterodontosaurus* specimen and was compared with other ornithischian (see Chapters 5 and 8). See Table 4.4 for RBF results at the predentary as well as the rostral, middle, and caudal teeth.

TABLE 4.4. Actual RBF value across heterodontosaurid tooth row.

Genus	Spec. #	Input Lever Angle in ° (mAMEP)	Predentary RBF	Rostral Tooth RBF	Middle Tooth RBF	Caudal Tooth RBF
Heterodontosaurus	SAM-PK-K337	51.28	0.378	0.449	0.588	0.842

RBF values were plotted in a line graph to visualize the general trend of bite forces throughout the jaw (Fig. 4.21).

Mechanical Advantage

Heterodontosaurus, the representative heterodontosaurid genus in this lever arm study, shows relatively moderate relative bite forces (RBFs) along the tooth row and a higher predentary RBF compared to most thyreophorans (see Chapter 5) and many basal genera of both Ornithopoda and Marginocephalia (see Chapter 8). It is plausible that this higher predentary RBF and moderate RBF across the tooth row is an adaptation concurrent with the formation of caniniform dentary dentition as well as highly

specialized crushing teeth. Lower RBFs are shown throughout thyreophorans as a whole compared to the rest of Ornithischia.

FIGURE 4.21. Plot of *Heterodontosaurus* RBF values across tooth row.

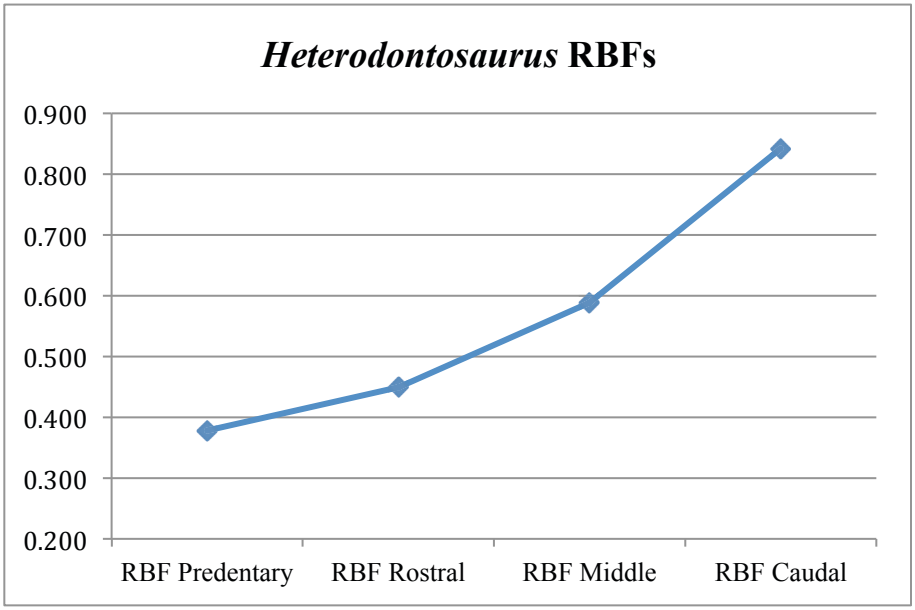

Perturbation analysis (Otten, 1983; 1985) results are shown below with RBF values with both the coronoid eminence removed and the jaw joint raised to the level of the maxillary tooth row:

TABLE 4.5. Hypothetical RBFs across heterodontosaurid tooth row with coronoid process removed (left, black) and articular raised to level of the tooth row (right, white).

Genus	Spec. #	Input Lever Angle in ° (mAMEP)		Predentary RBF		Rostral Tooth RBF		Middle Tooth RBF		Caudal Tooth RBF	
Heterodontosaurus	SAM-PK-K337	52.69	51.28	0.364	0.284	0.432	0.343	0.566	0.454	0.809	0.671

Results show that RBF values at all tooth positions are hypothetically lower if the jaw joint is raised to the level of the tooth row than they are it is if the coronoid was removed. This suggests that lowering the jaw joint ventrally has a larger influence on mechanical advantage than increasing the elevation of the coronoid eminence process, thereby indicating that it is the most influential factor in early ornithischian evolution, given the basal status of heterodontosaurids. See Chapter 8 for evolutionary implications.

Chapter 5: Thyreophoran Craniomandibular Anatomy

Thyreophoran mandibular morphology is discussed in depth below with emphasis on functional interpretation (see Table 5.1 for specimens examined; see Fig. 5.1 for phylogenetic relationships among genera). As some of the postdentary elements do not show as much functional significance other than as a rigid unit, only a brief discussion of each postdentary bone is given below to illustrate the general shape of this region. Cranial elements with direct contact to the mandible (i.e., the premaxilla, maxilla, and quadrate) provide functional implications in thyreophoran jaw mechanisms and are also described for further completeness. Cranial elements holding significance with regards to the jaw adductor musculature are described as needed in the Jaw Musculature section.

FIGURE 5.1. Phylogeny of Thyreophora. A, Phylogeny from basal Thyreophora showing all of Stegosauria and its divide with Ankylosauria (Butler et al., 2008; Maidment, 2010); B, Phylogeny of Ankylosauria (Thompson et al., 2012).

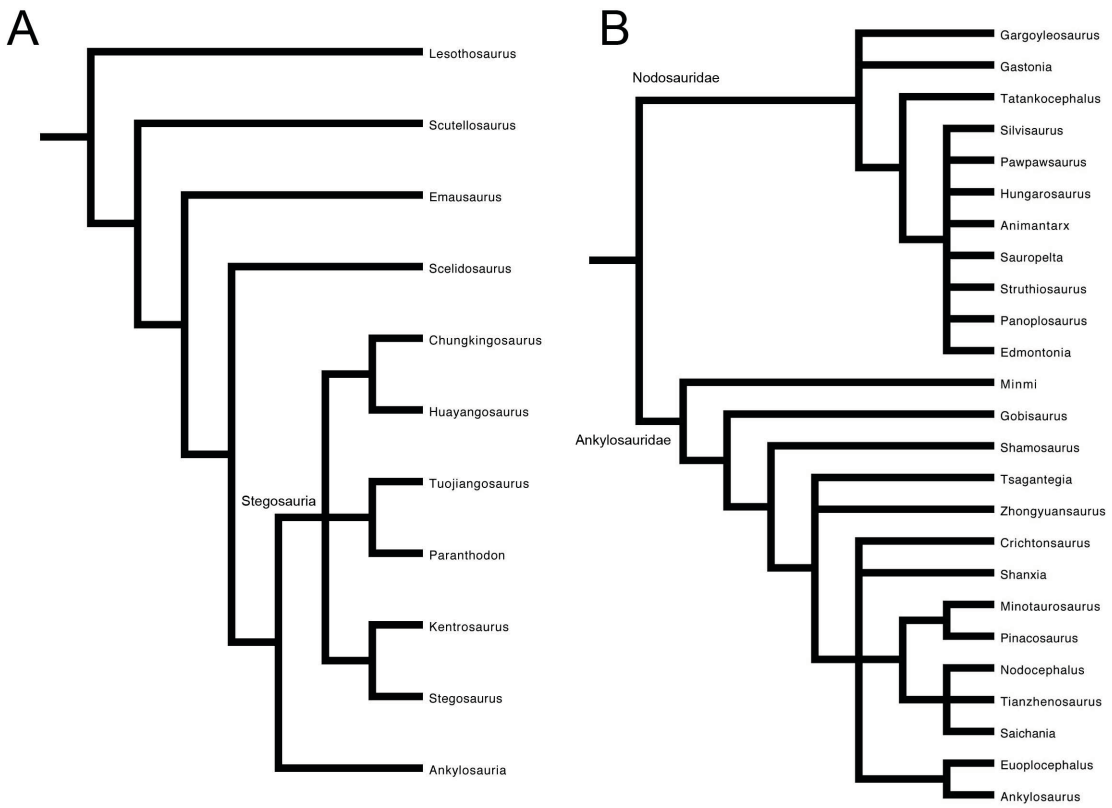

TABLE 5.1. Thyreophoran specimens examined in this study. (Note: most specimens were examined by the author, except for *Huayangosaurus*, which was examined from detailed photographs taken by Han Feng-Liu and provided by Karen Poole.)

Taxon	Specimen	Elements
Basal Thyreophora		
Lesothosaurus	BMNH R8501	Complete jaw and skull
	BMNH R11956	Partial jaw and skull
	BMNH R2422	Partial r. dentary
Scelidosaurus	BMNH R1111	Paired jaws (no predentary)

		and skull
Scutellosaurus	BMNH R11534 (Cast)	Partial l. dentary
Stegosauria		
Huayangosaurus	IVPP V6728	Complete jaw and skull
Regnosaurus	BMNH R2422	Partial r. dentary
Stegosaurus	CMNH 106	R. dentary; quadrate; partial skull
	CMNH 41681	L. jaw ramus
	USNM 481111 (Cast)	Complete jaw and skull
	USNM 4934	Complete jaw and skull
	USNM 4935	Partial r. dentary; skull
	ROM 60192 (Cast)	Complete jaw and skull
Ankylosauria		
Ankylosaurus	AMNH 5214	Complete jaw and skull
Edmontonia	AMNH 5337	Complete jaw and skull
	USNM 11868	R. dentary; skull
Euoplocephalus	ROM 788	Skull
	AMNH 5405	Predentary; r. jaw ramus; skull
	AMNH 5403	Predentary; paired jaws
Gastonia	Cast	Skull

Panoplosaurus	ROM 814	Partial skull
	ROM 1215	L. dentary; skull
	TMP 1981.00.03 (Cast)	Complete jaw and skull
Pawpawsaurus	Cast	Skull
Pinacosaurus	AMNH 6523	Complete jaw and skull
	ZPAL MgD-II/1 (Cast)	Complete jaw and skull
Sarcolestes	BMNH R2682	Partial l. dentary
Silvisaurus	KUVP 1348	L. dentary; skull

OSTEOLOGICAL DESCRIPTION: BASAL THYREOPHORA

The following descriptions were based on my examination of specimens. See also Colbert 1981; Haubold (1990), Sereno (1991), Barrett (2001), and Norman et al., 2004 for further descriptions of this paraphyletic clade.

FIGURE 5.2. Basal thyreophoran cranial material in right lateral view. A, *Lesothosaurus* (based on BMNH R8501); B, *Scelidosaurus* (based on BMNH R1111). Scale bars = 1 cm.

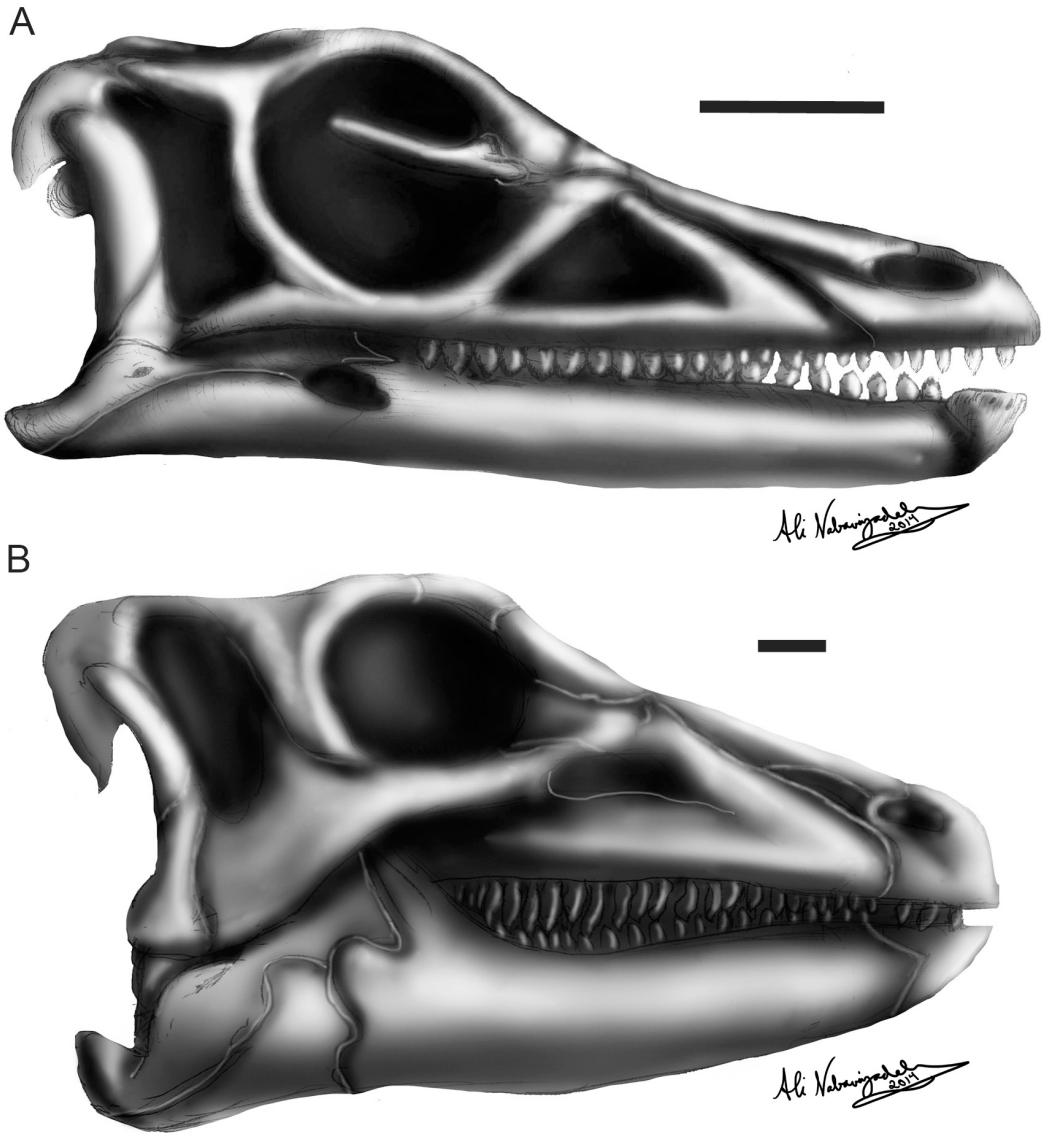

Cranium

Basal Thyreophora is a paraphyletic group, including *Lesothosaurus* (Fig. 5.2A; 5.3), *Scelidosaurus* (Fig. 5.2B), *Emausaurus*, and *Scutellosaurus* (Norman et al., 2004; Butler et al., 2008). Like many small-bodied, bipedal herbivorous dinosaurs, their crania are somewhat elongate and triangular in dorsal view. *Lesothosaurus* (e.g., BMNH

R8501) has the most slender skull of the four taxa, while *Scelidosaurus* (BMNH R1111) and *Emausaurus* (Haubold, 1990) have a relatively deeper occiput caudally. Complete cranial material of *Scutellosaurus* has not been described (Colbert, 1981). Basal thyreophorans tend to have a narrow, triangular palate in ventral view that tapers medially at the rostral tip. The entire palate in *Scelidosaurus* (BMNH R1111; Barrett, 2001) shows both vomers are fused at the midline to create the nasal passages.

Basal thyreophorans have large, oval orbits with an obliquely angled, narrow, rectangular infratemporal fenestra. The antorbital fenestra is prominent and triangular in *Lesothosaurus* (BMNH R8501; Sereno, 1991), dorsoventrally narrower in *Emausaurus* (Haubold, 1990), and minute or almost non-existent in *Scelidosaurus* (BMNH R1111). In *Lesothosaurus*, the jugal has a straight lower edge that runs ventral to the orbit to where it articulates with the quadratojugal caudally. In *Scelidosaurus* and *Emausaurus* (Haubold, 1990), the jugal is narrow beneath the orbit but then, just caudal to the orbit, abruptly tapers ventrally to eventually articulate with the quadrate caudoventrally. The jaw joint is offset just ventral to the tooth row, as in many ornithischians. The paroccipital processes are prominent, expanded, and squared-off distally, with a lateral orientation with respect to the occiput in caudal view.

FIGURE 5.3. *Lesothosaurus* cranium in left lateral view (generalized). Abbreviations: aof, antorbital fenestra; f, frontal; itf, infratemporal fenestra; la, lacrimal; j, jugal; m, maxilla; n, nasal; or, orbit; p, palpebral; pa, parietal; pf, prefrontal; pm, premaxilla; po, postorbital; pop, paroccipital process; pt, pterygoid; q, quadrate; qj, quadratojugal; sq, squamosal; stf, supratemporal fenestra. Scale bar = 1 cm.

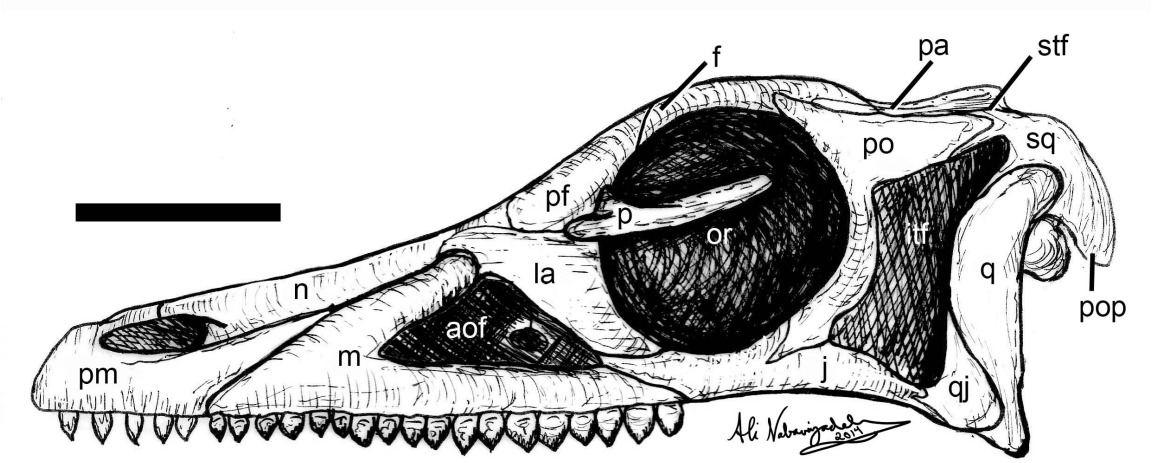

Premaxilla—The most complete basal thyreophoran premaxillae have been described in *Lesothosaurus* (Sereno, 1991), *Emausaurus* (Haubold, 1990), and *Scutellosaurus* (Colbert, 1981). In ventral view, the premaxillae in basal thyreophorans normally meet at the midline to form a flat rostral palate (Fig. 5.4). In lateral view, the oral margin of the premaxilla in *Lesothosaurus* and *Emausaurus* is straight and level with the ventral edge of the maxillary. This oral margin is rugose at the tip, suggestingindicating the presence of a keratinous beak covering it from tip to the first tooth premaxillary tooth crown in life. The premaxilla has a very small narial process dorsal to the nostril and an elongate caudolateral process ventral to the nostril that fits between the nasal and maxilla. This process is more blunt in *Emausaurus*, which also has a blunter snout relative to the elongate and narrow snout in *Lesothosaurus*. *Lesothosaurus*, *Scutellosaurus*, and *Emausaurus* are all known to possess premaxillary dentition, which is described below in the Dentition section.

FIGURE 5.4. *Lesothosaurus* (BMNH R8501) premaxilla palatal view, with premaxillary dentition visible (see Dentition section below). Scale bar = .5 cm.

Maxilla—The maxilla is bordered by the premaxilla rostrally and dorsally, the palatine and vomer medially, the ectopterygoid caudomedially, and the lacrimal and jugal caudodorsally. In *Lesothosaurus* (BMNH R8501; R11956), *Scelidosaurus* (BMNH R1111), and *Emausaurus* (Haubold, 1990), the maxilla is deeply triangular and flat in lateral view, with the antorbital fenestra bound by it rostrally and ventrally, except in *Scelidosaurus*, where the antorbital fenestra is small and narrow. The maxillary tooth row runs along the ventral margin of the maxillary body. *Lesothosaurus*, *Emausaurus*, and *Scutellosaurus* (Colbert, 1981) have a relatively straight to slightly lingually bowed maxillary tooth row in ventral view while the tooth row of *Scelidosaurus* is bowed lingually to a much greater degree (Fig 5.5), like its dentary counterpart (see below). The maxillary tooth rows are subparallel to each other in ventral view, with the mesial dentition closest in proximity to one another. The medial alveolar margin is somewhat thickened because of the presence of dentition. A slightly medially inset tooth row with

an overhanging dorsal maxillary ridge, characteristic of most ornithischian dinosaurs, is known to be present in *Scelidosaurus* and *Emausaurus*, but absent in *Lesothosaurus*. See Dentition section below for a description of dental morphology in basal thyreophorans.

FIGURE 5.5. *Scelidosaurus* (BMNH R1111) right maxillary tooth row (palatal view) showing medially bowed dentition. Ruler units in cm.

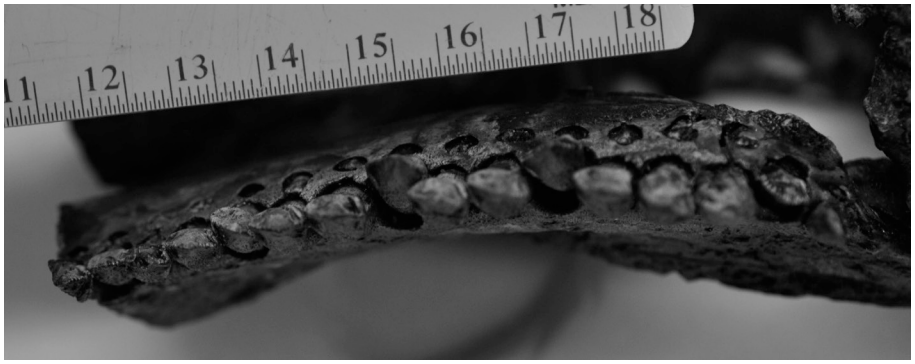

Quadrate—The quadrate is known in *Lesothosaurus* (BMNH R8501) and *Scelidosaurus* (BMNH R1111) among basal thyreophorans. The head of the quadrate is rounded at its margins and fits between two ventrally-oriented processes (pre- and postquadratic processes) in a deep concavity on the ventral margin of the squamosal. According to Barrett (2001), the median skull roof elements in *Scelidosaurus*, such as the parietals, frontals, nasals, as well as the dorsal head of the quadrate, were fused together tightly so as to prevent any bending in this part of the skull. The shaft is tall and approximately dorsoventrally straight with a small degree of rostral bowing, seen most in *Scelidosaurus*. It is mediolaterally compressed and twisted around its long axis. The quadrate is stabilized by rostrally oriented wings contacting the quadratojugal laterally and the pterygoid more internally. The ventral head of the quadrate is generally

mediolaterally expanded, with taxa such as *Scelidosaurus* having an almost bicondylar head, with the medial condyle dorsoventrally narrower than the distally flatter lateral condyle (Fig. 5.6). The mandibular condyles are ventrally offset relative to tooth row, causing a ventrally offset jaw articulation in life.

FIGURE 5.6. Ventral head of left quadrate in *Scelidosaurus*, showing bicondylar head in caudal view.

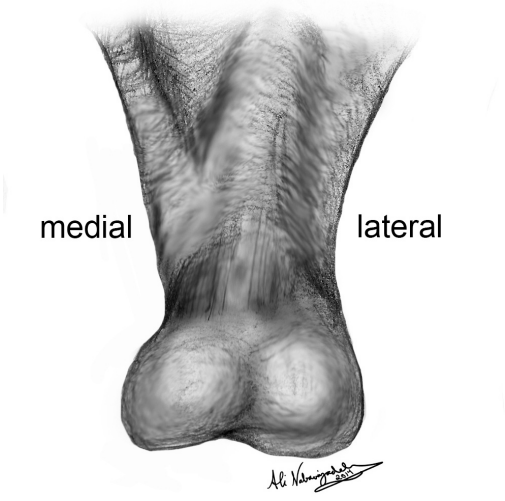

Predentary

Predentary morphology is known only in *Lesothosaurus* (BMNH R8501; Fig. 5.7; 5.8), the most basal among known members of Thyreophora. It is a single, small element, likely covered by a keratinous rhamphotheca, which united both dentaries at their rostral ends and thereby stabilized the mandibular symphysis during the act of ingesting vegetation. In ventral view, the predentary is shaped like a short-shafted arrow. In dorsal

view, the outer dorsal rim of the predentary forms a sharp ridge laterally and the main body of the predentary is shallowly cupped mediolaterally.

FIGURE 5.7. Restored *Lesothosaurus* predentary (after Sereno, 1991). A, lateral view; B, dorsal view.

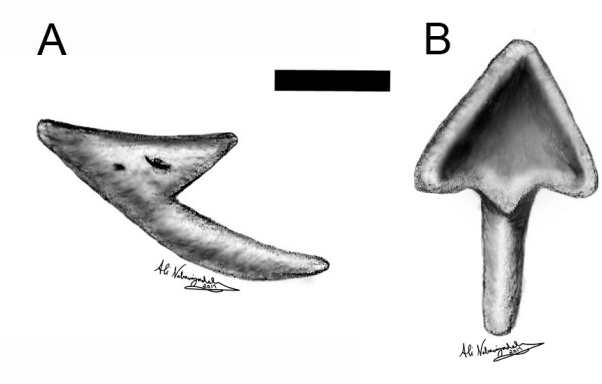

The predentary has a elongate median ventral process directed caudally that cradles the rostroventral ends of both dentaries ventrally, as well as a shorter, caudolaterally projecting process that articulates with the rostrodorsal edge of each respective dentary. The median ventral process is broad and comes to a blunt point caudally and possesses shallow pits on its dorsal surface for articulation with the surface at the rostroventral tip of each dentary. The ventral process has a curved articulation with the ventral aspect of the dentaries, creating a cradle for the dentaries together, although there is freedom for slight lateral excursion of the dentaries because of its narrow articulation.

FIGURE 5.8. *Lesothosaurus* (BMNH R8501) predentary with rostral end of left dentary. Abbreviations: d, dentary; p, predentary. Ruler units in cm.

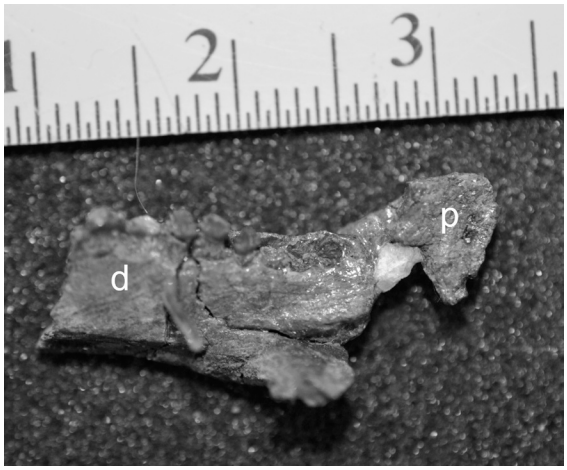

The two shorter, caudolaterally-oriented processes are triangular and taper distally, adjoining with the rostrodorsal edge of each respective dentary at a sharp, grooved surface on the caudoventral edge of the predentary, leaving gaps between the predentary and dentary at the suture (Fig. 5.9). Sereno (1991) interpreted this loose articulation as a sign of slight mobility of each dentary at the predentary-dentary symphysis and potential allowance of controlled "twisting" of each mandibular corpus around its long axis during feeding. He also noted that this joint could have been synovial; however, due to the nonexistence of a symphyseal synovial joint in the extant phylogenetic bracket of Archosauria, it can conservatively only be labeled as a ligamentous or fibrocartilagenous joint until further studies portray otherwise (Thulborn, 1970; Sereno, 1991). The predentary bone is unknown in *Scelidosaurus*, *Emausaurus*, and *Scutellosaurus*.

FIGURE 5.9. *Lesothosaurus* predentary-dentary articulation, with visible gaps between the elements (after Sereno, 1991). Abbreviations: d, dentary; p, predentary.

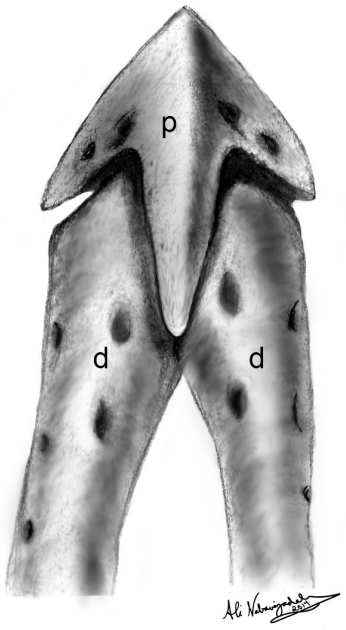

FIGURE 5.10. *Lesothosaurus* mandible (generalized). A, lateral view; B, medial view. Abbreviations: a, angular; ar, articular; c, coronoid; d, dentary; p, predentary; pa, prearticular; rap, retroarticular process; sa, surangular; sp, splenial. Scale bar = 1 cm.

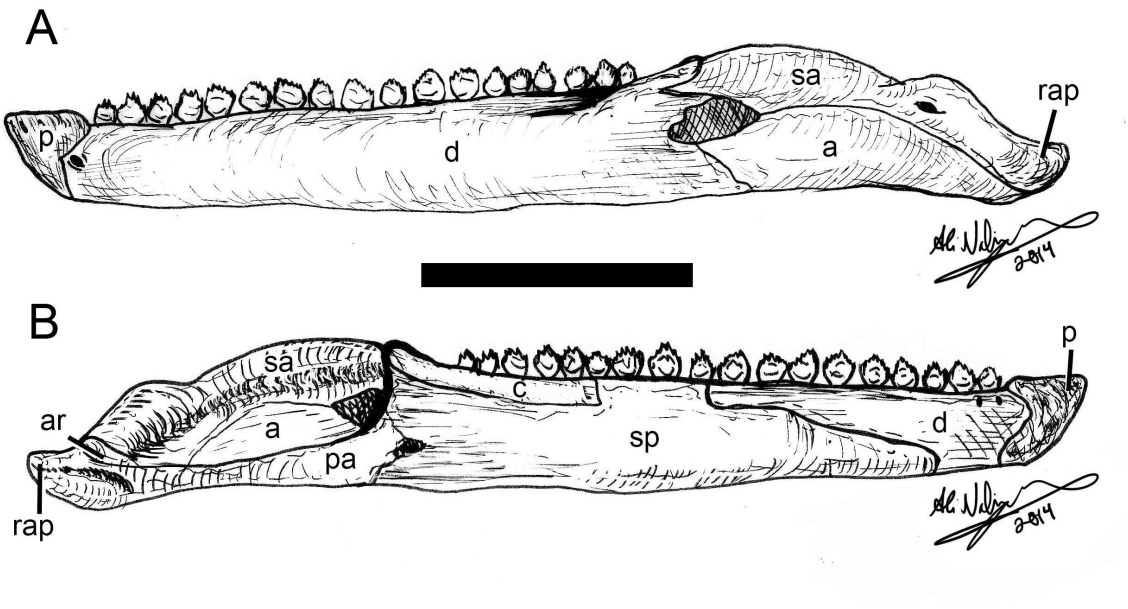

FIGURE 5.11. *Scelidosaurus* (BMNH R1111) left mandibular ramus. A, lateral view. B, medial view. Scale bar = 2 cm.

Dentary

The dentary (Fig. 5.10; 5.11) is the largest element in the thyreophoran mandible of basal thyreophorans. It articulates with the predentary and the opposite dentary rostrally, the splenial medially, and the surangular, angular, coronoid, and prearticular splenial caudally. In lateral view, the dentary is elongate and expands dorsoventrally at its caudal end.

The dentary is variable in morphology depending on the taxon. In *Lesothosaurus* (BMNH R8501) and *Scelidosaurus* (BMNH R1111), the ventral margin of the dentary is straight with only a slight ventral bowing at mid-length (Fig. 5.11).

In *Emausaurus* (Haubold, 1990), and to a much lesser extent in *Scutellosaurus* (Colbert, 1981), the ventral margin of the dentary is tapered ventrally at both its rostral and caudal ends, creating a dorsal bowing of the dentary at mid-length. Some basal thyreophorans, such as *Scelidosaurus* (BMNH R1111) exhibit the beginnings of a buccal emargination with a medially-inset tooth row for supposed "cheeks" or other form of buccal soft tissue (Fig. 5.12; see also Barrett, 2001). *Lesothosaurus*, *Scutellosaurus*, and *Emausaurus* arguably have little to no buccal emargination, although the material known for *Scutellosaurus* is not adequate to make such an assertion. The dentition in these three taxa is more marginally placed along the dorsal edge of the dentary, which has a relatively flat lateral surface. This dorsal ridge ascends dorsally to reach the coronoid eminence, which is rather short in all taxa relative to more derived ornithischians.

FIGURE 5.12. *Scelidosaurus* right dentary (dorsal view) showing medial curvature of tooth row and buccal emargination. Abbreviations: em, emarginated region.

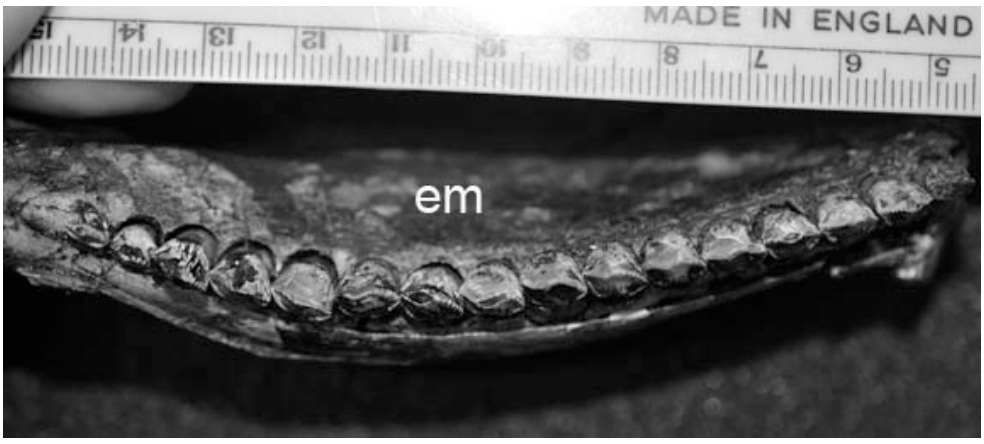

The rostral part of the dentary is dorsoventrally expanded and mediolaterally flattened, but ends in a somewhat rounded rostral edge that contacts its counterpart

medially, securing the dentary-dentary suture and the predentary rostrally and laterally. In dorsal view, the dentaries articulate in a v-shape, as the dentaries are at an acute angle relative to one another. Slight rugosity is apparent at its rostral edge indicating that each dentary the dentaries rubbed against their counterpart in life. A large foramen on the lateral surface of the rostral tip of the dentaries supplied neurovasculature (likely the mental artery and nerve as seen in extant archosaurs) rostrally to the predentary, as did a concentration of other smaller foramina caudal to it. These foramina likely supplied both the predentary and the skin covering the more rostral surface of the dentaries themselves. The alveolus-bearing dorsal ridge of oral margin of the dentary is relatively straight in *Lesothosaurus*, *Emausaurus*, and *Scutellosaurus* and the dentaries are somewhat sub-parallel to each other. In contrast, this dorsal edge is bowed medially in *Scelidosaurus*. See Dentition section below for a description of dental morphology in basal thyreophorans.

The rostral portion of the coronoid eminence is composed of the dentary as it extends dorsally just caudal to and in line with the dentition. The remainder of the coronoid eminence is composed of the coronoid bone, coming to a point (at the apex) of the coronoid eminence (with the exception of *Emausaurus*, with no described coronoid bone), and by the surangular, gradually descending caudally at a more shallow angle than rostral dentary portion. In caudal view, the mandibular canal is large and runs from immediately ventral to the caudal surface of the coronoid process down to the ventromedial aspect of the dentary body ventral to the dentition. Caudally, the coronoid eminence is continuous with the adductor fossa where the jaw adductor musculature inserts. The inferior alveolar branch of the trigeminal nerve (CN V_3), which would have

been found in the mandibular canal, innervated the dentition as well as ultimately the skin around the mandible and the keratinous rhamphotheca that sheathed the predentary. The caudal aspect of the dentary encapsulates and articulates with the coronoid, surangular, angular, and prearticular. The caudal margin of these elements as well as the splenial form the caudal boundaries of the mandibular canal.

Coronoid

The coronoid bone (Fig. 5.10) is described in all basal thyreophoran taxa except *Emausaurus* (Haubold, 1990). It is a slender sheet of bone that forms the apex of the medial coronoid eminence, extending just caudal to the dentary and continuous with the slightly descending dorsal margin of the surangular, forming a shallow coronoid eminence altogether. It typically curves rostroventrally to the alveolar margin of the dentary. The dorsal-most aspect of the coronoid is rugose, indicative of adductor muscle insertion.

Splenial

The splenial (Fig. 5.10) is a thin, sheet-like bone that covers the ventromedial aspect of the dentary and the caudal portion of the mandibular canal with a dorsoventrally broad expansion before it abruptly becomes thinner as it extends rostrally. The caudal portion of the splenial bifurcates where it articulates with the coronoid dorsally and the angular and prearticular ventrally.

Angular

The angular (Fig. 5.10) is an elongate, narrow, and laterally-compressed bone ventral to the mandibular canal and caudal to the dentary along its caudoventral margin, with an external mandibular fenestra between the two elements. The articular bone sutures with the surangular caudodorsally to create the ventromedial edge of the mandibular corpus caudally. The angular forms the floor of the adductor chamber and articulates with the splenial rostrally and the articular caudodorsally. The angular also acts as the ventral brace of the articular glenoid and it, along with the surangular and prearticular, helps brace the articular for sturdy articulation with the quadrate.

Surangular

The surangular (Fig. 5.10) forms the dorsal margin of the mandible and the continuation of the coronoid eminence caudal to the dentary and coronoid bones. It has a thick dorsal margin rostral to the jaw joint, contacting the dentary and coronoid rostrally, and forms the lateral margin of the adductor fossa for the jaw adductor musculature as well as the dorsolateral margin of the mandibular canal. The ventral portion of the surangular contacts the dentary at a suture ventral to the coronoid eminence but immediately dorsal to the small external mandibular fenestra formed by the dentary and angular. The surangular curves contacting the prearticular rostral to the articular and forms the ventrolateral lip of the craniomandibular glenoid as well as the lateral aspect of the retroarticular process caudal to this glenoid.

Prearticular

The prearticular (Fig. 5.10) is a gracile element covering the caudomedial portion of the mandible and contacting the splenial as it extends rostrally. It forms the floor of the adductor fossa in medial view as it meets the surangular immediately rostral to the articular glenoid. It envelops the articular medially and extends caudally forming the ventromedial aspect of the retroarticular process immediately caudal to the glenoid.

Articular

The articular (Fig. 5.10; 5.13) is square in dorsal view and is held in place by the surangular laterally, the angular ventrally, and prearticular medially. It forms a slightly concave glenoid which is rostrocaudally as well as the transversely expanded for articulation with the bicondylar ventral head of the quadrate inside the synovial cavity in life (Fig. 5.13; Barrett, 2001). The margins surrounding the glenoid are raised dorsally into ridges, created by the articular medially and surangular laterally. The jaw articulation is ventrally offset from the level of the tooth row.

FIGURE 5.13. Caudal aspect of *Scelidosaurus* right mandible with indication of where the quadrate meets the articular glenoid surface at the craniomandibular joint. Abbreviations: ar, articular surface; q, quadrate.

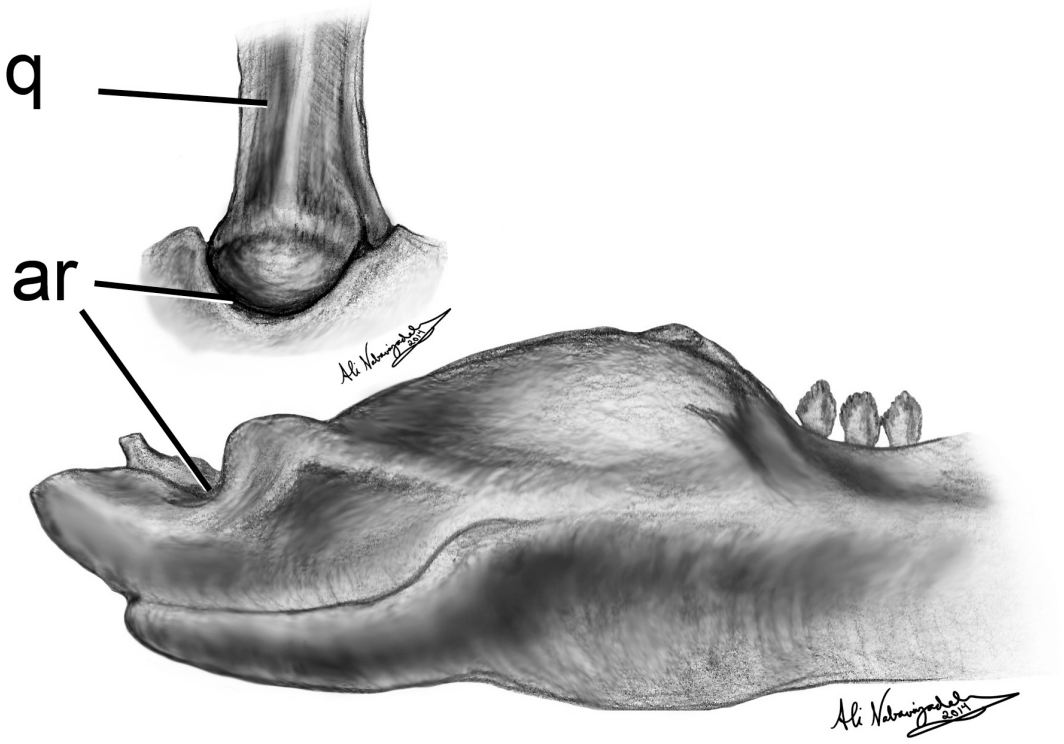

Dentition

Lesothosaurus (BMNH R8501), *Scutellosaurus* (Colbert, 1981), and *Emausaurus* (Haubold, 1990) are all known to possess premaxillary teeth, with six tooth positions in *Lesothosaurus* and *Scutellosaurus* and five tooth positions in *Emausaurus*. The premaxillary teeth (Fig. 5.14) are conical, lacrimiform, and are slightly recurved distally. They rested against the lateral edge of the keratinous rhamphotheca of the predentary in life.

FIGURE 5.14. *Lesothosaurus* left premaxillary tooth in first tooth position.

The maxillary dentition in basal thyreophorans is closely packed with mesiodistally spade-shaped teeth with apicobasal ridges running along the buccal and lingual surfaces (Fig. 5.15). These ridges form denticles at the apical ridges of the teeth. The wear facets on the teeth of *Scelidosaurus* are small at the apex of the teeth, unlike the dentary teeth described below (BMNH R1111; Barrett, 2001). *Lesothosaurus* had about 15 to 16 maxillary teeth, *Scelidosaurus* and *Scutellosaurus* (Colbert, 1981) had as many as 18 teeth, and *Emausaurus* (Haubold, 1990) had about 21 teeth.

FIGURE 5.15. *Lesothosaurus* left maxillary dentition in first four tooth positions.

The dentary teeth in basal thyreophorans often retain the primitive appearance of ornithischian teeth, unlike the unusually derived morphology of the more primitive heterodontosaurids. They are typically spade-shaped in labial and lingual views, with a

mesiodistally-expanded base that extends apically to a point; ridges run apicobasally along the lingual and labial surfaces that create denticles at the apical ridges (Fig. 5.16). Approximately seven round-to-pointed denticles are found at each apical tooth edge in *Lesothosaurus* (e.g., BMNH R8501), four to six denticles in *Emausaurus* (Haubold, 1990) and *Scutellosaurus* (Colbert, 1981), and six to nine denticles in *Scelidosaurus* (Barrett, 2001), usually with a single denticle present at the apex of the tooth crown. The root is narrow and columnar. In *Scelidosaurus*, the apex of the tooth is somewhat asymmetrical and the teeth posses a shelf, due to a buccal expansion at its base (Barrett, 2001).

The dentary tooth count in basal thyreophorans is variable. *Lesothosaurus* has between 11-14 teeth (BMNH R8501; Sereno, 1991), *Scelidosaurus* has at least 16 teeth (BMNH R1111; Barrett, 2001), *Scutellosaurus* (Colbert, 1981) has 18 teeth, and *Emausaurus* (Haubold, 1990) has 21 teeth, all of which are described below. The smaller tooth count in the most basal *Lesothosaurus* shows an increase in tooth number in more derived basal thyreophoran taxa, although the number is still quite variable among the three more derived of these basal taxa.

FIGURE 5.16. *Scelidosaurus* right dentary tooth.

OSTEOLOGICAL DESCRIPTION: STEGOSAURIA

The following descriptions were based on my examination of specimens. See also Gilmore (1914), Sereno and Dong (1992), Barrett (2001), and Galton and Upchurch (2004) for further descriptions of this clade.

FIGURE 5.17. Stegosaur skulls. A, *Huayangosaurus*; B, *Stegosaurus*. Right lateral view; Scale bars = 5 cm.

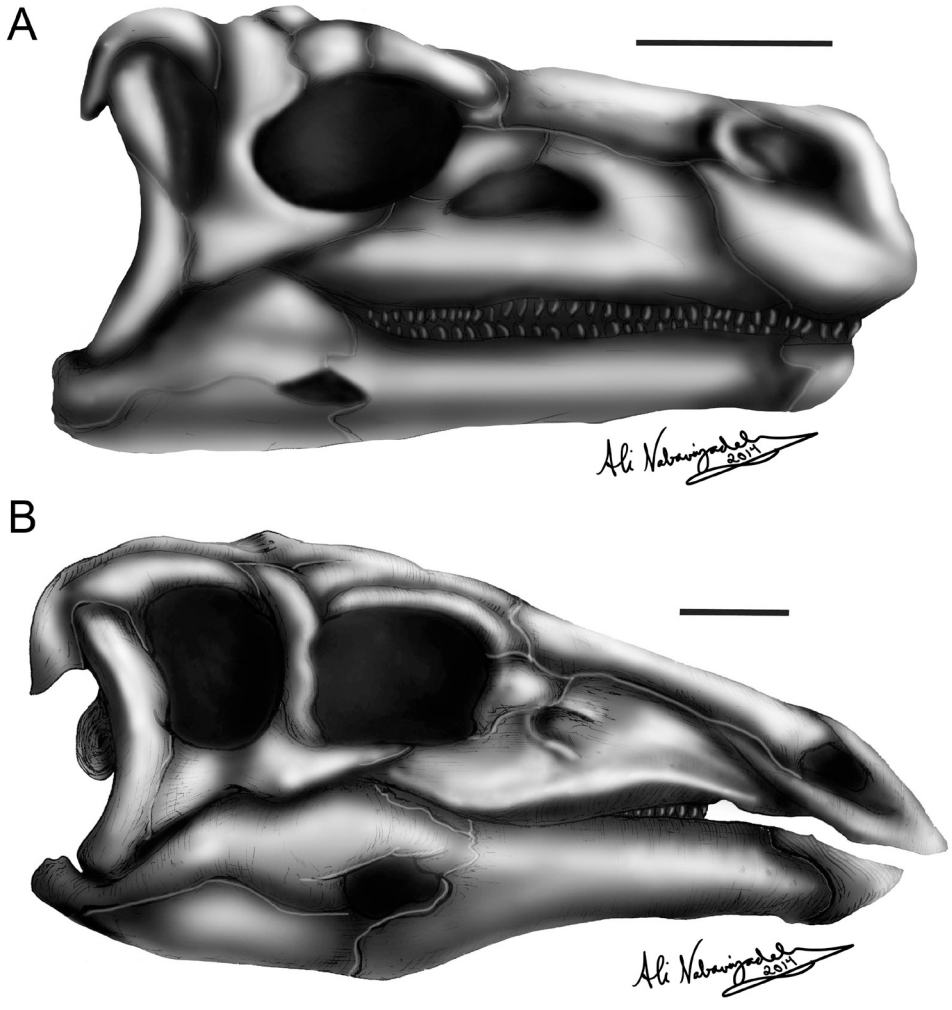

Cranium

Stegosaur skulls (Fig. 5.17; 5.18) are miniscule compared to the size of their postcrania and are generally elongate and slender in lateral view, tapering to a beaked snout rostrally, where the ventral angle is abruptly heightened at the level of the external nares. Stegosaurs have large, elliptical orbits that slightly taper rostrally. Caudal to the orbit is an infratemporal fenestra that is approximately square, except its caudodorsal corner is raised relative to its rostrodorsal corner. The antorbital fenestra is bounded by the maxilla, lacrimal, and jugal. It is triangular in *Huayangosaurus* (IVPP V6728; Sereno and Dong, 1992) and highly reduced or nonexistent in *Stegosaurus* (e.g., USNM 4934; Gilmore, 1914). The jugal is straight and level relative to the ventral edge of the rest of the skull and this straight edge is continuous with the quadrate, which has a ventral head extending below the level of the tooth row. The dorsal edge of the nasal is continuous with the tapering of the dorsal edge of the rest of the skull. The paroccipital processes are triangular and robust, angled laterally with respect to the occiput in caudal view.

FIGURE 5.18. *Stegosaurus* skull in left lateral view (generalized). Abbreviations: itf, infratemporal fenestra; la, lacrimal; j, jugal; m, maxilla; n, nasal; or, orbit; pa, parietal; pf, prefrontal; pm, premaxilla; po, postorbital; pop, paroccipital process; q, quadrate; sor, supraorbital; sq, squamosal; stf, supratemporal fenestra. Scale bar = 5 cm.

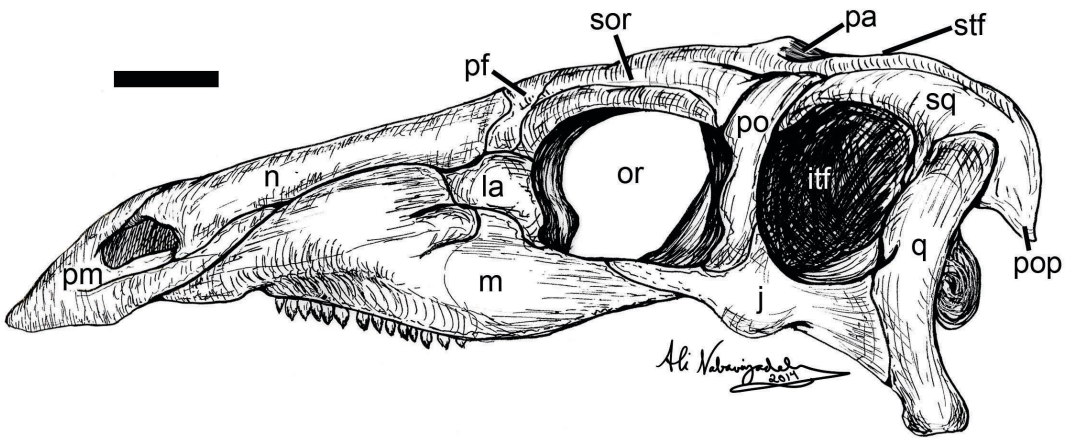

Premaxilla—Most stegosaur genera, including *Stegosaurus*, possess an edentulous premaxilla, with the exception of *Huayangosaurus* (see Dentition section below). The premaxillary teeth in *Huayangosaurus* (IVPP V6728) likely rested against the lateral surface of the keratinous rhamphotheca of the predentary of the mandible. The premaxilla in all stegosaur genera is dorsoventrally deepened caudally, with a straight oral margin that is slightly ventrally offset relative to the maxilla at the point of articulation. A caudodorsally-oriented long, thin process extends between the external naris and nasal bone and the maxilla, which combined create the muzzle. The oral margin of the premaxilla is thicker and rugose, with implications of being covered by a keratinous rhamphotheca that would have occluded with its counterpart covering the predentary. In *Miragaia*, the rostral tip of each premaxilla comes to a point and the rostrolateral margin of the premaxilla curves ventrally, which is unseen in other stegosaurs (Mateus et al., 2009). The lateral rim of the premaxilla outside of the three premaxillary teeth in *Huayangosaurus* is bulged and convex lateral to the alveoli. *Huayangosaurus* possesses a depression at the premaxillary-maxilla suture laterally,

while all other known stegosaurs do not show such a depression (Sereno and Dong, 1992). Ventrally, the premaxillary palate is flat and broad.

Maxilla—The maxilla is sutured with the premaxilla rostrally and dorsally, the palatine and vomer medially, the ectopterygoid caudally, and the lacrimal and jugal caudodorsally. In lateral view, it is flat and triangular, tapering ventrally at its rostral end. The dorsoventral height of the maxilla is relatively greater (creating a deeper snout) in *Huayangosaurus* (IVPP V6728), *Paranthodon* (Galton and Coombs, 1981), and *Chungkingosaurus* (Dong et al., 1983) than is seen in *Stegosaurus* (e.g., USNM 4934), which is relatively shorter, yet elongate rostrocaudally. Over 20 alveoli are present in the stegosaur mandible and they are variable in number depending on the taxon. Because *Huayangosaurus* has a longer tooth row, it typically has a few more teeth than the more derived *Stegosaurus* (see Dentition section below for tooth counts), although the exact number likely depends on its stage of growth. A series of dental foramina are presented just dorsal to the dentition on the medial and lateral sides. The bony lateral edge of the maxillary tooth row is exaggerated laterally to form a buccal shelf, with its tooth row consequently situated in a medially inset, emarginated position, with the dentition shifted ventrally. See Dentition section below for a description of stegosaur dental morphology.

Quadrate—The quadrate (Fig. 5.19) is a columnar, slightly rostrally-concave element, with its caudodorsally-oriented, small, rounded dorsal head sitting securely in the ventral cotylus of the squamosal in a ball-and-socket articulation. As the shaft of the quadrate bows ventrally (concavely), it gives off the rostrally-oriented pterygoid ramus that securely overlaps with the pterygoid bone. The ventral head of the quadrate is transversely expanded into two broadened and flat condyles, the lateral condyle

positioned higher than the medial, causing a ventrolaterally angled distal quadrate. This transversely-widened ventral head accommodates the widened expanse of the articular glenoid of the mandible described below.

FIGURE 5.19. *Stegosaurus* quadrate in lateral view. (CMNH 106). Scale bar = 2 cm.

Predentary

Among stegosaurs, predentary morphology (Fig. 5.20; 5.21) is known only in the basal *Huayangosaurus* (e.g., IVPP V6728; Sereno and Dong, 1992) and the derived *Stegosaurus* (e.g., USNM 4934), the predentary of both being preserved *in situ* and very similar in shape. In these forms, it is a single element, likely covered by a keratinous rhamphotheca, which united both dentaries at their rostral ends providing stabilization at the mandibular symphysis, as in *Lesothosaurus* (BMNH R8501; Sereno, 1991). The predentary possesses a caudally-oriented median ventral process cradling both dentaries ventrally and two shorter, caudolaterally-projecting processes articulating with respective

dentaries, much like that seen in *Lesothosaurus*. The median ventral process is relatively much more slender than in *Lesothosaurus*, ending in a sharper caudal point, and it possesses a flat surface for slight articulation between both dentaries at their rostroventral surfaces. Both caudolateral processes are dorsoventrally expanded and subtriangular and rest flatly upon the beveled ridges of the rostrodorsal ends of each dentary, rather than adjoining fully at the rostral edge of each dentary as in *Lesothosaurus*. The more slender ventral process and flatter, broader caudolateral processes made for a visibly looser articulation of the predentary with the dentary (Fig. 5.21) than that seen in *Lesothosaurus*, which might have implications on the potential for very minimal long axis rotation of the mandibular corpora at the predentary symphysis in stegosaurs.

FIGURE 5.20. *Stegosaurus* predentary. A, lateral view; B, dorsal view. Scale bar = 2 cm.

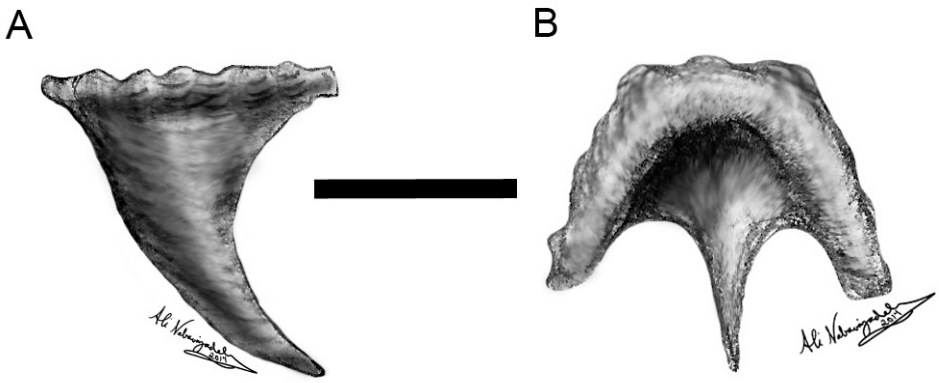

In superior view, the predentary is tapered and mediolaterally slightly u-shaped ventrally. The median rostral surface of the predentary is covered in many pits and neurovasculature foramina and, coupled with the rostral ends of the dentaries forms a more blunt, square-shaped rostral end of the mandible, in contrast to the more pointed

end of the mandible in *Lesothosaurus*. The rostral end of the predentary almost comes in contact with the tip of the rostroventral surface of the toothed premaxilla of the upper jaw in *Huayangosaurus*, creating only a slight overbite, based on the overhanging premaxillary teeth. In *Stegosaurus*, however, the toothless premaxilla rostrally overhangs the predentary much more significantly, creating a typically larger overbite (Gilmore, 1914; Barrett, 2001; Sereno and Dong, 1992).

FIGURE 5.21. Predentary-dentary articulation in *Stegosaurus* (USNM 4934) in ventral view. A, *in situ* specimen photo; B, illustration with gaps between elements visible. Abbreviations: d, dentary; p, predentary; pm, premaxilla. Scale bar = 2 cm.

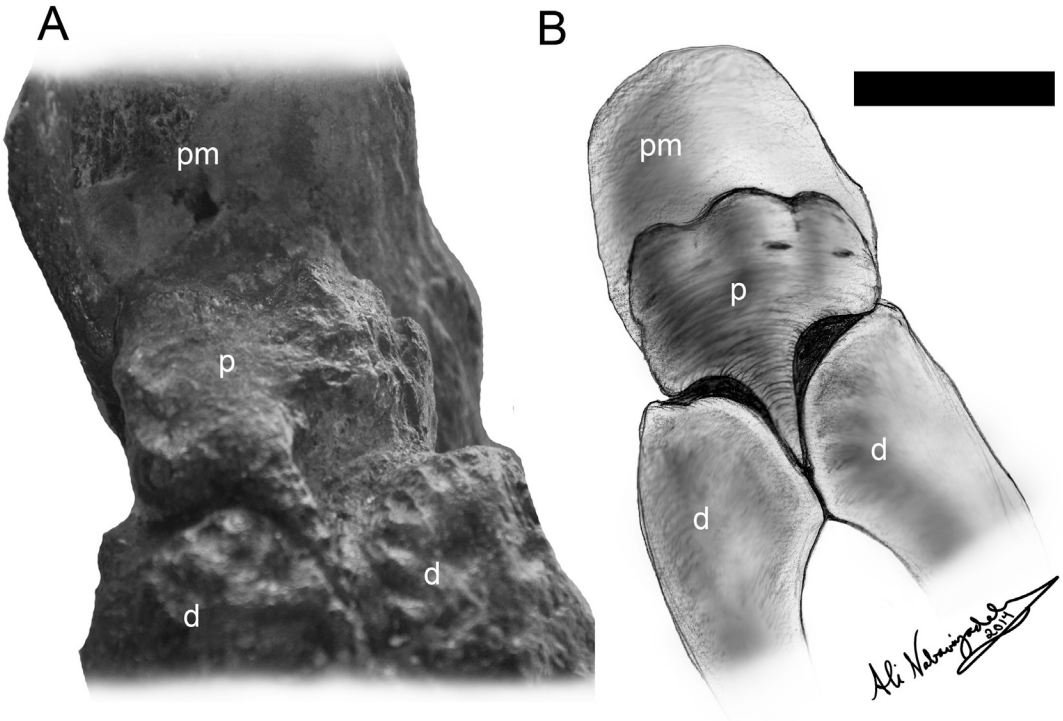

Dentary

The dentary (Fig. 5.22) is the largest element in the stegosaur mandible, articulating with the predentary and the opposite dentary rostrally, the splenial medially, and the surangular, angular, and coronoid caudally. It is elongate, narrow, and triangular in lateral view, with its greatest dorsoventral breadth at its caudal end.

FIGURE 5.22. *Stegosaurus* mandible (generalized). A, lateral view; B, medial view. Abbreviations: a, angular; ar, articular; c, coronoid; d, dentary; p, predentary; pa, prearticular; rap, retroarticular process; sa, surangular; sp, splenial. Scale bar = 5 cm.

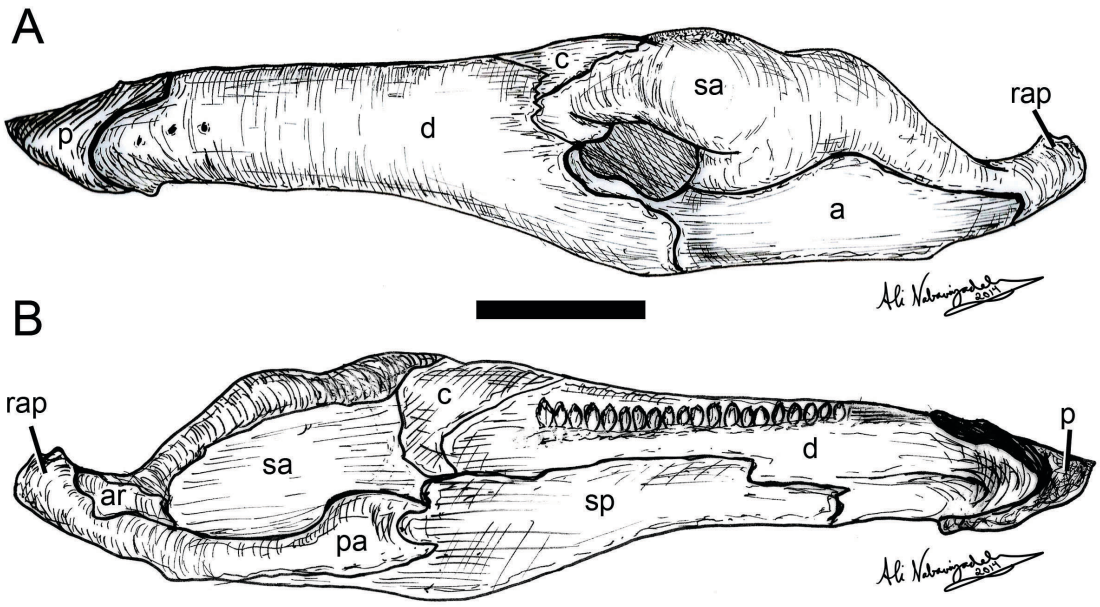

The dentary is mediolaterally-flattened element with a smooth lateral surface. In *Stegosaurus* (e.g., CMNH 41681; USNM 4934; 4935) and *Chialingosaurus* (Young, 1959), the greatest dorsoventral breadth and mandibular robustness is relatively greater

than that of most other stegosaurs, such as *Kentrosaurus* (Hennig, 1935), *Chungkingosaurus* (Dong et al., 1983), and *Tuojiangosaurus* (Dong et al., 1977), which have much narrower dentaries for their length. The ventral margin of the dentary is relatively straight throughout its length except at the rostral tip, where it curves ventromedially at the symphysis (Fig. 5.21). This ventromedial extension of the symphysis is especially exaggerated in *Kentrosaurus* (Hennig, 1935). In superior view, the symphyseal rim of the dentary is straight and rostrocaudally expanded. This rim adjoins its counterpart medially, forming a scoop-like morphology (Berman and McIntosh, 1986). The predentary articulates dorsal to the rostral tip of the adjoined dentaries, with the caudolateral processes of the predentary sitting inside of a depression in the thin rostrodorsal blade-like ridge caudal to the symphysis (Fig. 5.23) in *Stegosaurus* (unseen in *Kentrosaurus* [Hennig, 1935]) and the short ventral process of the predentary fit snugly between the dentaries at the symphysis. This articulation can especially be seen *in situ* in *Stegosaurus* (USNM 4934; Fig. 5.21), although with slight distortion offsetting the articulation of the predentary from its normal position. A minor gap surrounds the lateral articulation between the predentary and the dentaries that suggests the presence of a fibrocartilagenous or ligamentous material at this junction. This symphyseal morphology suggests the allowance of slight flexibility at this junction, although the amount of mobility would be minimal.

FIGURE 5.23. *Stegosaurus* (CMNH 41681) rostral end of dentary, highlighting symphyseal process and rostral ridge continuous with tooth row just caudal to it. Abbreviations: rr, rostral ridge; syp, symphyseal process. Ruler units in cm.

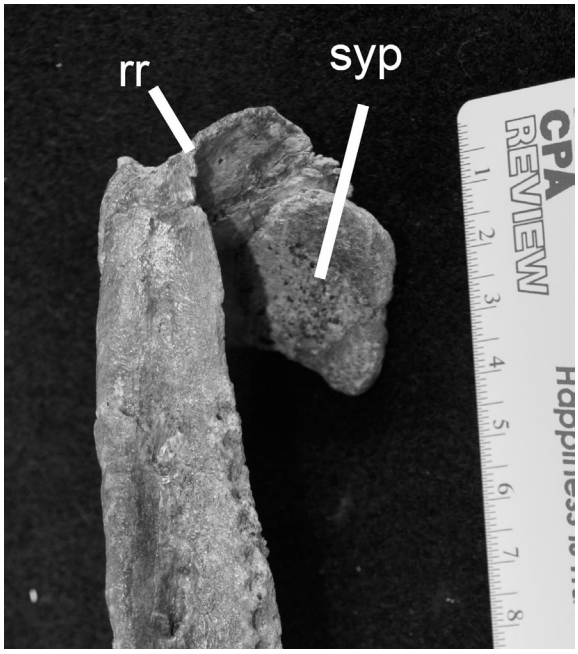

Along the dorsal rim of the stegosaur dentary, the tooth row is situated on the medial edge of a raised, mediolaterally-thickened ridge (CMNH 41681; Fig. 5.24). This ridge is slightly curved medially in superior view, creating a medially recurved tooth row occluding with the maxillary dentition during chewing. The alveoli are oriented primarily dorsomedially as the tooth row extends caudally, which is an unusual arrangement compared to many other ornithischian groups, except for the extreme case of ankylosaurs (see below). Although dentaries are only well-known in *Stegosaurus*, a partial dentary of *Kentrosaurus* (Hennig, 1935) shows it to have relatively larger alveoli, likely indicative of fewer teeth than in *Stegosaurus* (Berman and McIntosh, 1986; Barrett, 2001). As in the maxilla, tooth row length becomes shorter progressively through evolutionary time, with *Stegosaurus* having fewer teeth than the more basal *Huayangosaurus* (see Dentition section below). A series of dental foramina sits just ventral to the alveoli on the medial surface of the dentary. The medially arched, thickened dorsal rim and tooth row creates a

buccal emargination of the dentition in stegosaurs, as seen in most ornithischian dinosaur jaws (see *Stegosaurus* [CMNH 41681, USNM 4935] and *Regnosaurus* [BMNH 2422]).

FIGURE 5.24. *Stegosaurus* mandible CMNH (41681) in dorsal view highlighting buccal emargination and dorsally raised lamina as well as showing medially curved tooth row. Abbreviations: em, buccally emarginated area; lam, dorsal lamina buccal to tooth row. Scale bar = 2 cm.

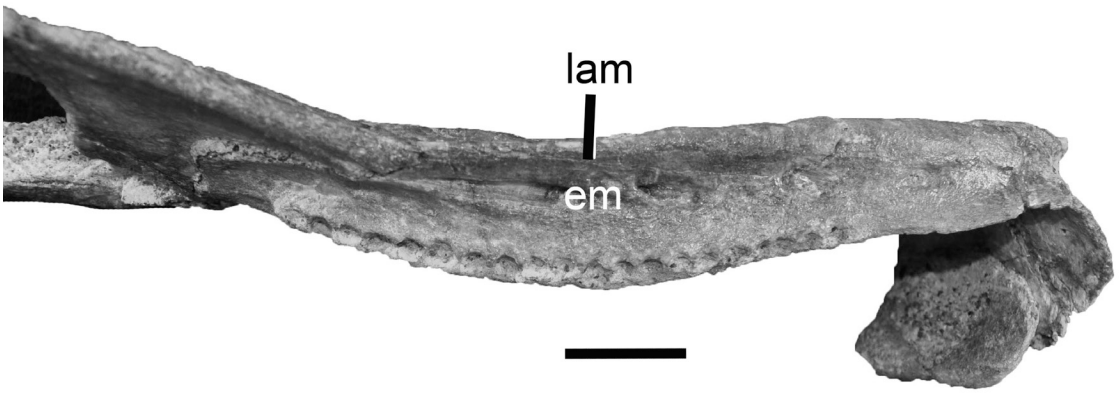

Stegosaurs are unique, however, in that the dorsally raised lamina extends off of the dorsal thickened ridge that extends rostrocaudally lateral to the dentition, hiding the distal portion of the tooth row in lateral view. In *Huayangosaurus* (IVPP V6728; Sereno and Dong, 1992), this dorsally-oriented lateral ridge extends caudally and is continuous with the coronoid eminence. Rostral to the tooth row, a dorsally raised, blade-like lip continues along the medial rim of the dorsal thickened ridge that continues to the predentary articulation, as seen in *Stegosaurus* (CMNH 41681). See Dentition section below for a description of stegosaur dental morphology.

The coronoid eminence in stegosaurs is made up primarily of the coronoid bone and surangular at its apex; however, the rostral region of the eminence is formed by the gradual dorsal rise of the dentary caudally in the same coronal plane as the tooth row. Although the dentary becomes dorsoventrally taller as it extends caudally, in lateral view, the caudodorsal aspect of the dentary ends much farther rostrally than its caudoventral extent, with a jagged caudal edge between the two points. Approximately mid-height, a thin sheet of bone of the caudal margin of the dentary extends a small tip contributing to the rostral extent of the elliptical external mandibular fenestra, created primarily by the surangular dorsally and the angular ventrally. Medially, the splenial covers the caudal two-thirds of the dentary just ventral to the alveoli. In caudal view, the isolated dentary (e.g., CMNH 41681**)** is hollow, creating the large elliptical mandibular fossa for the entrance of the mandibular canal and the inferior alveolar nerve (branch of CN V_3). The surrounding boundary of the mandibular fossa is a thin ridge throughout its circumference. The coronoid bone articulates with the caudodorsal rim of the dentary, the surangular contacts the dorsolateral rim, and the angular contacts the ventrolateral and ventral rim of the dentary.

Coronoid

The coronoid (Fig. 5.22) is a rather large triangular bone in medial view, with only a thin dorsal rim visible in lateral view. It forms the gradual ascent of the coronoid eminence from the alveoli of the dentary to just rostral to its apex made up of the surangular. The dorsal rim of the coronoid is a thin, blade-like ridge. It also forms a

portion of the rostromedial boundary of the adductor fossa, as seen in *Stegosaurus* (CMNH 41681; Berman and McIntosh, 1986).

Splenial

As in basal thyreophorans, the splenial in stegosaurs (Fig. 5.22) is a thin, sheet-like bone that covers the ventromedial aspect of the dentary and the caudal portion of the mandibular canal. It has roughly the same dorsoventral height throughout its length except for a caudally-extended ventral edge and a variably shaped rostral margin in medial view. It articulates with the angular and prearticular caudally.

Angular

The angular (Fig. 5.22) is an elongate, narrowed, laterally-compressed bone forming the ventral boundary of the mandibular canal and the adductor fossa, much like what is seen in basal thyreophorans. It is bordered dorsally by the surangular with a long, horizontal suture. Between the surangular and angular, a large, elliptical external mandibular fenestra is formed. The angular is also bordered by the dentary rostrolaterally, the splenial rostromedially, the prearticular dorsomedially, and helps brace the articular caudally for sturdy articulation with the quadrate.

Surangular

The surangular (Fig. 5.22) is a large bone that forms the apex of the coronoid eminence caudal to the dentary and coronoid bones. The apex of the coronoid eminence

is placed at approximately three-fifths of the length of the mandibular ramus (from rostral to caudal) in *Stegosaurus* (CMNH 41681; Berman and McIntosh, 1986). It has a roughened surface texture at the apex indicative of attachment site for the adductor musculature. It forms the caudolateral margin of the mandibular fossa and lateral boundary of the jaw adductor fossa. As described above, the surangular is bordered ventrolaterally by the angular and forms a large elliptical external mandibular fenestra between the two elements. The surangular curves to contact the prearticular rostral to the articular and has a thin extension of bone stretching caudally to the articular and contributing to the retroarticular process. It contributes to the actual glenoid of the mandible only at its lateral lip.

Prearticular

The prearticular (Fig. 5.22) is a narrow element covering the caudomedial portion of the mandible, articulating caudal to the splenial, dorsal to the angular, and ventrally covering the articular as it forms the glenoid to hold the quadrate. It envelops the articular medially and extends caudally to form the medial aspect of the retroarticular process immediately caudal to the glenoid.

Articular

As in basal thyreophorans, the articular (Fig. 5.22; 5.25) is square in dorsal view, held in place by the surangular laterally, the angular ventrally, and prearticular ventromedially. It forms a shallowly concave and rostrocaudally- as well as mediolaterally-expanded glenoid for articulation with the bicondylar distal end of the

quadrate (Fig. 5.25). Ridges extend dorsally around the outer edges of the glenoid formed by the prearticular and articular medially and surangular laterally. The articulation of the mandible with the quadrate is offset ventral to the level of the tooth row, as in most ornithischians.

FIGURE 5.25. *Stegosaurus* craniomandibular joint. A, caudal view of articular glenoid surface shown and retroarticular process for reference; B, quadrate-articular joint illustrated in caudal view. Abbreviations: ar, articular surface; q, quadrate; rap, retroarticular process. Scale bar = 2 cm.

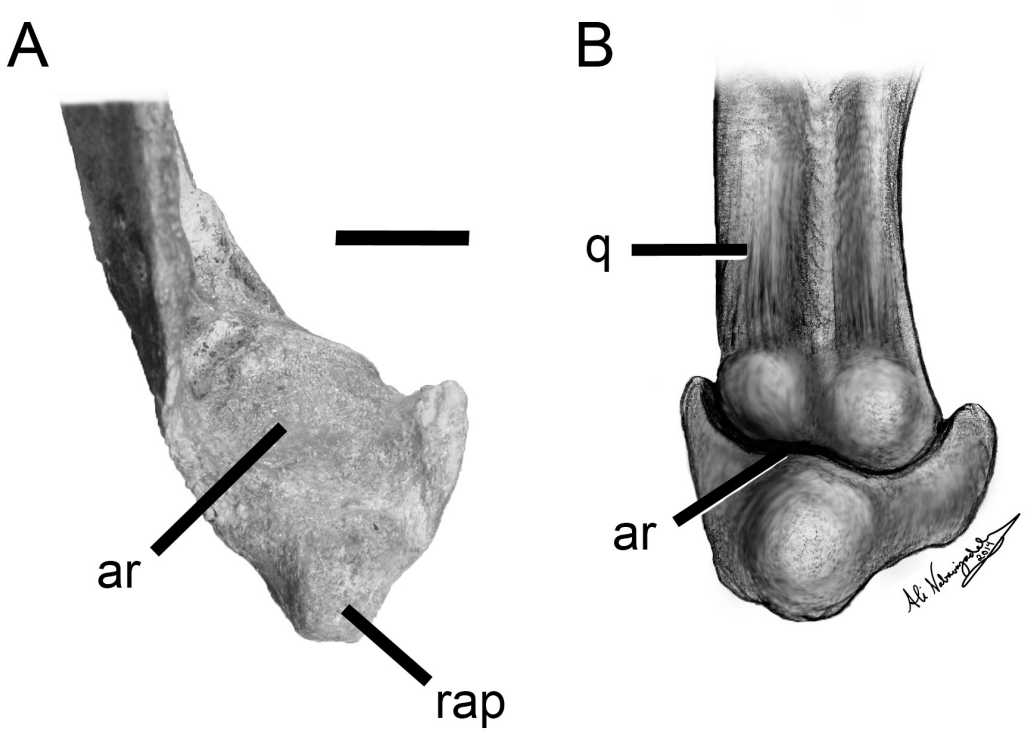

Dentition

Huayangosaurus (IVPP V6728; Sereno and Dong, 1992) bears seven roughly conical premaxillary teeth (Fig. 5.26) just caudal to the rostral edge of the premaxilla in lateral view. At occlusion, they rested against the lateral rim of the predentary, overhanging it. This rostral edge was likely used for puncturing vegetation at food acquisition. In contrast, in all other known stegosaur taxa, including *Stegosaurus*, the premaxilla is edentulous and rested against the dorsal rim of the predentary at occlusion.

FIGURE 5.26. *Huayangosaurus* left premaxillary tooth.

The maxillary and dentary teeth (Fig. 5.27) are generally spade-like with ridges that extend apicobasally along its buccal and lingual surfaces. They are buccolingually expanded and bulbous at the cingulum (especially in *Paranthodon* [Galton and Coombs, 1981]), with thin, cylindrical roots at the level of the alveoli. The apicobasal ridges create a variable number of blunted denticles (depending on the taxon) at the apical ridge of

each tooth. These denticles are much more blunt and less pointed than those seen in ankylosaur teeth (see below).

FIGURE 5.27. *Stegosaurus* left dentary tooth.

The tooth row consists of 20 to 23 tightly-packed teeth in *Stegosaurus*, whereas in the basal-most stegosaur, *Huayangosaurus* (IVPP V6728; Sereno and Dong, 1992), the tooth row has roughly 28 teeth (Sereno and Dong, 1992), meaning the tooth row shortened evolutionarily. Tooth wear is not commonly known in stegosaurs, as isolated teeth are rare and most teeth known are *in situ* and tightly packed to the point where it is not visible. The overall flattened shape of the teeth as well as slight wear on the apical rim of the teeth suggest a relatively orthal chewing action (Barrett, 2001). Minimal transverse movement of the jaw is plausible as well, performing a slight mortar-and-pestle-style jaw action in accordance with all other morphologies (see Chapter 8).

OSTEOLOGICAL DESCRIPTION: ANKYLOSAURIA

The following descriptions were based on my examination of specimens. See also Coombs (1971; 1978), Maryańska (1977), Vickaryous and Russell (2003), and Vickaryous et al. (2004) for prior descriptions of this clade. Due to the abundance of ankylosaur craniomandibular material, both examined by the author for this study and referenced in text, descriptions are based on observations of all specimens listed in Table 5.1 unless otherwise noted in the text.

FIGURE 5.28. Ankylosaur skulls in right lateral view showing shape differences in ankylosaurids vs. nodosaurids. A, *Euoplocephalus* (AMNH 5405; an ankylosaurid); B, *Panoplosaurus* (ROM 1215; a nodosaurid). Scale bars = 5 cm.

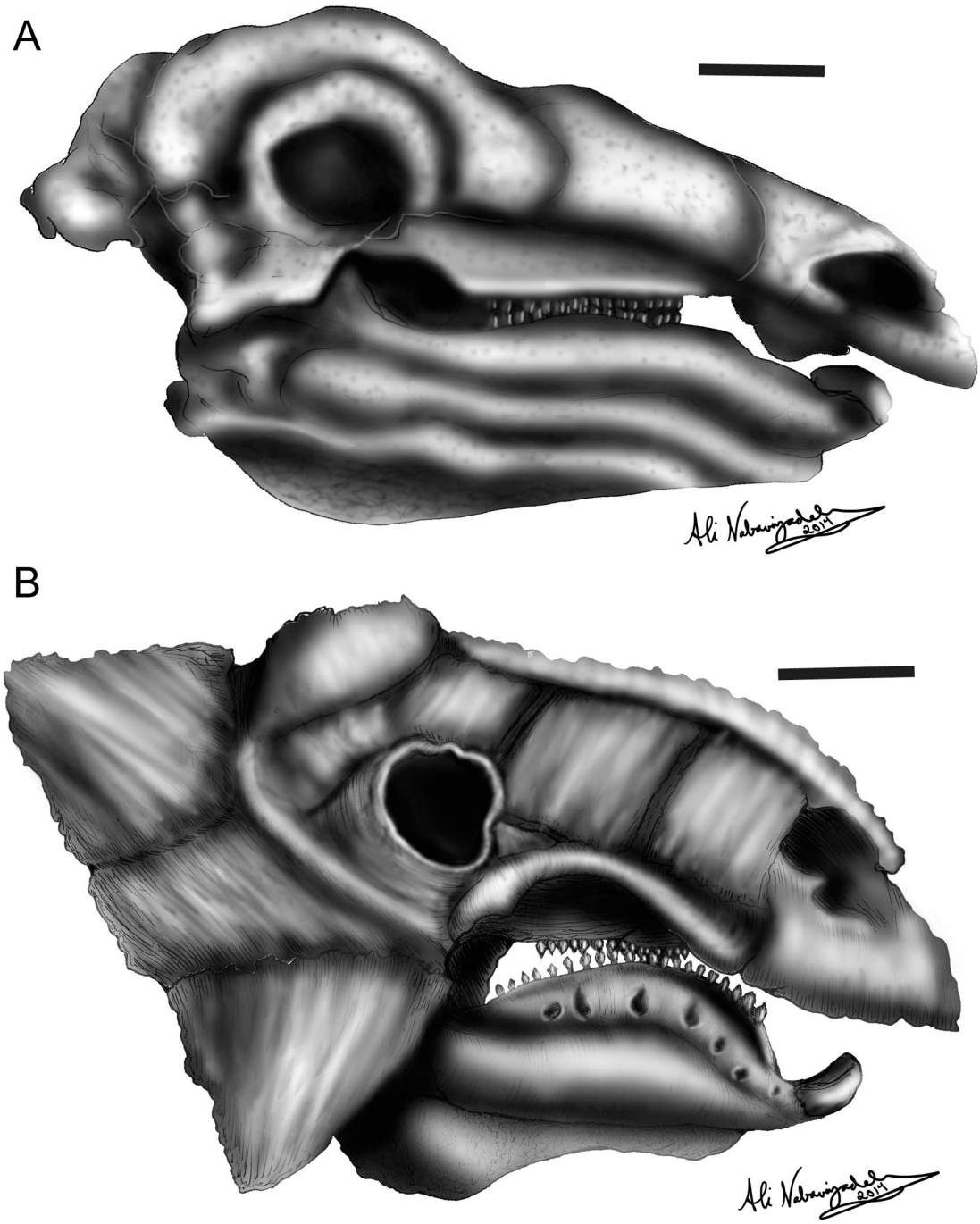

Cranium

Ankylosaurs are divided into Ankylosauridae (Fig. 5.28A) and Nodosauridae (Fig. 5.28B) (Coombs, 1978; Vickaryous et al., 2004), and these two clades will be referenced throughout these descriptions. The ankylosaur skull (Fig. 5.28; Fig. 5.29) is generally described as transversely broad and dorsoventrally short (Coombs, 1978). In dorsal view, the skull is approximately triangular, with a much broader rostral end and occiput in ankylosaurids than in nodosaurids, the latter having much narrower skulls with more pointed snouts than the former. *Zhongyuansaurus* is a possible exception, as it was originally thought to be a nodosaurid with its narrow snout (Xu et al., 2007), yet phylogenetic analysis by Thompson et al. (2012) suggests it is actually an ankylosaurid. Ankylosaurid skulls are transversely wider than they are rostrocaudally long, whereas the opposite is seen in nodosaurids skulls (Coombs, 1971; 1978). The skull is rostrocaudally short and squared off laterally in more basal ankylosaurids, such as *Minmi* (Molnar, 1996), *Crichtonsaurus* (Dong, 2002), and *Shamosaurus* (Tumanova, 1983; 1985), but becomes more elongate in more derived genera. The paroccipital processes are visible in dorsal view in nodosaurids but are not visible in ankylosaurids due to the caudally overhanging skull roof. Uniquely, the supratemporal fenestrae in neither clade is visible due to the robust surrounding dermal ossifications of various shapes and sizes tightly surrounding the dorsal surface of the skull (Coombs, 1978). In ankylosaurids, an ossified plate surrounding the quadratojugal region hides each infratemporal fenestra and quadrate in lateral view as well; however, in nodosaurids the infratemporal fenestrae are still exposed as caudally-slanted small rectangles. In special cases, such as *Edmontonia* and *Panoplosaurus*, an ellipsoid dermal ossified plate is positioned in the cheek region,

implying the presence of soft tissue in this area that would have to hold it in place (AMNH 5381; Lambe, 1919; Coombs, 1978; see Fig. 5.28B).

Ventrally, ankylosaurids have a broad palate while nodosaurids palates are much narrower. Most ankylosaurs possess a secondary palate as well. In nodosaurids, this secondary palate is made up of only a single sheet of bone running horizontally between the maxillary dentition and, in some cases, such as *Sauropelta*, it is non-existent (Coombs, 1978). In ankylosaurids, the secondary palate is more elaborate, made of two horizontal sheets of bone between the maxillary tooth rows. Due to these morphologies, the nasal passages in ankylosaurids, with several sinuses intact, are much more complex and sinuous than in nodosaurids (Coombs, 1978), although Witmer and Ridgely (2008), with the help of CT scanning, found more complex, looping nasal passages in nodosaurids than were previously known as well.

FIGURE 5.29. *Euoplocephalus* cranium in right lateral view (generalized with only select few elements labeled due to dermal ossifications surrounding skull). Abbreviations: jf, jugal flange; m, maxilla; n, nasal; or, orbit; pr, premaxilla; pt, pterygoid; sor, supraorbital. Scale bar = 5 cm.

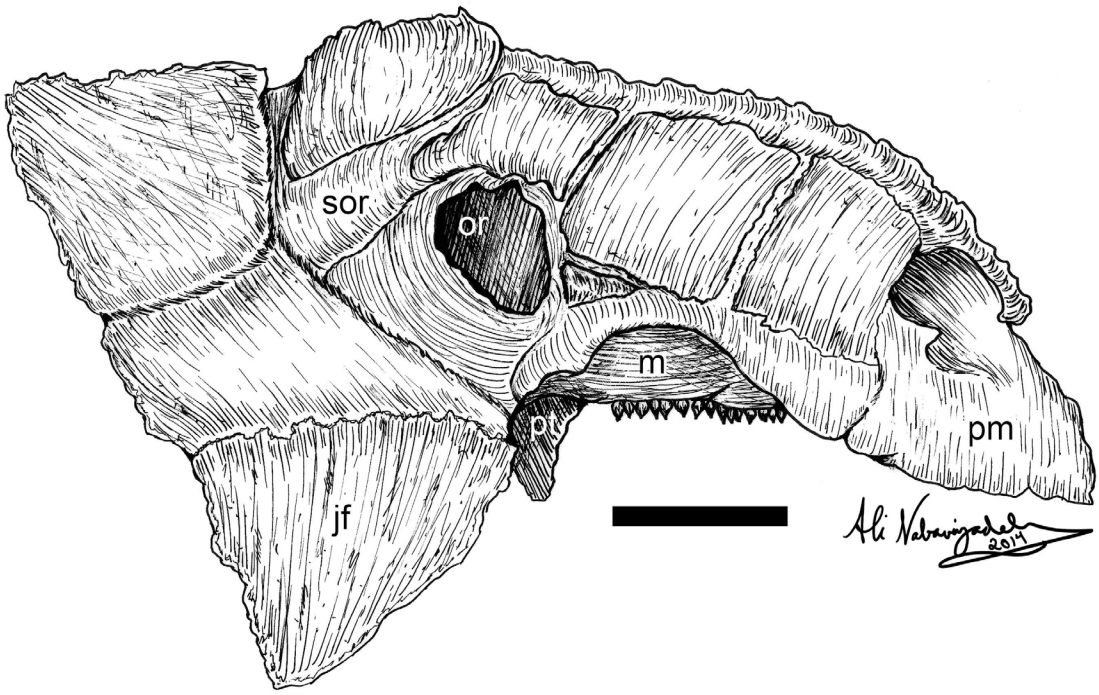

Premaxilla—The premaxilla is variably square among ankylosaurs, with a generally broader snout in ankylosaurids than in nodosaurids. In lateral view, the premaxilla typically extends and overhangs ventral to the level of the maxillary tooth row just caudal to it. All ankylosaur premaxillae have a rugose outer surface ventrally indicating that, in life, they were sheathed by a keratinous rhamphotheca around its outer and ventral edges, contacting the rhamphotheca of the predentary ventrally when the mouth was closed. The rostral and lateral borders form an irregular ventral thin edge called the tomial crest, which is caudally continuous with the lateral tomial crest of the maxilla. Both premaxillae are joined at the dorsal midline of the skull with two processes extending caudolaterally separating the external nares. The rostroventral tip of the interpremaxillary suture is demarcated by an inverted V-shape in ankylosaurids and by an even, flatter edge in nodosaurids. Ventrally, the premaxillae are sutured together in a

transversely broadened, square primary palate. The broad-snouted ankylosaurids possess a shorter ventral premaxillary palate. The narrower snouted nodosaurids possess a rostrally rounded, more elongate premaxillary palate with a caudomedially-oriented ridge that connects the cropping oral margin of the premaxilla to the maxillary tooth row. This connecting ridge is absent in ankylosaurids. The nodosaurids *Silvisaurus* (KUVP 1348; Eaton, 1960), *Gargoyleosaurus* (Kilbourne and Carpenter, 2005), *Tatankacephalus* (Parsons and Parsons, 2009), *Pawpawsaurus* (Lee, 1996), *Struthiosaurus*, and *Sauropelta* are the only ankylosaurs with known premaxillary teeth (Coombs, 1978; see Dentition section below), with a tooth row that bows out laterally along the inner ventral margins of the premaxilla. In most other ankylosaurs, however, including all ankylosaurids, the premaxilla is edentulous and overhangs the predentary by a few centimeters to create a large overbite in many derived ankylosaurs, especially ankylosaurids such as *Euoplocephalus* (e.g., AMNH 5405) and *Ankylosaurus* (AMNH 5214).

Maxilla—The maxilla in ankylosaurs is relatively short dorsoventrally and rounded at its lateral margin. The maxillary tooth row in ankylosaurs is medially inset, creating a buccal emargination. In more basal nodosaurids (e.g., *Silvisaurus* [KUVP 1348] and *Gastonia* [Kirkland, 1998]) and basal ankylosaurids (e.g., *Minmi* [Molnar, 1996], *Gobisaurus* [Vickaryous et al., 2001], *Tsagantegia* [Tumanova, 1993], and *Zhongyuansaurus* [Xu et al., 2007]), the maxillary tooth row is relatively much straighter rostrocaudally, although they are slightly subparallel to each other, angled closer together rostrally. Convergently, however, in both derived nodosaurids (e.g., *Panoplosaurus* [ROM 1215], *Gargoyleosaurus* [Kilbourne and Carpenter, 2005], and *Edmontonia* [USNM 11868]) and ankylosaurids (e.g., *Ankylosaurus* [AMNH 5214], *Euoplocephalus*

[AMNH 5405], *Pinacosaurus* [AMNH 6523], *Tianzhenosaurus* [Pang and Cheng, 1998], and *Minotaurasaurus* [Miles and Miles, 2009]), however, the tooth row curves medially at its mid-length and extends laterally again to a much greater extent caudally, corresponding to the medially-curved tooth row of the dentary (Fig. 5.30). This bowing morphology results in the caudal ends of both corresponding maxillary tooth rows farther apart than the rostral ends. The tomial crest of the premaxilla is continued by the maxilla along its ventrolateral margin. In ankylosaurids, the maxillary tooth row is separated from the lateral edge by a flat, transverse maxillary shelf, whereas in nodosaurids, it is confluent with a sinuous ridge originating on the ventral surface of the premaxilla, described above. The alveolar border in ankylosaurs generally projects ventrally as a separate small ridge containing the dentition. See Dentition section below for a description of ankylosaur dental morphology.

FIGURE 5.30. Palatal view of *Panoplosaurus* skull (ROM 1215) with arrows showing medially bowed maxillary tooth rows.

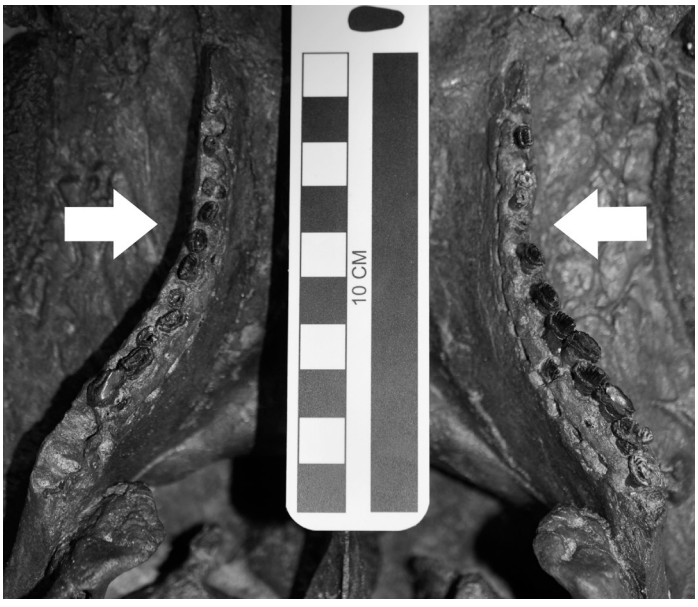

Quadrate—The quadrate (Fig. 5.31) in ankylosaurs is usually short, columnar and angled rostroventrally. In some forms, the rostroventral angle of the quadrate is greater at variable degrees, such as in *Pinacosaurus* (Maryańska, 1977), *Silvisaurus* (KUVP 1348), *Gastonia* (Kirkland, 1998), *Tsagantegia* (Tumanova, 1993), *Tatankacephalus* (Parsons and Parsons, 2009), *Gobisaurus* (Vickaryous et al., 2001), *Pawpawsaurus* (Lee, 1996), and *Gargoyleosaurus* (Kilbourne and Carpenter, 2005), whereas in other taxa, such as *Ankylosaurus* (AMNH 5214), *Euoplocephalus* (e.g., AMNH 5403; 5405), *Minmi* (Molnar, 1996), and *Cedarpelta* (Carpenter et al., 2001), the quadrate is less rostroventrally angled and instead nearly vertical. Whether an ankylosaur is an ankylosaurid or nodosaurid does not seem to correlate with variability in quadrate angle. In ankylosaurids, the quadrate has a more visible articulation with the ventral aspect of the squamosal, with the ball of the dorsal head of the quadrate and the quadratic fossa of the squamosal clearly visible in lateral view, indicating an unfused articulation between the two elements. In nodosaurids, in contrast, the dorsal (proximal) head of the quadrate is typically coossified with the squamosal, yet narrower at this end than in ankylosaurids (Kilbourne and Carpenter, 2005). As the body of the quadrate extends ventrally, a rostrally-oriented pterygoid wing is present along its rostral edge that contacts the pterygoid and acts as the origin for m. adductor mandibulae posterior (see below).

The mandibular condyle of the quadrate is hidden in lateral view by the quadratojugal-jugal flange and epijugal in ankylosaurids, but it is typically visible in nodosaurids. This condyle is rounded and has a narrow, elliptical (e.g., ankylosaurids like *Euoplocephalus* [AMNH 5405]) or triangular (e.g., nodosaurids like *Edmontonia* [AMNH 5337; USNM 11868]) outline in ventral view, with a rostromedial to

caudolateral axis. It is slightly bicondylar, with its medial condyle offset ventral to the level of its lateral condyle.

FIGURE 5.31. Ventral view of *Panoplosaurus* (ROM 1215) quadrate head. Scale bar = 1 cm.

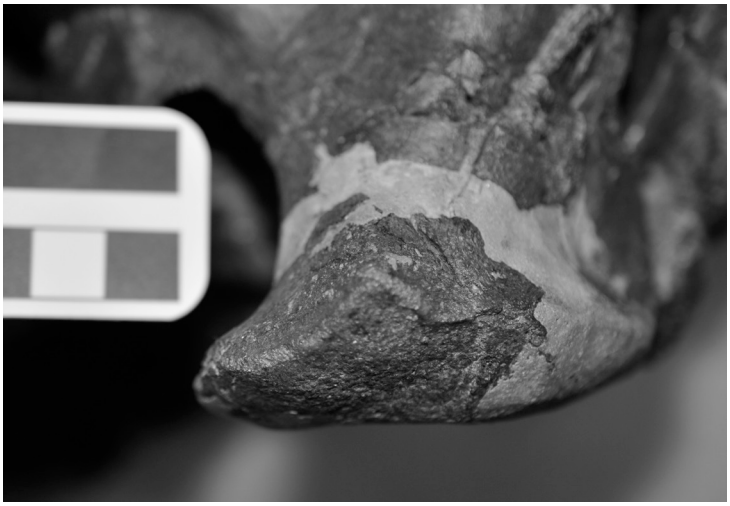

Predentary

Predentaries are known from only a few taxa within Ankylosauria (Fig. 5.32; 5.33). Among them are the ankylosaurids *Euoplocephalus* (AMNH 5403; 5405), *Saichania* (Maryańska, 1977), *Pinacosaurus* (AMNH 6523), and *Minotaurasaurus* (Miles and Miles, 2009), and the nodosaurid *Panoplosaurus* (TMP 1981.00.03; Lambe, 1919). As in all ornithischians, the predentary is a single, unpaired element, likely covered with a keratinous rhamphotheca, which conjoined both dentaries together at the rostral mandibular symphysis. On its rostral external surface, the predentary topology is highly rugose and is sporadically covered in pits and foramina indicating neurovasculature to the keratinous rhamphotheca. These foramina are relatively larger

than those seen in stegosaurs. Computed tomography scans of the predentary in *Euoplocephalus* (AMNH 5405) show vast interlocking channels throughout the predentary leading to the numerous foramina (Fig. 5.32).

FIG. 5.32. *Euoplocephalus* predentary. A, dorsal view reconstruction (AMNH 5403); B, caudal view reconstruction (AMNH 5403); C, dorsal view photograph (AMNH 5403); D, CT scan coronal slice of predentary (AMNH 5405) showing interconnected neurovascular canals. CT scans courtesy of Dr. Larry Witmer. Scale bar = 5 cm.

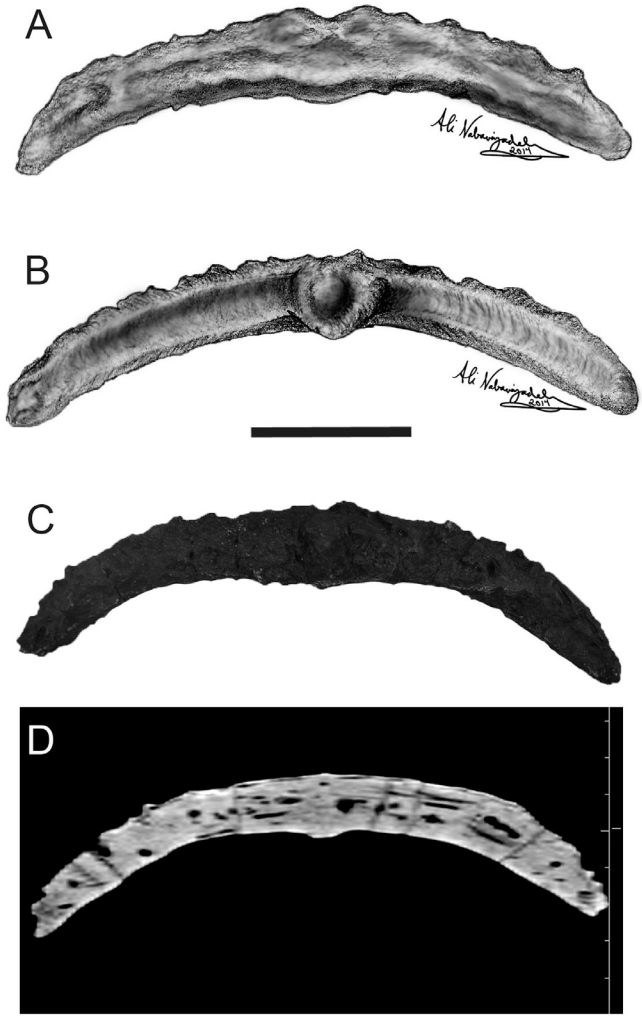

Due to the widened nature of the rostrum, the predentary is typically elongate mediolaterally with a diminished ventral process. It has a narrow and rounded body of variable dorsoventral depth that is recurved caudally and comes to a blunt point laterally on both sides. The ventral process is small and variably lies either between the rostral ends of the dentary symphysis or just ventral to them, cradling the dentaries. In some cases, as in *Euoplocephalus* (AMNH 5403; 54055), the ventral process is diminished so much that it is only represented by a small eminence on the ventromedial edge of the predentary. The extent to which the predentary body curves caudally at each lateral end is variable. In *Euoplocephalus*, the caudal orientation of each lateral tip is relatively small and forms a crescent in dorsal view. In other ankylosaurids (i.e., *Saichania* [Maryańska, 1977], *Pinacosaurus* [AMNH 6523], and *Minotaurasaurus* [Miles and Miles, 2009]) and the nodosaurid *Panoplosaurus* (Lambe 1919), however, the predentary is much more of squared-off bracket-shape in dorsal and ventral view (Fig. 5.33), with each caudolateral end directed more caudally with a narrow but rounded caudal margin. Each caudolaterally-oriented tip rests on the dorsal ridge of the spout-like rostral extension of the dentaries (Fig. 5.33). The articular surfaces on the caudal aspect of the predentary are smooth and rounded, especially in *Euoplocephalus*, but are still slightly flatter than its rostral, rugose surface. This smooth caudal surface of the lateral rami of the predentary does not articulate tightly with the rostral end of the dentaries and was, instead, likely attached by a flexible fibrocartilagenous or ligamentous tissue, permitting mobility at this junction, especially in *Euoplocephalus*, where articulation is the weakest.

FIGURE 5.33. Predentary-dentary articulation in *Pinacosaurus* (AMNH 5523) with gaps visible between elements. A, ventral view photograph; B, reconstruction. Abbreviations: d, dentary; p, predentary. Ruler in cm.

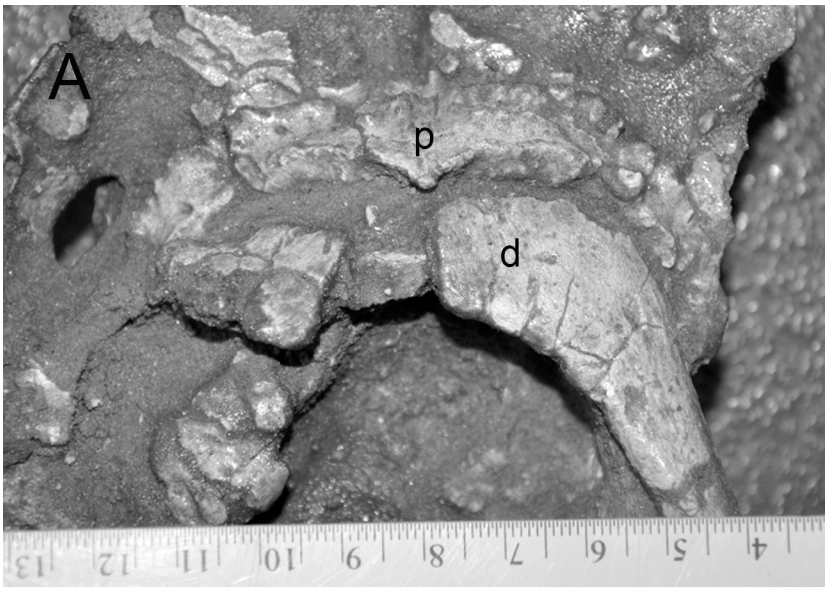

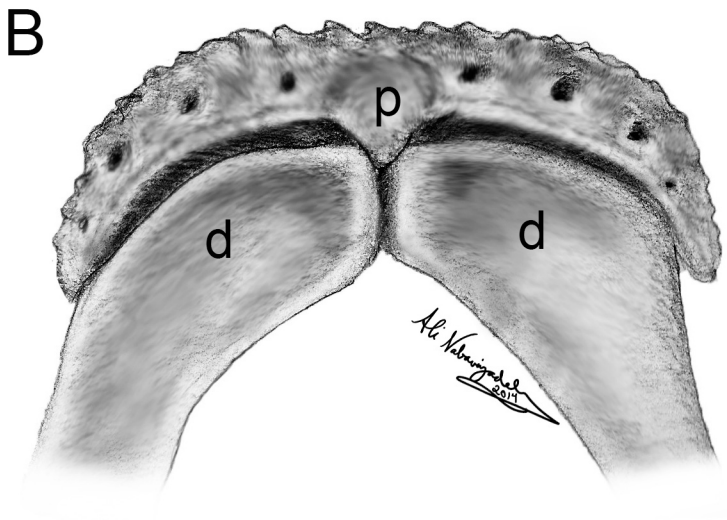

Dentary

The dentary (Fig. 5.34; 5.35; 5.36; 5.37; 5.38) is the largest element in the ankylosaur mandible and is, for the most part, similar in shape in both ankylosaurids and nodosaurids, with slight variations mostly insignificant to the overall function. It

articulates with the predentary and the opposite dentary rostrally, the splenial medially, the angular ventrally, and the surangular and coronoid caudally.

FIGURE 5.34. *Euoplocephalus* mandible (generalized – shown without predentary). A, lateral view; B, medial view. Abbreviations: a, angular; ar, articular; c, coronoid; d, dentary; pa, prearticular; rap, retroarticular process; sa, surangular; sp, splenial. Scale bar = 5 cm.

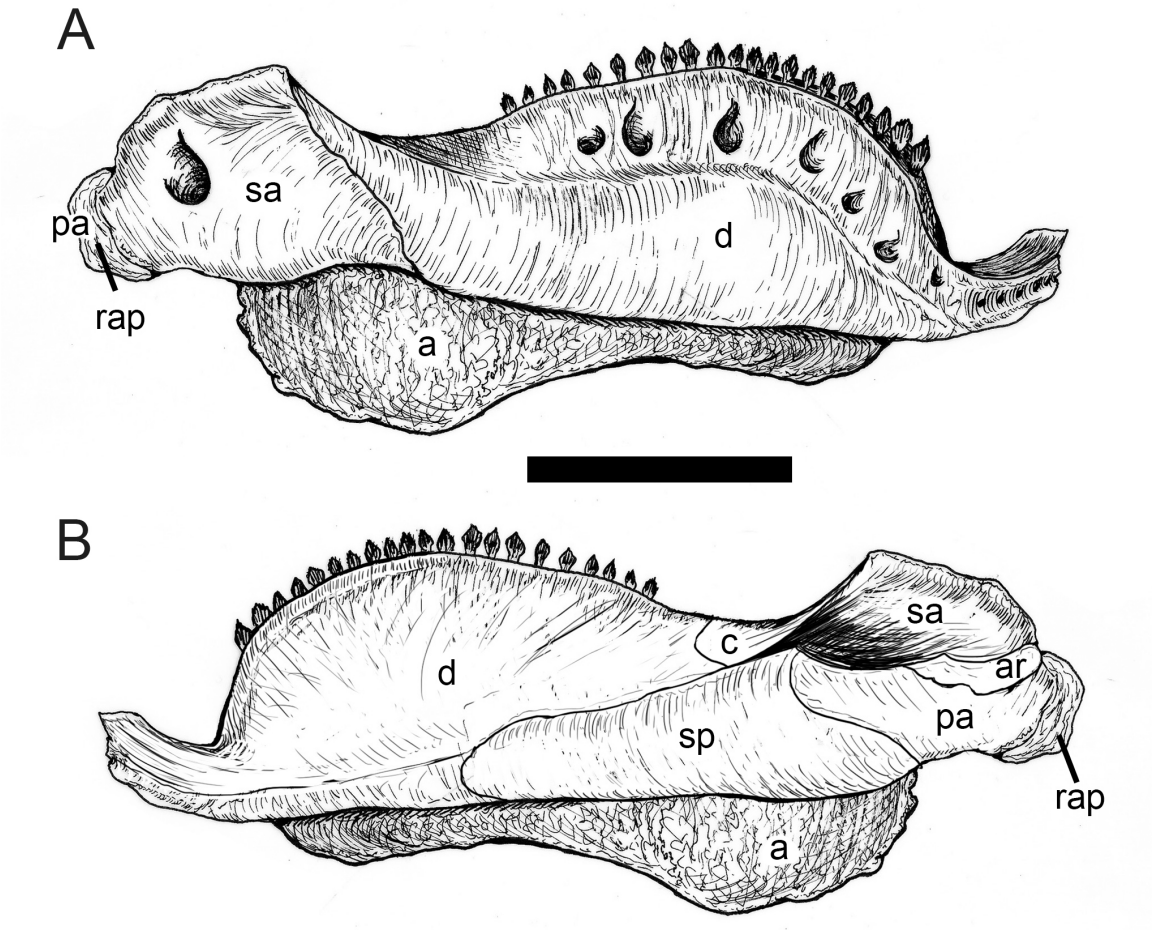

The ankylosaur dentary is very narrow at the rostroventral symphysis and abruptly curls dorsally until the arch of the tooth row reaches its maximum height at about mid-length. The dorsoventral height then remains level to its caudal end (e.g., *Ankylosaurus* [AMNH 5214]), except in *Euoplocephalus* (AMNH 5405) where the tooth row tapers ventrally again before reaching its caudal end. The ventral margin of the dentary is typically straight throughout most of its length, except at the symphysis where it curves slightly ventrally. The symphysis curves medially, with a concave symphyseal process on its medial surface like that seen in many hadrosauroid ornithopods (see Ornithopod Chapter). In few more basal cases (e.g., *Minmi* [Molnar, 1996]), the rostral tip of the dentary is vertical and flat, as seen in basal thyreophorans. In most derived ankylosaurs, however, the symphyseal process curves medially, forming a rostrocaudally elongate and narrow, slightly medially-arched rim which is characteristically slightly convex dorsoventrally and rugose along its length (Fig. 5.33; 5.35). This morphology suggests the possibility of mediolateral rotation around the long-axis of the dentaries against each other at this junction and in association with the predentary, contrary to what was suggested by Rybczynski and Vickaryous (2001), who suggested the preclusion of this movement. The smooth caudal surface of the lateral rami of the predentary rests against the rostral rim of the conjoined dentaries (Fig. 5.33), likely attached by a flexible fibrocartilagenous or ligamentous attachment. These cartilages and ligaments would further permit mediolateral rotation of the mandibular corpora around their long axes in all ankylosaurs, as described in the Predentary section above.

From its rostral tip, the dentary forms a caudolaterally-oriented and laterally-arched rostral edge of an otherwise dorsally-flat and rostrocaudally-narrow symphyseal

process. Along the dorsal rim of the dentary symphyseal process, an elongate and concave sulcus extends caudally.

FIGURE 5.35. Rostral view of *Ankylosaurus* (AMNH 5214) dentary exhibiting lateral groove and medial curvature at mandibular symphysis. Ruler units in cm.

Numerous foramina are lined up along the inner surface of the rostral sulcus, likely acting as an exit path of the mental nerve (a branch of CN V_3) to reach the predentary. This rostral edge is interrupted by a sharp dorsal turn that curls caudodorsally to form the mesial tip of the tooth row, with alveoli that are oriented slightly dorsolaterally. The dorsal rim of the dentary tooth row has a very sinuous morphology along its long axis (Fig. 5.35). As the tooth row extends caudally, it curves medially and

the alveoli are gradually oriented more dorsally and, in extreme cases such as *Euoplocephalus*, slightly dorsomedially.

FIGURE 5.36. Dorsal view of *Euoplocephalus* mandibular ramus showing curved tooth row with buccal emargination, the elongate symphyseal process, and the wide articular surface at the glenoid. Abbreviations: ar, articular surface; em, emarginated area; syp, symphyseal process.

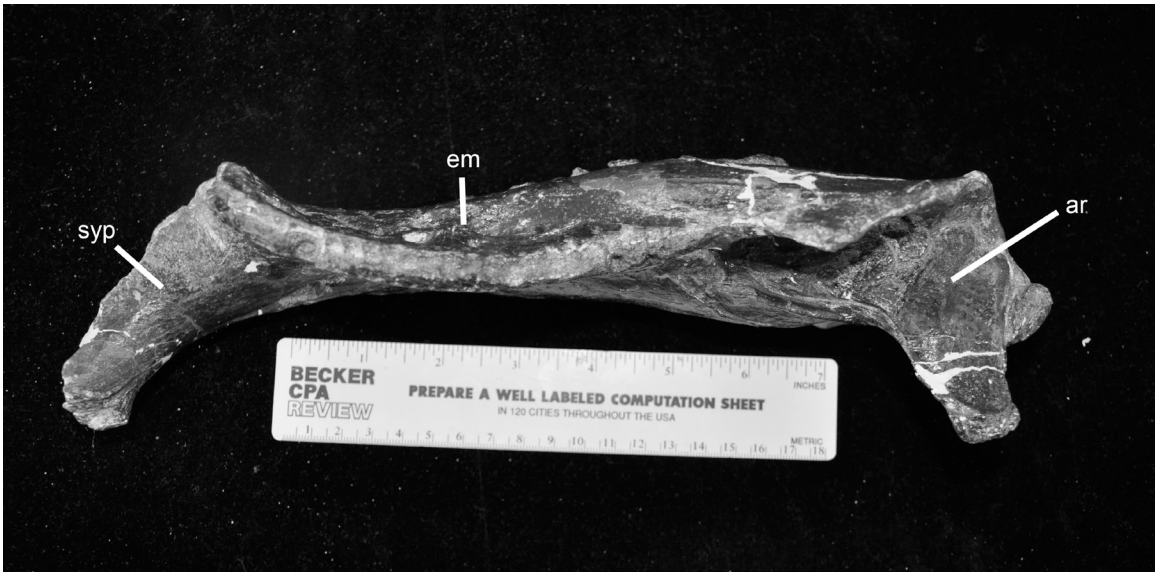

At the distal extreme of the tooth row, just rostral to the coronoid eminence of the mandible, the tooth row is at a more lateral position. This ultimately creates a medially arched tooth row in dorsal view, just as in the maxillary tooth row in ventral view. The transition from caudolaterally- to caudomedially-oriented alveoli from the mesial to the distal edge, however, creates a more complex tooth row that is unseen in almost any other vertebrate group, except for some non-hadrosauroid iguanodontian genera (see

Ornithopod chapter). See Dentition section below for a description of ankylosaur dental morphology.

With the medial arching of the dentary tooth row, a clear buccal emargination is formed with the dentary alveoli in a medially inset position that is most exaggerated at about mid-length before it is narrowed caudally (Fig. 5.36; 5.37). In lateral view, a clear ridge marks the lateral margin of the caudal portion of the emargination. This ridge continues dorsally until it forms the caudodorsally-oriented rostral edge of the sharp coronoid eminence of the mandible.

FIGURE 5.37. Comparison of ankylosaurid right lower mandibles, with *Euoplocephalus* (AMNH 5405) above and *Ankylosaurus* (AMNH 5124). Note differences in length and tooth row curvature. Ruler units in cm.

The coronoid is also made up of the coronoid bone rostromedially and the surangular at the apex and caudally descending ridge. At about mid-length, the body the dentary becomes laterally convex, creating a rounded, cylindrical long-axis that is exaggerated farther caudally in the mandible.

FIGURE 5.38. Comparison of nodosaurid right lower mandibles. A, *Edmontonia*; B, *Panoplosaurus* (ROM 1215). Note differences in coronoid eminence shape projecting dorsally on the left as well as difference in tooth row curvature. Scale bar in cm.

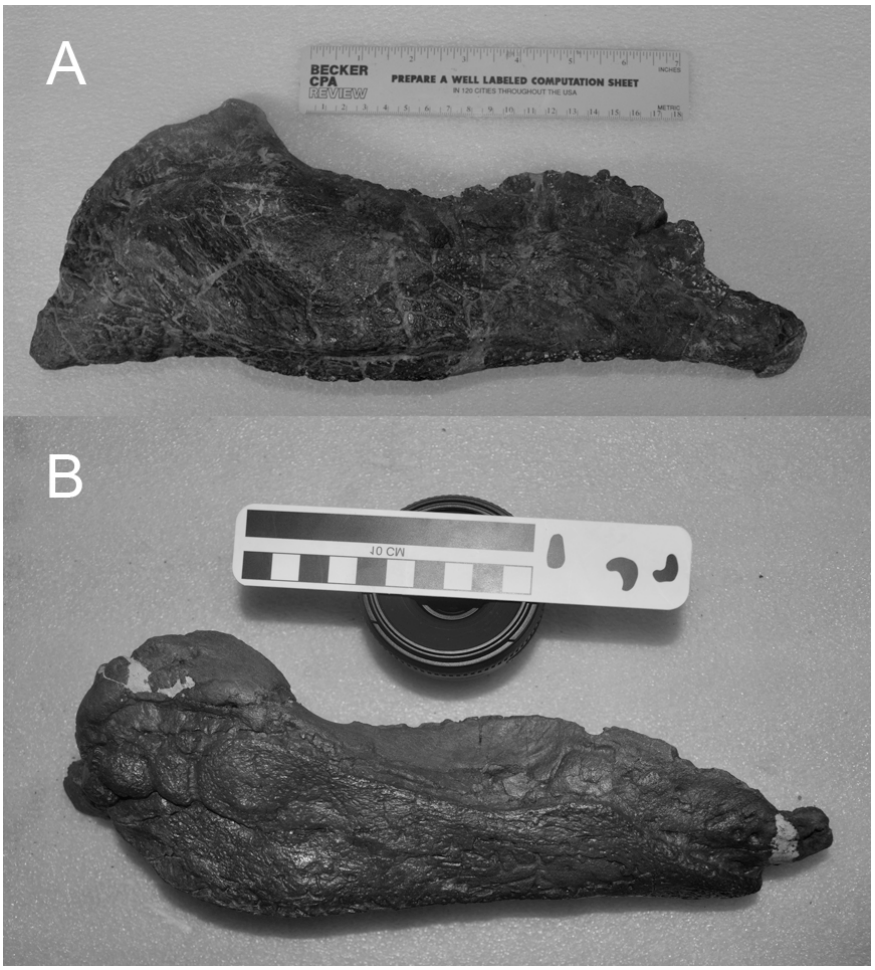

In lateral view, the body of the dentary, ventral to the tooth row, gradually extends caudodorsally, narrowing and contributing to the rostral edge of the coronoid eminence. It is sutured along a straight edge with the surangular caudally and the angular ventrally. The suture with the angular extends approximately the length of the tooth row, from its caudal edge to the level of the mesial extreme of the tooth row, where the dentary transitions into the symphyseal process. No mandibular fenestra is visible in ankylosaurs, likely because of the overlapping osteoderms covering the lateral surface of the mandible. Medially, the coronoid bone articulates with the caudodorsal point of the dentary. The caudal region of the dentary makes up the dorsal half of the mandibular height, with the splenial medially overlapping roughly the caudal two-thirds of the dentary ventral to the alveoli and making up most of the ventral region, except for the angular forming the ventral rim. The dentary is hollow, with a thinly rimmed, elliptical mandibular fossa (bounded also by the splenial medially and surangular laterally) where the mandibular cartilage and the inferior alveolar nerve (CN V_3) were located.

Coronoid

The coronoid (Fig. 5.34) is a small, thin bone in medial view. It forms the medial aspect of the dorsal gradual ascent of the coronoid eminence from the alveoli of the dentary and curves dorsally to create the medial apex of the coronoid eminence. In forms such as *Pinacosaurus* and *Saichania*, the coronoid is typically larger, with the rostral tip reaching about a third the caudal extent of the tooth row (Maryańska, 1977). The medial surface of the coronoid is covered in ridges in *Euoplocephalus* (Vickaryous and Russell, 2003), indicative of adductor muscular insertion.

Splenial

As in basal thyreophorans and stegosaurs, the splenial in ankylosaurs (Fig. 5.34) is a thin, sheet-like bone that covers the ventromedial aspect of the dentary and caudal portion of the mandibular canal. In medial view, it gradually increases in height from its rostral tip to about two-thirds its length, where it narrows caudally at the rim that creates the medial boundary of the mandibular canal. It articulates with the angular ventrally and prearticular caudally with slightly rounded sutures.

Angular

The angular in ankylosaurs (Fig. 5.34) is an elongate, narrow, laterally-compressed bone that forms the ventral boundary of the mandibular canal and adductor fossa throughout much of the length of the mandible. Laterally, it articulates with the dentary rostrodorsally and the surangular caudodorsally with a long, horizontal suture for each articulation. Medially, the angular is bordered by the splenial dorsally. In some taxa, the angular wraps medially to contact the prearticular (e.g., in *Edmontonia*), whereas in other taxa (e.g., *Euoplocephalus*) it does not contact the prearticular (Vickaryous and Russell, 2003). A large, robust osteoderm blankets the lateral and ventral surfaces of the angular of most ankylosaurs, further adding to the protection of the ankylosaur skull as a whole.

Surangular

The surangular (Fig. 5.34) is a large, triangular bone that forms the caudolateral portion of the apex of the coronoid eminence. The apex of the coronoid eminence is placed approximately four-fifths the length (from rostral to caudal) of the mandibular ramus. Compared to most other ornithischian clades, the coronoid eminence in ankylosaurs is much shorter rostrocaudally with respect to mandibular length and is placed much more caudally along the mandible. As in stegosaurs, it forms the caudolateral margin of the mandibular fossa and the lateral boundary of the jaw adductor fossa. As described above, the surangular is bordered ventrolaterally by the angular. The surangular is sutured with the prearticular and articular caudally. Laterally, it stretches caudal to the articular and forms the lateral surface of the retroarticular process and the lateral lip of the glenoid.

Prearticular

The prearticular (Fig. 5.34) is an elongate, narrow element covering the caudomedial portion of the mandible, articulating caudal to the splenial, dorsal to the angular, and, along with the surangular, ventrally cradling the articular that forms the mandibular glenoid. It envelops the articular medially and extends caudally to form the medial aspect of the retroarticular process just caudal to the glenoid. As it extends dorsally in medial view, it forms the ventral and ventromedial border of the adductor fossa of the mandible. As mentioned above, the prearticular contacts the angular as the angular wraps around medially in some taxa (i.e., in *Edmontonia*), but this is not the case

in others, such as *Euoplocephalus*, in which they do not touch (Vickaryous and Russell, 2003).

Articular

The articular (Fig. 5.34; 5.39; 5.40) is ellipsoidal to rectangular in dorsal view and is held in place by the surangular laterally and prearticular ventromedially. It forms a flat and mediolaterally-expanded glenoid for articulation with the ventral head of the quadrate (Fig. 5.40). It is also rostrocaudally expanded, more so than the rostrocaudal width of the ventral quadratic head, and without clear boundaries, suggesting some degree of rostrocaudal movement of the mandible along the quadrate (Rybczynski and Vickaryous, 2001).

FIGURE 5.39. Comparison of ankylosaurid mandibular glenoids. A, *Euoplocephalus* (AMNH 5405); B, *Ankylosaurus* (AMNH 5124). Note differences in breadth and general shape. Ruler units in cm.

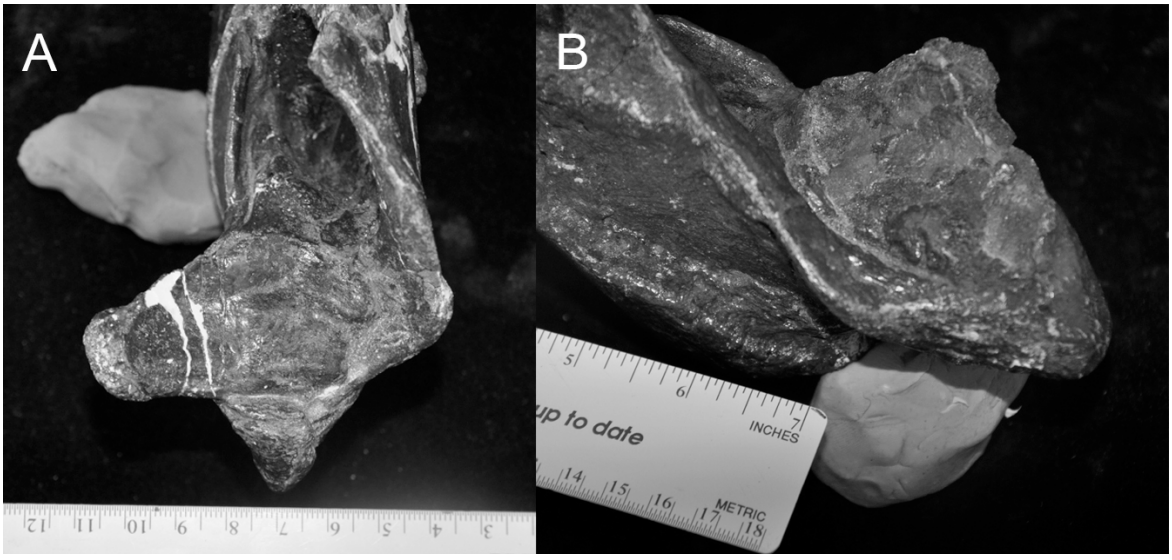

There are also dorsally-raised rims around the medial and lateral edges of the glenoid formed by the prearticular and articular medially and surangular laterally; this morphology likely permitting mediolateral rotation of the mandibular corpora, contrary to what was suggested by Rybczynski and Vickaryous (2001). This cupping morphology does have variation within subclades, however. For example, *Ankylosaurus* (AMNH 5124) is much more cupped in glenoid morphology than *Euoplocephalus*, which incidentally is also less rostrocaudally expanded and likely could not use as much of a propalinal chewing stroke as *Ankylosaurus* (Fig. 5.39). These differences are important to consider when investigating degree and method of mandibular rotation between genera of a given subclade. In nodosaurids, the lateral lip is raised higher than in ankylosaurids typically and is continuous with the coronoid eminence (Fig. 5.40). The articulation of the mandible with the quadrate is offset ventral to the level of the tooth row, as in most ornithischians.

FIGURE 5.40. *Edmontonia* quadrate-articular craniomandibular joint in caudal view. Abbreviations: ar, articular surface; q, quadrate; rap, retroarticular process.

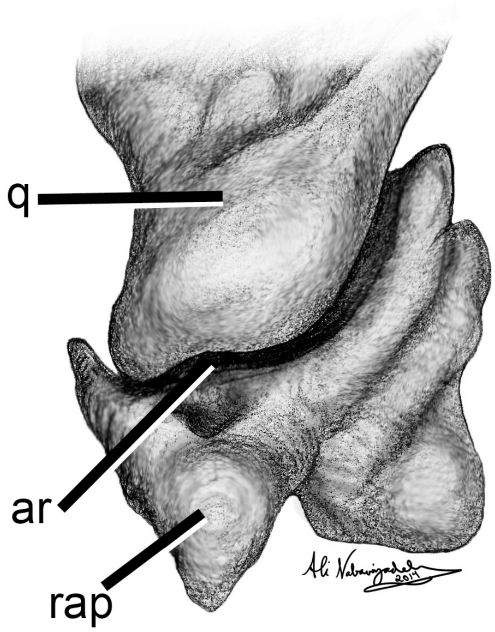

Dentition

The nodosaurids *Silvisaurus* (KUVP 1348; Eaton, 1960), Premaxillary dentition (Fig. 5.41) is found only in the nodosaurids *Silvisaurus* (KUVP 1348; Eaton, 1960), *Gargoyleosaurus* (Kilbourne and Carpenter, 2005), *Tatankacephalus* (Parsons and Parsons, 2009), *Pawpawsaurus* (Lee, 1996), *Struthiosaurus*, and *Sauropelta* and is typically peg to conical with a flattened edge, although seemingly much more stubby than in stegosaurs. Roughly eight or nine premaxillary teeth are present at the tip of the snout and flare laterally along the lateral edge before following the caudomedial ridge that connects with the maxillary tooth row.

FIGURE 5.41. *Silvisaurus* left premaxillary tooth.

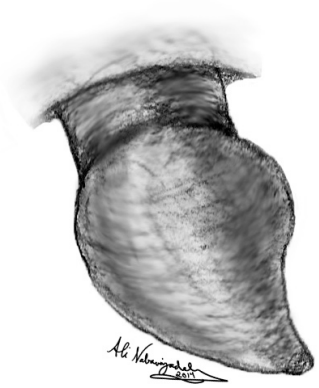

Ankylosaur maxillary and dentary teeth (Fig. 5.42), were likely only used minimally as indicated by the limited wear seen on isolated teeth (Barrett, 2001; Rybczynski and Vickaryous, 2001) and, for the most part, are very similar in shape to stegosaur teeth, although not entirely. Like stegosaurs, they are generally laterally compressed and spade-like with ridges that extend apicobasally along its buccal and lingual surfaces. They are buccolingually expanded and bulbous at the base (cingulum) with thin, cylindrical roots at the level of the alveoli. Unlike stegosaurs, however, the apicobasal ridges create sharp denticles at the mesial and distal apical ridge of each tooth, rather than the more blunted denticles seen in stegosaurs. Typically, no more than two or three replacement teeth can be seen beneath each alveolus and the teeth do not interlock. In ankylosaurids, the crown is small relative to the length of the roots, whereas in nodosaurids the crown is much larger in comparison. Although all ankylosaur teeth are swollen at the base, nodosaurids typically have a more distinct cingulum.

FIGURE 5.42. *Silvisaurus* right dentary tooth.

Tooth wear is not commonly seen in ankylosaurs, especially since many ankylosaur jaw specimens lack dentition and those that have dentition have poorly preserved tooth wear. Rybczynski and Vickaryous (2001) noted rostrocaudally angled tooth wear on an individual *Euoplocephalus* tooth, suggest propalinal motion; however, there are not sufficient data of ankylosaur microwear that would infer this with confidence.

JAW MUSCULATURE

Placement of jaw musculature in thyreophorans has only been commented on in a minimal and speculatory way through studies of muscle scarring as well as phylogenetic-bracketing methodology (Haas, 1969; Holliday, 2009). Haas (1969) originally described jaw adductor musculature in the ankylosaurid *Euoplocephalus*, indicating that the ankylosaurid skull morphology is highly modified and complex compared to most dinosaurs and, for this reason, skull musculature is difficult to discern with confidence. Holliday (2009) then went on to further discuss jaw adductor morphology in Dinosauria, referring to *Stegosaurus* and *Panoplosaurus* as the representative thyreophorans. These descriptions were used as a baseline for speculating about morphology and usage of jaw musculature in the present study. The descriptions below are generalized for all thyreophorans, unless otherwise noted.

M. depressor mandibulae

M. depressor mandibulae (mDM; Fig. 5.43) was likely the primary muscle used in opening the lower jaw. According to Haas (1969), this muscle originated on the caudodorsal and caudolateral surfaces of the paroccipital processes of the exoccipitals on the caudal-most extent of the cranium. M. depressor mandibulae stretched ventrally inserting onto the dorsal aspect of the shorter retroarticular process at the caudal-most region of the jaw past the mandibular joint. When the jaw is closed, the mDM looks to have been relatively dorsoventrally in basal thyreophorans and stegosaurs, however in ankylosaurs it looks to have extended at a much smaller angle in ankylosaurs, being

oriented much more rostroventrally. This is due to a more caudal displacement of the orbits in ankylosaurs as well as an expanded region of the skull caudal to the orbit, placing the paroccipital process much more caudally as well.

M. adductor mandibulae posterior

Palinal motion of the jaw mechanism was likely accommodated by the enlarged m. adductor mandibulae posterior (mAMP; Fig. 5.43). This muscle originated on the lateral surface of the rostrally-oriented pterygoid ramus of the quadrate in thyreophorans. It stretched rostroventrally to insert into the medial mandibular fossa on the inner caudal aspect of the dentary. This would make for a direct line of action for the muscle to contract and pull the jaw caudodorsally for stripping vegetation. As it is typically a very large muscle, it likely produced a great deal of force in the caudal direction and made for a substantial bite force.

As is seen in Table 5.2, muscle fiber orientations differ drastically between many genera. Among basal thyreophorans, *Emausaurus* shows a much higher angled mAMP than the basal-most *Lesothosaurus* and the more derived *Scelidosaurus*. This higher angle suggests a special case of a more dorsoventral contraction of mAMP in *Emausaurus*' jaw mechanism. Within Stegosauria, however, there is a drastic decrease in mAMP angle from the more basal *Huayangosaurus* (which has a much higher mAMP angle than basal thyreophorans) to the more derived *Stegosaurus*, reverting back to a more caudally oriented muscle contraction. Ankylosaurids show relatively similar mAMP angles (all higher than the more basal *Lesothosaurus* and *Scelidosaurus*), with sister genera *Ankylosaurus* and *Euoplocephalus* being almost equal angles and *Pinacosaurus* being

slightly lower (or more caudally oriented). The nodosaurids *Edmontonia* and *Pinacosaurus* have almost a 15 degree difference in mAMP muscle angle, with *Edmontonia*'s mAMP being much more caudally oriented.

TABLE 5.2. Thyreophoran mAMP muscle vector angles.

Genus	Spec. # / Ref.	mAMP(°)
Ankylosaurus	AMNH 5214	44.18
Edmontonia	USNM 11868	31.56
Emausaurus	(Haubold, 1990)	40.39
Euoplocephalus	AMNH 5405	46.72
Huayangosaurus	IVPP V6728	50.16
Lesothosaurus	BMNH R8501	27.56
Panoplosaurus	ROM 1215	45.31
Pinacosaurus	ZPAL MgD-II/1	37.31
Scelidosaurus	BMNH R1111	27.64
Stegosaurus	USNM 4934	29.45

M. pseudotemporalis

M. pseudotemporalis (mPST; represented by superficialis in Fig. 5.43) was likely made of two bellies in thyreophorans: m. pseudotemporalis superficialis and profundus. Together, these two muscle bellies would have assisted in pulling the jaw closed during chewing cycles.

M. pseudotemporalis superficialis—M. pseudotemporalis superficialis (mPSTS) likely originated at the rostral-most portion section of the supratemporal fenestra as well as the rostral portion of the sagittal crest in most thyreophorans except ankylosaurids. Haas (1969) placed the origin of mPSTS on the laterosphenoid in ankylosaurids because of the hindrance of the postocular shelf covering the supratemporal fenestra. MPSTS extended rostroventrally to insert on the dorsal apex of the coronoid eminence and the

rostral portion of the medial mandibular fenestra, likely through a tendinous sheet (Haas, 1969; Holliday, 2009).

M. pseudotemporalis profundus—M. pseudotemporalis profundus (mPSTP) likely originated on the lateral surface of the epipterygoid in thyreophorans, as seen in extant archosaurs. Like mPSTS, its insertion was likely the dorsal apex of the coronoid eminence and the rostral portion of the medial mandibular fenestra, likely through a tendinous sheet (Haas, 1969; Holliday, 2009).

FIGURE 5.43. Comparison of thyreophoran jaw musculature (m. pseudotemporalis [superficialis only], m. adductor mandibulae posterior, and m. depressor mandibulae). A, *Lesothosaurus* (basal thyreophoran); B, *Scelidosaurus* (basal thyreophoran); C, *Stegosaurus* (stegosaur); D, *Panoplosaurus* (ankylosaur). Abbreviations: mAMP, m. adductor mandibulae posterior; mDM, m. depressor mandibulae; mPST, m. pseudotemporalis. Left lateral views. See Figs. 5.2, 5.17, and 5.28 for scale bars.

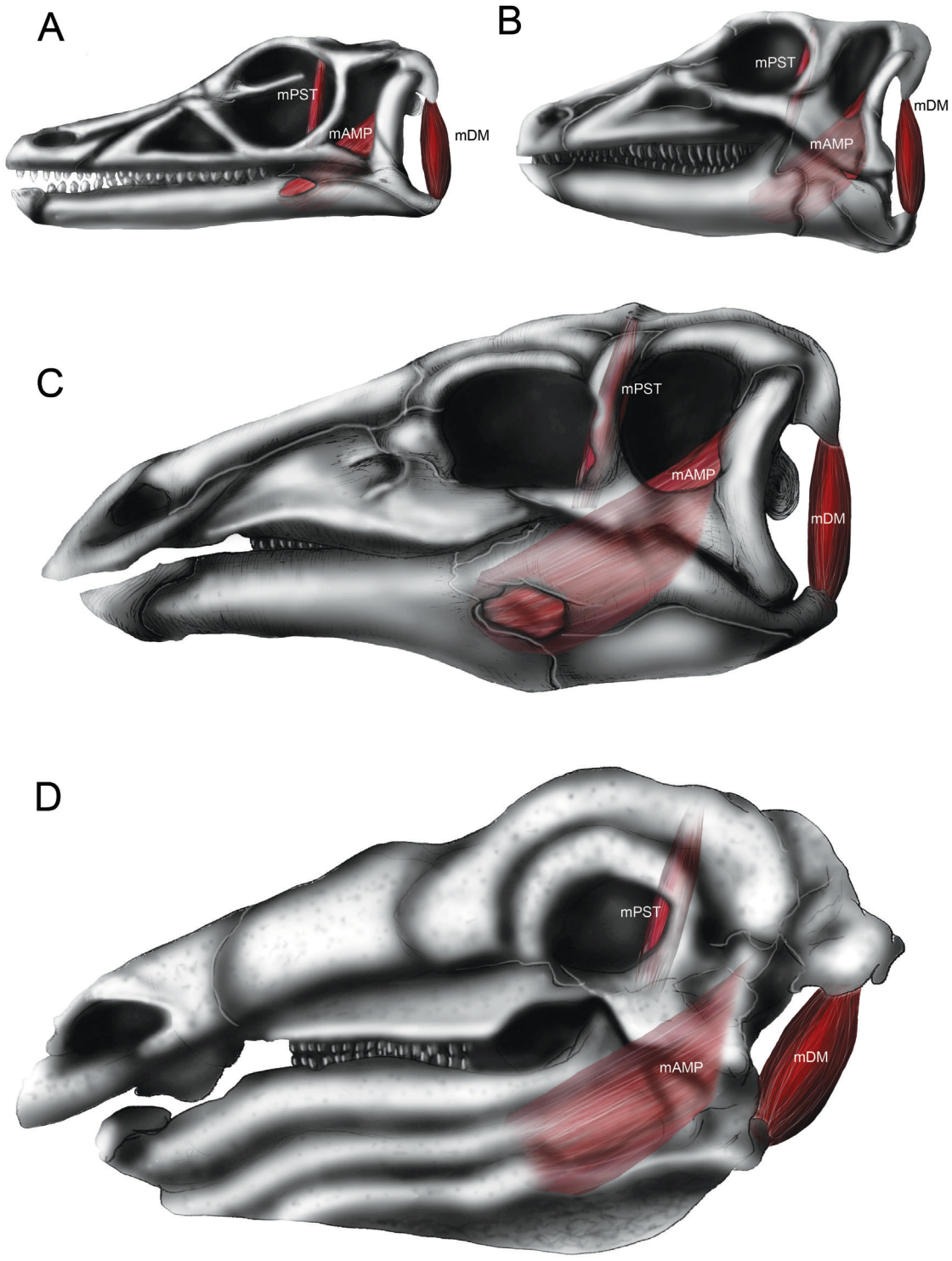
A
mPST
mAMP
mDM
B
mPST
mDM
mAMP
C
mPST
mAMP
mDM
D
mPST
mAMP
mDM

M. adductor mandibulae externus

The primary group of muscles likely acting to raise the jaw to occlusion is the adductor mandibulae externus (mAME; Fig. 5.44) muscle group. All of the muscles in this group likely originated on or near the squamosal and the temporal region, as is seen in extant archosaur relatives, together functioning as a large fan of muscle (Haas, 1969; Holliday, 2009). See Table 5.3 for muscle fiber orientations.

M. adductor mandibulae externus superficialis—According to Holliday (2009), m. adductor mandibulae externus superficialis (mAMES) likely originated on the medial ridge of the supratemporal arch, made of the postorbital and squamosal, as can be seen in extant archosaurs and lepidosaurs. The supratemporal bar is visible in basal thyreophorans, stegosaurs, and nodosaurids; however, it is hidden from lateral and superior view in ankylosaurids due to the postocular shelf and dermal ossifications surrounding the skull. M. adductor mandibulae externus superficialis expanded along the more lateral portion of the dorsal rim of the surangular and likely the more caudal portion of the coronoid eminence.

M. adductor mandibulae externus medialis—M. adductor mandibulae medialis (mAMEM) likely originated on the caudolateral surface of the supratemporal fossa just dorsal to the infratemporal fenestra (Holliday, 2009). It likely extended rostroventrally to insert onto the smooth medial aspect of the dorsal ridge along the surangular portion of the coronoid eminence. Exact demarcation of this muscle is unclear because, mAMEM likely shared a muscle body with mAMEP (see below).

M. adductor mandibulae externus profundus—M. adductor mandibulae externus profundus (mAMEP) likely originated on the caudomedial wall of the

supratemporal fenestra and caudal portion of the sagittal crest in superior view (Holliday, 2009), although this is not visible in ankylosaurs due to dermal ossification covering this area. This muscle is thought to have inserted at the caudodorsal apex of the coronoid eminence, which is made up mostly of the surangular in stegosaurs and ankylosaurs and mostly of the coronoid bone in basal thyreophorans.

MAME muscle vector angles—As is seen in Table 5.3, muscle fiber orientations and muscle fan sizes differ drastically among many genera. Among basal thyreophorans, although *Scelidosaurus* has the lowest mAMEP angle (i.e., most caudally oriented), the span of the entire mAME complex (from the caudal-most fibers of mAMEP to rostral-most fibers of mAMES) is by far the largest of the basal thyreophorans (including *Lesothosaurus* and *Emausaurus*), suggesting that it likely had a large range of directions to contract mAME, using different portions of it in different ways. Stegosauria, there is also an increase in muscle fiber orientation span from the more basal *Huayangosaurus* (which has a much higher mAMEP angle than the more basal thyreophorans *Lesothosaurus* and *Scelidosaurus*) to the more derived *Stegosaurus*. Ankylosaurids show relatively similar mAME fiber orientations (with a slightly larger mAMEP to mAMES range in *Pinacosaurus*). The nodosaurids *Edmontonia* and *Pinacosaurus* have a large difference in mAME fiber orientations, with *Edmontonia*'s mAME muscle complex being much more caudally oriented.

TABLE 5.3. Thyreophoran mAME muscle vector angles.

Genus	Spec. # / Ref.	mAMEP(°) (Coronoid Apex)	mAMEM(°) (Coronoid Mid-height)	mAMES(°) (Coronoid Base)
Ankylosaurus	AMNH 5214	56.41	67.85	70.33
Edmontonia	USNM 11868	22.86	36.32	45.72
Emausaurus	(Haubold, 1990)	68.57	76.9	85.42
Euoplocephalus	AMNH 5405	56.26	66.78	74.63
Huayangosaurus	IVPP V6728	63.57	77.97	85.18
Lesothosaurus	BMNH R8501	48.91	67.09	83.08
Panoplosaurus	ROM 1215	43.7	62.59	64.49
Pinacosaurus	ZPAL MgD-II/1	57.86	75.55	84.32
Scelidosaurus	BMNH R1111	33.08	60.3	79.22
Stegosaurus	USNM 4934	47.74	70.11	87.17

FIGURE 5.44. Comparison of thyreophoran m. adductor mandibulae externus muscle complex morphology showing variations in muscle vector angles of m. adductor mandibulae externus profundus. A, *Lesothosaurus* (basal thyreophoran); B, *Scelidosaurus* (basal thyreophoran); C, *Huayangosaurus* (stegosaur); D, *Stegosaurus* (stegosaur); E, *Panoplosaurus* (nodosaurid ankylosaur); F, *Euoplocephalus* (ankylosaurid ankylosaur). Left lateral views. See Figs. 5.2, 5.17, and 5.28 for scale bars.

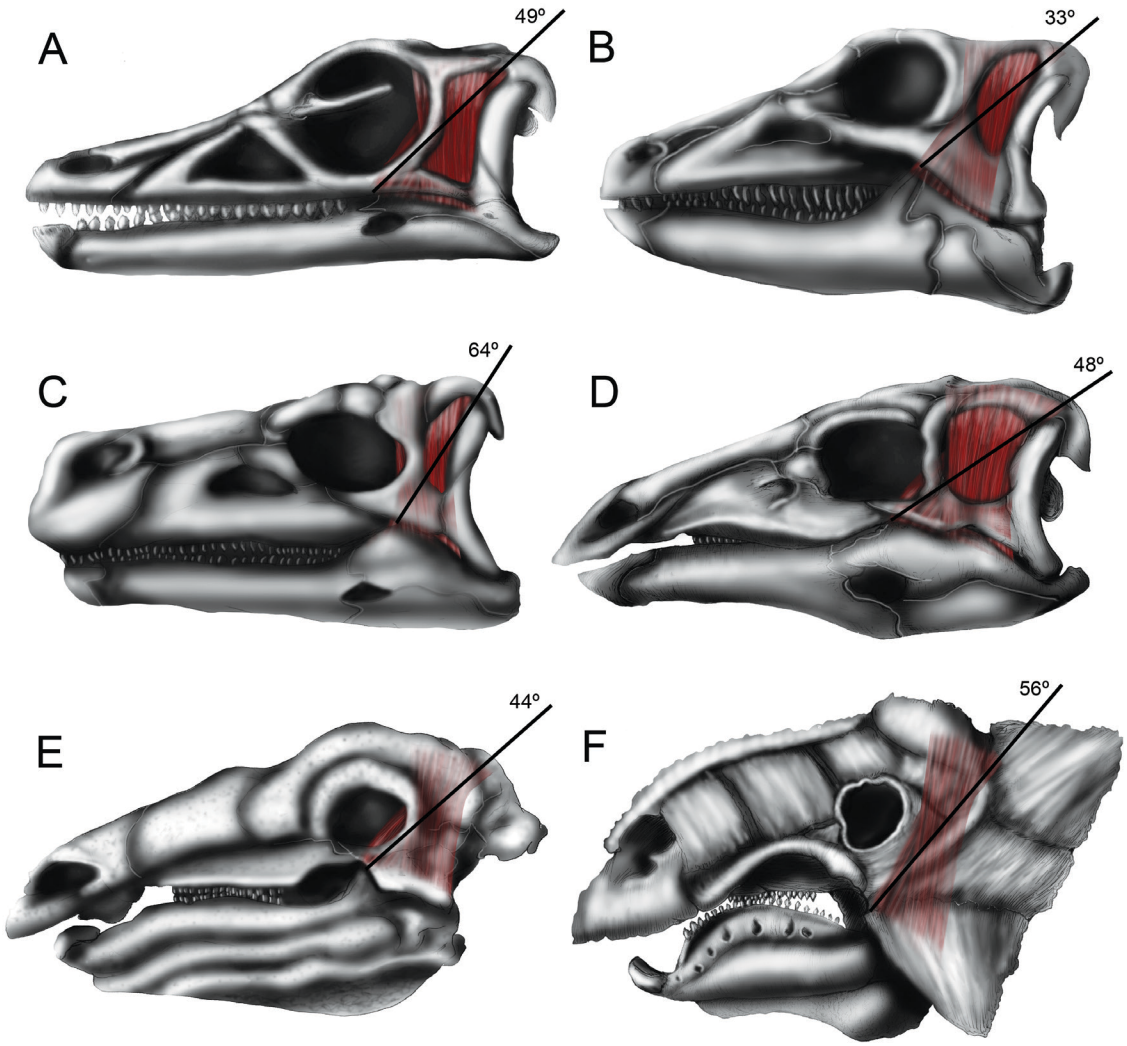

M. pterygoideus ventralis

M. pterygoideus ventralis (mPTV; Fig. 5.45) likely originated on the pronounced caudoventral surface of the pterygoid flange and on the palate ventral surface of the palate, demarcated by a slightly concave and smooth surface. This muscle would have run caudoventrally to wrap around the lateral aspect of the mandible and eventually to insert onto the ventrolateral aspect of the mandible (angular) and retroarticular process, although exact insertion is unclear due to lack of distinct muscle scarring. MPTV likely

functioned in medial movement, stabilization, or restriction of the mandibular corpus (Haas, 1969; Holliday, 2009).

M. pterygoideus dorsalis

M. pterygoideus dorsalis (mPTD; Fig. 5.45) likely originated on a rostrocaudally-elongate depressed region on the dorsal aspect of the pterygoid flange and on the palate. It ran caudoventrally around the medial aspect of its respective mandibular corpus. The insertion was likely on the medial aspect retroarticular process. Its function, opposing m. pterygoideus ventralis, it plausibly suited the medial movement or restriction of its corresponding ramus, depending on which side of the jaw is used in mastication (Haas, 1969; Holliday, 2009).

FIGURE 5.45. Comparison of thyreophoran m. pterygoideus ventralis (mPTV) and m. pterygoideus dorsalis (mPTD). A, B, *Lesothosaurus* (basal thyreophoran) (A, mPTV; B, mPTD); C, D, *Scelidosaurus* (basal thyreophoran) (C, mPTV; D, mPTD); E, F, *Stegosaurus* (stegosaur) (E, mPTV; F, mPTD); G, H, *Panoplosaurus* (ankylosaur) (G, mPTV; H, mPTD). Left lateral views. See Figs. 5.2, 5.17, and 5.28 for scale bars.

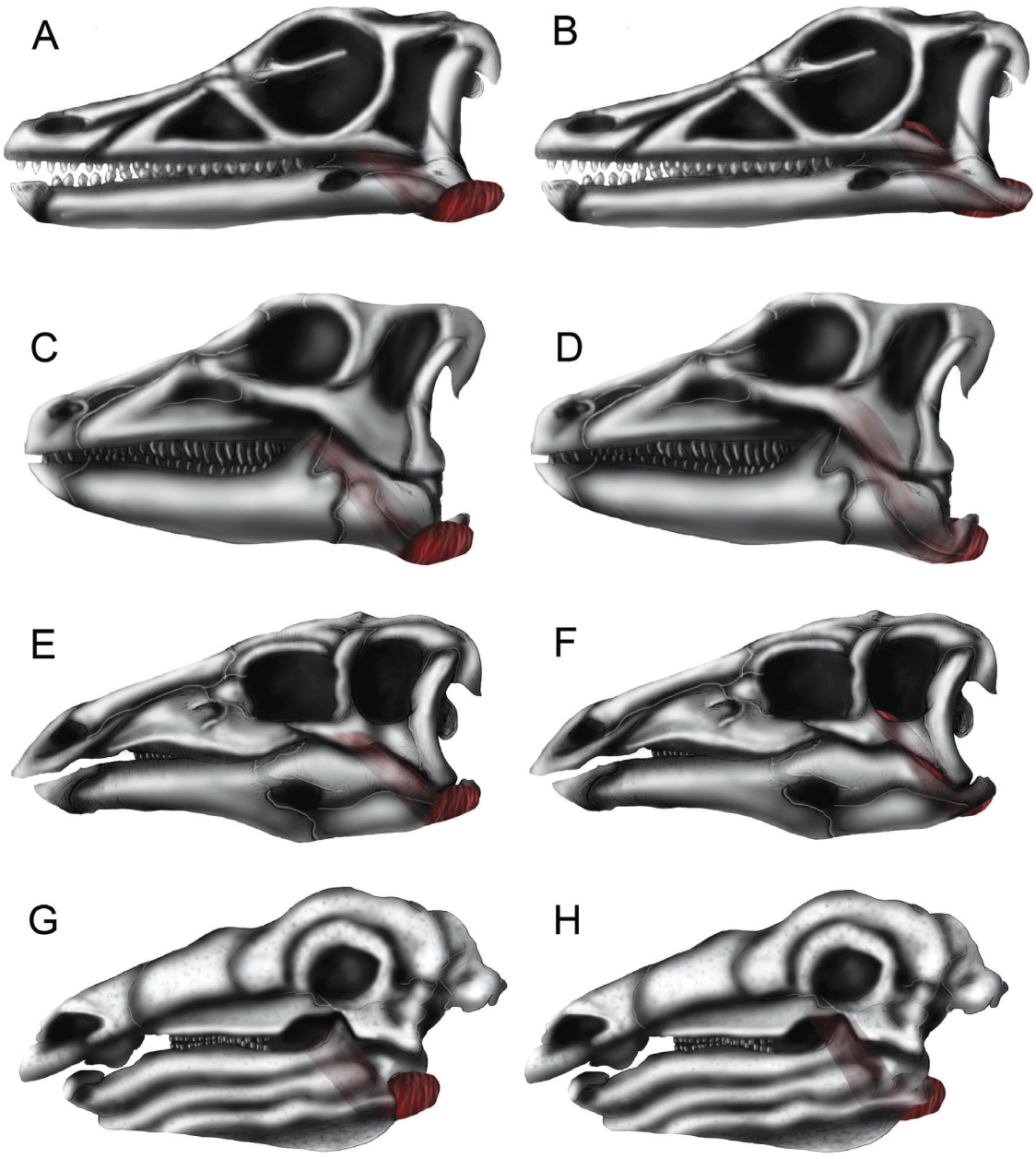
A
B
C
D
E
F
G
H

2D LEVER ARM ANALYSES

2D lever arm relative bite force (RBF) analysis was done on various thyreophoran genera and were compared with each other as well as the rest of Ornithischia (see Chapter 8). Below, the RBF results at the predentary as well as the rostral, middle, and caudal teeth are given (Table 5.4).

TABLE 5.4. Actual RBF values across thyreophoran tooth rows.

Genus	Spec. # / Ref.	Input Lever Angle in ° (mAMEP)	Predentary RBF	Rostral Tooth RBF	Middle Tooth RBF	Caudal Tooth RBF
Ankylosaurus	AMNH 5214	56.41	0.378	0.449	0.588	0.842
Edmontonia	USNM 11868	22.86	0.261	0.316	0.441	0.794
Emausaurus	(Haubold, 1990)	68.57	0.347	0.432	0.565	0.876
Euoplocephalus	AMNH 5405	56.26	0.288	0.312	0.418	0.642
Huayangosaurus	IVPP V6728	63.57	0.208	0.269	0.339	0.595
Lesothosaurus	BMNH R8501	48.91	0.249	0.263	0.382	0.696
Panoplosaurus	ROM 1215	43.7	0.261	0.282	0.407	0.731
Pinacosaurus	ZPAL MgD-II/1	57.86	0.212	0.267	0.374	0.616
Scelidosaurus	BMNH R1111	33.08	0.287	0.321	0.445	0.766
Stegosaurus	USNM 4934	47.74	0.384	0.412	0.560	0.885

RBF values were plotted in line graphs within various subgroups of Thyreophora to visualize the general trends of bite forces throughout the jaws (Fig. 5.46; 5.47; 5.48).

Mechanical Advantages Among Thyreophoran Jaws (with MANOVA Results)

For visualization of RBF values in a phylogenetic context, see Fig. 5.49.

Basal thyreophorans were neither significantly different in RBFs from derived stegosaurs ($p = 0.829$) or ankylosaurs ($p = 0.222$), although *Scelidosaurus* scored exceptionally higher throughout the entire jaw.

FIGURE 5.46. Basal thyreophoran RBFs (on Y-axis) across the tooth row compared to *Heterodontosaurus*. Bite points are at the predentary (PD) tip as well as the rostral, middle, and caudal teeth.

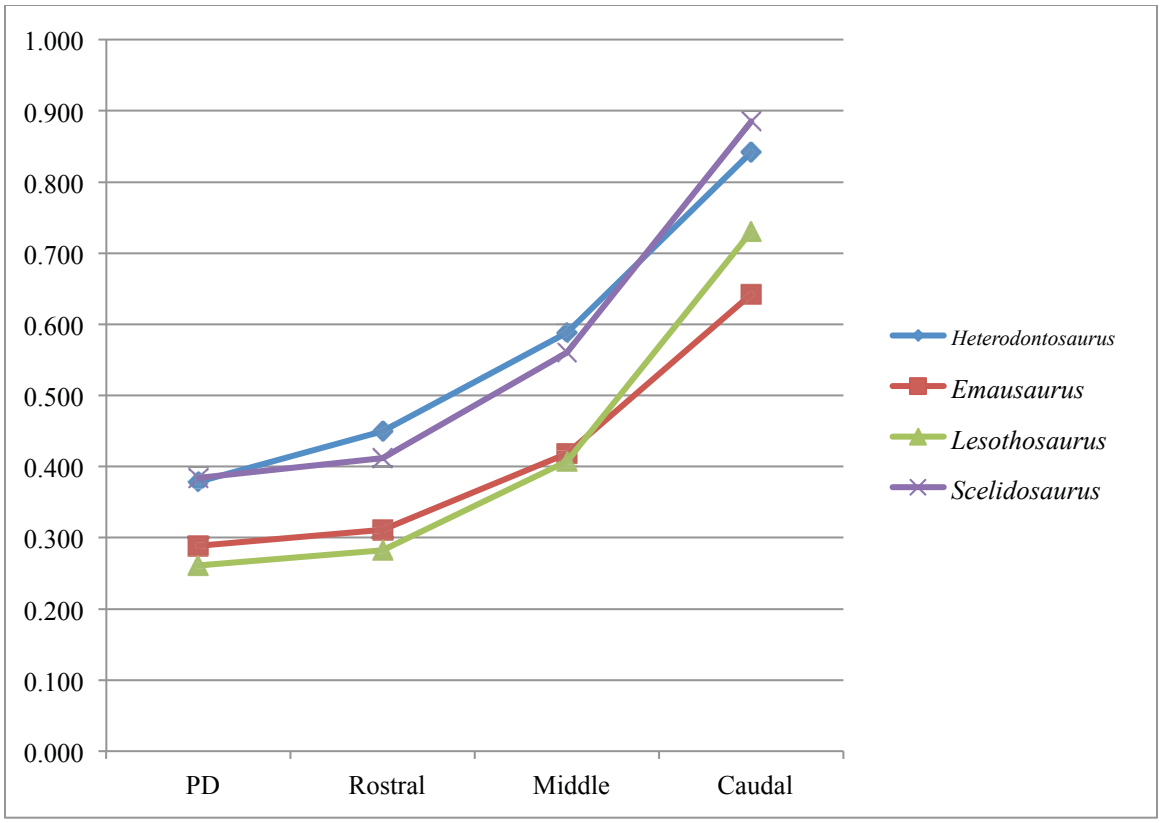

Stegosaurs and ankylosaurs also did not have a significant difference in RBFs ($p = 0.562$), which is indicative of likely inefficient feeding strategies in Thyreophorans as a

whole. Stegosaurs seem to have transitioned from a higher distal RBF in basal stegosaurs (i.e., *Huayangosaurus*) to a more mesially focused RBF in advanced stegosaurs (i.e., *Stegosaurus*). This is partially due to the fact that the stegosaur tooth row is actually shortened and displaced more rostrally in advanced forms, focusing on a rostral-focused bite in their characteristically elongate snout.

FIGURE 5.47. Stegosaur RBFs (Y-axis) across the tooth room compared to *Lesothosaurus*, a basal thyreophoran. Bite points are at the predentary (PD) tip as well as the rostral, middle, and caudal teeth.

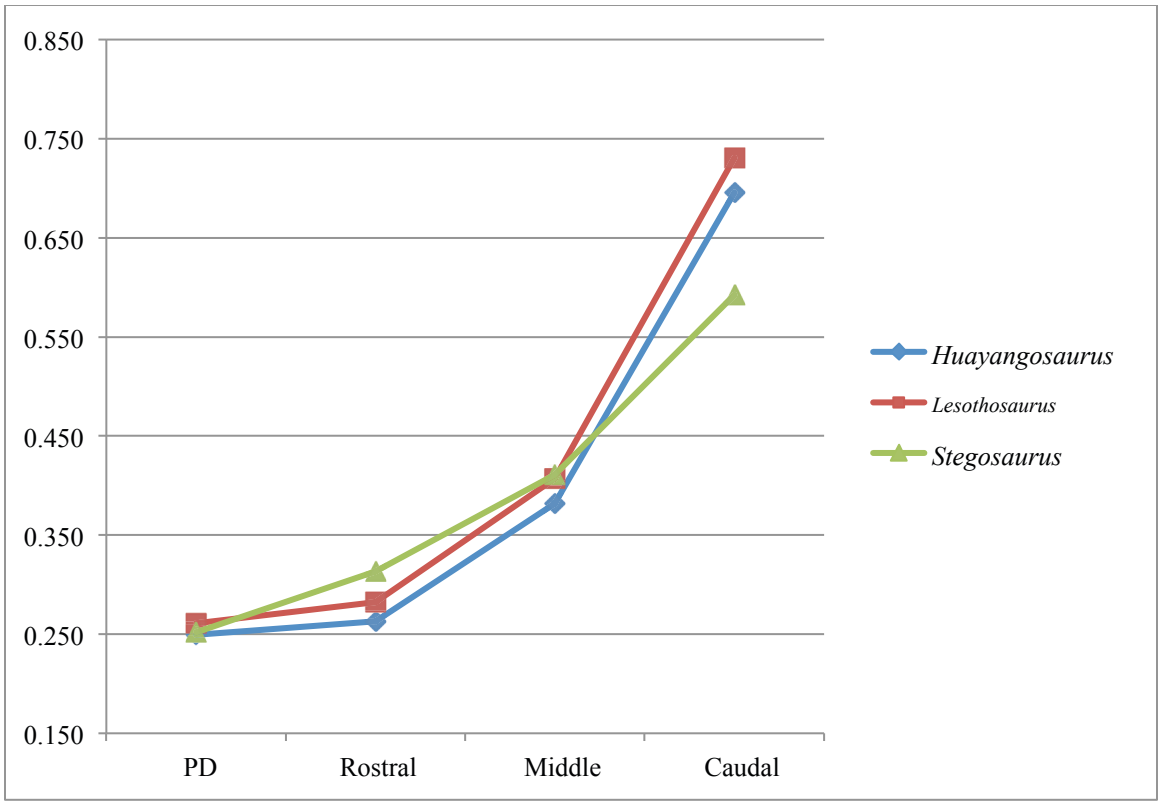

Among Ankylosauria, ankylosaurids and nodosaurids also do not significantly differ in RBF ($p = 0.733$). Mallon and Anderson (*in press*) note that nodosaurids

generally have a higher RBF than ankylosaurids. Their study only examined *Panoplosaurus* and *Euoplocephalus*, however. Although results in this study agree with Mallon and Anderson on both taxa, when adding in the nodosaurid *Edmontonia* and the ankylosaurids *Ankylosaurus* and *Pinacosaurus*, the distinction between nodosaurid and ankylosaurid RBFs is not as consistent with their results, as both ankylosaurids *Ankylosaurus* and *Pinacosaurus* both score higher in RBF totals than the *Panoplosaurus* (See Table 5.4). The ankylosaurid *Euoplocephalus* shows an exceptionally low RBF score compared to the other ankylosaurids. Much of this is due to the fact that *Euoplocephalus* possesses an exceptionally low coronoid process that is placed much more caudally along the length of the mandible compared to that of *Ankylosaurus*. Also, the lower mandible of *Ankylosaurus* is proportionately longer as well than the lower mandible of *Euoplocephalus*. Among nodosaurids, *Panoplosaurus* shows a lower RBF than that of *Edmontonia*, especially at the distal-most tooth, where *Edmontonia* exceeds the rest of the ankylosaurs. Although these two taxa have been deemed very similar, with some arguing they represent a single genus, there is a very distinctive morphological difference in mandibular shape between the two. *Panoplosaurus* has a much more rounded coronoid process with an articular glenoid that is placed much closer to the level of the tooth row, whereas *Edmontonia* possesses a coronoid process that is more triangular with a much more ventrally displaced articular glenoid. These differences in shape do much to affect the outcome of mechanical advantage and resulting RBF and should be considered.

FIGURE 5.48. Ankylosaur RBFs across the tooth room compared to *Lesothosaurus*, a basal thyreophoran, and *Stegosaurus*. Bite points are at the predentary (PD) tip as well as the rostral, middle, and caudal teeth.

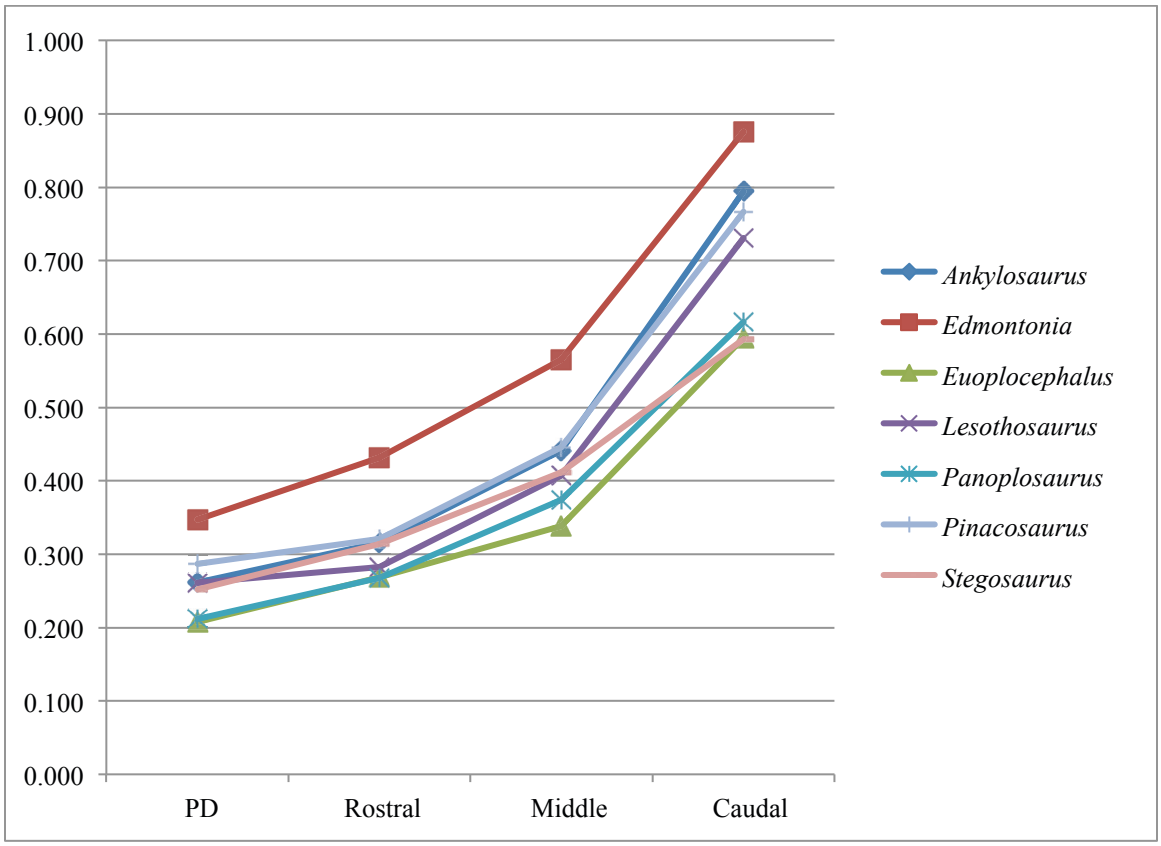

The phylogeny below visualizes the above results with optimized RBF values of the predentary and the caudal tooth compared to one another. Cooler colors (e.g., blue and purple) show the lowest RBF values and warmer colors (e.g., red, orange, and yellow) show gradually larger RBF values.

FIGURE 5.49. Phylogenetic mapping of RBFs across thyreophoran taxa, comparing predentary and caudal tooth RBF values. *Heterodontosaurus* is used as the outgroup taxon. (Compiled phylogeny [Butler et al., 2008; Maidment, 2010; Thompson et al., 2012].)

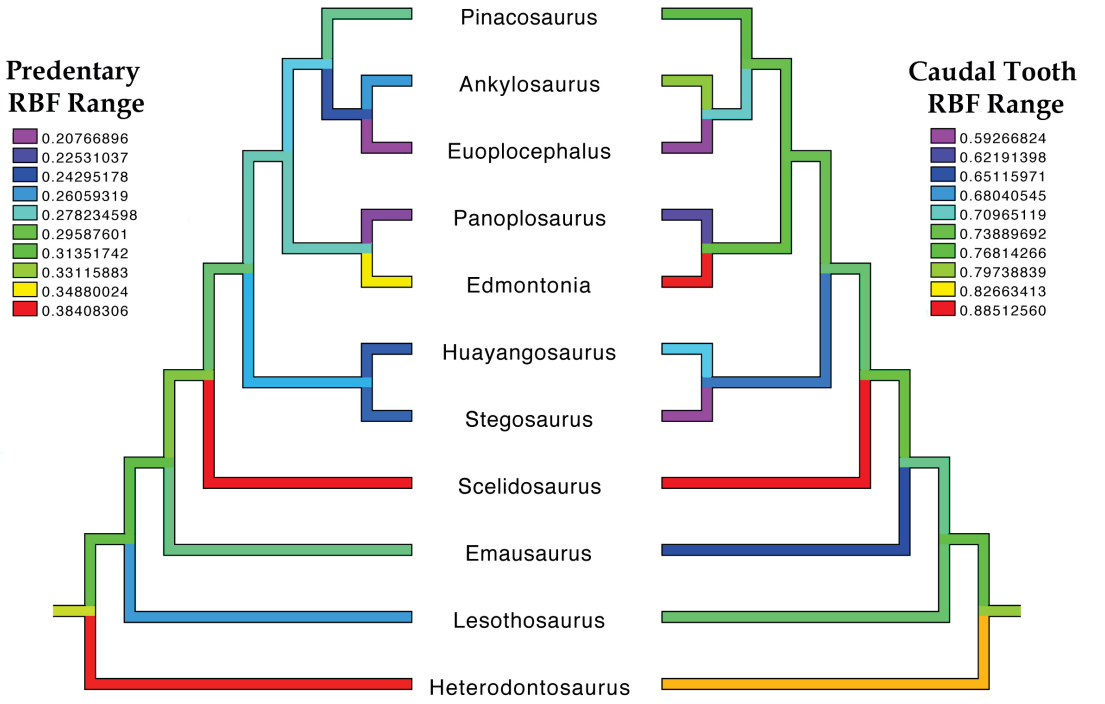

Perturbation analysis (Otten, 1983; 1985) results are shown below with RBF values with both the coronoid eminence removed and the jaw joint raised to the level of the maxillary tooth row:

TABLE 5.5. Hypothetical thyreophoran RBFs with coronoid process removed (left, black) and articular raised to level of the tooth row (right, white).

Genus	Spec. # / Ref.	Input Lever Angle in ° (mAMEP)		Predentary RBF		Rostral Tooth RBF		Middle Tooth RBF		Caudal Tooth RBF	
Ankylosaurus	AMNH 5214	58.26	56.41	0.232	0.208	0.280	0.255	0.392	0.361	0.705	0.674
Edmontonia	USNM 11868	35.29	22.86	0.258	0.200	0.321	0.254	0.420	0.345	0.651	0.563
Emausaurus	(Haubold, 1990)	70.72	68.57	0.281	0.279	0.303	0.303	0.407	0.406	0.625	0.629
Euoplocephalus	AMNH 5405	58.98	56.26	0.175	0.144	0.226	0.184	0.285	0.241	0.501	0.432
Huayangosaurus	IVPP V6728	65.97	63.57	0.231	0.214	0.243	0.227	0.354	0.329	0.645	0.616
Lesothosaurus	BMNH R8501	50.93	48.91	0.245	0.226	0.264	0.245	0.382	0.352	0.685	0.635
Panoplosaurus	ROM 1215	48.93	43.70	0.152	0.110	0.193	0.142	0.270	0.202	0.444	0.351
Pinacosaurus	ZPAL MgD-II/1	59.18	57.86	0.272	0.235	0.305	0.265	0.423	0.372	0.729	0.657
Scelidosaurus	BMNH R1111	40.54	33.08	0.332	0.257	0.356	0.276	0.484	0.383	0.765	0.627
Stegosaurus	USNM 4934	51.29	47.74	0.239	0.209	0.297	0.259	0.389	0.341	0.561	0.495

Results show that RBF values at all tooth positions in all taxa are hypothetically lower if the jaw joint is raised to the level of the tooth row than it is if the coronoid was removed. This suggests that lowering the jaw joint ventrally has a larger influence on mechanical advantage than the coronoid, thereby retaining the basal condition seen in heterodontosaurids (see Chapter 4). Also, note how removing the coronoid process increases the input muscle vector angle, as is expected. See Chapter 8 for evolutionary implications.

Chapter 6: Ornithopod Craniomandibular Anatomy

As in previous chapters, ornithopod mandibular morphology is discussed in depth below with emphasis on functional interpretation (see Table 6.1 for specimens examined; see Fig. 6.1 for phylogenetic relationships). As some of the postdentary elements do not show as much functional significance as others, only a brief discussion of each postdentary element of the mandible is given below to illustrate the general shape of this region with a larger emphasis on functionally-significant morphology. Cranial elements with direct contact to the mandible (i.e., the premaxilla, maxilla, and quadrate) provide functional implications in ornithopod jaw mechanisms and are also described for the sake of completeness. Cranial elements holding significance with regards to the jaw adductor musculature are described as needed in the Jaw Musculature section.

FIGURE 6.1. Phylogeny of Ornithopoda. A, Basal Ornithopoda until Hadrosauridae (compiled phylogeny from Butler et al., 2011 and McDonald et al., 2013); B, Hadrosauridae (Prieto-Marquez, 2010).

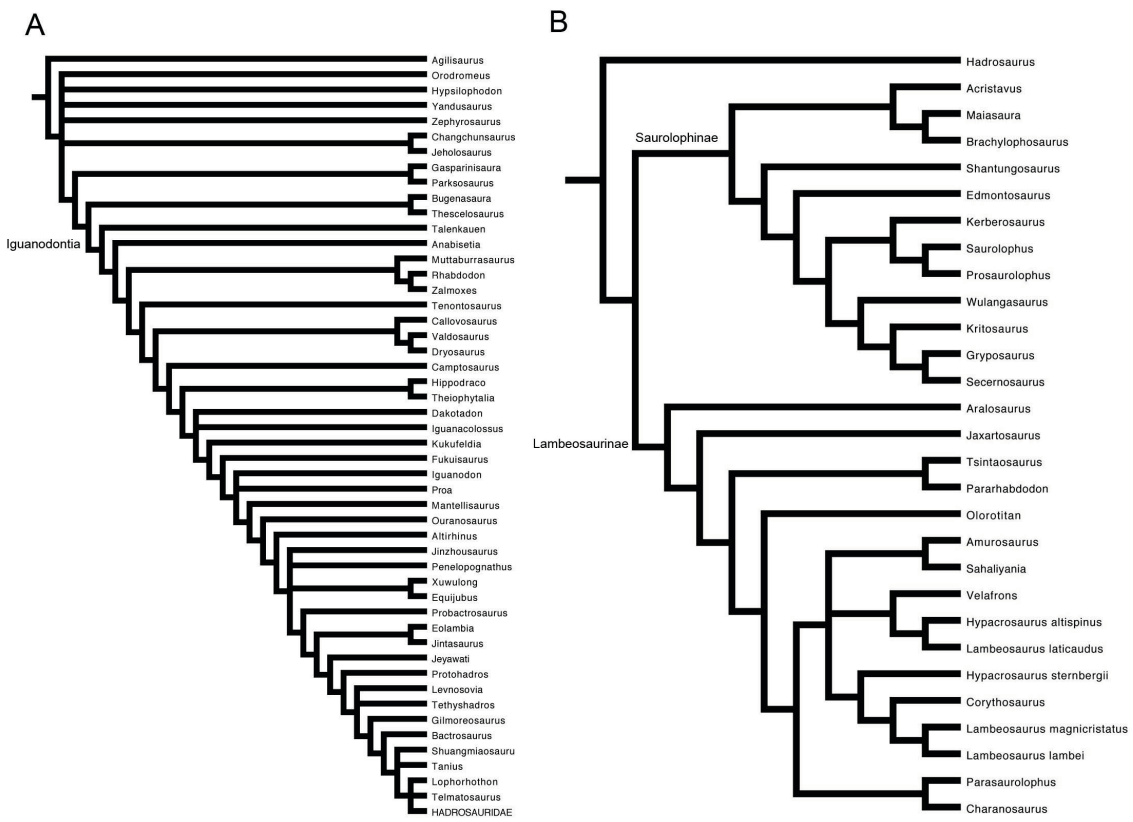

TABLE 6.1. Ornithopod specimens examined in this study. (Note: most specimens were examined by the author; however, some specimens were photographed in detail by Karen Poole and used in this study with permission.)

Taxon	Specimen	Elements
Agilisaurus (b. cerapodan)	ZDM 6011	R. jaw ramus; skull
Altirhinus	Cast	Partial jaw and skull
Anabisetia	PVPH 74	Partial paired dentaries
Bactrosaurus	AMNH 6553	Paired dentaries; l. maxilla
	AMNH 6372	Predentary

	AMNH 6365	Partial skull
	AMNH 6366	Skull roof
Bugenasaura	MOR 979	Paired dentaries; skull
Camptosaurus	AMNH 3017	Partial paired dentaries
	UMNH VP 16455	R. dentary; r. maxilla
	UMNH VP 16458	Quadrate
	USNM 4281	R. dentary
Changchunsaurus	JLUM L0403-j–Zn2	Complete skull and jaw
Corythosaurus	AMNH 3971	L. dentary
	AMNH 5240	Complete jaw and skull
	AMNH 5338	Complete jaw and skull
	AMNH 5461	Complete jaw and skull
	BMNH R9528	Partial skull with quadrate
	CMNH 1074	R. dentary; partial r. maxilla
	CMNH 11376	Paired dentaries
	ROM 759	Complete jaw and skull
	ROM 776	Complete jaw and skull
	ROM 777	Complete jaw and skull
	ROM 868	Complete jaw and skull
	ROM 869	Surangular
	ROM 870	Complete jaw and skull
	ROM 871	Complete jaw and skull
	ROM 1933	Complete jaw and skull

	USNM 11893	Predentary; paired dentaries
	USNM 16600	Predentary; r. dentary; complete skull
Dakotadon	SDSM 0863	Predentary; partial r. dentary; partial skull
Dryosaurus	CMNH 3392	Complete jaw and skull
	CMNH 11340	Complete jaw and skull
	DMNH 9001	Partial jaw and skull
Edmontosaurus	AMNH 5046	R. dentary; skull
	AMNH 5879	Paired maxillae
	BMNH R8927	Complete jaw and skull
	CMNH 9970	R. dentary
	ROM 801	Complete jaw and skull
	ROM 867	Complete jaw and skull
	ROM 64076	L. dentary; quadrate
	USNM 2155	Paired jaw (no predentary), partial skull
	USNM 3814	Complete jaw and skull
	USNM (uncatalogued)	L. dentary
Eolambia	CEUM 3191	Dentary
	CEUM 35742	Predentary
Equijubus	Cast of IVPP V12534	Complete jaw and skull
Gasparinisaura	MUCPv 208	Paired jaws (no predentary)

		and skull
Gryposaurus	ROM 764	Partial jaw and skull
	ROM 873	Complete jaw and skull
	TMP 1980.022.0001	Complete jaw and skull
Hippodraco	UMNH VP 20500	Partial jaw and skull
Hypacrosaurus	AMNH 5278	Paired jaws (no predentary); complete skull
	AMNH 5357	L. dentary; l. maxilla
	MOR 548	Complete jaw and skull
	ROM 789	Complete jaw and skull
	ROM 61784	Predentary; partial paired dentaries
Hypsilophodon	BMNH R192	L. jaw ramus; partial r. jaw ramus
	BMNH R193	Partial r. dentary
	BMNH R196	Partial jaw and skull
	BMNH R197	Complete jaw and skull
	BMNH R2470	Predentary; partial r. dentary
	BMNH R2477	Partial jaw and skull
Iguanodon	BMNH R754	Partial dentary
	BMNH R1831	R. dentary
	BMNH R11521	Predentary; l. jaw ramus

	IRSNB R51	Complete jaw and skull
	IRSNB R52	Complete jaw and skull
	IRSNB R56	Complete jaw and skull
	IRSNB Vert-05144-00001	Complete jaw and skull
	IRSNB Vert-1544-1714	Complete jaw and skull
	IRSNB Vert-1544-1715	Complete jaw and skull
	IRSNB Vert-5144-1362	Complete jaw and skull
	IRSNB Vert-5144-1639	Complete jaw and skull
	IRSNB Vert-5144-1657	Complete jaw and skull
	IRSNB Vert-5144-1716	Complete jaw and skull
Jeholosaurus	IVPP V12529	Complete jaw and skull
Kritosaurus	AMNH 5799	Complete jaw and skull
	USNM 8629	L. jaw ramus
Kukufeldia	BMNH R28660	R. dentary
Lambeosaurus	AMNH 5353	Complete jaw and skull
	AMNH 5373	Complete jaw and skull
	AMNH 5382	Partial jaw (no predentary); partial skull
	BMNH R9527	R. dentary; skull
	ROM 758	Complete jaw and skull
	ROM 794	Complete jaw and skull
	ROM 869	Complete jaw and skull
	ROM 1218	Complete jaw and skull

	TMP 1966.004.0001	Complete jaw and skull
	TMP 1981.37.1	Partial jaw and skull
	USNM 10309	Predentary; r. dentary; quadrate
Maiasaura	ROM 44770	Complete jaw and skull
	ROM specimen	Predentary; r. dentary; skull
	ROM Cast of MOR Juv.	Complete jaw and skull
Mantellisaurus	BMNH R5764	R. dentary
	IRSNB R57	Complete jaw and skull
Orodromeus	MOR 294	Complete jaw and skull
Ouranosaurus	Cast	Complete jaw and skull
Parasaurolophus	NMMNH P-25100	L. jaw ramus; l. maxilla
	ROM 768	Complete jaw and skull
Parksosaurus	ROM 804	Partial jaw and skull
Prosaurolophus	ROM 787	Complete jaw and skull
	ROM 789	Complete jaw and skull
	USNM 12712	Complete jaw and skull
Saurolophus	AMNH 5220	Complete jaw and skull
	AMNH 5221	Paired dentaries; paired premaxillae; paired maxillae
	ROM 21703 (Cast)	Partial jaw and skull
Telmatosaurus	AMNH 5145 (cast of	Paired jaws (no predentary);

	holotype)	partial skull
Tenontosaurus	AMNH 3034	Partial jaw and skull
	YPM 5456	Complete jaw and skull
Theiophytalia	YPM 1887	Partial jaw and skull
Thescelosaurus	NCSM 15728	Complete jaw and skull
	USNM 14686	L. jaw ramus
Velafrons	ROM 53490 (Cast)	R. dentary; l. maxilla
Yandusaurus	ZDM 6001	Partial jaw and skull
Zalmoxes	BMNH R3389	Quadrate
	BMNH R3392	R. dentary
	BMNH R3393	Quadrate
	BMNH R3394	Predentary
	BMNH R3407	R. dentary
	BMNH R3410	Predentary
	BMNH R4899	Partial l. dentary
	BMNH R4900	Partial r. dentary
	BMNH R4910	Partial jaw
	BMNH R4912	L. dentary
Unidentified hadrosaurids	AMNH 5285	Predentary
	AMNH 21523	L. dentary
	AMNH 21524	L. dentary
	AMNH 21529	Predentary; l. dentary; maxilla

	AMNH 5899	Paired dentaries; quadrate
	KUVP 17400	L. dentary
	KUVP 96884	Dentary
	KUVP 96887	Dentary
	TMP 1975.11.45	Predentary
	TMP 1991.36.311	Predentary

OSTEOLOGICAL DESCRIPTION

The following descriptions were based on personal examination of specimens. For further descriptions, see Lambe (1920), Ostrom (1961), Galton (1974; 1983), Weishampel (1984), Horner (1992), Boyd et al. (2009), Norman (1984), Norman (1986), Norman (2004), Norman et al. (2004), Horner et al. (2004), Evans (2010), and more referenced below. Due to the large abundance of ornithopod craniomandibular material, both personally examined for this study and referenced in text, descriptions are based on observations of all specimens listed in Table 6.1 unless otherwise noted in the text.

FIGURE 6.2. Diversity of ornithopod skulls. A, *Hypsilophodon*; B, *Thescelosaurus*; C, *Dryosaurus*; D, *Iguanodon*; E, *Edmontosaurus*; F, *Prosaurolophus*; G, *Gryposaurus*; H, *Corythosaurus*; I, *Parasaurolophus*. Left lateral views. Scale bars = 5 cm.

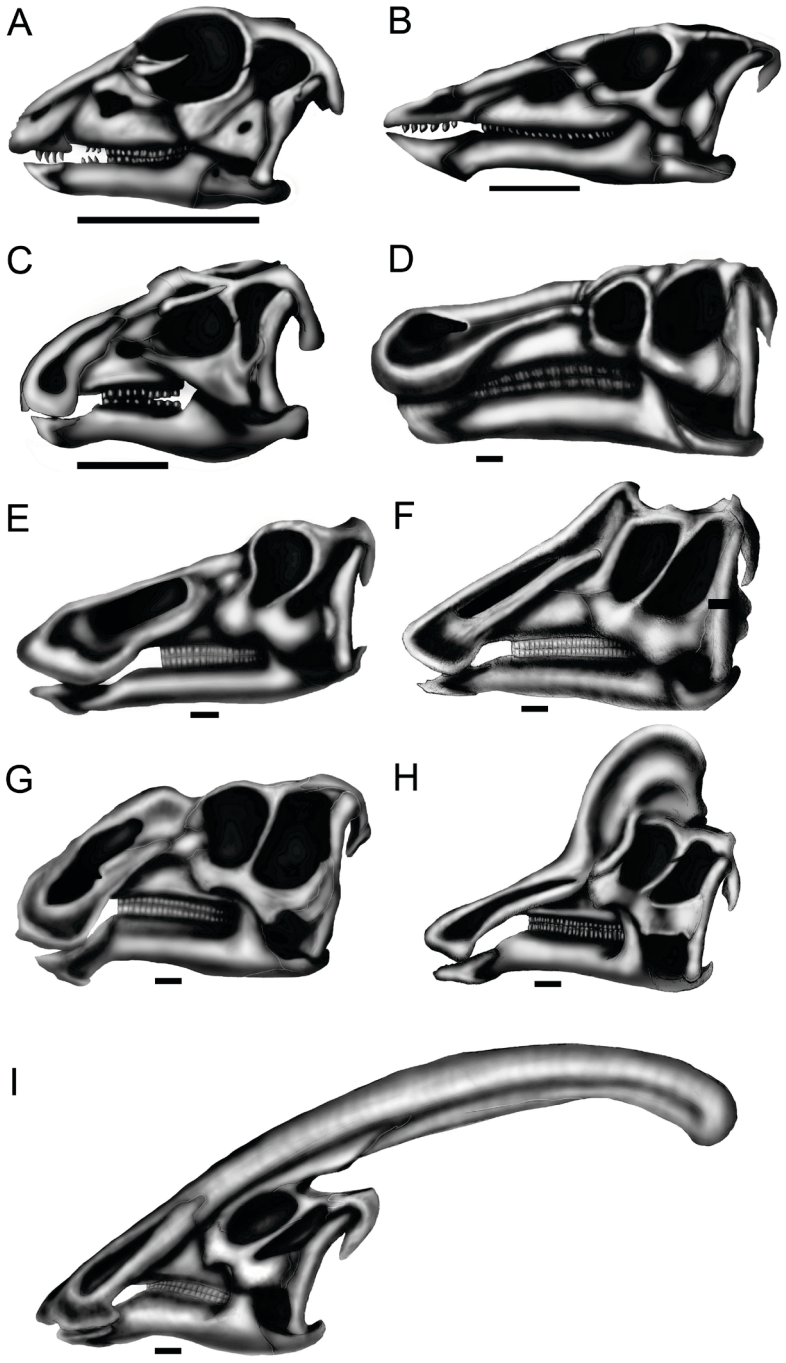

Cranium

Ornithopod crania (Fig. 6.2; 6.3) are generally wedge-shaped in lateral view, being rostrocaudally blunter relatively in more basal forms and more elongate in the derived iguanodontians. Ornithopod skulls in general are triangular in dorsal and palatal view. The derived hadrosauroids evolved a dorsoventrally compressed rostrum, creating what is commonly described as an edentulous duckbill (Morris, 1970). Basal ornithopods and non-hadrosauroid iguanodontians typically have large, circular orbits, whereas the orbits of hadrosauroids tend to be dorsoventrally elongate and elliptical. Caudal to the orbit, the infratemporal fenestra is small and circular in basal ornithopods and much larger and rectangular in iguanodontians, with a thin upper temporal bar dorsally. The postorbital process, made by the postorbital and jugal, is a very thin rod and both elements are joined at a flat articular surface. A small, rounded antorbital fenestra is seen in basal ornithopods and becomes either highly reduced or disappears in the derived iguanodontians. The external naris is typically small and circular. The jugal is roughly continuous with the caudoventrally-oriented ventral rim of the cranium in the most basal ornithopods (*Hypsilophodon* [BMNH R197], *Yandusaurus* [ZDM 6001], *Orodromeus* [MOR 294], *Gasparinisaura* [MUCPv 208], *Parksosaurus* [ROM 804], *Changchunsaurus* [JLUM L0403-j–Zn2], *Jeholosaurus* [IVPP V12529], *Bugenasaura* [MOR 979], and *Thescelosaurus* [NCSM 15728]), but becomes much more flange-like and triangular in the derived iguanodontians, extending caudoventrally with respect to the ventral margin of the maxillary tooth row. The quadrate, where it forms half of the jaw joint, has a ventral head that extends below the level of the tooth row, as described below.

FIGURE 6.3. *Corythosaurus* (hadrosaurid) skull (generalized). Abbreviations: itf, infratemporal fenestra; la, lacrimal; j, jugal; m, maxilla; n, nasal; or, orbit; pf, prefrontal; pm, premaxilla; po, postorbital; pop, paroccipital process; q, quadrate; sq, squamosal; stf, supratemporal fenestra. Left lateral view. Scale bar = 10 cm.

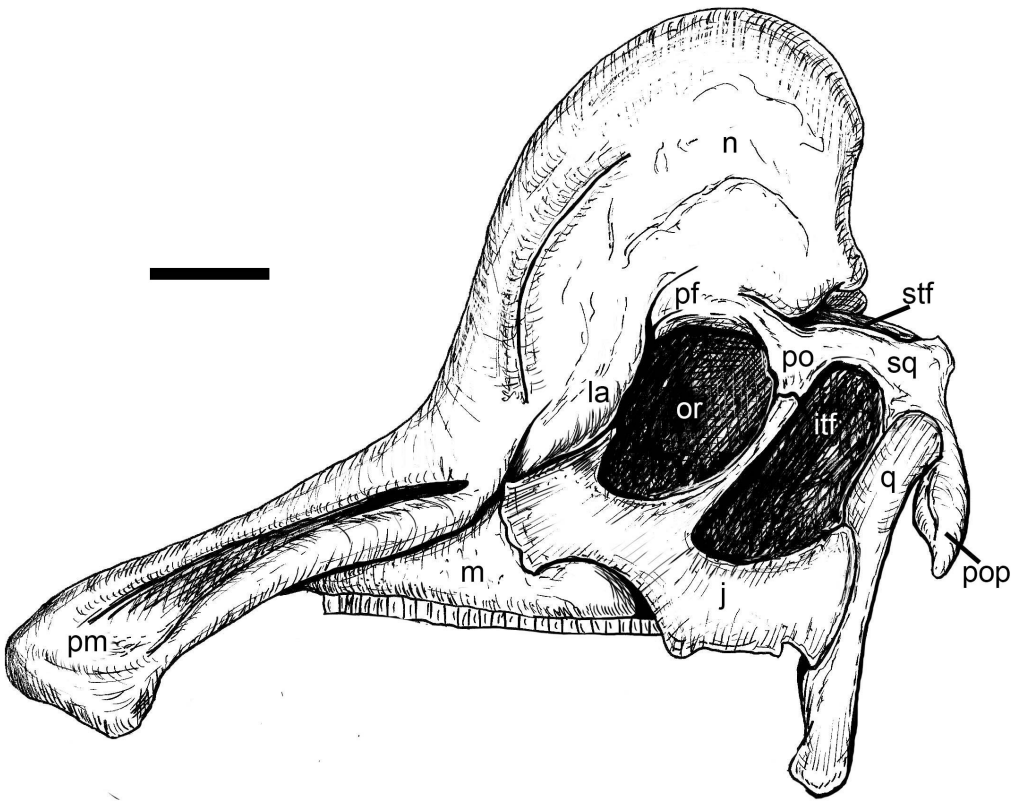

The dorsal edge of the nasal continues the rostral tapering of the skull in dorsal view and is situated in between the paired premaxillae. In lambeosaurine hadrosaurids, the nasal, along with other dorsal cranial elements, is integrated into an elaborate hollow crest, with each taxon possessing its own unique morphology from a long tube-like structure, such as in *Parasaurolophus*, to a hump-like crest, such as in *Corythosaurus*, to extravagant crests, such as in *Lambeosaurus*. The paroccipital processes are triangular

and robust, angled slightly laterally with respect to the occiput in caudal view.

Premaxilla—The premaxilla articulates with the maxilla, nasal, and vomer caudally. It has a rostral narial process that forms the rostral margin of the naris and contacts the nasals above the naris. Behind the naris is a more robust caudodorsally- long, thin process extends between the nasal and the maxilla, creating the dorsal margin of the external naris. This process joins with the nasal and maxilla caudal to it and joins the snout together. In lateral view, the premaxilla in many basal ornithopods, including basal-most iguanodontians, is either dorsoventrally deep, as in *Hypsilophodon* (BMNH R197) and *Iguanodon* (e.g., IRSNB R51), or rostrocaudally elongate, like that in *Thescelosaurus* (NCSM 15728) (Fig. 6.4).

FIGURE 6.4. Lateral view of basal ornithopod premaxillae. A, *Hypsilophodon* (BMNH R197); B, *Thescelosaurus* (NCSM 15728). Scale bars = 1 cm.

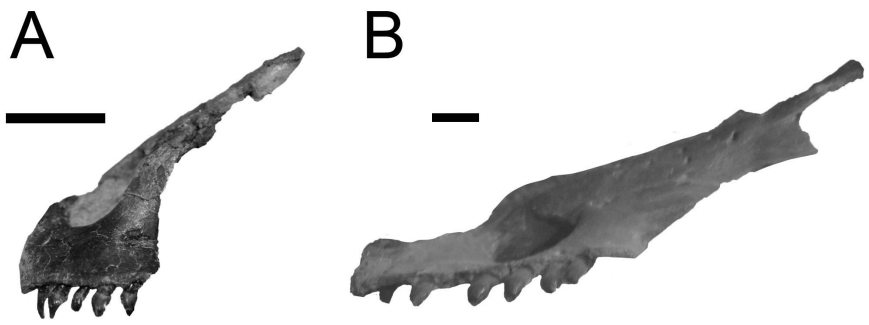

Basal ornithopods and their close relatives bear around five conical teeth on the ventrolateral margin of each premaxilla (see Dentition section below). These teeth occluded with the lateral surface of the keratinous rhamphotheca of the predentary at the

rostral tip of the mandible. Later ornithopods reduce the number of premaxillary teeth, then lose them altogether. In all ornithopods, the premaxilla is ventrally offset relative to the maxilla, sutured immediately caudal to it. In basal ornithopods and non-hadrosauroid iguanodontians, the ventral oral margin of the premaxilla is relatively horizontal in lateral view, whereas in hadrosauroids, it is typically angled rostroventrally along the oral margin. The rostral-most predentary always has an edentulous oral margin of varying sizes.

The premaxilla forms a majority of the dorsoventrally compressed, "duckbill" structure seen in hadrosauroid snouts, forming a large, rounded shape of the rostral snout when both premaxillae are joined medially in rostral view (Fig. 6.5). Iguanodontians possess an edentulous premaxilla. The ventral rim of this toothless rostral end of the premaxilla in these taxa is thick and rugose, with implications of being enveloped by a keratinous rhamphotheca that likely occluded with its counterpart covering the predentary. Ventrally, the premaxillary palatal roof is especially broad in iguanodontians and joins the vomer caudomedially.

FIGURE 6.5. *Corythosaurus* (ROM 776) premaxilla in lateral view showing dorsoventrally compressed duckbill morphology.

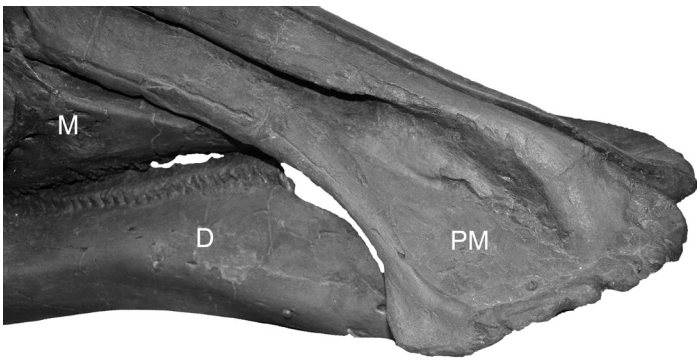

Maxilla—The maxilla (Fig. 6.6) borders the premaxilla rostrally and dorsally, the palatine and vomer medially, the pterygoid and ectopterygoid caudally, the lacrimal dorsally, and the jugal caudodorsally. In lateral view, the maxilla is triangular with a rostrally-oriented process. In hadrosaurids, the rostrodorsal margin of the hadrosaurid maxilla possesses two elongate, thin, and parallel sheets of bone that run caudodorsally, upon which the premaxilla rests dorsally, a suture at which the maxilla is said to have rotated in the pleurokinetic feeding model (Weishampel, 1984a; Norman and Weishampel, 1985)**.** A series of dental foramina are present just dorsal to the dentition on the medial and lateral sides, with hadrosaurids possessing a dorsally displaced, arched row of alveolar foramina on its medial surface, for entry of the maxillary nerve (V_2) and artery to supply the dentition.

FIGURE 6.6. *Parasaurolophus* (NMMNH P-25100**)** maxilla in lateral view. Scale bar = 5 cm.

The maxilla forms the ventral margin of the antorbital fenestra in basal ornithopods. This fenestra is either highly reduced or non-existent in the derived hadrosaurids. The bony lateral edge of the maxillary tooth row is convex laterally forming a visible buccal shelf, with its tooth row consequently situated in a medially inset, emarginated placement, with the dentition oriented ventrally. This emargination had been suggested to be the attachment of a cheek-like soft tissue structure (Galton, 1973; however, see Papp and Witmer (1995) for a rebuttal of this). See Dentition section below for a description of ornithopod dental morphology.

Quadrate—The quadrate is a tall, columnar element, with its rounded dorsal head, which, in most cases, fits securely in the ventrolaterally-facing cotylus of the squamosal in a ball-and-socket articulation between the pre- and post-quadratic processes. In some specimens, however, such as in *Corythosaurus* (ROM 776), the dorsal head of the quadrate is smaller than the squamosal socket, which suggests considerable mobility, as is suggested in the pleurokinetic feeding model (Fig. 6.7; Weishampel 1984a, Norman and Weishampel, 1985).

FIGURE 6.7. *Corythosaurus* (ROM 776) proximal quadrate head exhibiting rare case of loose articulation with squamosal.

Much like that seen in heterodontosaurids and other ornithischians, the quadrate, as it descends to the jaw joint, arches rostrally in lateral view until the quadratojugal blocks it from view laterally. This arching is especially apparent in *Dryosaurus* (CMNH 3392; Fig. 6.8), for example, which has an exaggerated rostral curvature of the quadrate mid-shaft.

FIGURE 6.8. *Dryosaurus* (CMNH 3392) rostrally bowed quadrate in lateral view. Scale bar = 2 cm.

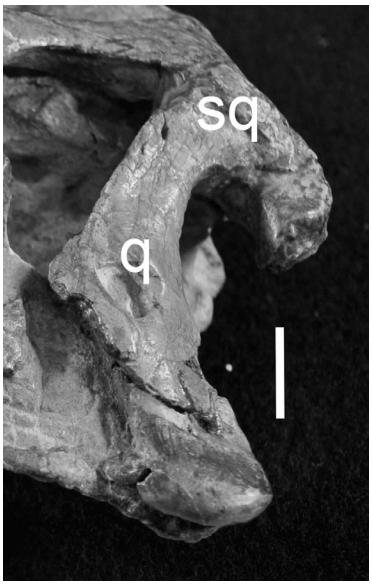

It exhibits an embayment on its rostral edge with a rostrally-arched . A sheet of bone extending from its the rostromedial edge of the quadrate shaft creating the pterygoid wing that overlaps the quadratic wing of the pterygoid. The quadratojugal sutures with the embayed rostrolateral margin of the quadratic body and covers the lateral side of the quadrate ventrally, but not at its most ventral head. The quadrate is only slightly angled rostrally, but is relatively straight in many ornithopods compared to other ornithischians, with some variable exceptions within Hadrosauridae, such as *Parasaurolophus* (e.g., ROM 768; Fig. 6.9) and *Edmontosaurus* (e.g., BMNH 8927), where the quadrate is angled rostrally to a much higher degree, although some of this might be due to taphonomic distortion.

FIGURE 6.9. *Parasaurolophus* (ROM 768) quadrate in lateral view showing slight rostroventral angle.

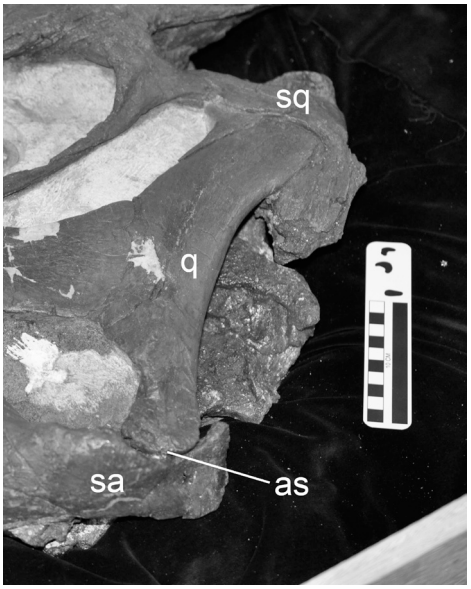

The ventral head of the quadrate extends farther than the level of the maxillary tooth row, to a variable degree depending on the taxon, resulting in a ventrally offset jaw articulation. In some basal ornithopods, such as *Thescelosaurus* (NCSM 15728), the ventral head of the quadrate is even deflected caudally again, as is seen in heterodontosaurids. The quadrate in most hadrosauroids is notably very spherical at its ventral end, where it is almost completely ball shaped in derived hadrosauroids.

Conversely, in basal hadrosauroids and other ornithopods, the ventral head of the quadrate typically has two condyles situated mediolaterally, forming a mediolaterally-elongate ventral head. This morphology creates more of a bicondylar, albeit asymmetrical, hinge synovial joint in non-hadrosaurids and more of a ball-and-socket synovial joint in hadrosaurids at which the mandibular corpus could potentially rotate mediolaterally as well as rostrocaudally within the synovial capsule (Fig. 6.10).

FIGURE 6.10. Ventral head of ornithopod quadrates. A, *Iguanodon* (*Mantellisaurus)* (left) (BMNH R11521); B, *Edmontosaurus* (right) (ROM 64076).

Predentary

The predentary (Figs. 6.11; 6.12; 6.13; 6.14; 6.15; 6.16; 6.17; 6.18; 6.19; 6.20) is a single, unpaired, median element resting upon the rostral end of the articulated paired dentaries. It is edentulous and forms the lower bill that comes in contact with the premaxilla when the oral cavity is closed. It is the only part of the mandible that contacts the premaxilla, occluding rostrally. A keratinous rhamphotheca likely surrounded the rostral and lateral surfaces of the predentary, as indicated by a rugose outer surface (Morris, 1970).

Depending on the taxon, ornithopod predentaries have a great diversity of beak morphologies. In the most basal ornithopods (*Hypsilophodon* [BMNH R197; Fig. 6.12], *Changchunsaurus* [JLUM L0403-j–Zn2], *Jeholosaurus* [IVPP V12529], and

Thescelosaurus [NCSM 15728; 6.11]), as well as in *Dryosaurus* (CMNH 3392; 11340), it is triangular and has a rostrally pointed, scoop-shaped tip. This tip is elongate in *Jeholosaurus* and even more so in *Thescelosaurus* and *Changchunsaurus*, both of which have much longer and sharper rostral snouts. Predentaries of this arrow-like shape generally have a thin dorsal oral margin with a very thin, mediolaterally-expanded dorsal edge that occluded with the premaxilla.

FIGURE 6.11. *Thescelosaurus* (NCSM 15728) predentary in right lateral view and its articulation with dentary. Scale bar = 2 cm.

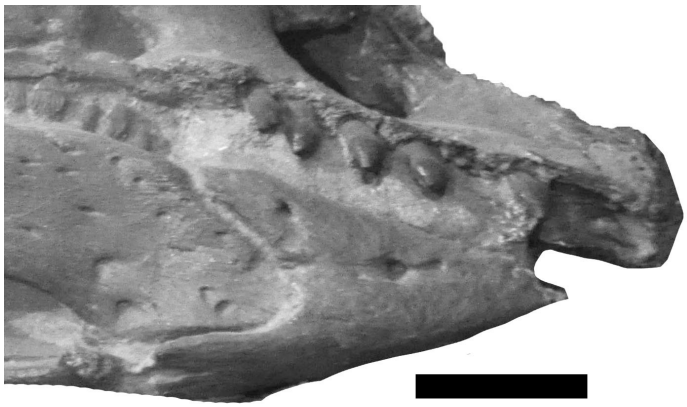

In lateral view, predentaries of this form taper rostrodorsally to the tip and a longitudinal groove runs from the rostral tip along the lateral margin of the predentary, dividing the caudolateral and ventral processes (described below). One or two foramina are usually present on the caudal half of this groove for neurovasculature to the keratinous sheath. The inner, oral surface is moderately concave transversely and slopes dorsally to the rostral margin. Dorsally-projecting denticles are usually not present in the most basal ornithopod predentaries. *Dryosaurus*, along with the sharp rostromedial

process, also possesses a dorsally-projecting, flat, triangular denticle on each lateral side, creating a three-pronged, tiara-like appearance of the predentary.

FIGURE 6.12. *Hypsilophodon* predentary restored. A, lateral view. B, dorsal view. Based on BMNH R197 and Galton (1974). Scale bar = 1 cm.

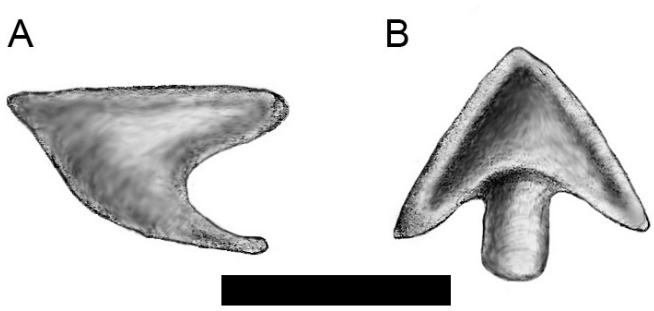

A predentary with a broadly expanded, U-shaped rostral edge is seen in *Zalmoxes* (BMNH R3394; R3410; Weishampel et al., 2003; Fig. 6.14), *Tenontosaurus* (YPM 5456), *Iguanodon* (e.g., BMNH R11521; IRSNB R51; R52; R56; Figs. 6.13; 6.15; 6.16), *Equijubus* (IVPP V12534), *Eolambia* (CEUM 35742), *Gilmoreosaurus* (Prieto-Marquez and Norell, 2010), *Bactrosaurus* (AMNH 6372), and most other non-hadrosaurid iguanodontians, although, interestingly, it can also be seen in the hadrosaurid "*Kritosaurus*" (AMNH 5799; see Fig. 6.20).

FIGURE 6.13. *Iguanodon* (IRSNB R56) predentary in rostrodorsal view.

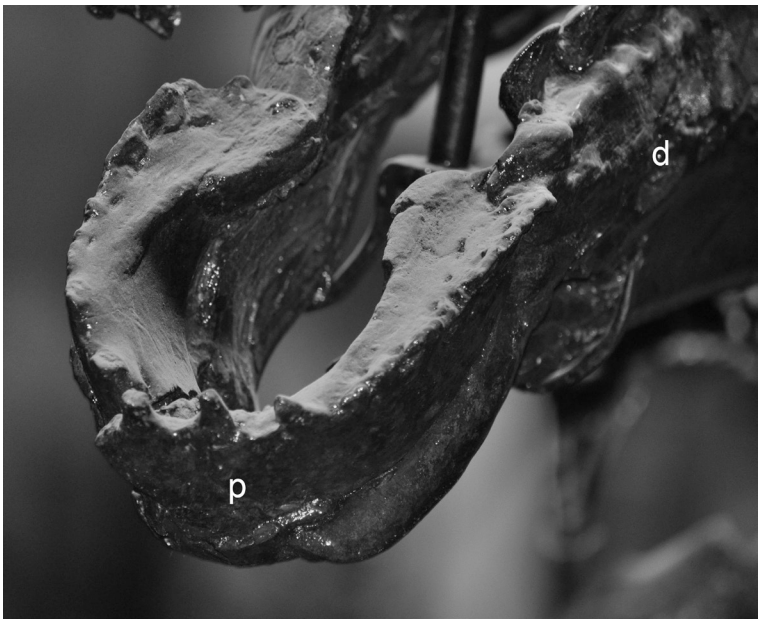

These predentaries have parallel caudolateral processes (see below), although in *Ouranosaurus* (Taquet, 1976) is a special case in which the caudolateral processes are only parallel at the very distal lateral tips, forming a much straighter ventral edge and rod-like body. The caudolateral processes also have a gently transversely concave inner oral surface that tapers to the dorsal margins. The dorsal margins of these predentaries, for the most part, have pointed (e.g., *Iguanodon* and *Equijubus*) or rounded (e.g., *Probactrosaurus* [Norman, 2002]), dorsally-projecting denticles, with one midline denticle the largest and the subsequent denticles on either side slightly shorter or of equal height. These denticles are not seen, however, in *Zalmoxes* or "*Kritosaurus*". These taxa instead have a smooth, flattened dorsal edge, with a slight slope on the inner side. *Zalmoxes* is unusual among ornithopods in that it has a relatively much deeper predentary body dorsoventrally that encloses the dentaries at the symphysis.

FIGURE 6.14. *Zalmoxes* predentary restored. A, lateral view. B, dorsal view. Based on BMNH R3394, BMNH R3410, and Weishampel et al. (2003). Scale bar = 2 cm.

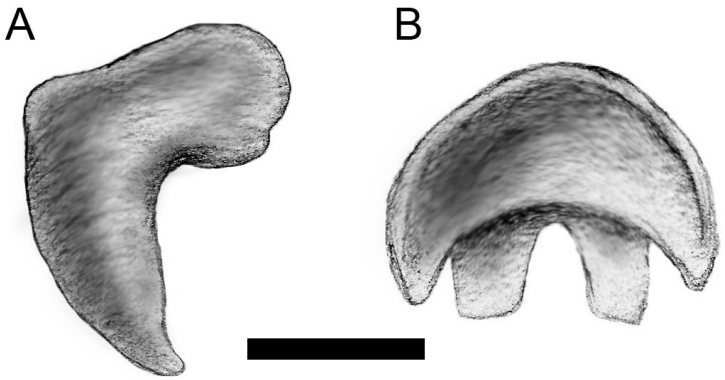

In most other hadrosaurids, with the exception of "*Kritosaurus*", both lambeosaurines and hadrosaurines, the predentary forms a flat, expanded, shovel-like rostral edge. Along the rostrodorsal border, between four to eight blunt, sub-rectangular (sometimes conical) projections that protrude dorsally on either side of the sagittal plane (with a midline projection in some cases) form a denticulate dorsal edge, much like the ventrally oriented denticulate edge of the premaxilla. Just ventral to these projections is a series of foramina that pierce rostrocaudally the rostral ridge, the largest of which is immediately lateral to the sagittal plane. These foramina likely housed branches of the mental artery and nerve (c.n. V), as they branched from the inferior alveolar artery and nerve that provided blood and nerve supply to the keratinous bill (Ostrom, 1961).

FIGURE 6.15. *Iguanodon* predentary (generalized). A, lateral view. B, dorsal view. Scale bar = 4 cm.

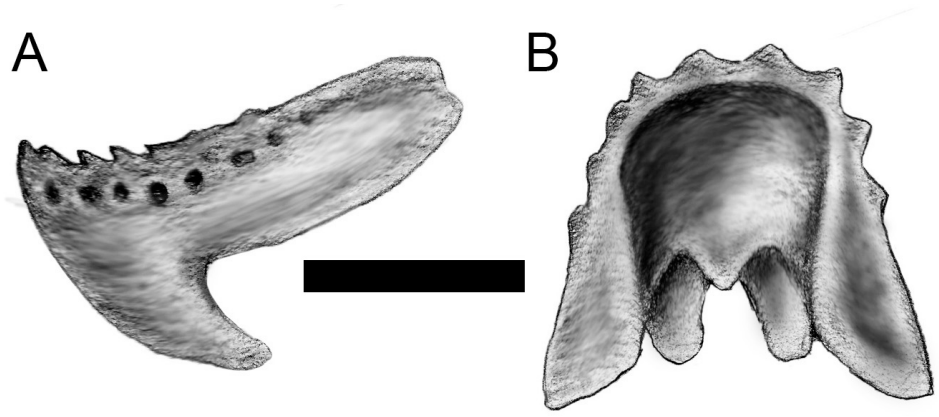

Four processes contact the paired dentaries in ornithopods, except for in basal ornithopods, (e.g., *Hypsilophodon*, *Jeholosaurus*, *Thescelosaurus*, and *Changchunsaurus*) as well as *Dryosaurus* and *Zalmoxes*, which only have three processes. Two extend caudally along the sagittal plane, both on the dorsal and ventral aspect of the predentary. In non-hadrosauroid iguanodontians, the dorsal process is a small, triangular caudal protrusion from the articular surface that braces the dorsal margin of the dentary symphysis.

FIGURE 6.16. *Iguanodon* (*Mantellisaurus*) (BMNH R11521) predentary in lateral view in articulation with dentary. Ruler units in cm.

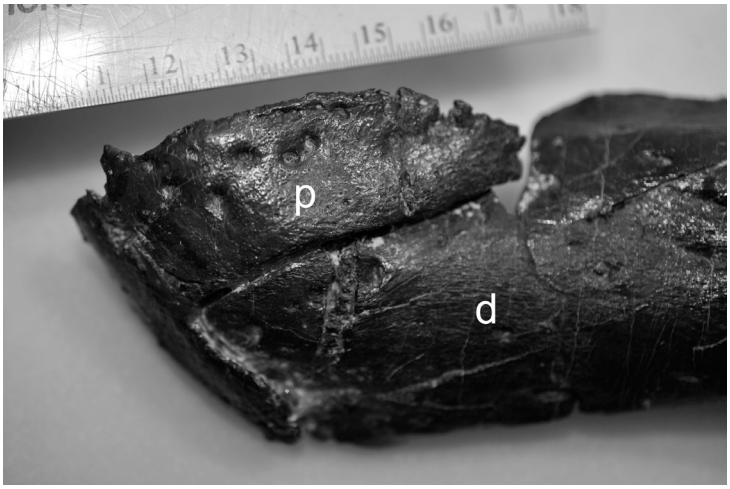

In hadrosauroids, the dorsal process is elongate, straight, and rod-like with a sub-triangular dorsal ridge and a conical caudal tip, also resting upon and bracing the dorsal aspect of the dentary symphysis (Figs. 6.17; 6.18; 6.19). The ventral process is prominent and braces the ventral surface of the dentary symphysis. In basal ornithopods, this ventral process is a single midline projection that extends caudoventrally in either a pointed (e.g., *Hypsilophodon*, *Jeholosaurus*, and *Thescelosaurus*) or laterally broadened, plate-like morphology (e.g., *Jinzhousaurus* [Barrett et al., 2009]). In lateral view, *Hypsilophodon* has a shorter ventral process than dorsal process, unlike *Jeholosaurus* and *Thescelosaurus*, which have a longer ventral process underlying the symphysis like that seen in the basal ceratopsian *Archaeoceratops* (IVPP v1114). In most other derived ornithopods, the ventral process is broad, mediolaterally flat, and bilobate, with each lobe supporting its corresponding dentary at its rostroventral aspect. In lambeosaurines, the caudodorsal process is longer than the ventral process, whereas in hadrosaurines it is typically the opposite.

FIGURE 6.17. Generalized hadrosauroid predentary (based mainly on *Lambeosaurus*, USNM 10309). Note that there is much variation between species. A, dorsal view, top is rostral; B, rostroventral view; C, lateral view. Abbreviations: clp, caudolateral process; d, denticle; dp, dorsal process; f, foramen; vp, ventral process. Scale bar equals 5 cm.

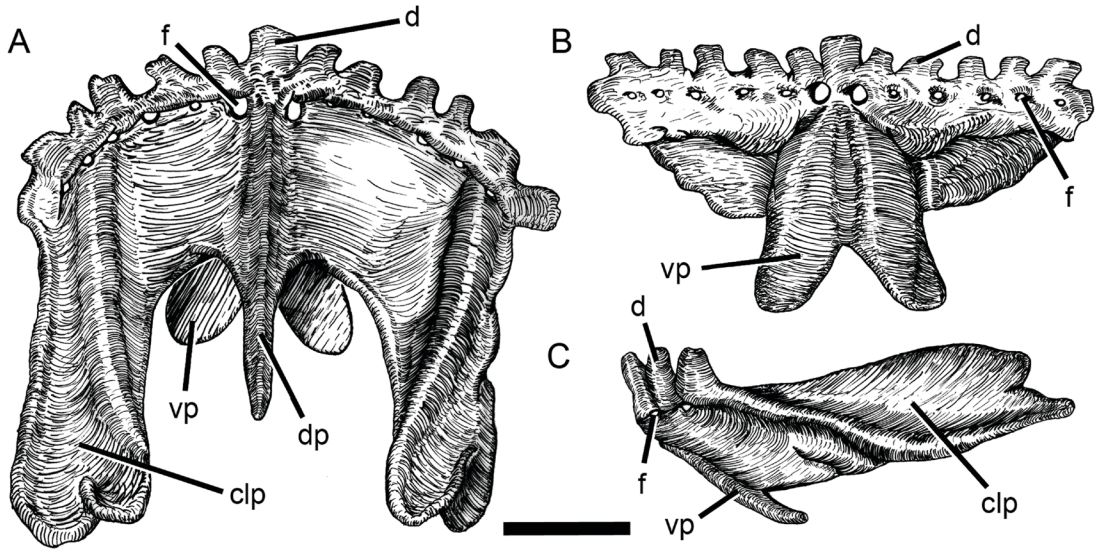

Two larger processes project caudolaterally to rest upon the rostrodorsal edge of each dentary. In dorsal view, depending on the taxon, the processes of the predentary provide its characteristic V- or U-shape with both caudolateral processes forming a broad, triangular plane on each side as they continue rostrally, forming a butterfly-like shape in hadrosauroids (e.g., *Corythosaurus* [USNM 11893], *Lambeosaurus* [USNM 10309] and many others [see also Table 6.1]).

FIGURE 6.18. Hadrosauroid predentaries. A-C, hadrosaurid predentary (TMP 1991.36.311); A, dorsal view; B, lateral view; C, caudoventral view depicting articular surface; D-F, *Lambeosaurus* predentary (USNM 10309); D, dorsal view, rostral up; E, rostral view; F, close-up of caudoventral view with arrows depicting caudomedial space of predentary between the dorsal and ventral processes where both dentaries articulated with the predentary and each other. Abbreviations: as, articular surface; clp, caudolateral process; d, denticle; dp, dorsal process; f, foramen; vp, ventral process. Scale bars equal 5 cm.

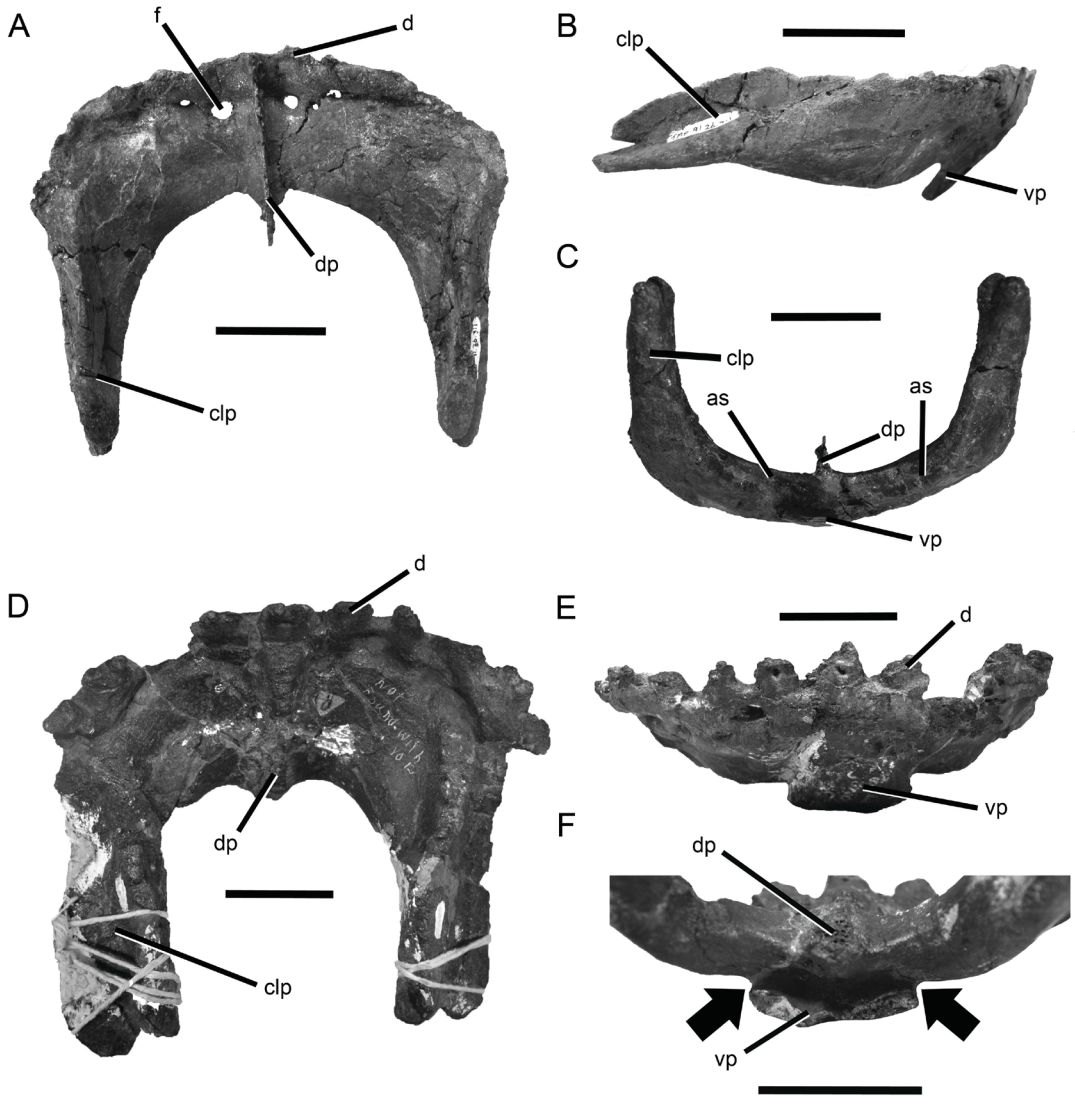

In caudal view, the end of each process is broadened and laterally compressed. In basal ornithopods, it consists of a unilobate projection, but in most iguanodontians, it is typically bilobate, and sometimes bowed slightly medially. Each process is angled, forming a flat, dorsomedial to ventrolateral plane. This plane on the medial side of each process continues rostrally and becomes less broadened and shallowly concave on the medial side midway to the rostral border (Figs. 6.19; 6.20). This makes for an osteologically unstable articulation with the sharp, rostral ridge of the dentary on both sides; there is no tight, clasping junction and it provides a surface on which the dentary was able to move freely (Figs. 6.19; 6.20).

FIGURE 6.19. Surface scan of *Corythosaurus* (USNM 11893) predentary showing articular surface. A, Dorsal view showing predentary shape; B, caudoventral view with darker shaded area depicting wide range on which the sharp, dorsal ridge of the rostral end of the dentary variably articulates. Abbreviations: as, articular surface; clp, caudolateral process; dp, dorsal process; p, pit (see Discussion section); vp, ventral process. Scale bar equals 3 cm.

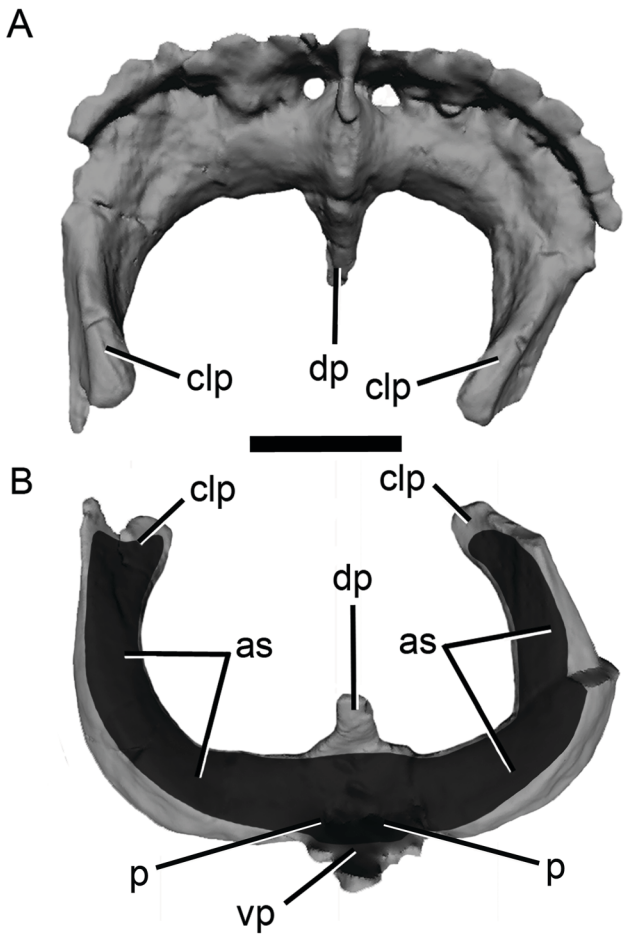

When the dentary is articulated with the ventral portion of the medial aspect of the large caudolateral process of the predentary, a gap is formed on the dorsal portion of that articular surface. Conversely, when the dentary is articulated with the dorsal portion of that articular surface, another gap on the ventral region is found between the smooth surface of the predentary and dentaries. This morphology further indicates a broad, flat surface area against which the dentaries were potentially able to articulate freely in relation to the predentary. Together these spaces show that membranous or ligamentous tissues, at least in Hadrosauroidea, likely held the two elements together.

FIGURE 6.20. Predentary-dentary articulation of *Kritosaurus* (AMNH 5799). A, restored illustration with arrows depicting gaps between the elements; B, photograph of articulated specimen indicating mediolaterally expanded caudolateral process of predentary resting perpendicularly upon thin, grooved ridge of dentary diastema. Abbreviations: clp, caudolateral process of predentary; de, dentary; di, diastema of dentary; pr, predentary.

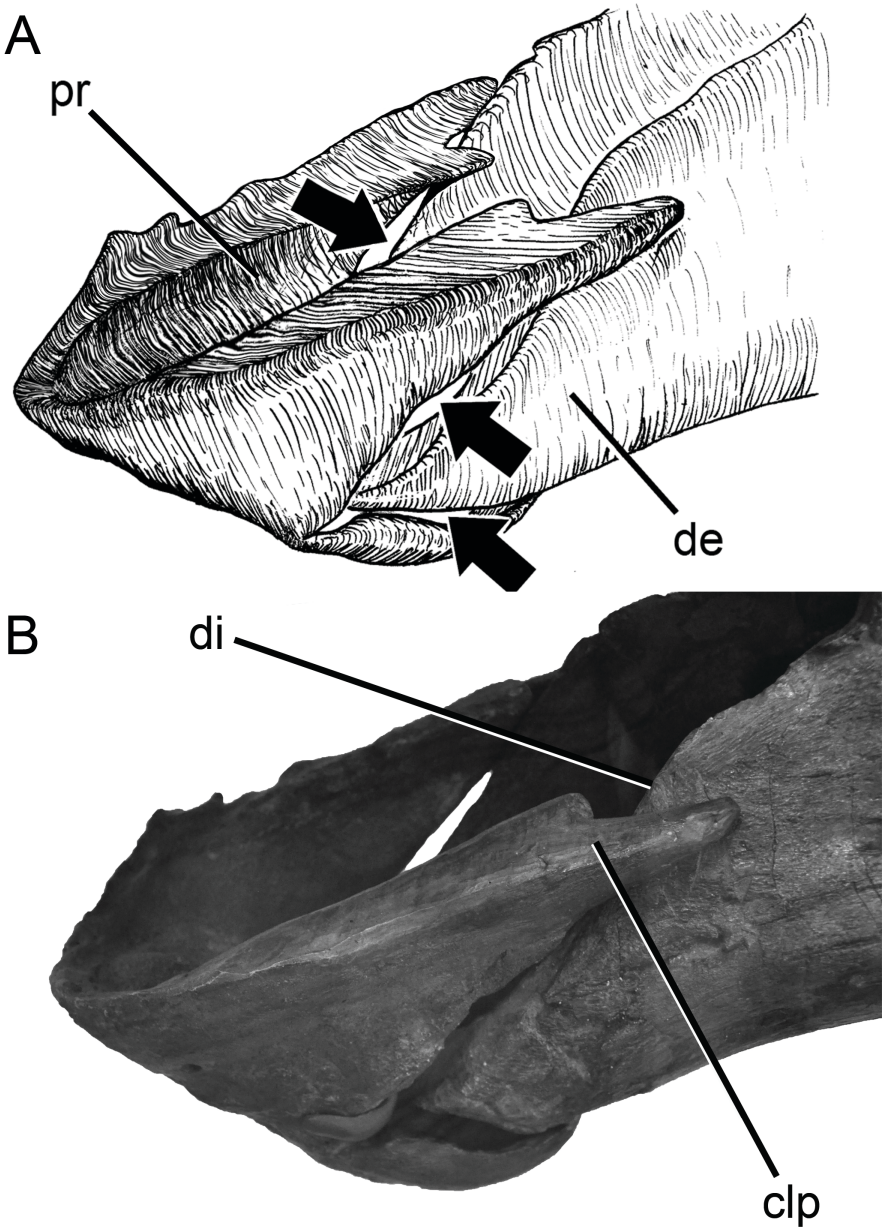

Dentary

The dentary (Fig. 6.21; 6.22; 6.23;6.24; 6.25; 6.26) is the largest element in the ornithopod mandible. It articulates with the predentary and the opposite dentary rostrally, the splenial medially, and the surangular and angular caudally. In lateral view, the ventral edge is elongate and relatively straight in basal ornithopods and many basal iguanodontians, whereas in other iguanodontians, including all hadrosauroids, the ventral margin bends ventrally at its rostral end toward the symphysis at varying degrees. The lateral surface forms a low ridge lateral to the dental battery, producing emargination of the dentary dentition. Several foramina on the lateral surface are more or less linearly disposed ventral to the dental series along the emargination and they likely transmitted neurovasculature to skin on the lateral surface of the mandible. One large laterally-placed foramen at the rostral tip of the dentaries supplied neurovasculature (mental artery and nerve) rostrally to the predentary. Three or more foramina are also distinctive and placed caudally but still in the rostral end of the lateral surface, likely also acting as the mental foramina supplying both the predentary and the skin of the rostral surface of the dentaries themselves.

FIGURE 6.21. *Corythosaurus* (hadrosaurid) mandible (generalized). A, lateral view; B, medial view. Abbreviations: a, angular; ar, articular; d, dentary; p, predentary; rap, retroarticular process; sa, surangular; sp, splenial. Scale bar = 5 cm.

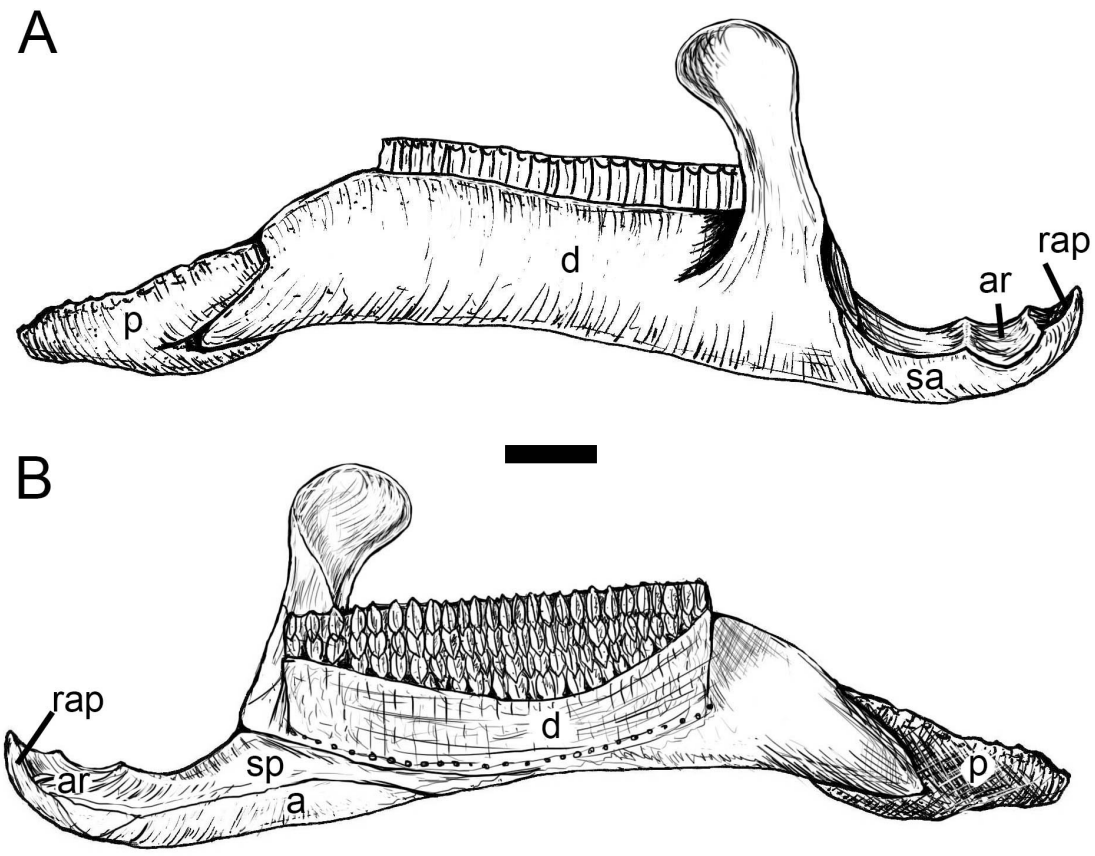

In basal ornithopods (e.g., *Hypsilophodon* [BMNH R197], *Yandusaurus* [ZDM 6001], *Gasparinisaura* [MUCPv 208], *Parksosaurus* [ROM 804], *Changchunsaurus* [JLUM L0403-j–Zn2], *Jeholosaurus* [IVPP V12529], *Bugenasaura* [MOR 979], and *Thescelosaurus* [NCSM 15728]) and *Dryosaurus* (CMNH 3392) the rostral margin of the dentary is relatively straight dorsoventrally with respect to the long axis of the rest of the mandibular corpus and ends in a rounded rostral tip that articulates with its counterpart. Derived ornithopods, including thescelosaurids and all iguanodontians, have a rostral dentary tip that is recurved medially (Fig. 6.22), which is exaggerated and ventrally deflected in the derived hadrosauroids to variable degrees, and ends in a rostrodorsally-

expanded straight edge where it comes into contact with its counterpart at the symphysis. The rostral and dorsal margin is very blunt with numerous seemingly random tongue-and-groove ridges suggesting bone remodeling induced by forces from movement against the opposite dentary in life. These ridges are seen in nearly all hadrosauroid dentary specimens and are especially exaggerated in adult forms. Articulation with the predentary at the rostral end is discussed above.

FIGURE 6.22. *Iguanodon* (*Mantellisaurus)* (BMNH R11521); left predentary and dentary in medial view (with predentary cut at the symphysis showing symphyseal articulation. Abbreviations: d, dentary; p, predentary; sym, symphysis. (Ruler in cm.)

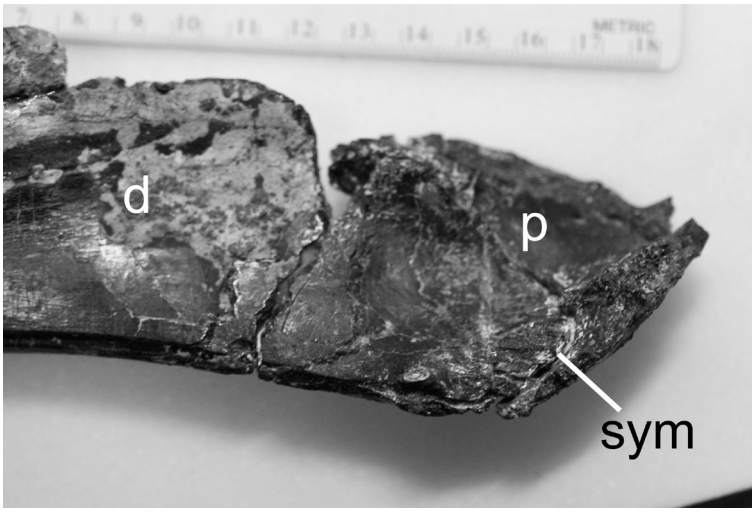

From rostral to caudal, the dentary curves out laterally and then straightens. Within the area between the symphysis and the dental battery is a distinct diastema in iguanodontians that is recurved and flat with a cupped medial surface (Fig. 6.23). A distinct thin, recurved ridge with a slight groove upon which the predentary rested (see Predentary section). This dorsal ridge curves to become parallel with and close to the

dorsal ridge of its counterpart before reaching the dental battery, which is also parallel to its counterpart (see Dentition section below for a description of ornithopod dental and tooth battery morphology). The lateral surface then diverges more laterally mid-length in an arch until reaching the dorsally oriented coronoid process, which is the most lateral portion of the dentary.

FIGURE 6.23. Hadrosaurid sub-adult left dentary (KUVP 17400). A, medial view of anterior diastema with arrow depicting curved articular surface for predentary to rest upon; B, caudal view of dentary depicting medial curvature of coronoid process and mandibular canal (lateral side on left). Abbreviations: cp, medially curved coronoid process; db, dental battery; mc, mandibular canal. Scale bar equals 2 cm.

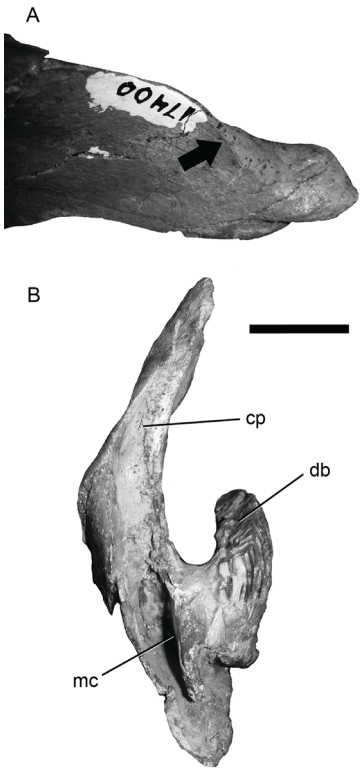

The coronoid process (Fig. 6.24) varies in shape depending on the taxon. Basal ornithopods (e.g., *Hypsilophodon* [BMNH R197], *Yandusaurus* [ZDM 6001], *Orodromeus* [MOR 294], *Gasparinisaura* [MUCPv 208], *Parksosaurus* [ROM 804], *Changchunsaurus* [JLUM L0403-j–Zn2], *Jeholosaurus* [IVPP V12529], *Bugenasaura* [MOR 979], and *Thescelosaurus* [NCSM 15728]), and *Dryosaurus* (CMNH 3392) possess a triangular coronoid process, which is not as prominent as more derived iguanodontians, but still provides attachment for the main jaw adductor musculature, as described below. In more derived ornithopods, the coronoid process is usually much larger and extends more dorsally; it is convex on the rostral and lateral sides and concave with thin outer edges on the caudal side of its body.

FIGURE 6.24. Comparison of ornithopod coronoid processes. A, *Dryosaurus* (CMNH 3392); B, *Mantellisaurus* (BMNH R5764); C, *Parasaurolophus* (hadrosaurid) (NMMNH P-25100). Abbreviations: cp, coronoid process. Not to scale.

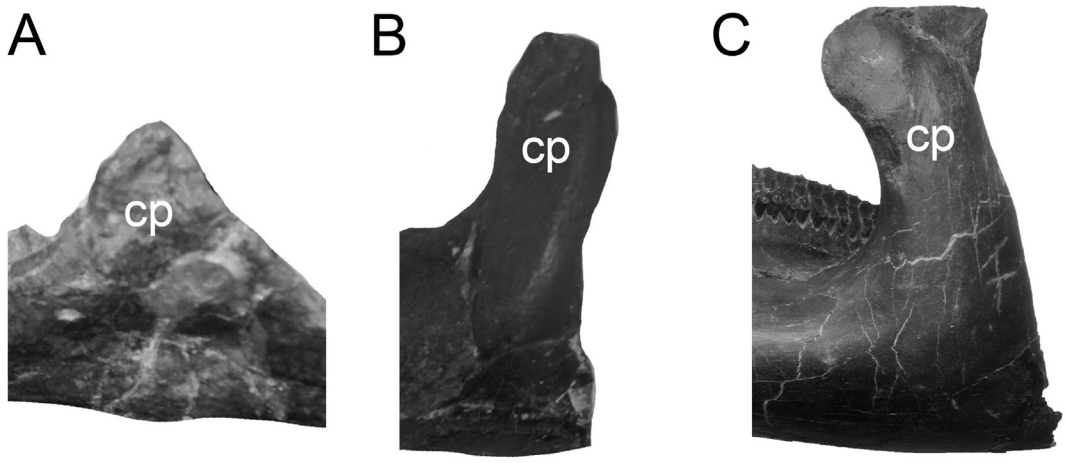

The coronoid process projects straight dorsally in *Zalmoxes* (e.g., BMNH R3392; R3407) and basal iguanodontians such as *Iguanodon* (e.g., BMNH R11521; IRSNB R51; R52; R56), *Kukufeldia* (BMNH R28660), *Ouranosaurus* (Taquet, 1976), *Altirhinus* (Norman, 1998), and *Equijubus* (IVPP V12534, plus others [see Figure 6.1 for more genera]). It should be noted that the coronoid process in basal iguanodontians is shorter and placed relatively more caudally with respect to the length of the jaw as compared to hadrosauroids. In hadrosauroids, the coronoid process extends even farther dorsally and angles slightly rostrally toward the orbit and narial region rather than caudally as in most vertebrates (Ostrom, 1961). Ventrally, the coronoid process bows laterally from the lateral surface of the dentary body, forming a convex surface flush with the rest of the dentary. It then extends dorsally, curving medial to the arch of the jugal and at acute angle with respect to it (Fig. 6.25).

FIGURE 6.25. *Lambeosaurus* (hadrosaurid) (ROM 794) right coronoid process projecting medial to jugal flange and lateral to maxilla. Abbreviations: cp, coronoid process; j, jugal; m, maxilla.

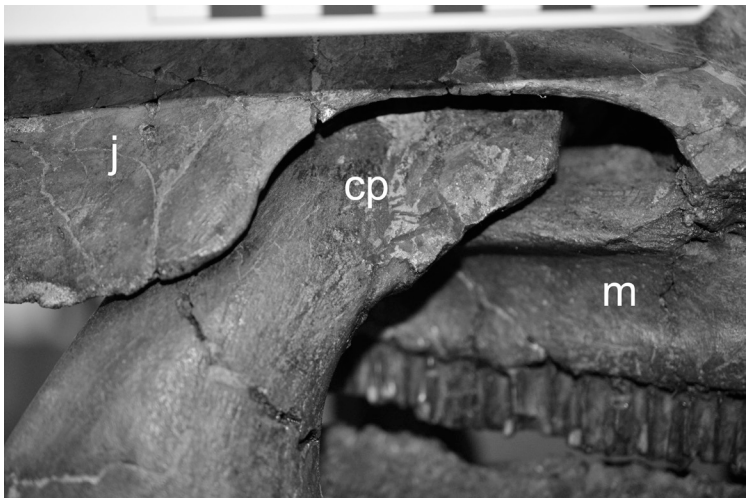

The caudal aspect of the dental battery typically ends just rostral to the coronoid process in basal ornithopods and non-hadrosauroid iguanodontians, but continues and lies just medial to the coronoid process in most hadrosauroids. The medial aspect of the coronoid process is much less convex and sometimes is dorsoventrally straight. The most dorsal aspect of the coronoid process in hadrosauroids is slightly expanded rostrocaudally.

In caudal view, the mandibular canal is large and runs from immediately ventral to the concavity of the caudal surface of the coronoid process to the ventromedial aspect of the dentary body ventral to the dental battery. Two elongate, flat, triangular processes make up the dorsal and ventral parts of the mandibular groove on the medial side and articulate with the surangular. Ventral to the mandibular groove is a flat surface for articulation with angular. At the caudal end of the dental battery, a bony caudal process also supports the splenial on its medial and dorsal surface.

FIGURE 6.26. *Gryposaurus* left dentary (AMNH 5465). A, lateral view; B, medial view. Abbreviations: cp, coronoid process; db, dental battery; di, ventrally curving diastema; em, emargination; mc, mandibular canal; sy, tongue-and-groove symphysis. Scale bar equals 10 cm.

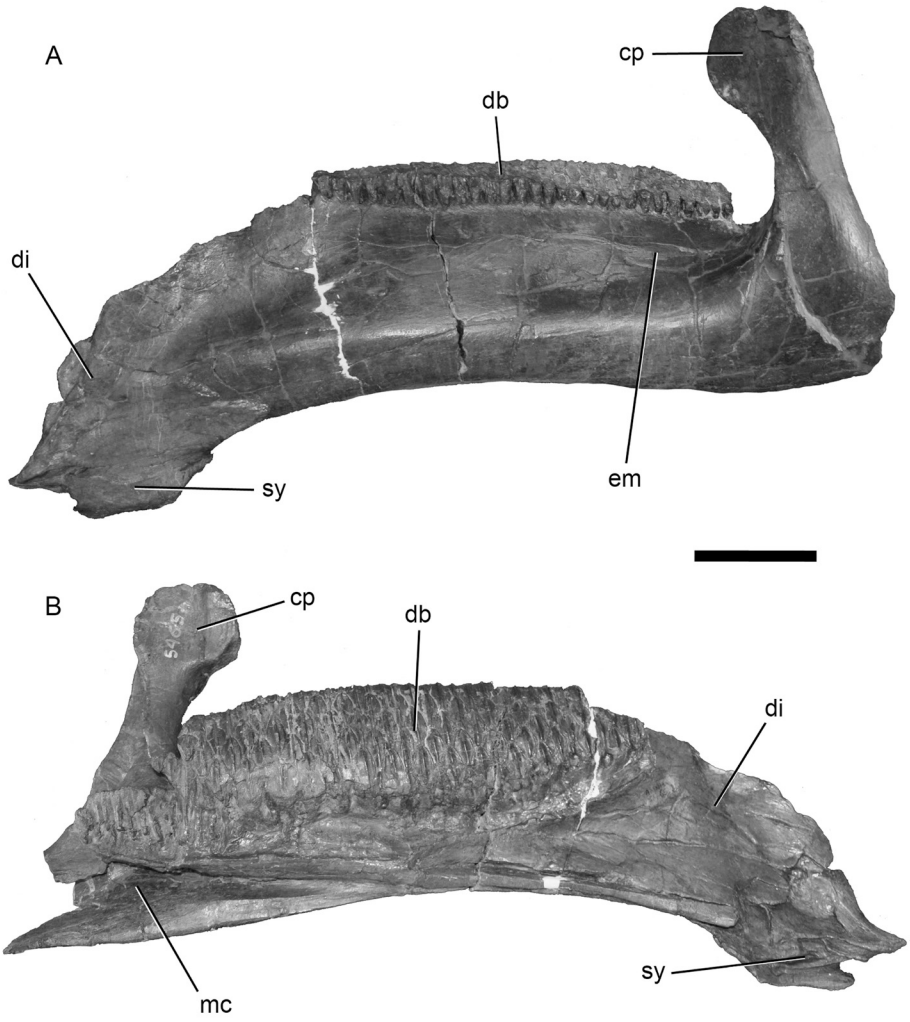

Coronoid

The coronoid is known in basal ornithopods as well as in non-hadrosauroid iguanodontians, except for *Altirhinus, Eolambia, Protohadros,* and *Probactrosaurus*. The coronoid is a relatively small element that adheres to the medial aspect of the dorsal coronoid process and sometimes extends slightly dorsally above the level of the dentary portion of the coronoid, providing an attachment site for m. pseudotemporalis and m. adductor mandibular externus (see below).

Splenial

The splenial (Fig. 6.21) is thin, sheet-like, and covers the ventromedial aspect of the dentary and dental battery, covering the alveolar foramina on that side, but is not firmly adhered to the dental battery. The splenial is triangular rostrally where it meets the splenial process of the dentary by means of a shallow groove and also articulates with the surangular, angular, and articular caudally with a jagged articular surface.

Angular

The angular (Fig. 6.21) is an elongate, narrowed, and laterally-compressed bone ventral to the mandibular groove located on the medial surface of the dentary rostrally and surangular caudally. It forms the ventromedial edge of the caudal portion of the mandibular corpus and articulates with the splenial rostrodorsally and the articular caudodorsally. It, along with the surangular, braces the articular for sturdy articulation with the quadrate.

Prearticular

The prearticular contacts the dentary, surangular, and articular to form the medial boundary of the adductor fossa. It is elongate and braces the surangular and articular rostral to the retroarticular process in basal ornithopods and non-hadrosauroid iguanodontians. In hadrosauroids, it is a small wedge-shaped bone on the medial aspect of the jaw that makes up part of the wall of the adductor fossa leading to the mandibular canal.

Surangular

The surangular (Fig. 6.21) makes up the largest portion of the mandibular body caudal to the dentary. It forms the walls of the caudal end of the mandibular canal and also possesses an ascending sheet of bone (thinner in hadrosaurids) that forms a part of the caudal portion of coronoid process, made up mostly by the dentary. It also articulates with the splenial medially and the angular ventromedially. Caudally it extends and articulates with the articular, forming the caudal-most retroarticular process. A dorsally extended lateral lip, or buttress, forms the lateral portion of the articular surface on which the quadrate articulates, forming the synovial craniomandibular joint (see Articular section below).

Articular

The articular (Figs. 6.21; 6.27) is small, flattened, and subrectangular, barely forming the most medial aspect of the articular surface with the quadrate (mostly made up by the surangular) as the synovial craniomandibular joint. Along with the surangular, it also forms the retroarticular process. It articulates with the surangular rostrally and rostrolaterally, the angular ventrally, and splenial rostromedially.

As the dorsal aspect of the surangular-articular complex extends caudally, it is elongate and becomes shallowly concave, both rostrocaudally and mediolaterally, sloping upwardly in each direction (Fig. 6.27). When articulated with the ventral portion of the quadrate, the quadrate covers roughly half to two-thirds of the rostrocaudal length of the articular surface, showing that there was a range of movement, especially in hadrosauroids, for the quadrate to translate in that direction against the articular as the

mandible moves. The shallow concavity on the mediolateral surface of the articular also shows that the mandible was not locked in place across this plane, but allows mediolateral rotation of the mandibular corpus against the quadrate (although there is room for medial rotation as the lateral side of the articular surface is obstructed by the dorsally extended lateral lip, or buttress, of the surangular). As noted above, the quadrate is notably very spherical at its ventral end in hadrosauroids (Figs. 6.10; 6.27), creating a ball-and-socket synovial joint allowing mediolateral rotation of the mandibular corpora as well as rostrocaudally displacement within the synovial capsule (Fig. 6.27).

FIGURE 6.27. Hadrosauroid jaw joint quadrate-articular articulation. A, ventral portion of hadrosaurid quadrate (AMNH 5220) depicting spherical end; B, surangular-articular basin (*Telmatosaurus* cast) depicting where quadrate sits; C, depiction of craniomandibular articulation caudal to dentary. Abbreviations: as, articular surface where quadrate rests at the jaw joint; cp, coronoid process of dentary; dll, dorsal lateral lip of surangular; ju, jugal; qu, quadrate; rap, retroarticular process; sa, surangular; vq, spherical ventral portion of quadrate.

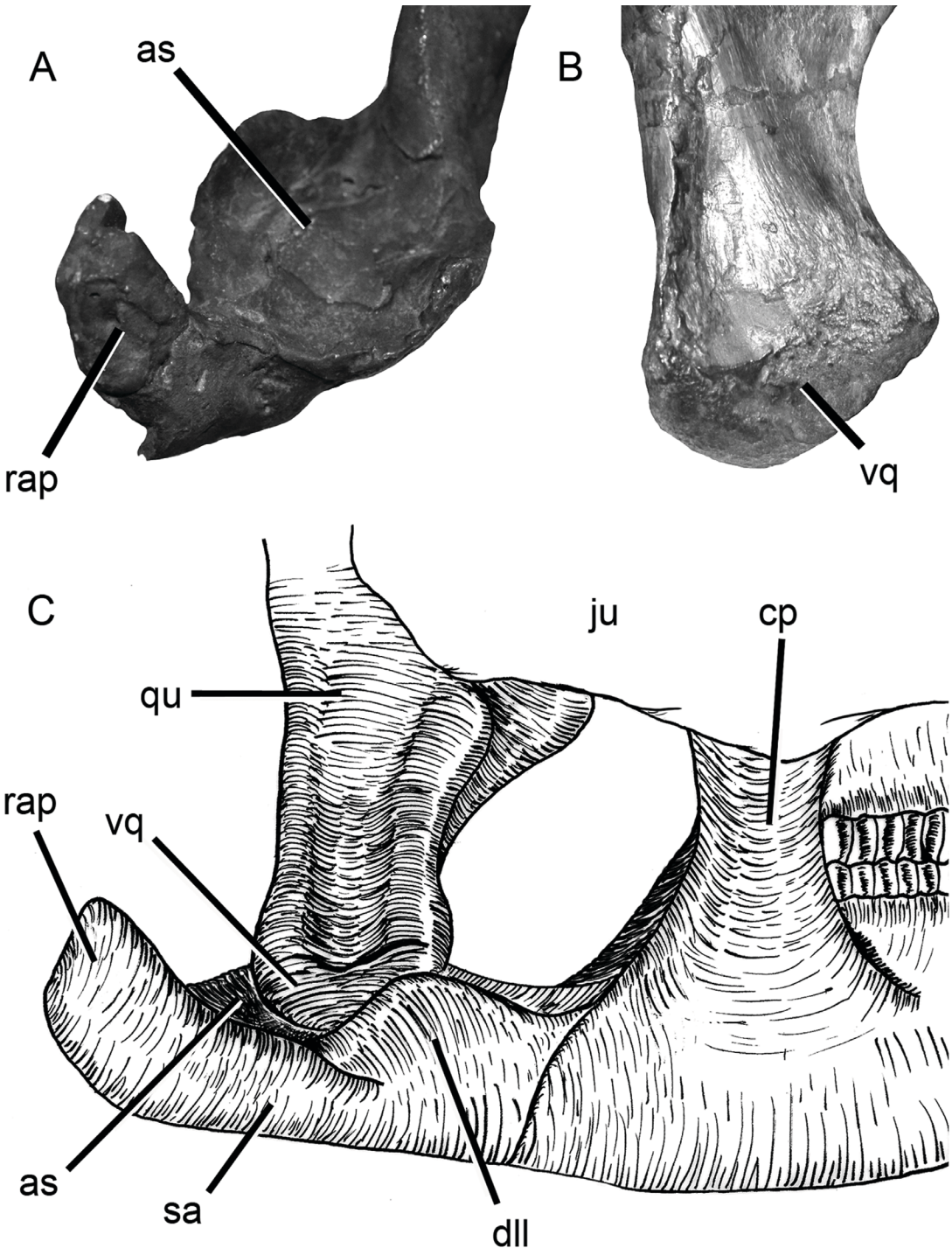
A
as
rap
B
vq
C
ju
cp
qu
rap
vq
as
sa
dll

Dentition

Basal ornithopods have roughly five conical premaxillary teeth that are sometimes lacrimiform and have a pointed apex, with a cupped inner enamel surface (e.g., *Hypsilophodon* (BMNH R197; Fig. 6.28). These teeth run along the lingual margin of the premaxilla on either side and were suitable for puncturing vegetation at the initial bite. Premaxillary dentition is then lost in subsequently more derived ornithopods (i.e., iguanodontians).

FIGURE 6.28. *Hypsilophodon* left premaxillary tooth.

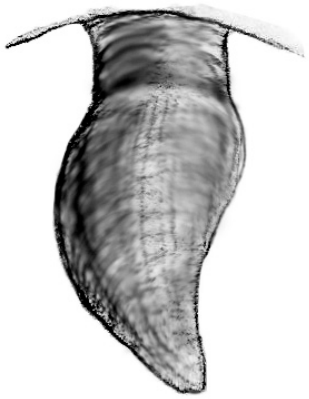

The maxillary teeth (Fig. 6.29) are rounded in basal forms (e.g., *Hypsilophodon*) to diamond-shaped (e.g., iguanodontians; Fig. 6.30), apicobasally elongate, and have thin ridges running along the outer surface (usually one median ridge with one or two ridges

parallel on either side). Hadrosaurids have a single thin midline ridge on the lingual side on an elongate, diamond-shaped tooth crown running the height of the tooth. In iguanodontians, especially hadrosaurids, the tooth row in the maxilla does not contain nearly as many teeth, with only a tightly packed row of single teeth seen in lateral view. The continuous occlusal surface is oriented ventromedially, occluding with the dorsolateral occlusal surface of the dentary tooth battery described below.

FIGURE 6.29. *Hypsilophodon* maxillary tooth (above) coming into occlusion with dentary tooth (below).

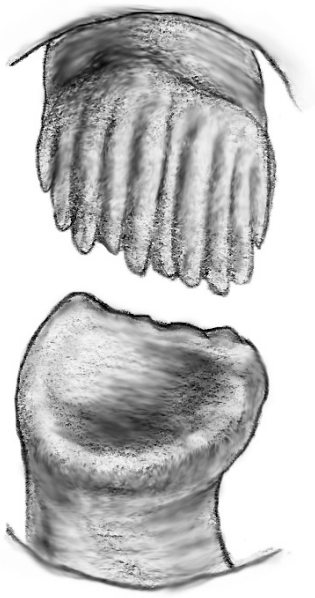

The most distinctive feature of the ornithopod dentary is the tooth row (Fig. 6.30; 6.31), which is formed into a dental battery in hadrosauroids. It covers more than half the length of the dentary. The tooth row begins at the rostral-most oral margin of the dentary

in more basal ornithopods, but just caudal to the diastema in most iguanodontians. The dentary contains roughly 10 to 15 teeth in basal forms and up to 40 or more tightly packed columns of teeth in hadrosaurids. The number of tooth positions varies with ontogeny and species, each extending dorsally from an elongate row of alveoli. The tooth row extends even farther caudally than the coronoid process, which lies lateral to it, especially in hadrosauroids. Positioning of teeth in basal ornithopods is a typical reptilian tooth row with teeth in line with each other. Non-hadrosauroid iguanodontians have a tooth row with fewer teeth that are larger with respect to the size of the dentary itself and have visible replacement teeth, although only with two or three replacement teeth per tooth position (Weishampel and Jianu 2011). The tooth row in non-hadrosauroid iguanodontians is unique in that, much like that seen in ankylosaurs, the tooth row has a sinusoidal configuration with alveoli that are oriented slightly dorsolaterally at the rostral end and, as the tooth row extends caudally, curves medially and the alveoli are gradually oriented dorsally and, in the most extreme cases such as *Ouranosaurus* (Taquet, 1976), slightly dorsomedially. In hadrosauroids, in which dental batteries have many more teeth, all tooth columns jointly form a medially-convex configuration extending dorsally to form a flat, smooth occlusal surface. This occlusal surface faces dorsolaterally and occludes with the ventrolateral orientation of the dentition of the maxilla dorsally. In medial view, the alveoli are V-shaped, with both rostral and caudal ends closest to the dorsal surface with the fewest teeth in the column. A thin, rugose layer of bone conceals the ventral half of the medial surface of the dental battery.

FIGURE 6.30. *Iguanodon* dentary tooth. A, medial view; B, lateral view.

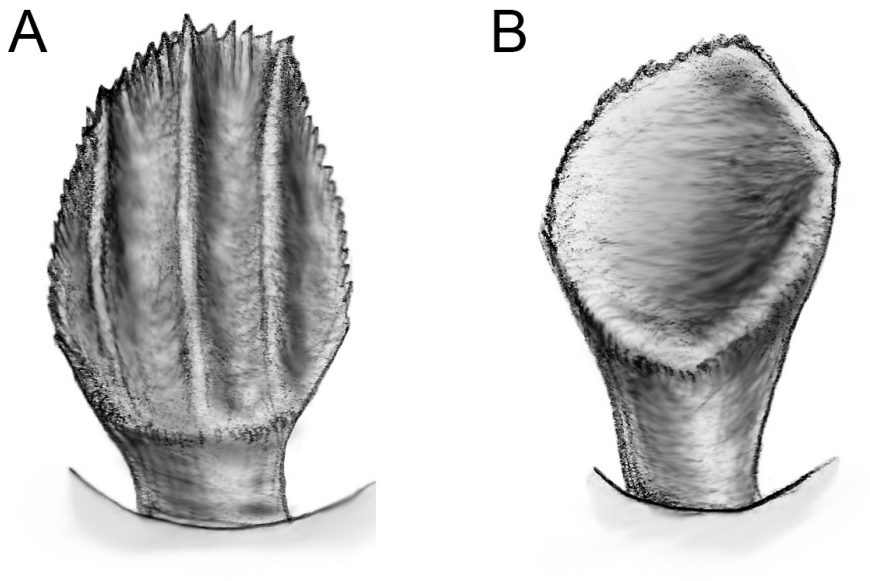

Individual dentary teeth, like maxillary teeth, are rounded with a straight and thin apex in basal forms (e.g., *Hypsilophodon*) to diamond-shaped and apicobasally elongate (e.g., iguanodontians). A thin midline ridge on the lingual side runs the height of the tooth in hadrosaurids. Basal ornithopods possess many more apicobasally-oriented ridges along the outer surface of the teeth that form rounded denticle-like protrusions on the apical ridge of the dentition in basal ornithopods, but not typically in iguanodontians. A worn edge along the lingual edge of the teeth is present at variably acute angles. Non-hadrosauroid iguanodontians, such as *Iguanodon*, possess a much more mesiodistally expanded apical ridge with a denticle formed apically by the large midline ridge and a large wear facet laterally (Fig. 6.30). The midline ridge in the derived hadrosauroids, when reaching the continuous occlusal surface mentioned above, creates a serrated edge running the mesiodistal length of the lingual side of the tooth row when combined with the rest of the tooth columns. This serrated edge forms a saw blade configuration of the

tooth row that is bowed dorsally in the center that would help strip vegetation (Fig. 6.31). A description of dental micro- and mesowear is given below.

FIGURE 6.31. Hadrosaurid tooth battery in dentary (medial of left mandible).

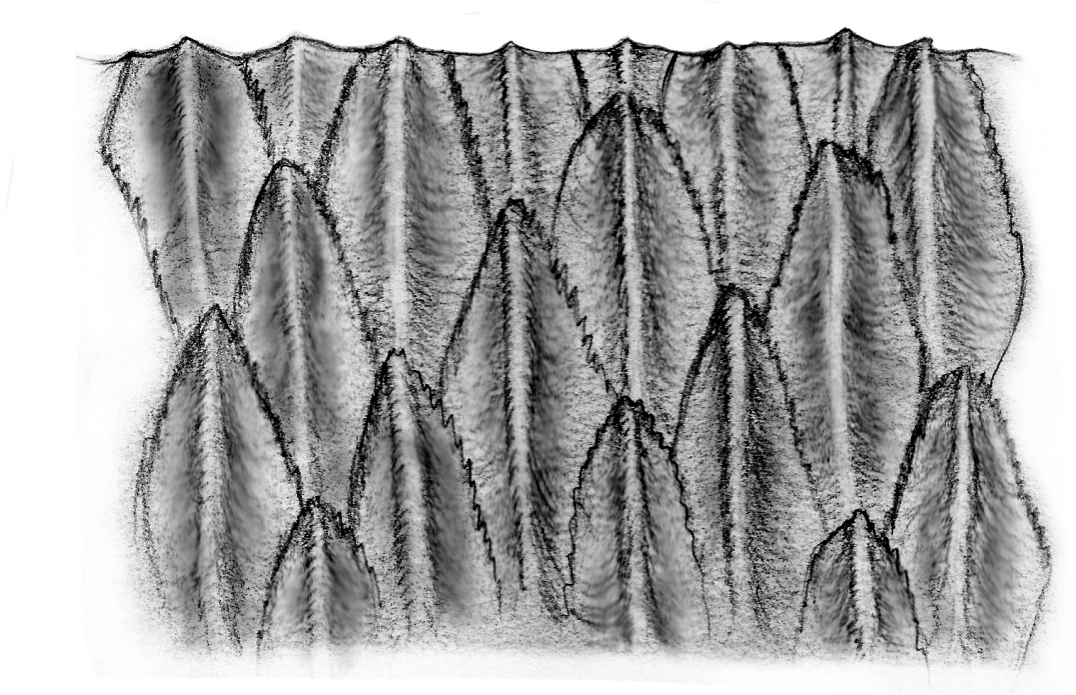

Dental wear patterns in basal ornithopods and non-hadrosaurid iguanodontians are very similar. The occlusal surfaces of the maxillary tooth row are oriented medially while the dentary occlusal surfaces are oriented laterally. Occlusal surfaces of both teeth are either show a slightly cupped wear plane, as in *Hypsilophodon* and *Thescelosaurus*, or a flatter wear plane, as in many larger non-hadrosaurid iguanodontians. Hadrosaurid dental microwear is well understood (Ostrom, 1961; Weishampel, 1983, 1984; Williams et al., 2009). When observed occlusally, with the midline denticle (on the lingual side) on top of

the field of view, the occlusal surface of a single dentary tooth is U-shaped capped with a three-point crown, the middle point represented by the midline ridge forming a single denticle of the serrated tooth row.

Microwear observations show wear in both the mesiodistal and buccolingual directions (Fig. 6.32). The mesiodistal microwear is largely present along the occlusal surface of the lingual denticulate margin at the tooth apex. United they form a shelf of wear along that edge displaying a propalinal aspect of its jaw mechanism. The buccolingual microwear is very prominent along the majority of the occlusal surface and many of the scratches stretch nearly the entire height of the occlusal surface. This microwear displays a strong transverse movement of the mandibular corpus as well on both sides of the jaw. Given the dorsolateral orientation of the occlusal surfaces of both dentary tooth rows, a transverse mechanism of the entire lower jaw acting as one unit is unlikely (Weishampel, 1984; Williams et al., 2009).

Mesowear patterns come in two levels on the dentary tooth row: a higher step on the buccal edge and a lower step on the lingual edge that ends at the lingual edge of the occlusal surface of the tooth (Fig. 6.32). The sections at which these two steps meet represent the point at which the maxillary teeth began or ended occlusion with the dentary teeth. Between the dentaries, these wear edges are produced on opposite sides of each other, meaning that on both dentaries the higher steps are both positioned on the labial side of the dentary and the lower steps are both positioned on the lingual side of the dentary. Also, an acute angle (~20°) at which the higher mesowear level meets the lower level along the tooth row indicates offset occlusion (Fig. 6.32).

On the maxillary occlusal surface, a concave pit represents the region where the dentary teeth initially occluded with the maxillary teeth. On the lingual edge, instead of a sharp corner, a rounded margin permits rotation at the end of occlusion of the dentary against the maxilla (Fig. 6.32). This was most plausibly done by rotation of the dentary teeth medially so that the maxillary teeth wear in a rounded manner. Many specimens of hadrosauroid maxillae examined show this edge to be chipped away throughout the tooth row, indicating extensive wear. This condition, along with the offset occlusal patterns and microwear of the dentary teeth, indicates that the dentaries move in opposite directions to maneuver the vegetation through the oral cavity, therefore providing both dentaries the ability to independently and simultaneously rotate mediolaterally.

FIGURE 6.32. Hadrosauroid dental micro- and mesowear. A, dentary tooth (KUVP 96884) occlusal surface (lingual edge at top) with arrows depicting an example of both mesiodistal and buccolingual wear; B, occlusal surface of multiple dentary teeth (KUVP 17400) with denticulate serrated edge of dental battery seen on lingual edge (at top). Arrows depict step-ladder mesowear where the edge of the maxilla occludes with dentary; C, same dentary teeth with lines showing 20 degree angle of maxilla-dentary occlusion; D, maxillary teeth (KUVP 96887) with arrows depicting curling of denticulate edge from dentary rotation.

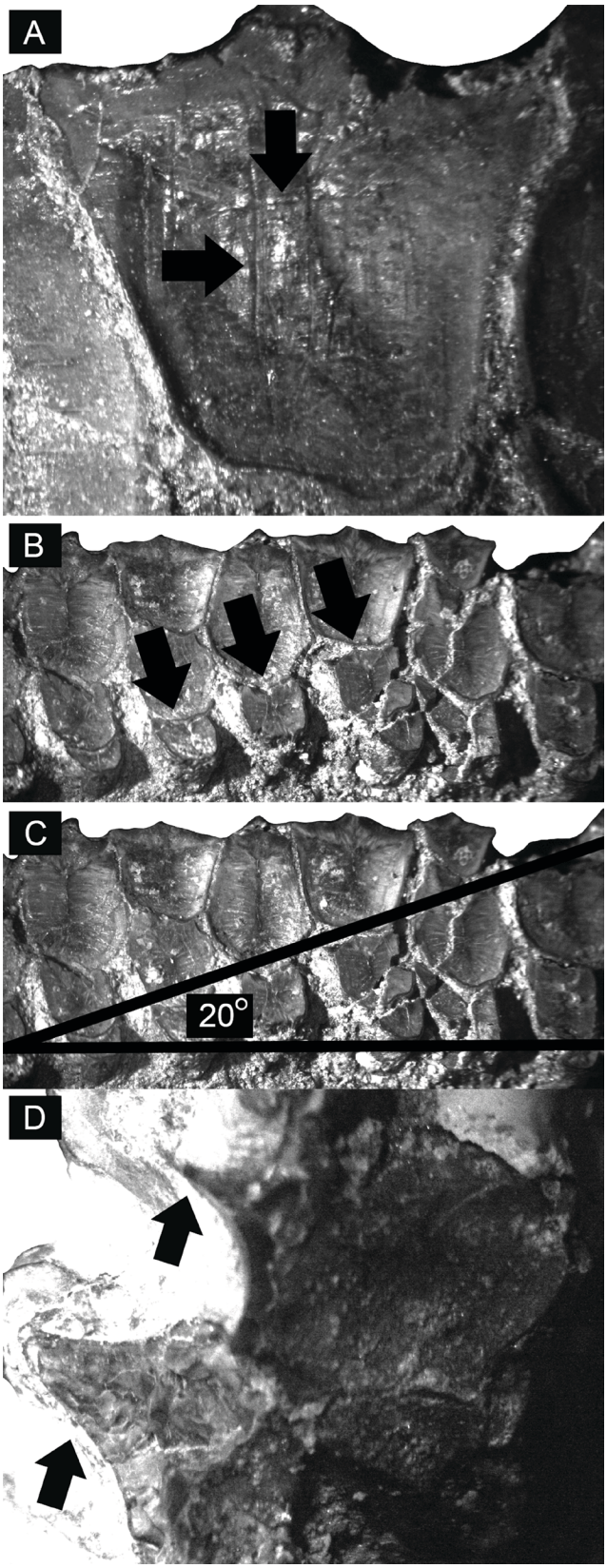
A
B
C
20°
D

JAW MUSCULATURE

Reconstruction of jaw musculature in ornithopods comes to us through studies of muscle scarring as well as phylogenetic bracketing methodology (Ostrom, 1961; Galton, 1974; Holliday, 2009). These descriptions were used as a baseline for inferring the morphology and use of jaw musculature. The descriptions below are generalized for all ornithopods, unless otherwise noted.

M. depressor mandibulae

M. depressor mandibulae (mDM; Fig. 6.33) was likely the primary muscle acting to lower the jaw. According to Ostrom (1961), it is likely that this muscle originated on the caudodorsal and caudolateral surfaces of the paroccipital processes of the exoccipitals on the most caudal extent of the cranium. M. depressor mandibulae inserted ventrally onto the dorsal aspect of the retroarticular process at the most caudal region of the jaw, past the jaw joint. In more basal ornithopods, mDM is oriented at an acute angle rostroventrally due to a caudally expanded occiput (as in *Hypsilophodon* and *Thescelosaurus*). In basal iguanodontians, mDM becomes a lot more dorsoventrally vertical due to a straighter quadrate (as in *Dryosaurus* and *Iguanodon*). The mDM in many derived hadrosaurids, however, reverts to a mDM with a more acute angle, with extreme cases such as in *Corythosaurus* and *Parasaurolophus*.

M. adductor mandibulae posterior

The palinal motion of the jaw was likely initiated by the large m. adductor mandibulae posterior (mAMP; Fig. 6.33). This muscle likely originated on the lateral surface of the rostrally-oriented pterygoid wing of the quadrate body in ornithopods. It likely inserted rostroventrally into the opening of the medial mandibular adductor fossa on the inner caudal aspect of the dentary. This would make for a direct line of action for the muscle to pull the jaw caudally. This might have aided to strip the animal to strip vegetation against its the dentition in that direction. As it was a very large muscle, mAMP likely produced a lot of force in the caudal direction for a substantial bite force.

As is seen in Table 6.2, muscle fiber orientations likely remained relatively stable throughout ornithopod evolution, being maintained between 30 degrees to 50 degrees. There is no clear pattern within subclades of Ornithopoda, even among hadrosaurids. In some cases, such as *Parasaurolophus* and *Hypacrosaurus*, the quadrate has a more exaggerated rostroventral orientation of the ventral head, which would result in a slightly more caudally oriented mAMP angle.

TABLE 6.2. Ornithopod mAMP muscle vector angles.

Genus	Spec. #	mAMP(°)
Agilisaurus	ZDM 6011	39.93
Gasparinisaura	MUCPv 208	34.58
Anatotitan	Cast of holotype	34.6
Camptosaurus	(Marsh, 1879)	30.9
Corythosaurus	ROM 777	37.56
Dryosaurus	CMNH 3392	32.9
Edmontosaurus	ROM 801	40.87
Gryposaurus	ROM 873	42.05
Hypacrosaurus	ROM 789	37.55

Hypsilophodon	BMNH R197	34.6
Jeholosaurus	IVPP V12529	33.27
Altirhinus	Cast of holotype	38.29
Equijubus	IVPP V12534	43.89
Iguanodon	IRSNB R51	37.68
Ouranosaurus	(Taquet, 1976)	35.57
Kritosaurus	AMNH 5799	47.37
Lambeosaurus	ROM 1218	39.78
Maiasaura	Cast - MOR	48.38
Parasaurolophus	ROM 768	34.7
Parksosaurus	ROM 804	40.68
Prosaurolophus	ROM 787	43.62
Saurolophus	AMNH 5220	42.08
Tenontosaurus	AMNH - display	32.86
Thescelosaurus	NSCM 15728	40.33

M. pseudotemporalis

M. pseudotemporalis (Fig. 6.33) was likely made of two bellies in ornithopods: superficialis and profundus. Together, these muscles would have assisted in pulling the jaw closed during chewing cycles.

M. pseudotemporalis superficialis—According to Holliday (2009), m. pseudotemporalis superficialis (mPSTS) likely originated at the dorsal margin of the temporal fossa, showing that no muscle scarring can be found to give any indication of it. This muscle likely extended rostroventrally to insert inside the medial mandibular fenestra as well as on the dorsal apex of the coronoid eminence or process in ornithopods. This insertion was likely through a tendinous sheet, as indicated by distinct muscle scarring (Ostrom, 1961; Galton, 1974; Holliday, 2009).

M. pseudotemporalis profundus—Because ornithopods have lost the epipterygoid, M. pseudotemporalis profundus (mPSTP) likely originated on the lateral

surface of the brain case inside of a depression, or fossa. Like mPSTS, its insertion was likely the dorsal apex of the coronoid eminence and the rostral portion of the medial mandibular fenestra, likely through a tendinous sheet (Ostrom, 1961; Galton, 1974; Holliday, 2009).

FIGURE 6.33. Comparison of ornithopod jaw musculature (m. pseudotemporalis, m. adductor mandibulae posterior, and m. depressor mandibulae). A, *Hypsilophodon* (basal ornithopod); B, *Iguanodon* (basal iguanodontian); C, *Corythosaurus* (hadrosaurid). Abbreviations: mAMP, m. adductor mandibulae posterior; mDM, m. depressor mandibulae; mPST, m. pseudotemporalis. Left lateral view. See Fig. 6.2 for scale bars.

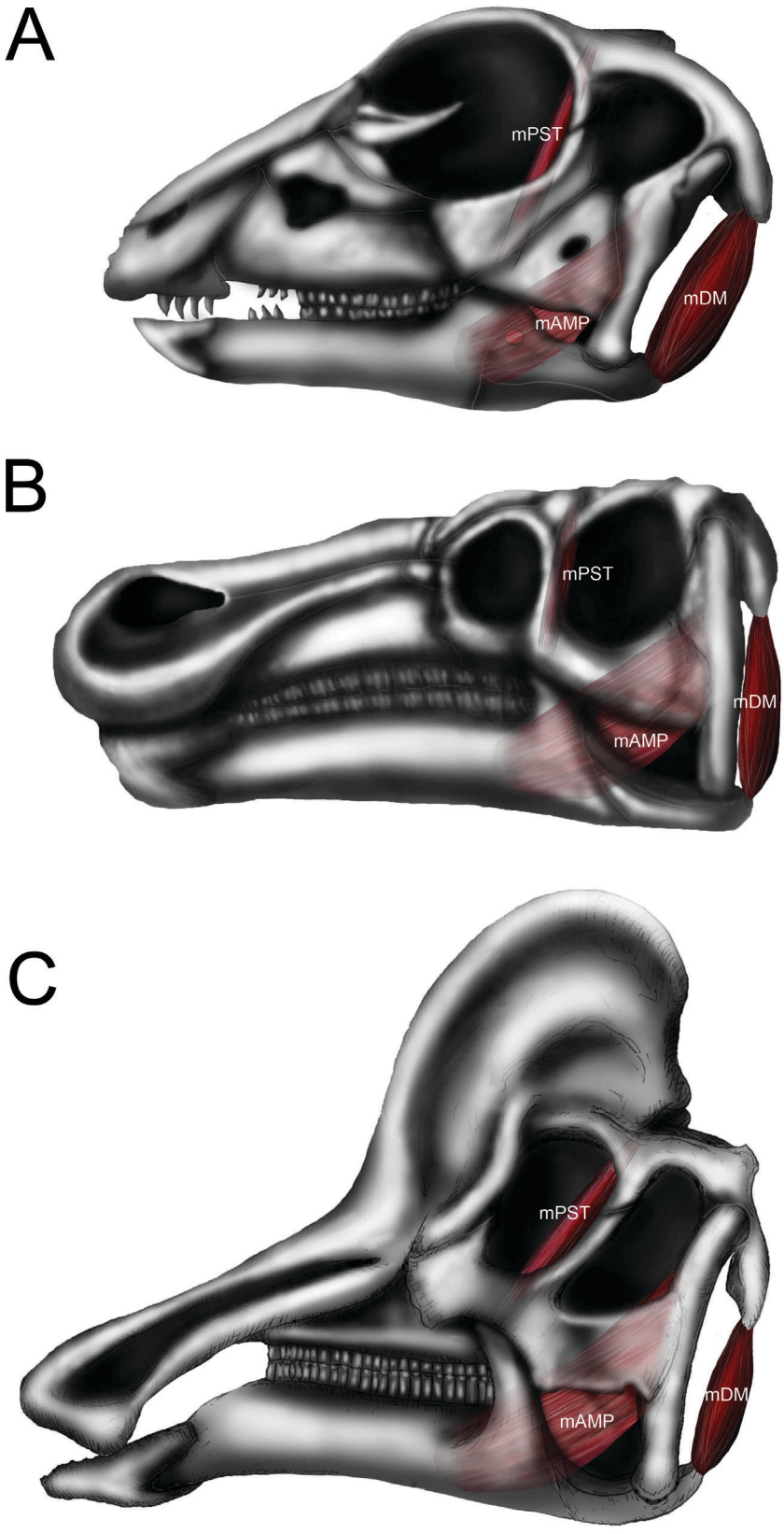
A
mPST
mDM
mAMP
B
mPST
mDM
mAMP
C
mPST
mDM
mAMP

M. adductor mandibulae externus

The primary group of muscles likely acting to raises the jaw to occlusion is the adductor mandibulae externus muscle group (Fig. 6.35). The muscles of this group likely all originated on or near the squamosal, together functioning as one large fan of muscle (Ostrom, 1961; Galton, 1974; Holliday, 2009).

M. adductor mandibulae externus superficialis—According to Holliday (2009), as seen in most other ornithischians, m. adductor mandibulae externus superficialis (mAMES) likely originated on the medial ridge of the supratemporal bar - this bar is, made of the postorbital and squamosal -, as can be seen, for example, in extant lepidosaurs. Ostrom (1961) indicated that it also occupied the lateral surface of the rostral portion of the squamosal. The evidence for this was because of a distinct depression just rostral to the quadrate in lateral view, forming an embayment on the caudal aspect of the infratemporal fenestra internally. Some hadrosaurs, such as *Gryposaurus* (ROM 873) and "*Kritosaurus*" (AMNH 5799), possess a much wider infratemporal fenestra rostrocaudally, likely indicative of larger surface area for musculature (Ostrom, 1961). Other hadrosaurs, such as *Parasaurolophus* (ROM 768) and *Edmontosaurus* (e.g., ROM 801; 867), conversely show a rostrocaudally narrowed infratemporal fenestra, indicating less room for adductor musculature (Fig. 6.34).

FIGURE 6.34. Hadrosaurid infratemporal fenestrae. A, *Gryposaurus* (ROM 873 flipped) (wider); B, *Parasaurolophus* (ROM 768) (narrower). Abbreviations: itf, infratemporal fenestra; o, orbit. Not to scale.

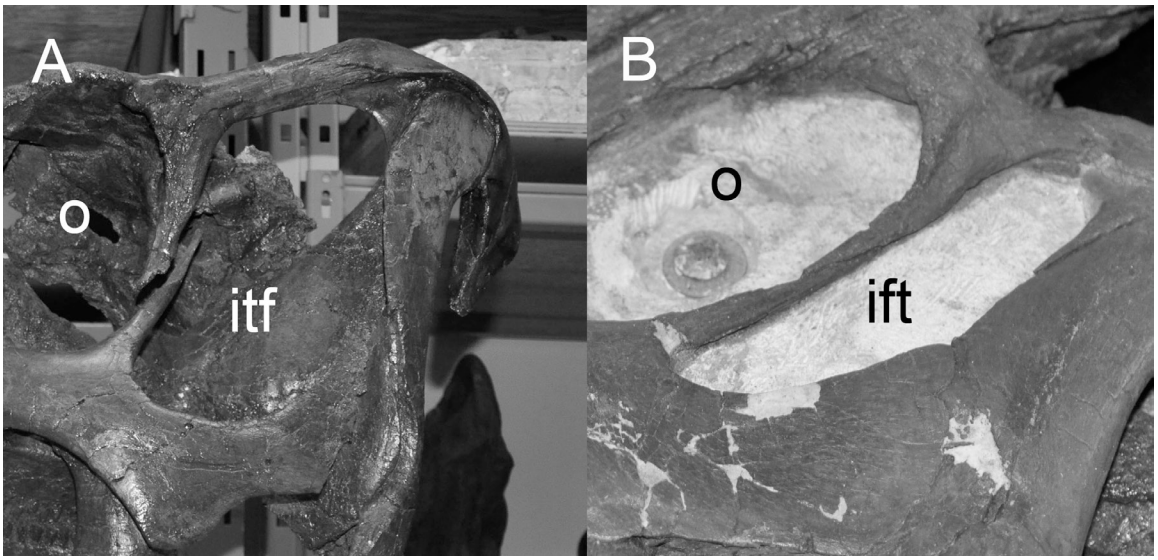

The mAMES then expanded along the lateral portion of the dorsal rim of the surangular and likely the caudal ridge of the dorsal aspect of the coronoid process. Basal ornithopods exhibit a shallow fossa along the dorsal surface of the element that likely demarcates the insertion of this muscle. This margin is less clear in iguanodontians, especially hadrosaurids. However, this margin is still the most plausible insertion (Holliday, 2009).

M. adductor mandibulae externus medialis—M. adductor mandibulae medialis (mAMEM) likely originated on the caudolateral surface of the supratemporal fossa just dorsal to the internal margin of the infratemporal fenestra. It likely extended rostroventrally to insert onto the medial surface of the dorsal ridge along the surangular portion of the coronoid process, just rostral to the insertion of mAMES. Exact

demarcation of this muscle is unclear because, in many cases, mAMEM joins with mAMEP (see below) and this insertion is not completely visible.

M. adductor mandibulae externus profundus—M. adductor mandibulae externus profundus (mAMEP) likely originated on the lateral aspect of the skull roof on the parietal and squamosal, covering the caudomedial wall of the supratemporal fenestra and caudal portion of the sagittal crest in superior view (Ostrom, 1961; Holliday, 2009). This muscle is proposed to have inserted at the caudodorsal apex of the coronoid process, which is made up of the dentary and coronoid bone in non-hadrosauroid ornithopods, but is only made of the dentary alone in hadrosauroids. (Ostrom, 1961; Galton, 1974; Holliday, 2009; see above).

MAME muscle vector angles—As is seen in Table 6.3, muscle fiber orientations and muscle fan sizes are quite variable among genera. Among basal ornithopods, mAME orientation is low relative to the more derived basal iguanodontians. There is a trend from mAMEP muscle vector angles between 30 degrees and 45 degrees in basal ornithopods to a much higher mAMEP muscle vector angle in iguanodontians such as *Dryosaurus* and *Iguanodon*, which are both over 50 degrees. MAME muscle span from the rostral-most mAMES fiber to the caudal-most mAMEP fiber seems to cover a larger range as well in more derived ornithopods. This is likely indicative of more complex musculature becoming necessary for more complex feeding mechanisms. Many hadrosaurids seem to have more larger room for the mAME muscle span, such as *Gryposaurus*. Other hadrosaurids, however, especially lambeosaurines but also saurolophines such as *Edmontosaurus*, revert back to a more acute angle of mAME musculature with a much smaller muscle span. This is due to an angled quadrate as well as a caudally displaced

orbit. In the case of lambeosaurines, it is also due to the caudal movement of skull elements (nasals and premaxillae making up the hollow. These hadrosaurids with only a small amount of room for mAME musculature may have, in turn evolved the recruitment of larger pterygoideus musculature to make up for the bite forces needed for feeding. Further three-dimensional studies from CT scans (with muscle body size estimations) are necessary to make such an assertion, however.

TABLE 6.3. Ornithopod mAME muscle vector angles.

Genus	**Spec. #**	**mAMEP(°) (Coronoid Apex)**	**mAMEM(°) (Coronoid Mid-height)**	**mAMES(°) (Coronoid Base)**
Agilisaurus	ZDM 6011	43.04	53.52	65.5
Gasparinisaura	MUCPv208	36.07	47.62	58.57
Anatotitan	Cast of holotype	32.25	52.47	68.73
Camptosaurus	(Marsh, 1879)	34.06	66.55	88.32
Corythosaurus	ROM 777	40.87	65.09	77.93
Dryosaurus	CMNH 3392	52.41	70.27	83.5
Edmontosaurus	ROM 801	54.69	72.74	81.69
Gryposaurus	ROM 873	55.57	75.86	86.73
Hypacrosaurus	ROM 789	35.65	62.03	74.97
Hypsilophodon	BMNH R197	41.03	53.46	63.12
Jeholosaurus	IVPP V12529	42.01	62.09	71.07
Altirhinus	Cast of holotype	45.36	78.94	93.7
Equijubus	IVPP V12534	47.33	75.17	83.87
Iguanodon	IRSNB R51	52.43	79.59	95.31
Ouranosaurus	(Taquet, 1976)	39.08	67.21	79.72
Kritosaurus	AMNH 5799	59.34	76.49	84.93
Lambeosaurus	ROM 1218	52	77.69	84.68
Maiasaura	Cast - MOR	62.73	81.31	88.68
Parasaurolophus	ROM 768	40.16	63.88	81.37
Parksosaurus	ROM 804	45.75	74.25	85.94

Prosaurolophus	ROM 787	54.67	74.3	81.85
Saurolophus	AMNH 5220	41.63	71.95	77.26
Tenontosaurus	AMNH - display	40.31	58.8	71.88
Thescelosaurus	NSCM 15728	39.9	69.99	78.25

FIGURE 6.35. Comparison of ornithopod m. adductor mandibulae externus muscle complex morphology showing variations in muscle vector angles of m. adductor mandibulae externus profundus. A, *Hypsilophodon* (basal ornithopod); B, *Thescelosaurus* (basal ornithopod); C, *Dryosaurus* (basal ornithopod); D, *Iguanodon* (basal iguanodontian); E, *Edmontosaurus* (saurolophine hadrosaurid); F, *Prosaurolophus* (saurolophine hadrosaurid); G, *Gryposaurus* (saurolophine hadrosaurid); H, *Corythosaurus* (lambeosaurine hadrosaurid); I, *Parasaurolophus* (lambeosaurine hadrosaurid). Note: angles listed are based on specimen data, not the illustration. Left lateral views. See Fig. 6.2 for scale bars.

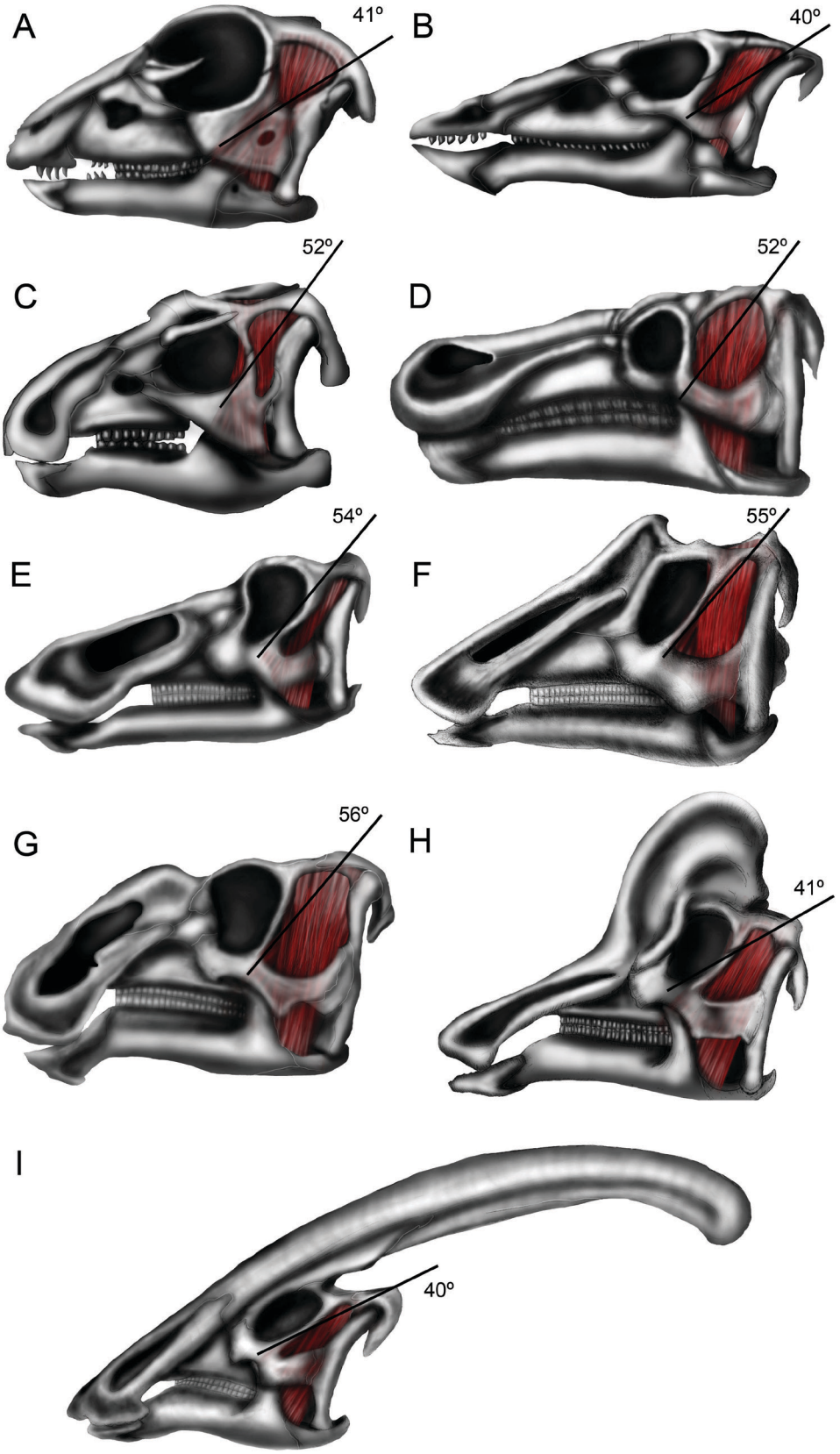
A
41º
B
40º
C
52º
D
52º
E
54º
F
55º
G
56º
H
41º
I
40º

M. pterygoideus ventralis

M. pterygoideus ventralis (mPTV; Fig. 6.36) originated on the broad caudoventral surface of the pterygoid and on the ventral surface of the palate, indicated by a smooth surface. Ostrom (1961) also suggested that this muscle possessed an extra slip that also attached to the caudoventral flange of the pterygoid. The mPTV likely wrapped caudoventrally around the lateral aspect of the mandible and eventually inserted onto the ventrolateral aspect of the mandible and retroarticular process, although exact insertion is unclear due to lack of muscle scarring on the outer surface of the bone (Ostrom, 1961; Holliday, 2009). Holliday (2009) suggested that hadrosaurs might have had an insertion of this muscle on the lateral surface of the jugal flange (wrapping around and past the mandible laterally) due to observed scarring on this surface. This seems unlikely, however, due to the fact that the muscle fibers would have to course all the way to the its original height of their origins after a considerable descent toward the mandible. For such a muscle to function, it would need to be extremely long-fibered (as in a human m. sartorius) or contain several intertendinous junctions (as in a human m. rectus abdominis); neither morphology has been suggested for any ornithischian jaw adductor. MPTv likely functioned in medial movement, stabilization, or restriction of the mandibular corpus. As stated above, this muscle might have been enlarged due to the narrowing of space allowing mAME musculature to expand, though further studies are necessary to make such an assertion.

M. pterygoideus dorsalis

M. pterygoideus dorsalis (mPTD; Fig. 6.36) likely originated on a rostrocaudally elongate depressed region on the dorsal aspect of the pterygoid flange and palatine bones, although these attachments are difficult to observe due to the smooth surface likely formed by passages within the nasal cavity (Holliday, 2009). According to Ostrom (1961), mPTD also had a portion that originated on the maxillary shelf ventral and medial to the jugal dorsal to the caudal half of maxillary dentition. The mPTD stretched caudoventrally around the medial aspect of its respective mandibular corpus. The insertion was likely on the medial aspect of the retroarticular process of the mandible (Ostrom, 1961; Galton 1974; Holliday, 2009). Its function, with m. pterygoideus ventralis, plausibly acted as a sling to stabilize the lower jaw. Being placed on opposite sides of the mandibular corpus, mPTD and mPTV would work well together in mediolateral movement or restriction of the mandibular corpus in general.

FIGURE 6.36. Comparison of ornithopod m. pterygoideus ventralis (mPTV) and m. pterygoideus dorsalis (mPTD). A, B, *Hypsilophodon* (basal ornithopod) (A, mPTV; B, mPTD); C, D, *Iguanodon* (basal iguanodontian) (C, mPTV; D, mPTD); E, F, *Corythosaurus* (hadrosaurid) (E, mPTV; F, mPTD). Left lateral views. See Fig. 6.2 for scale bars.

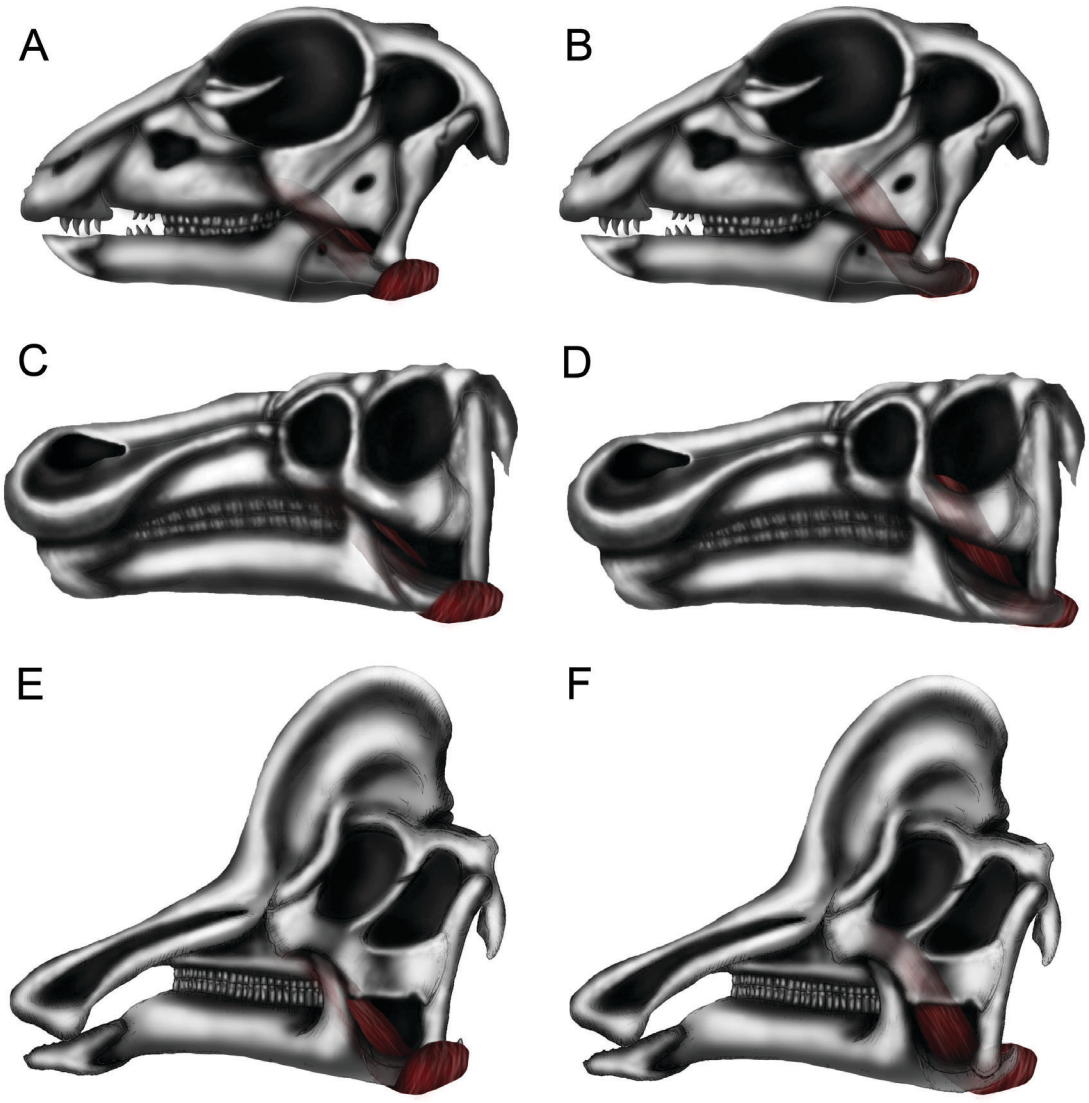
A
B
C
D
E
F

2D LEVER ARM ANALYSES

2D lever arm relative bite force (RBF) analysis was done on several ornithopod genera and were compared with each other as well as the rest of Ornithischia (see Chapter 8). Below, the RBF results at the predentary as well as the rostral, middle, and caudal teeth are given (Table 6.4).

TABLE 6.4. Actual RBF values across ornithopod tooth row.

Genus	**Spec. #**	**Input Lever Angle in ° (mAMEP)**	**Predentary RBF**	**Rostral Tooth RBF**	**Middle Tooth RBF**	**Caudal Tooth RBF**
Agilisaurus	ZDM 6011	43.04	0.306	0.341	0.491	0.855
Gasparinisaura	MUCPv 208	36.07	0.350	0.377	0.535	0.907
Anatotitan	Cast of holotype	32.25	0.279	0.547	0.837	1.806
Camptosaurus	(Marsh, 1879)	34.06	0.303	0.373	0.533	0.930
Corythosaurus	ROM 777	40.87	0.403	0.606	0.882	1.585
Dryosaurus	CMNH 3392	52.41	0.325	0.413	0.559	0.881
Edmontosaurus	ROM 801	54.69	0.282	0.535	0.856	2.027
Gryposaurus	ROM 873	55.57	0.424	0.570	0.879	1.826
Hypacrosaurus	ROM 789	35.65	0.451	0.704	1.057	1.701
Hypsilophodon	BMNH R197	41.03	0.346	0.429	0.620	1.022
Jeholosaurus	IVPP V12529	42.01	0.247	0.305	0.431	0.747
Altirhinus	Cast of holotype	45.36	0.374	0.463	0.657	1.136
Equijubus	IVPP V12534	47.33	0.405	0.536	0.708	1.035

Iguanodon	IRSNB R51	52.43	0.365	0.467	0.677	1.263
Ouranosaurus	(Taquet, 1976)	39.08	0.262	0.355	0.509	0.899
Kritosaurus	AMNH 5799	59.34	0.375	0.546	0.829	1.655
Lambeosaurus	ROM 1218	52.00	0.423	0.568	0.883	1.848
Maiasaura	Cast - MOR	62.73	0.346	0.548	0.817	1.569
Parasaurolophus	ROM 768	40.16	0.371	0.508	0.790	1.820
Parksosaurus	ROM 804	45.75	0.319	0.430	0.562	0.807
Prosaurolophus	ROM 787	54.67	0.358	0.510	0.793	1.741
Saurolophus	AMNH 5220	41.63	0.277	0.483	0.731	1.501
Tenontosaurus	AMNH - display	40.31	0.360	0.442	0.606	0.947
Thescelosaurus	NSCM 15728	39.90	0.252	0.348	0.510	0.915

Mechanical Advantages Among Ornithopod Jaws (with MANOVA Results)

There is a notable trend in the transition from a more evenly distributed RBF throughout the jaw in basal ornithopods and many non-hadrosaurid iguanodontians to a substantially stronger caudal RBF in hadrosaurids. Mallon and Anderson (*in press*) performed a 2D lever arm analysis of the jaw apparatus in genera prevalent in the Dinosaur Park Formation (Late Cretaceous, Alberta).. They studied multiple individuals within each genus and found that there is no significant difference between RBFs in individuals within a given genus of hadrosaurid, showing consistency throughout individuals within a given genus. Furthermore, they also found that there is no significant difference between genera within Hadrosauridae itself. In the current study, genera are compared in Ornithopoda within groupings of Basal Ornithopoda (+ *Dryosaurus* and *Camptosaurus*, since these genera, although iguanodontians, are arguably more basal in jaw morphology) (Fig. 6.37), more derived non-hadrosaurid Iguanodontia (Fig. 6.38), and

Hadrosauridae (Fig. 6.39). The groupings Lambeosaurinae and Hadrosaurinae are also compared within Hadrosauridae.

FIGURE 6.37. Basal ornithopod RBFs (Y-axis values) across the tooth row compared to Heterodontosaurus and Agilisaurus. Bite points are at the predentary (PD) tip as well as the rostral, middle, and caudal teeth.

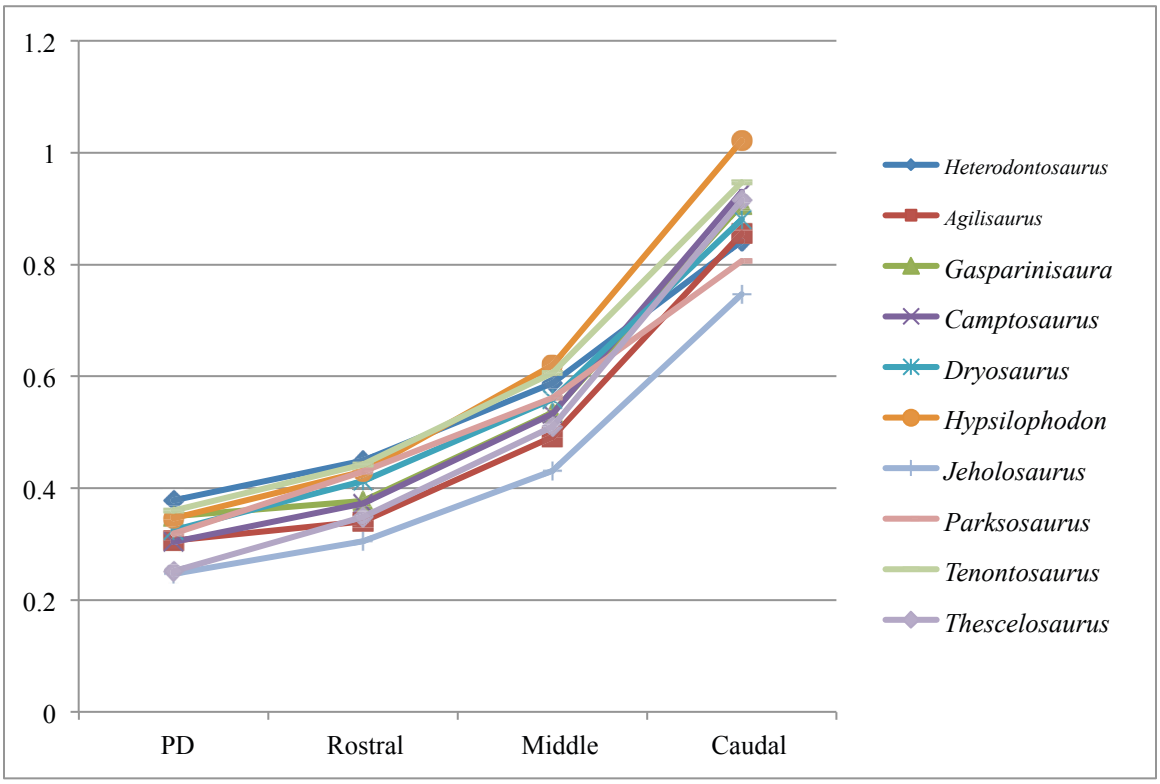

Results show, first of all, that basal ornithopods and more derived non-hadrosaurid iguanodontians are not significantly different in terms of RBF across the tooth row ($p = 0.099$). They all show relatively low RBFs in the caudal bite point especially, with *Iguanodon* and *Altirhinus* showing a slightly higher value. As is expected, however, basal ornithopods do show a highly significant difference in RBF than the highly derived Hadrosauridae ($p < 0.001$).

FIGURE 6.38. Basal iguanodontian RBFs across the tooth row. Bite points are at the predentary (PD) tip as well as the rostral, middle, and caudal teeth.

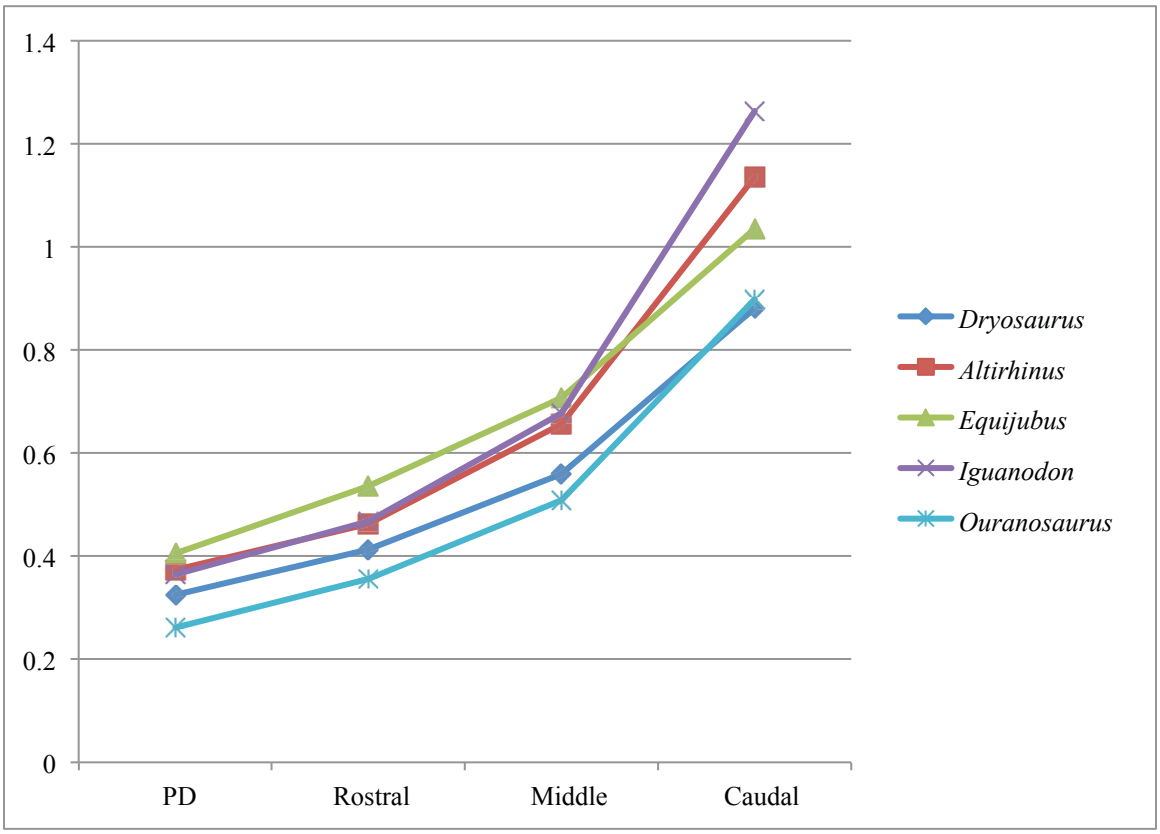

This evolutionary transition is actually seen much later in within Ornithopoda, as the non-hadrosaurid iguanodontians and derived hadrosaurids also show a highly significant difference in RBF ($p = 0.001$). This significance likely has a lot to do with the middle and caudal bite forces in hadrosaurids being substantially higher than in the rest of Iguanodontia, due to a caudally extended tooth row creating a shorter load arm caudally. The two subclades within Hadrosauridae, Lambeosaurinae and Hadrosaurinae, show no significant difference in RBF values across the tooth row ($p = 0.352$). Notable differences within Hadrosauridae are a substantially lower RBF value in the predentary of the hadrosaurines *Edmontosaurus, Anatotitan*, and *Saurolophus*, likely because of the highly

elongate diastema stretching the bill farther rostrally, and the generally higher predentary RBFs in the lambeosaurines, especially *Lambeosaurus*. *Edmontosaurus* also shows a greater RBF at the caudal end of the tooth row, showing how it is especially adapted for caudal forces rather than rostral.

FIGURE 6.39. Hadrosaurid RBFs across the tooth row compared to *Iguanodon*. Bite points are at the predentary (PD) tip as well as the rostral, middle, and caudal teeth.

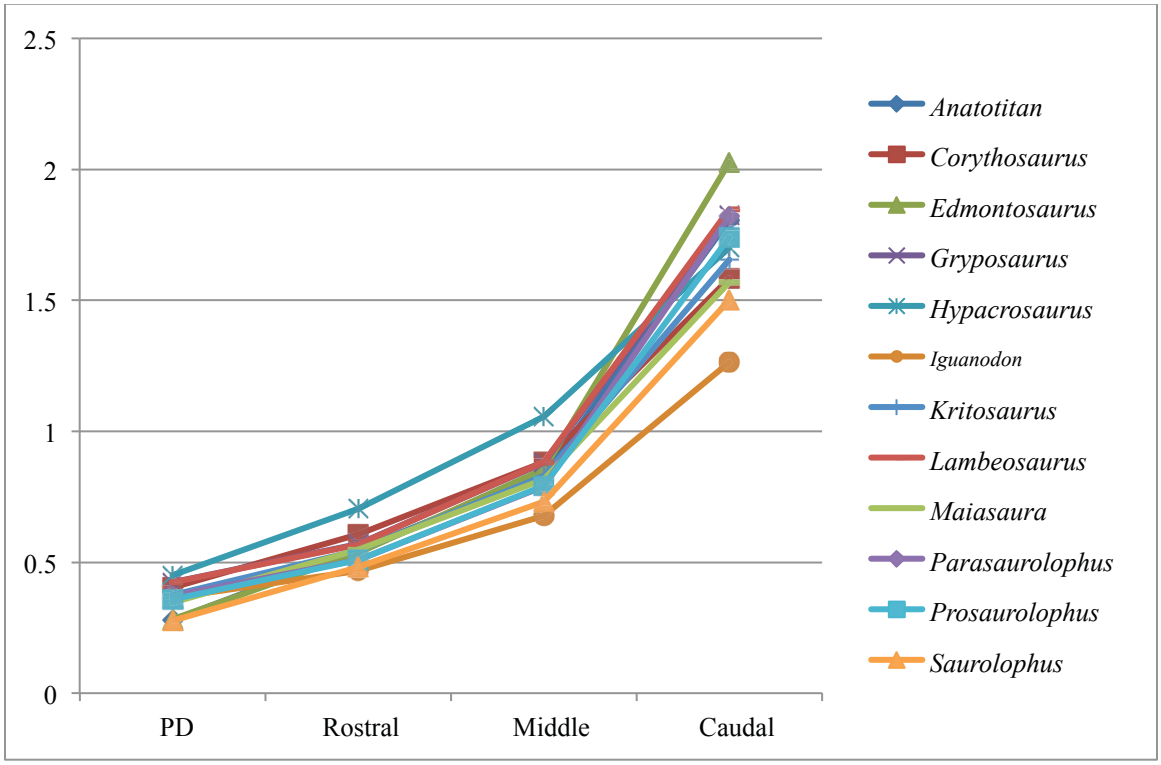

The phylogeny below (Fig. 6.40) visualizes the above results with optimized RBF values of the predentary and the caudal tooth compared to one another. Cooler colors show the lowest RBF values and warmer colors show gradually larger RBF values.

FIGURE 6.40 Phylogenetic mapping of RBFs across ornithopod taxa, comparing predentary and caudal tooth RBF values. *Agilisaurus* is used as the outgroup taxon. (Compiled phylogenies [Butler et al., 2011; McDonald et al., 2013; Prieto-Marquez, 2010].)

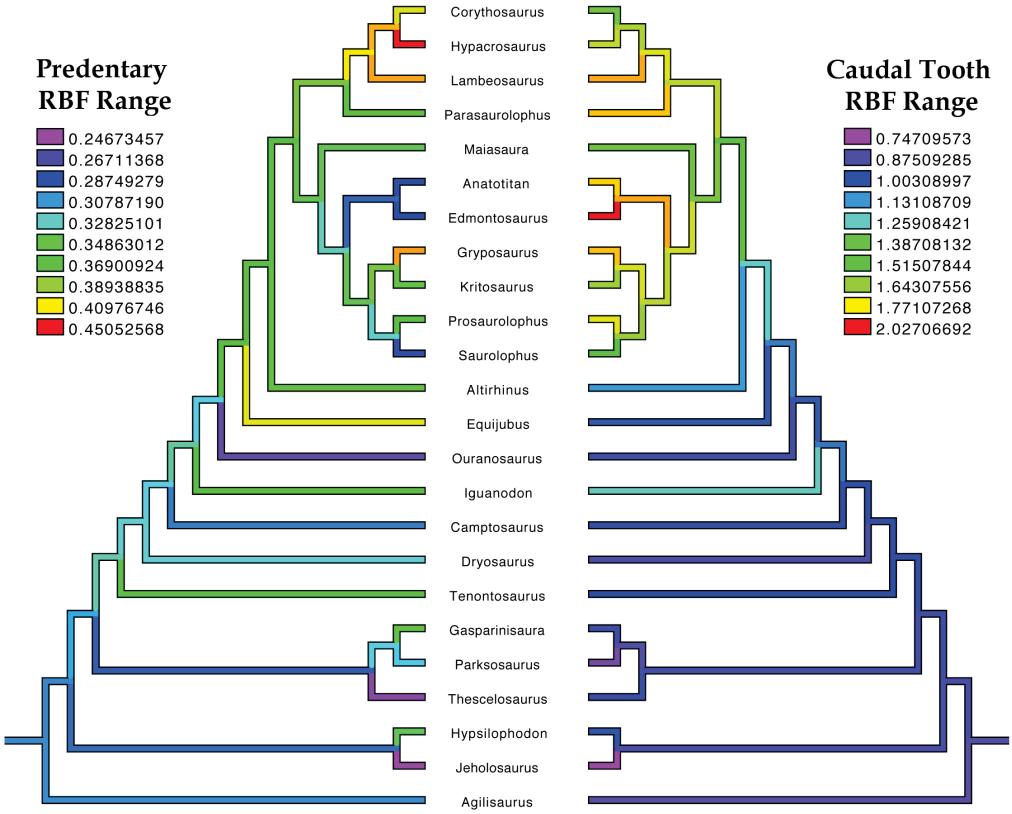

Perturbation analysis (Otten, 1983; 1985) results are shown below (Table 6.5) with RBF values with both the coronoid eminence removed and the jaw joint raised to the level of the maxillary tooth row:

TABLE 6.5. Hypothetical ornithopod RBFs with coronoid process removed (left) and articular raised to level of the tooth row (right).

Genus	Spec. #	Input Lever Angle in ° (mAMEP)		Predentary RBF		Rostral Tooth RBF		Middle Tooth RBF		Caudal Tooth RBF	
Agilisaurus	ZDM 6011	47.78	43.04	0.257	0.187	0.286	0.211	0.412	0.312	0.717	0.590
Gasparinisaura	MUCP v 208	40.84	36.07	0.306	0.211	0.329	0.226	0.467	0.332	0.793	0.594
Anatotitan	Cast of holotype	41.20	32.25	0.215	0.210	0.422	0.421	0.646	0.658	1.393	1.422
Camptosaurus	(Marsh, 1879)	41.93	34.06	0.265	0.192	0.325	0.237	0.465	0.347	0.811	0.639
Corythosaurus	ROM 777	51.90	40.87	0.316	0.292	0.476	0.462	0.692	0.695	1.243	1.446
Dryosaurus	CMNH 3392	56.49	52.41	0.307	0.286	0.391	0.368	0.529	0.501	0.833	0.804
Edmontosaurus	ROM 801	56.05	54.69	0.217	0.260	0.411	0.496	0.657	0.794	1.556	1.966
Gryposaurus	ROM 873	63.25	55.57	0.339	0.333	0.457	0.467	0.704	0.747	1.462	1.873
Hypacrosaurus	ROM 789	48.17	35.65	0.312	0.316	0.488	0.538	0.733	0.851	1.180	1.946
Hypsilophodon	BMNH R197	44.67	41.03	0.298	0.182	0.370	0.230	0.534	0.346	0.881	0.706
Jeholosaurus	IVPP V12529	46.72	42.01	0.217	0.173	0.268	0.215	0.380	0.309	0.658	0.547
Altirhinus	Cast of holotype	56.50	45.36	0.301	0.284	0.372	0.364	0.528	0.525	0.914	0.952
Equijubus	IVPP V12534	57.98	47.33	0.318	0.277	0.421	0.380	0.556	0.518	0.813	0.817
Iguanodon	IRSNB R51	60.82	52.43	0.305	0.289	0.392	0.375	0.567	0.557	1.058	1.108
Ouranosaurus	(Taquet, 1976)	48.34	39.08	0.219	0.189	0.298	0.260	0.426	0.377	0.753	0.683
Kritosaurus	AMNH 5799	68.20	59.34	0.284	0.301	0.413	0.456	0.627	0.718	1.251	1.701
Lambeosaurus	ROM 1218	62.55	52.00	0.331	0.345	0.445	0.479	0.691	0.760	1.447	1.835
Maiasaura	Cast - MOR	69.91	62.73	0.280	0.307	0.443	0.499	0.661	0.751	1.269	1.508
Parasaurolophus	ROM 768	53.53	40.16	0.286	0.321	0.392	0.442	0.609	0.696	1.403	1.660
Parksosaurus	ROM 804	49.91	45.75	0.295	0.186	0.398	0.256	0.520	0.355	0.747	0.529
Prosaurolophus	ROM 787	63.85	54.67	0.281	0.292	0.400	0.426	0.623	0.677	1.368	1.637
Saurolophus	AMNH 5220	56.10	41.63	0.215	0.218	0.374	0.386	0.567	0.599	1.165	1.331
Tenontosaurus	AMNH - display	44.06	40.31	0.322	0.203	0.395	0.255	0.541	0.361	0.847	0.631

Thescelosaurus	NSCM 15728	49.30	39.90	0.191	0.193	0.264	0.267	0.387	0.391	0.694	0.726

Results show that RBF values at all tooth positions in basal ornithopod taxa are hypothetically lower if the jaw joint is raised to the level of the tooth row than it is if the coronoid was removed. This suggests that lowering the jaw joint ventrally has a larger influence on mechanical advantage than the coronoid, thereby retaining the basal condition seen in heterodontosaurids as well as thyreophorans (see Chapter 4 and 5). Also, note how removing the coronoid process increases the input muscle vector angle, as is expected. In the derived hadrosaurids, however, due to the enlargement of the coronoid process, it is clear that the reverse is true. The evolved coronoid process takes over as a much more influential character in increased mechanical advantage. This is also seen in the derived ceratopsids (see Chapter 7). See Chapter 8 for evolutionary implications.

Chapter 7: Marginocephalian Craniomandibular Anatomy

Marginocephalian mandibular morphology is discussed in depth below with emphasis on functional interpretation (see Table 7.1 for specimens examined; see Fig. 7.1 for phylogenetic relationships). As some of the postdentary elements do not show as much functional significance as others, only a brief discussion of each postdentary element of the mandible is given below to illustrate the general shape of this region with a larger emphasis on functionally significant morphology. Cranial elements with direct contact with the mandible (i.e., the premaxilla, maxilla, quadrate, and rostral in ceratopsians) provide functional implications in marginocephalian jaw mechanisms and are also described for further completeness. Cranial elements holding significance with regards to the jaw adductor musculature are described as needed in the Jaw Musculature section.

FIGURE 7.1. Marginocephalian phylogenies. A, Pachycephalosauria (Evans et al., 2013); B, Ceratopsia (compiled phylogenies of Mackovicky and Norell (2006 [with integrated *Auroraceratops* placement of You and Dodson (2003)]) for basal ceratopsians, Sampson et al., (2012), and Sampson et al. (2013) for ceratopsids.

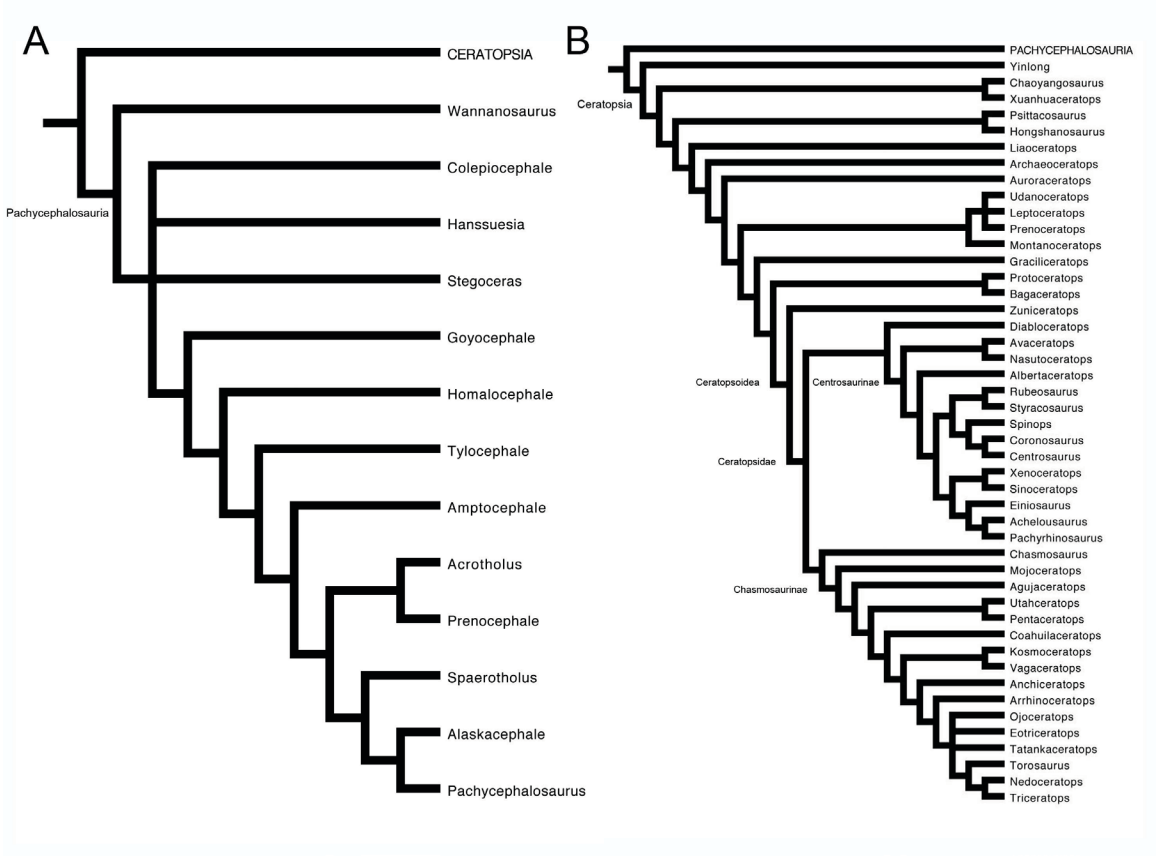

TABLE 7.1. Marginocephalian specimens examined in this study. (Note: many specimens were examined by the author; however, a large number of specimens, especially those from Chinese and Mongolian museums, were examined from detailed photographs. These photographs were provided courtesy of Frank Varriale and are used in this study with permission.

Taxon	Specimen	Elements
Pachycephalosauria		
Dracorex	TCMI 2004.17.1	Skull
Pachycephalosaurus	AMNH 1696	Complete jaw and skull
Prenocephale	ZPAL MgD-I/104	Skull
Spherotholus	NMMNH P30067	L. jaw ramus
Stegoceras	UALVP 2	Paired jaws (no predentary; skull
Tylocephale	ZPAL MgD-I/105	Partial skull
Wannanosaurus	IVPP V4447	L. jaw ramus
Ceratopsia		
Achelousaurus	MOR 485	Partial l. dentary; quadrate
	MOR 591	Predentary; partial l. jaw ramus; l. maxilla
Albertoceratops	TMP 2001.26.01	Partial skull with l. maxilla
Anchiceratops	NMC 8535	Skull
	ROM 802	Partial skull
Archaeoceratops	IVPP V1114	Complete jaw and skull
Arrhinoceratops	NMC 8882	R. dentary
	ROM 796	Skull
	ROM 1439	Complete jaw
Auroraceratops	IGCAGS 2004-VD001	Complete jaw and skull

Bagaceratops	GI SPS 100-528	Complete jaw and skull
	ZPAL MgD-I 123	Partial jaw and skull
	ZPAL MgD-I 125	Complete jaw and skull
	ZPAL MgD-I 127	Partial jaw and skull
	ZPAL MgD-I 137	L. dentary
	ZPAL MgD-I 153	R. jaw ramus
	ZPAL MgD-II 117	Partial jaw and skull
Brachyceratops	MOR 373	Predentary; r. dentary; quadrate
	MOR 571	Surangular
	USNM 7951	Predentary; dentary; skull
	USNM 7952	Rostral
Centrosaurus	AMNH 5351	Complete jaw and skull
	AMNH 5377	Paired dentaries
	NMC 348	Complete jaw and skull
	NMC 8795	Complete jaw and skull
	ROM 767	Complete jaw and skull
	TMP 1965.012.0006	R. dentary
	TMP 1979.011.0014	R. dentary
	TMP 1979.011.0053	R. dentary
	TMP 1979.011.0096	R. dentary
	TMP 1980.018.0022	Predentary
	TMP 1980.018.0080	L. dentary

	TMP 1980.018.0090	Quadrate
	TMP 1980.018.0148	Surangular
	TMP 1980.018.0265	L. dentary
	TMP 1980.018.0311	L. dentary
	TMP 1981.018.0066	R. dentary
	TMP 1982.018.0111	Predentary
	TMP 1982.018.0127	L. dentary
	TMP 1986.018.0068	R. dentary
	TMP 1986.126.0001	Predentary; paired dentaries
	TMP 1997.085.0001	Complete skull and dentary
	USNM 8897	Complete jaw and skull
Ceracinops	MOR 300	Partial jaws (no predentary); quadrate
Chaoyangosaurus	IGCAGS V3781	Complete jaws; partial skull
Chasmosaurus	NMC 284	R. dentary
	NMC 2245	Complete jaw and skull
	NMC 8801	R. dentary
	ROM 839	Compete jaw and skull
	ROM 843	Complete jaw and skull
	TMP 1981.019.0175	Skull
Diabloceratops	Carnegie Cast	Skull
Einiosaurus	MOR 456	Complete jaw
Gryphoceratops	ROM 56635	Partial r. dentary

Hongshanosaurus	IVPP V12617	Complete jaw and skull
Leptoceratops	NMC 8889	Complete jaw and skull
	TMP 1995.012.0006	Partial l. dentary
Liaoceratops	IVPP V12633	Complete jaw and skull
	IVPP V12738	Complete jaw and skull
Magnirostris	IVPP V12513	Complete jaw and skull
Micropachycephalosaurus	IVPP V5542	Partial l. dentary
Monoclonius	NMC 1173	Predentary; quadrate
	NMC 8790	Complete jaw and skull
Nedoceratops	USNM 2612	Skull
Pachyrhinosaurus	NMC 10645	Predentary; r. jaw ramus
	TMP Display Skull	Complete jaw and skull
	TMP 1987.055.0243	L. dentary
	TMP 1988.055.0002	L. dentary
	TMP 1988.055.0161	Predentary
	TMP 1989.055.0030	Predentary
	TMP 1989.055.0057	L. dentary
	TMP 1989.055.0723	R. dentary
Pentaceratops	AMNH 1624	Partial jaw; skull
	AMNH 6325	Skull
	KUVP Specimen	Predentary
	KUVP 16100	Skull
	NMMNH P21098	Predentary; r. dentary

	OMNH 10165	Lower jaw; Partial skull
Prenoceratops	TCMI 2001.96.14	Complete jaw and skull
Protoceratops	AMNH 2352	Predentary
	AMNH 6438	Complete jaw and skull
	AMNH 6466	Complete jaw
	GI SPS 100-500	Complete jaw and skull
	GI SPS 100-507	Complete jaw; partial skull
	GI SPS 100-521	Complete jaw and skull
	GI SPS 100-522	Complete jaw and skull
	GI SPS 100-527	Partial jaw and skull
	UCMP 62185	Complete jaw; partial skull
	ZPAL MgD-II 02	Complete jaw and skull
	ZPAL MgD-II 04	L. dentary; maxilla
Psittacosaurus	AMNH 6254	Complete jaw and skull
	BNHM BPV-24	Complete jaw and skull
	BNHM BPV-119	Complete jaw and skull
	BNHM BPV-120	Complete jaw and skull
	IVPP V738	Complete jaw and skull
	IVPP V7705	Complete jaw and skull
	IVPP 12-0888	Complete jaw and skull
Styracosaurus	AMNH 5372	Complete jaw and skull
	NMC 344	Complete jaw and skull
Torosaurus	MOR 1122	Partial jaws; skull

Triceratops	AMNH 972	Predentary
	AMNH 5237	Dentary
	MOR 004	Complete jaw and skull
	MOR 699	Complete jaw and skull
	MOR 1110	Predentary; skull
	MOR 1199	Complete jaw and skull
	OMNH 10170	Complete jaw
	ROM 55380	Complete jaw and skull
	TCMI 2001.93.1	Complete jaw and skull
	UCMP 133908	Predentary
	USNM 4928	Predentary; skull
Yinlong	IVPP V14530	Complete jaw and skull
Zuniceratops	MSM P2224	L. dentary
	MSM P3201	L. dentary
	MSM P4175	Predentary

OSTEOLOGICAL DESCRIPTION: PACHYCEPHALOSAURIA

The following descriptions were based on personal examination of specimens. For further descriptions, see Gilmore (1924), Maryańska and Osmólska (1974), Sues and Galton (1987), Maryańska et al. (2004), and others referenced below.

FIGURE 7.2. *Stegoceras* skull. Scale bar = 5 cm.

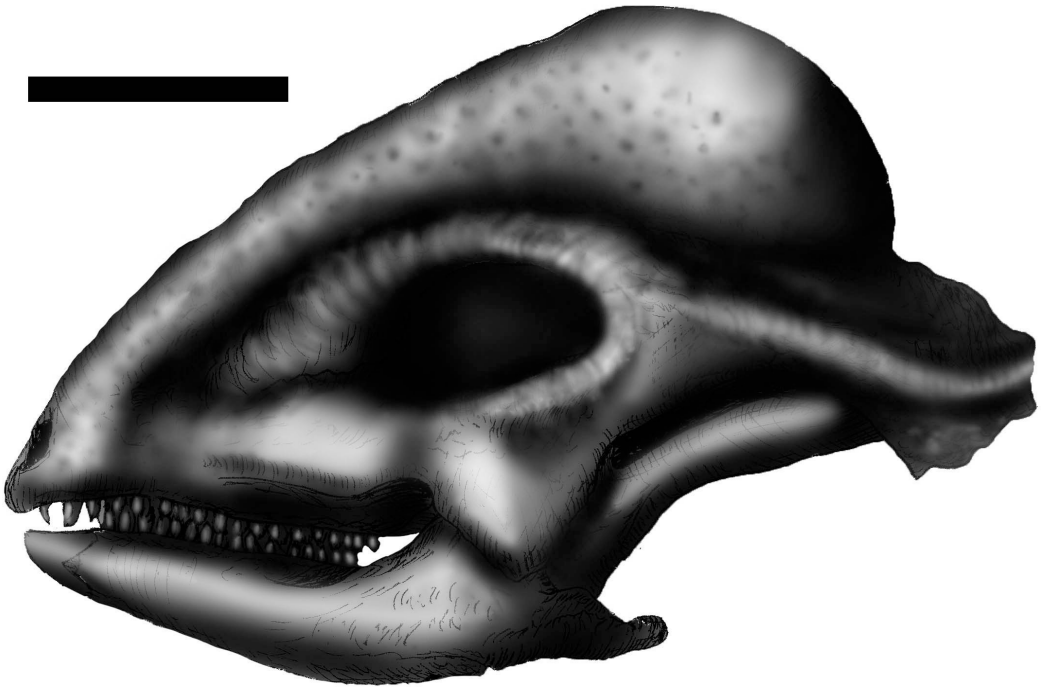

Cranium

The most distinctive character of pachycephalosaur skulls is the prominent thickening of the skull roof into a dome (Figs. 7.2; 7.3). This dome is made of the frontal and parietal as well as some supraorbital and postorbital along its lateral margins, and has variable thicknesses depending on the taxon (Gilmore, 1924; Maryańska and Osmólska, 1974). Skull thickening was previously thought to have protected the small brain and basicranium from damage during head butting; however, histological studies showed internal structures inconsistent with head butting behavior suggesting that it might have been for species recognition or sexual display (Goodwin and Horner, 2004). Along with the thickening of the skull roof, most articulations of skull elements are co-ossified and akinetic. Immediately rostral to the thickened skull roof, the nasal slopes ventrally down to the rostral tip. In *Pachycephalosaurus* (AMNH 1696), this is more of a straight preorbital descent to the rostral tip of the premaxilla, creating a triangular skull profile in lateral view, whereas in many other pachycephalosaurs, such as *Stegoceras* (UALVP 2) and *Prenocephale* (ZPAL MgD-I/104), the nasals are more dorsally arched. Pachycephalosaurs possess a large, circular orbit, but usually have no antorbital fenestra, except for *Prenocephale*, in which it is small.

FIGURE 7.3. *Stegoceras* cranium (generalized). Abbreviations: : itf, infratemporal fenestra; la, lacrimal; j, jugal; m, maxilla; n, nasal; or, orbit; pa, parietal; pf, prefrontal; pm, premaxilla; q, quadrate; sor, supraorbital; sq, squamosal (right lateral view). Scale bar = 5 cm.

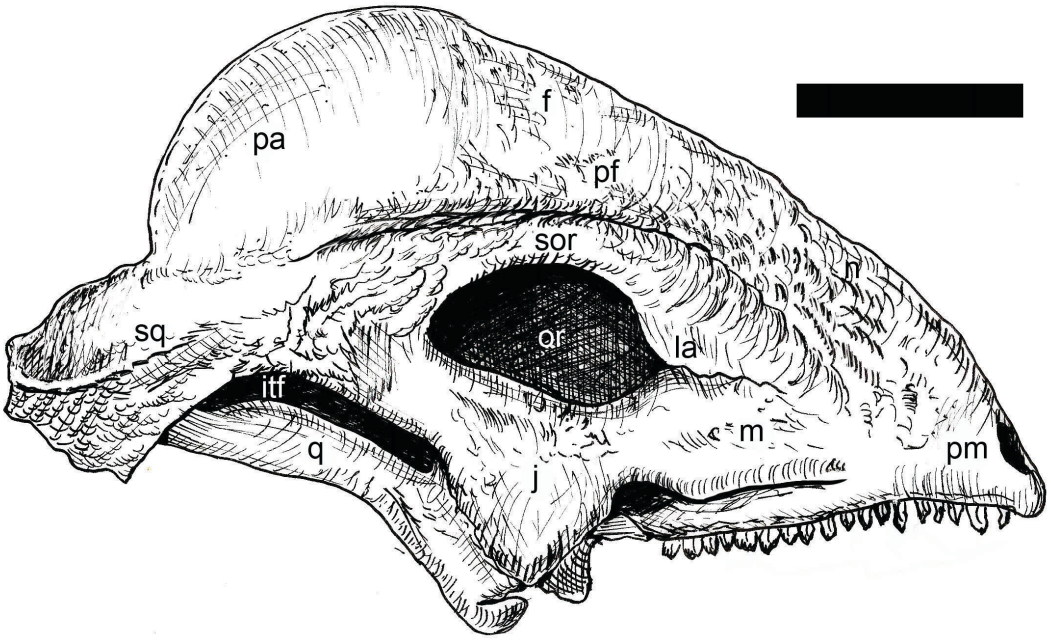

Ventrally, the premaxilla is set slightly lower with respect to the level of the maxillary tooth row, although it is not known in *Pachycephalosaurus* or *Homalocephale* (Maryańska and Osmólska, 1974). The palate is narrow in ventral view and each maxillary tooth row is medially arched with respect to its dentary counterpart. The jugal is fused to the quadratojugal, creating a large triangular flange oriented caudoventrally and protruding ventral to the level of the maxillary tooth row. A lateral expansion of the squamosals that overhangs the occiput as well as a dorsoventral heightening of the occiput itself characterizes pachycephalosaurs as a clade. In the more basal *Homalocephale* as well as *Stegoceras*, circular supratemporal fenestrae are still present, albeit they are much smaller and nearly closed in *Stegoceras*. Most other pachycephalosaur taxa, however, do not have supratemporal fenestrae because they are

been closed of during skull thickening. The infratemporal fenestra is present, but rostrocaudally compressed as a thin oval to a crescentic opening. The quadrate is angled rostrally with respect to its dorsal articulation, as is discussed below. Pachycephalosaur skulls also have many rounded or conical osteoderms, usually on the squamosals and on the narial region.

Premaxilla—The premaxilla is small and blunt, mostly because the enlarged nasals overtake much of the rostrodorsal margin of the snout. This element is situated rostrally between the maxilla and nasal and does not reach far caudally. It borders most of the ventral margin of the small external naris, however. The ventral edge of the premaxilla is prominent and rugose, and is slightly ventral to the level of the maxillary tooth row. Much like all ornithischians, in lateral view, the rostral-most region of the premaxilla does not bear any dentition. However, immediately caudal to this margin, three teeth are present (see Dentition section below). There is a slight diastema between the premaxillary and maxillary dentitions, although the extent of premaxillary or maxillary contribution to this diastema is variable.

Maxilla—The maxilla is, a dorsoventrally tall, nearly-triangular element bordered by the premaxilla rostrally, the nasal and lacrimal dorsally, and the jugal caudally. Ventrally, the maxilla rests against its counterpart medially at the palate, with the vomer just caudal to it (Fig 7.4). There is no antorbital in any pachycephalosaur except for a small one in *Prenocephale* (ZPAL MgD-I/105), which is created within the maxilla-lacrimal suture. This region in pachycephalosaurs has been associated with a paranasal sinus, with structures much like nasal turbinates (Maryańska and Osmólska, 1974). There is a buccal swelling of the lateral maxilla immediately dorsal to the tooth row, indicating

creating a medially inset emargination of the tooth row, possibly supporting soft tissue on its lateral margin. The maxillary tooth rows form an acute angle with respect to its counterpart in ventral view, with the mesial-most teeth closest together and the distal-most teeth farthest apart. See Dentition section below for a description of dental morphology.

FIGURE 7.4. Ventral view of *Stegoceras* (UALVP 2) palate showing acute angle between tooth rows. Rostral at top. Scale bar = 5 cm.

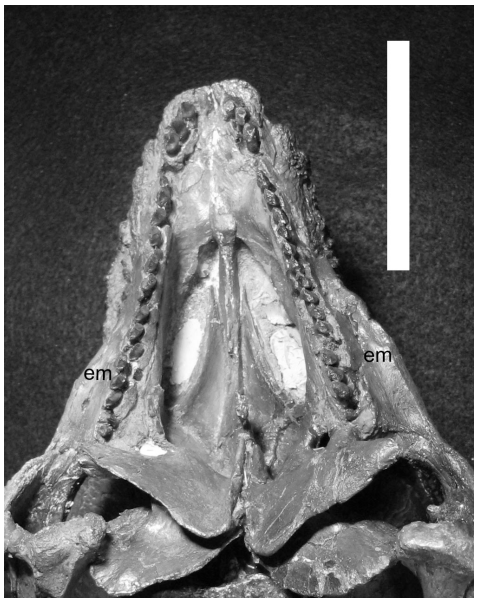

Quadrate—The quadrate (Figs. 7.5; 7.6) is a tall, columnar element at the caudal margin of the skull bilaterally. Dorsally, it is rounded and wedged ventral to the squamosal. It is, at variable degrees, angled rostroventrally forming much of the caudal margin of the infratemporal fenestra at its dorsal half.

FIGURE 7.5. *Prenocephale* (ZPAL MgD-I/104) left quadrate in lateral view showing rostral bowing. Abbreviations: itf, infratemporal fenestra; q, quadrate; sq, squamosal. Photo courtesy of Frank Varriale. Scale bar = 5 cm.

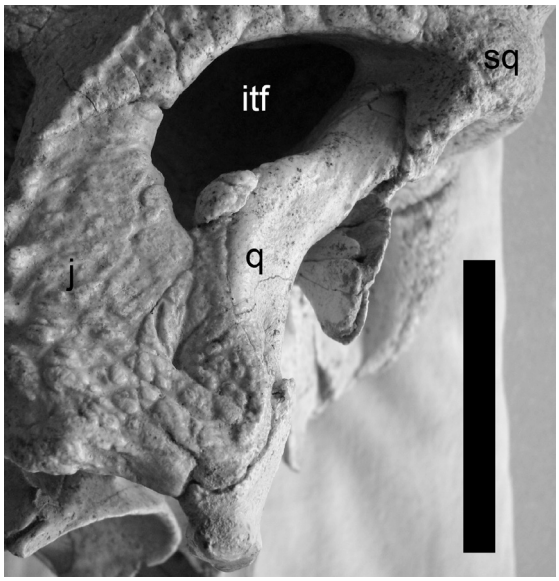

A large, expanded pterygoid process projects rostrally from the midshaft of the quadrate, which overlaps the pterygoids. The ventral head the quadrate extends to the level of the maxillary tooth row; here it is rostrocaudally round, with a mediolateral expansion where it articulates with the articular surface of the mandible and acts like a hinge joint. The quadrate is rostrally fused to the quadratojugal, which, along with the jugal, forms a large, triangular jugal flange that hides the rest of the mediolateral expanse of the quadrate in lateral view, precluding any streptostyly.

FIGURE 7.6. *Prenocephale* (ZPAL MgD-I/104) left quadrate in caudal view showing laterally expanded ventral head. Abbreviations: q, quadrate. Photo courtesy of Frank Varriale. Scale bar = 2 cm.

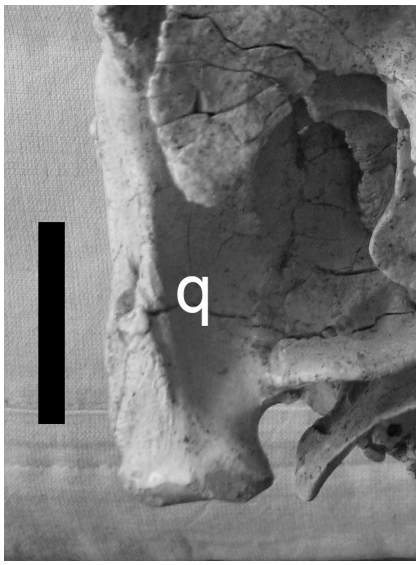

Predentary

There are currently no described predentaries for Pachycephalosauria, although articular impressions on the dentaries (described below) indicate its presence is likely (Sues and Galton; 1987; Maryańska et al., 2004).

Dentary

The dentary (Figs. 7.7; 7.8; 7.9) is the largest element in the pachycephalosaur mandible, extending roughly two-thirds the length of the mandible (Sues and Galton, 1987; Maryańska et al., 2004). It articulates with the predentary as well as its counterpart rostrally, the splenial medially, and the surangular, angular, and coronoid caudally.

FIGURE 7.7. *Stegoceras* right mandible (generalized without predentary). A, lateral view; B, medial view. Abbreviations: a, angular; ar, articular; c, coronoid; d, dentary; rap, retroarticular process; sa, surangular; sp, splenial. Scale bar = 5 cm.

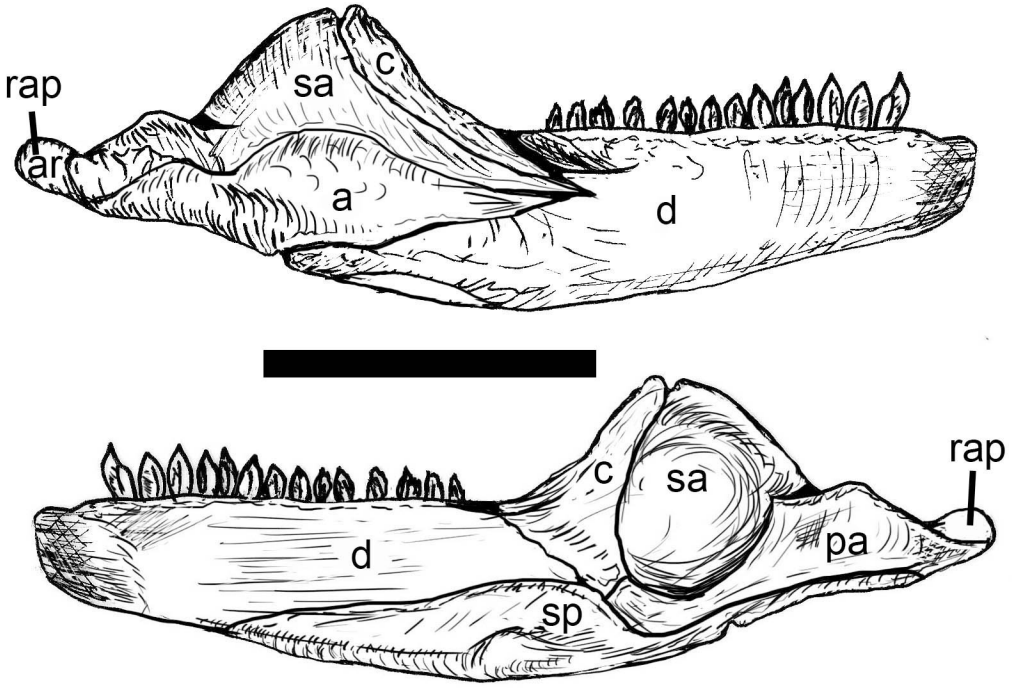

Dentaries (and mandibles in general) are rarely found in pachycephalosaurs, known only in *Stegoceras*, *Pachycephalosaurus* (AMNH 1696; "*Dracorex*" [TCMI 2004.17.1]), *Goyocephale* (Perle et al., 1982), *Tylocephale* (Maryańska and Osmólska, 1974), and *Wannanosaurus* (Hou, 1977). The dentary is thin mediolaterally and elliptical in shape rostrocaudally, with its rostral end tapering to a thin, mediolaterally-flattened, and subrectangular margin. The dentaries are not fused at the symphysis nor are they fused to the predentary. The medial surface of the symphysis bears fine rugosities and

ridges, suggesting bone remodeling induced by forces from movement against the opposite dentary in life (Fig. 7.8).

FIGURE 7.8. *Stegoceras* (UALVP 2) rostral end of right dentary in medial view showing rugose mandibular symphysis. Abbreviations: sym, symphysis. Photo courtesy of Frank Varriale.

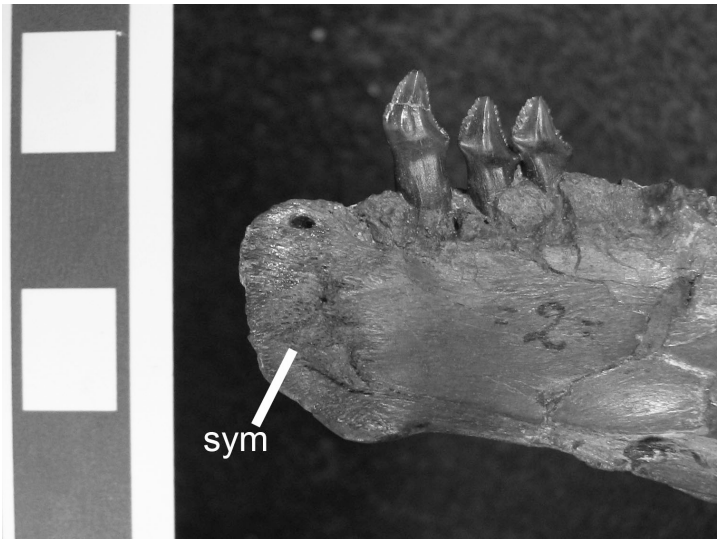

Shallow grooves on the lateral margins of the dentary, however, suggest an articulation with a small predentary that likely had caudolateral processes. Two or three small foramina on the lateral surface of the rostral edge of the dentary indicate neurovasculature supplying a keratinous covering of the predentary.

The tooth row starts just caudal to the rostral expansion, or diastema, of the dentary on its dorsal margin. In occlusal view, the dentary tooth rows are at an acute angle to each other and each is more or less straight, with only a slight medial curvature at its caudal end. Buccal widening just ventral to the tooth row, creates a medially inset

tooth row, as is seen in the maxilla, likely supporting soft tissue along its lateral margin (Fig. 7.9). The tooth row extends just medial to the coronoid eminence at its caudal extent. See Dentition section below for a description of dental morphology.

FIGURE 7.9. *Stegoceras* (UALVP 2) right mandible in dorsal view showing medial emargination of tooth row on dentary. Abbreviations: em, emargination. Photo courtesy of Frank Varriale. Scale bar units in cm.

The coronoid eminence is taller relative to that of other more basal ornithischians, and triangular in lateral view. Rostrally it is composed of the dentary but also of the coronoid and surangular. Its caudodorsal margin is where the jaw adductor musculature, aiding in jaw elevation, likely inserted (see below). The mandibular fossa of the caudal margin of the dentary likely accommodated the mandibular nerve (V_3) and the insertion of part of m. adductor mandibulae externus. A shallow concavity on the caudomedial aspect of the dentary clearly indicates this fossa. The dentary caudal aspect of the dentary is concave, with the surangular and coronoid bordering its caudolateral margin and the angular bordering its ventral margin. There are no eternal mandibular fenestrae present.

Coronoid

The coronoid (Fig. 7.7) in pachycephalosaurs is not well known, but is small and thin, continuous with the surangular at its dorsal margin and creating the more caudal aspect of the coronoid eminence, with the dentary articulating immediately rostral to them. The coronoid possesses a grooved articulation with the surangular and has two processes; one contacting the dentary and the other articulating with the prearticular.

Splenial

The splenial (Fig. 7.7) is a thin sheet of bone that lies along the medial aspect of the dentary, covering a large portion of it and acting like a plate against the inferior alveolar branch of the mandibular nerve (V_3) within the mandibular canal of the dentary, as it does in extant archosaurs and, likely, in a majority of ornithischians.

Angular

The postdentary region of the mandible is short and the angular is the largest element of it. (Sues and Galton, 1987; Maryańska et al., 2004; Fig. 7.7). It articulates with the caudoventral aspects of the dentary and surangular. It creates a ventrally-concave, rostrocaudally-elongate groove and thereby forms the ventral aspect of the internal mandibular fossa that served as an insertion of m. adductor mandibulae posterior. It likely also created the medial margin of the craniomandibular jaw joint and elongate retroarticular process typical of pachycephalosaurs, although these sutures are difficult to discern.

Prearticular

This small element articulates with the angular rostrally and the articular caudally (Fig. 7.7). The suture between the prearticular and articular is not visible, indicating fusion between the two elements (Sues and Galton, 1987; Maryańska et al., 2004). It has a long, rostrally-oriented projection in medial view that likely served as an insertion of some muscle fibers from m. adductor mandibulae externus as well as m. adductor mandibulae posterior.

Surangular

The surangular (Fig. 7.7) is an irregularly-shaped, thin element that forms the more caudal aspect of the dorsally-oriented coronoid eminence. It borders the dentary and coronoid rostrally, the angular ventrally, and helps cradle the articular caudally, creating the lateral aspect of the craniomandibular joint, a majority of which is formed by the articular. It extends farther caudally, creating the lateral margin of the retroarticular process, which is notably elongate in pachycephalosaurs. Three small foramina on the lateral surface of the surangular probably supplied neurovasculature to the skin of the mandible (Sues and Galton; 1987).

Articular

As stated above, the articular is fused with the prearticular, extending caudally in a sinusoidal path, with its dorsal surface to form a concave surface for articulation with the ventral part of the quadrate (Figs. 7.7; 7.10; 7.11). This hinge joint likely imparted

orthal chewing action (Sues and Galton, 1987; Varriale, 2011) because a hinge joint like this would only allow rotation around the coronal axis of the quadratic condyle.

FIGURE 7.10. *Stegoceras* (UALVP 2) right mandibular glenoid in dorsal view, rostral to the left. Abbreviations: as, articular surface; lat, lateral side; med, medial side;;; rap, retroarticular process. Photo courtesy of Frank Varriale. Scale bar units in cm.

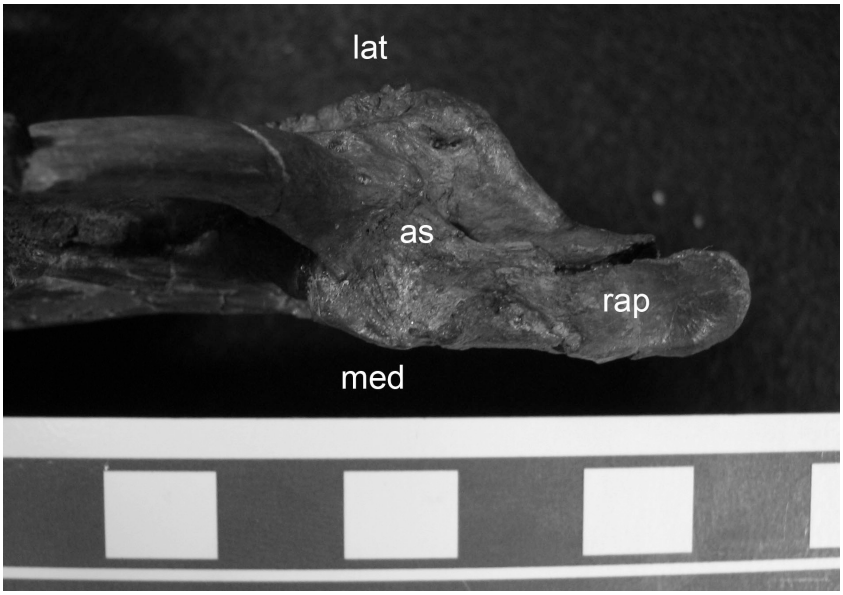

The caudal-most extent of the articular forms an elongate retroarticular process, relatively longer with respect to the mandible than in many other ornithischians, including ornithopods (Maryańska et al., 2004). This retroarticular process acted as the insertion for m. depressor mandibulae as well as m. pterygoideus musculature.

FIGURE 7.11. Pachycephalosaur quadrate/articular articulation in caudal view.

Abbreviations: ar, articular surface; q, quadrate; rap, retroarticular process.

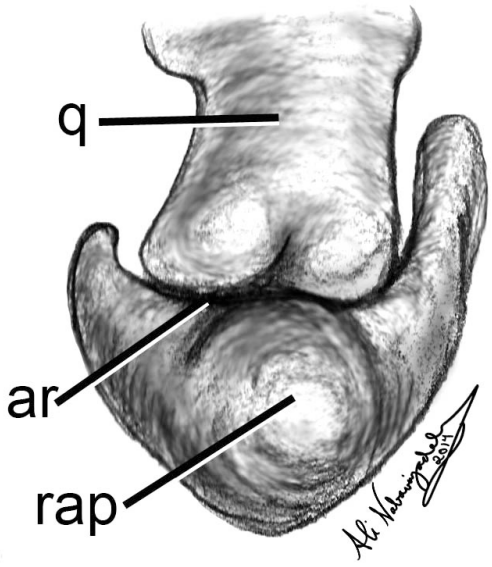

Dentition

Pachycephalosaurs typically have three conical, caudoventrally-recurved caniniform teeth in the premaxilla, each one larger than the one mesial to it. These teeth are seen in *Prenocephale* (ZPAL MgD-I/104; Maryańska and Osmólska, 1974), *Dracorex* (TCMI 2004.17.1), *Goyocephale* (Perle et al., 1982), and *Stegoceras* (UALVP 2; Gilmore, 1924), but likely existed in other pachycephalosaurs as well. They are denticulate on their distal margin and possess vertical wear facets (Sues and Galton 1987; Varriale, 2011), indicative of an orthal tooth-tooth movement.

FIGURE 7.12. "*Dracorex"* left premaxillary tooth; first tooth position.

The maxilla contains, for the most part, between 15 to 20 teeth that project ventrally at its ventrolateral margin, although *Goyocephale* had a relatively smaller tooth row (Perle et al., 1982). These maxillary teeth differ from those of the premaxilla in being small, triangular to lacrimiform, and mediolaterally compressed, with a slightly bulbous cingulum. The crown surfaces have apicobasally-oriented ridges that form marginal denticles at the apex, with the largest denticles in the center of the tooth. The teeth are almost in line with each other mesiodistally, with the mesial end of each more caudal tooth overlapped labially by the tooth mesial to it (Maryańska et al., 2004). The tooth crown is slightly convex lingually while the labial side is concave (Maryańska et al., 2004). The tooth roots are long and cylindrical.

The dentition of the dentary is similar to the maxillary dentition (Fig. 7.13). The crown is triangular to lacrimiform and projects dorsally from a bulbous base. The mesial dentition is typically larger in size than the more distal teeth. The crowns are ridged apicobasally, with the middle ridges the most pronounced. Wear is on the labial side of the dentition, meaning that the dentary teeth occluded with the maxillary teeth lingually (Maryańska et al., 2004).

FIGURE 7.13. *Stegoceras* dentary tooth. (Right side; middle tooth.)

Wear on the pachycephalosaur dentition is variable but shows orthal stroke with oblique wear in *Stegoceras* (Sues and Galton, 1987; Varriale, 2011). In some cases, such as *Goyocephale* and *Tylocephale* (ZPAL MgD-1), the wear on all teeth combined form one wear plane, indicative of uniform use of the tooth row as a whole in chewing (Maryańska et al., 2004).

OSTEOLOGICAL DESCRIPTION: CERATOPSIA

The following descriptions were based on personal examination of specimens. For further descriptions, see Hatcher et al. (1907), Lull (1933), Ostrom (1964), Ostrom (1966), Dodson (1996), Dodson et al. (2004), You and Dodson (2004), Tanoue et al. (2011), and more referenced below. Due to the large abundance of ceratopsian craniomandibular material, both personally examined for this study and referenced in text, descriptions are based on observations of all specimens listed in Table 6.1 unless otherwise noted in the text.

FIGURE 7.14. Comparison of ceratopsian skulls. A, *Psittacosaurus* (basal ceratopsian – psittacosaurid); B, *Archaeoceratops* (basal neoceratopsians); C, *Leptoceratops*; D, *Protoceratops*; E, *Centrosaurus* (centrosaurine ceratopsid); F, *Triceratops* (chasmosaurine ceratopsid); G, *Chasmosaurus* (chasmosaurine ceratopsid). Scale bars = 5 cm.

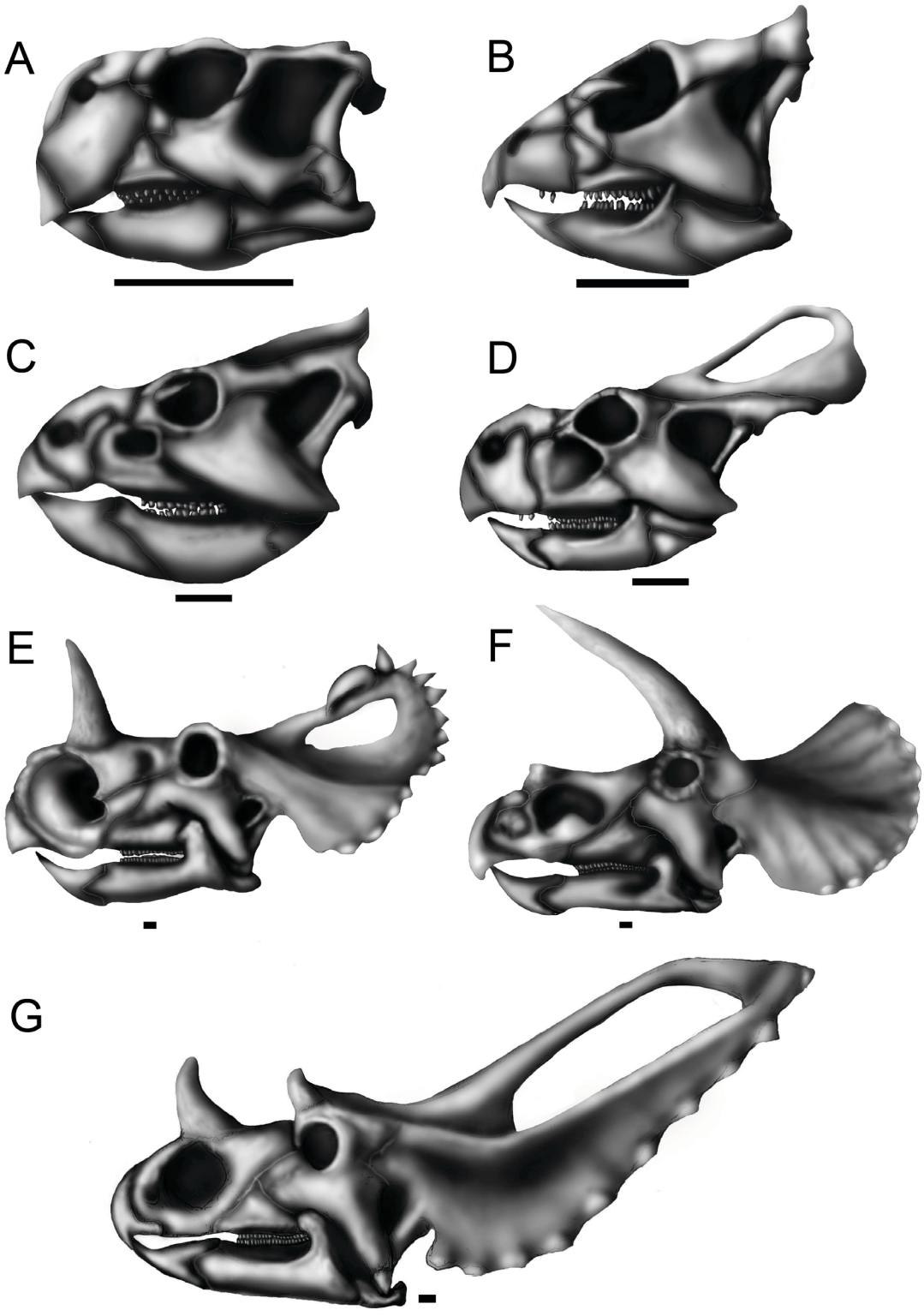
A
B
C
D
E
F
G

Cranium

Ceratopsians have arguably some of the most elaborate cranial anatomy of all dinosaurian subclades and of vertebrates as a whole (Figs. 7.14; 7.15. Except for the basal *Yinlong* (IVPP V14530) and psittacosaurids, ceratopsians are known primarily for their distinctive, caudodorsally expanded bony frill, which is formed by a caudal extension of the squamosal caudolaterally and the parietal medially, creating a median parietal bar. The frill possesses a series of small, bony protrusions, called epocciptials (episquamosals and epiparietals) that surround the distal edge of the frill circumference. These frills usually have two enlarged fontanelles on either side of the dorsal surface surrounding the parietal bar, except in *Triceratops*, which simply has a solid sheet of bone throughout the frill (see Table 7.1 for specimens; Hatcher et al., 1907; Dodson, 1996; Forster, 1996). Among the most derived ceratopsian clade, Ceratopsidae, chasmosaurines tend to have much more caudally elongate frills, whereas centrosaurines have relatively shorter frills. Rostrally, the frill is sutured to the jugal on either side of the skull, which is represented by a caudoventrally-oriented, triangular bony protrusion that slightly enlarges at its distal end. Just caudal to the jugals on both sides of the skull is an infratemporal fenestra, which, in derived ceratopsids, is small and triangular to circular and caudally bounded by the rostroventrally-oriented quadrate. The supratemporal fenestra in basal ceratopsians (e.g., *Yinlong*, psittacosaurids, and basal neoceratopsians) is larger and of circular to rectangular, as in the most basal ornithischians. In derived ceratopsids, however, it is reduced in size to a small opening, sometimes as small as a slit at the rostral border of either side of the frill and is only visible in dorsal view.

FIGURE 7.15. *Chasmosaurus* (chasmosaurine ceratopsid) cranium (generalized). Abbreviations: itf, infratemporal fenestra; j, jugal; la, lacrimal; m, maxilla; n, nasal; or, orbit; pa, parietal; po, postorbital; pm, premaxilla; q, quadrate; r, rostral; sq, squamosal. Right lateral view. Scale bar = 15 cm.

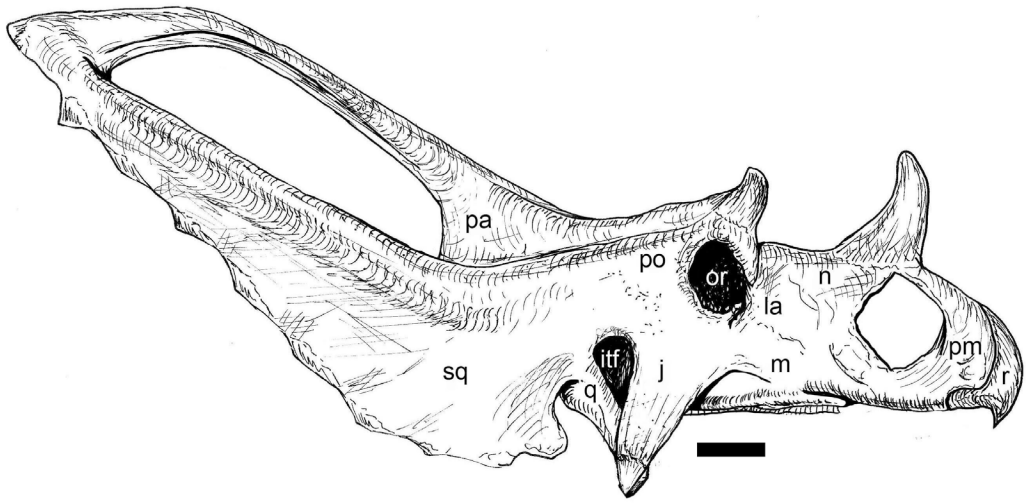

Ceratopsians are also known for their sharp beak, with a unique ventrally-curved and pointed rostral bone overhanging the equally pointed predentary rostrodorsally (described below). The rostral bone is a neomorph of ceratopsians. The external naris is relatively small in basal ceratopsians and grows in relative rostrocaudal breadth to extremely large in derived ceratopsids, which correlates with the reduction in size of the subtriangular antorbital fenestra in basal ceratopsians to obliteration in derived taxa. The circular orbits in ceratopsians also tend to decrease in relative size as genera become larger.

The signature long and pointed horns of ceratopsians are not particularly evident until the appearance of *Zuniceratops* and the derived Ceratopsidae. Vascular, keratinous

sheaths, like those of bovid mammals, surrounded ceratopsian horn cores (Dodson, 1996). Horn cores are known to be of different shapes and sizes, depending on the taxon. The chasmosaurine *Bauplan* is two long brow horn cores above the orbits with a smaller nasal horn core, although this is not always the case. Centrosaurines, on the other hand, possess a long nasal horn core and two small brow horn cores, again, with exceptions. In life, the horns would have been used either for defense or display and are what set apart most ceratopsians from the rest of Ornithischia.

Rostral—The rostral (Fig. 7.16), an unpaired, median element unique to Ceratopsians. It is sutured rostral to the nasals dorsally and premaxillae ventrally by two processes, oriented caudodorsally and caudolaterally respectively. *Chaoyangosaurus* (IGCAGS V3781) and psittacosaurids possess a slightly more rostrally rounded, cup-shaped rostral, which also has a flat ventral edge (see Table 7.1 for specimens; Tanoue et al., 2011). Psittacosaurid rostrals are distinctively short rostrocaudally, yet are dorsoventrally high, barely sutured with the nasal dorsally. The rostral of more derived ceratopsians, however, possesses a more mediolaterally compressed and, in some cases, ventrally hooked morphology with a pointed tip at its distal end like a parrot. Among the most derived ceratopsids, centrosaurines tend to possess a much straighter, triangular rostral, whereas the rostral of chasmosaurines tend to be much more rostrocaudally elongate, relatively shorter in height, and ventrally recurved (Dodson et al., 2004). The rostral indentation between the caudodorsal and caudolateral processes forms the rostral border of the large, high external naris. The rostral overhangs its ventral counterpart, the predentary, in front and is ventrally scoop-shaped with a dorsally sloped internal surface, where the predentary would fit inside during occlusion.

FIGURE 7.16. Rostral bones in relation to surrounding elements. A, Psittacosaurus (IVPP 12-0888; basal ceratopsian; photo courtesy of Frank Varriale); B, Centrosaurus (ROM 767; ceratopsid). Abbreviations: d, dentary; p, predentary; pm. Premaxilla; r, rostral. Scale bar in A = 2 cm. Scale bar units in B in cm.

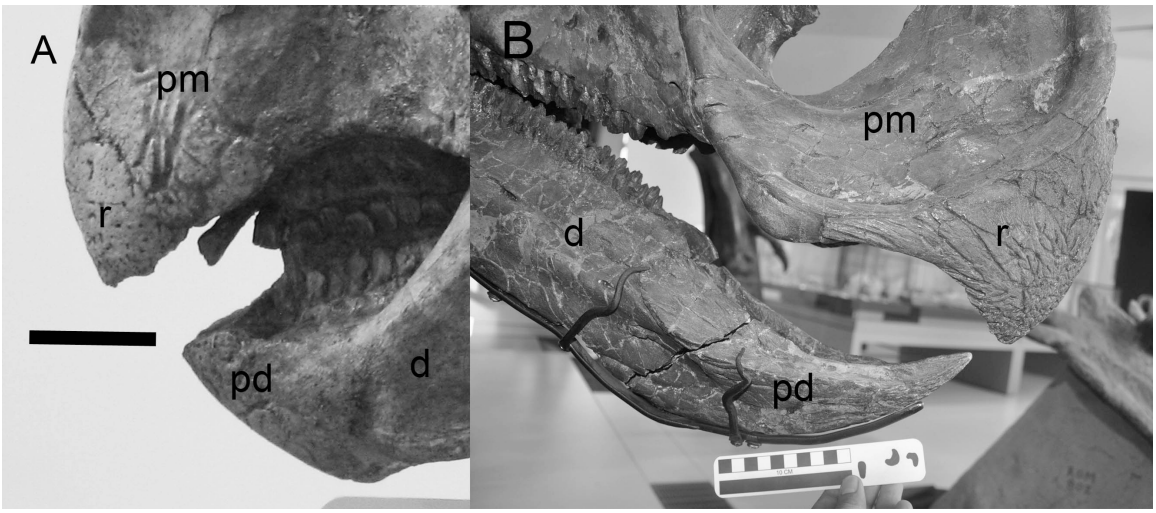

Premaxilla—Unlike the rest of Ornithischia, the premaxilla in ceratopsians (Fig. 7.17) does not form the rostral-most edge of the cranium. Instead, the premaxilla caudally borders the rostral, which has as one of its consequences the formation of a substantial region of the lateral surface of the skull by the premaxilla. For example the morphology of the latter element dictates the height and breadth of the lateral narial region. In psittacosaurids, the premaxilla is tall, with a broad, expansive dorsal half and a much narrower ventral half where it forms the rostral part of the oral margin, which creates a large portion of the parrot beak-like morphology of psittacosaurids. In some basal neoceratopsians, the premaxilla is almost square, with a dorsally higher caudal region, while in others, it retains the primitive, more elongate morphology. Premaxillae in protoceratopsids and leptoceratopsids possess a caudolateral process and leptoceratopsids

also possess another separate, more ventrally-placed caudal process. In protoceratopsids, the premaxilla as a whole is dorsoventrally taller than rostrocaudally elongate, whereas in leptoceratopsids it is the opposite. The ventral edge of the premaxilla is flat in the most basal ceratopsians, but it is bowed ventrally in leptoceratopsids, where it comes in contact with the caudal margin of the predentary.

In derived ceratopsids, an extensive enlargement of the oval-shaped external nares and the premaxilla forms a large portion of the ventral half of the narial margin. As a result, the premaxilla in ceratopsids is more irregular in shape; the rostral half more rostrally-expanded to form the rostral margin of the medially-indented narial region while the caudal half is much narrower where it articulates with the maxilla laterally. The rostral half of the premaxilla is joined medially with its partner to form a large septum, which creates the medial indentation of the external naris. In centrosaurines, the ventral oral margin is prominently bowed ventrally where it meets the caudal margin of the slightly ventrally-bowed and beveled oral margin of the predentary. In chasmosaurines, the ventral oral margin is much flatter and is continuous with flatter morphology of the oral margin typical of chasmosaurine predentaries (see below). Ventrally, the palatal processes of ceratopsian premaxillae extend caudally meeting the maxillae laterally and vomers medially, forming the primary palate. See Dentition section below for a description of morphology in premaxillae of *Yinlong*, basal neoceratopsians, and protoceratopsids.

FIGURE 7.17. *Triceratops* (ROM 55380; ceratopsid) premaxilla in articulation with surrounding elements exhibiting large narial opening. Abbreviations: m, maxilla; nar, narial opening; pm, premaxilla; r, rostral.

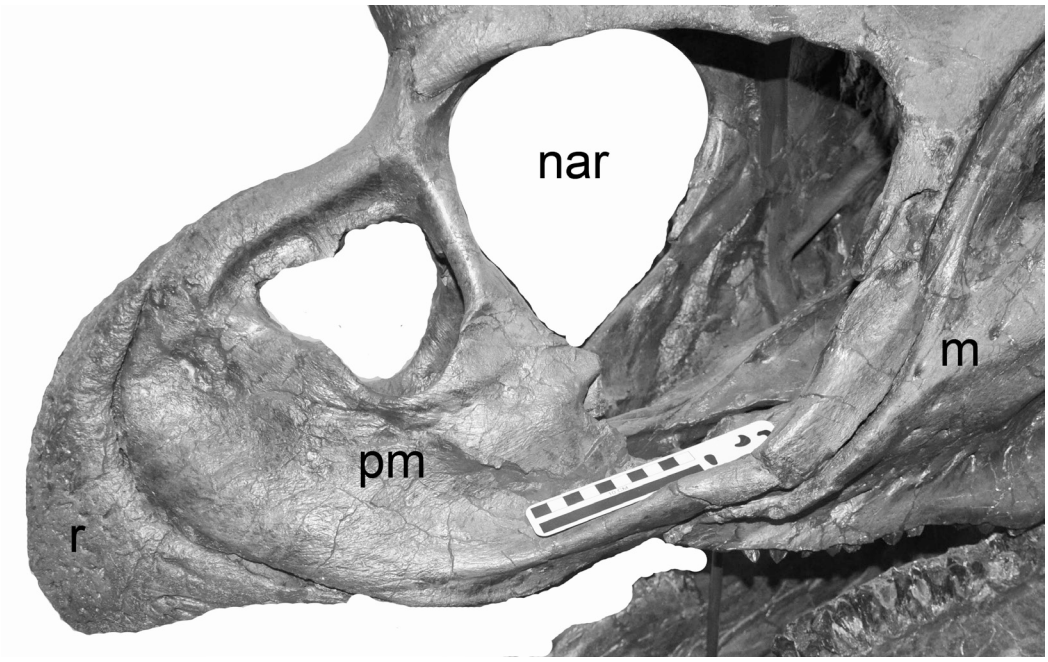

Maxilla—The maxilla is the main tooth-bearing element in the upper jaw. It is irregularly triangular and borders the premaxilla rostrally, the lacrimal dorsally, and the jugal and palate caudally. It creates much of the lateral surface of the skull, forming a majority of the ventral oral margin in more basal ceratopsian taxa. However, it is equal in length to the premaxilla in the derived ceratopsids, mainly due to the enlarged external nares. Dorsally, it forms the ventral margin of the antorbital fossa or fenestra in more basal ceratopsian taxa, except *Archaeoceratops* (IVPP V1114) and Ceratopsidae, which have no antorbital fenestra. A distinct buccal emargination of the ventral oral margin creates a medially inset tooth row, which likely allowed room for soft tissue to attach as a

means of retention of food as the animal chews (Galton, 1973; although, the fleshy, muscular nature of this soft tissue has been questioned [Papp and Witmer, 1998]). The medially inset tooth row is relatively straight in nature and caudally continues medial to the ventral jugal process in ceratopsids. See Dentition section below for a description of dental morphology.

Quadrate—The quadrate (Fig. 7.18) changes shape dramatically throughout ceratopsian evolution. In general, the quadrate is angled rostroventrally at different degrees depending on the taxon (Dodson, 1993); with basal ceratopsians possessing relatively much more vertically-oriented quadrates. In these basal taxa, the dorsal head of the quadrate is rounded and locked within the boundaries of the squamosal cotylus by the pre- and postquadratic processes. As ceratopsians evolved, the postquadratic process extends ventrally and, in protoceratopsids and leptoceratopsids, is continuous with the frill. The dorsal head of the quadrate in ceratopsids fits inside of a slot on the ventromedial surface of the squamosal, creating an immobile articulation (Weishampel, 1984). In most non-ceratopsid ceratopsians, the quadrate has a sigmoid shape, with the ventral end straightened dorsoventrally. As in all ornithischians, the quadrate is expanded at midshaft to form a thin pterygoid flange on its rostral surface that extends rostrally to articulate with the quadrate flange of the pterygoid. The greatest difference between basal ceratopsian and ceratopsid quadrates lies in the orientation of the ventral head of the quadrate. In *Yinlong* and psittacosaurids, the ventral head of the quadrate is arranged as it is in any basal member of other ornithischian clades, where the quadratojugal articulates rostrally and laterally to it and the caudal-most aspect of the jugal sits rostral to this articulation. In neoceratopsians, however, the arrangement rotates, with the three

elements oriented mediolateral, with the jugal the most lateral and the quadratojugal and quadrate sequentially more medial to it in a transverse articulation (Dodson, 1996; Fig. 7.18). The infratemporal fenestra is depressed ventrally due to the morphology of the jugal in more derived ceratopsians, especially ceratopsids. The ventral head of the quadrate is itself mediolaterally expanded and slightly bicondylar where it articulates with the articular surface of the mandible, the medial condyle enlarged slightly relative to the lateral condyle. It is narrow in lateral view, however, forming what acted well as a hinge joint with only slight room to move mediolaterally.

FIGURE 7.18. *Triceratops* (ROM 55380) quadrate in caudal view showing lateral articulations of quadratojugal and jugal. Also note mediolaterally expanded, bicondylar ventral quadrate head. Abbreviations: gl, glenoid; j, jugal; q, quadrate; qj, quadratojugal.

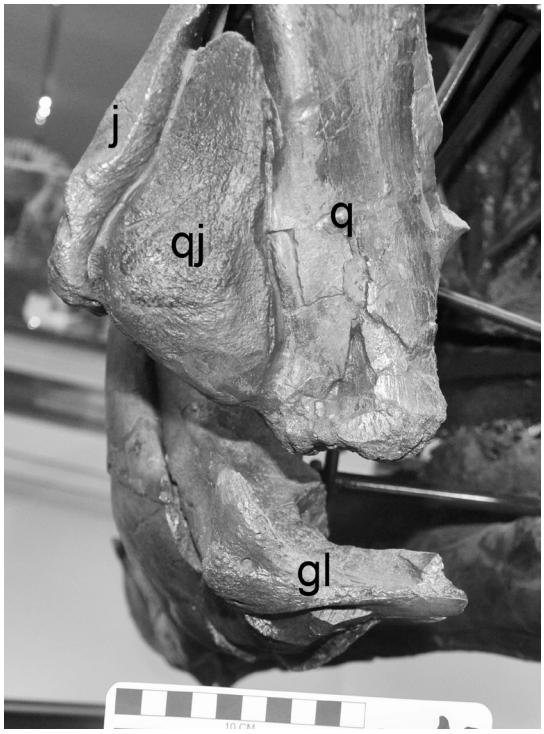

Predentary

The unpaired predentary (Figs. 7.19; 7.20; 7.21) is edentulous and fits inside the rostral during occlusion. The predentary was likely surrounded by a keratinous sheath around the rostral and lateral surfaces, as indicated by its highly vascularized and rugose outer surface. In dorsal view, the sloping and concave internal surface medial to the oral margin ascends rostrodorsally to the median pointed tip (Fig 7.20). The predentary in all ceratopsians is triangular in both lateral and dorsal view. The rostral tip is sagittally positioned in dorsal view and is oriented rostrodorsally in lateral view. The predentary in *Chaoyangosaurus* (IGCAGS V3781) and psittacosaurids is unique among ceratopsians in that it is more rounded around the oral margin in dorsal view and has a flatter surface at this margin (see Table 7.1 for specimens; Tanoue et al., 2011; Fig. 7.19). The predentary in *Yinlong* (IVPP V14530) is short and blunt rostrocaudally and shaped like an arrowhead in ventral view, with a mediolaterally expanded and rectangular ventral process contacting the dentary symphysis ventrally. It possesses two short caudodorsal processes, much like many other ornithischian taxa such as *Lesothosaurus*, stegosaurs, and basal ornithopods.

FIGURE 7.19. Ceratopsian predentary diversity (lateral views; not to scale). A, *Psittacosaurus* (psittacosaurid); B, *Archaeoceratops* (basal neoceratopsian); C, *Protoceratops* (protoceratopsid); D, *Leptoceratops* (leptoceratopsids); E, *Chasmosaurus* (chasmosaurine); F, *Centrosaurus* (centrosaurine). Scale bars = 1 cm.

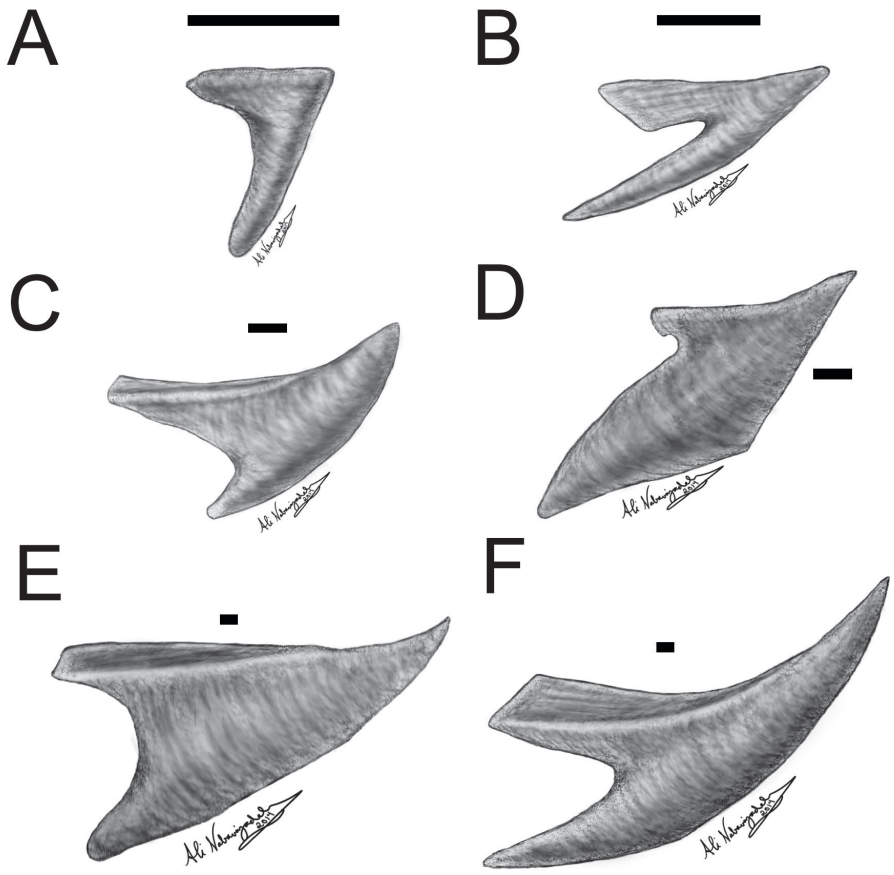

Throughout evolution time, the tip of the ceratopsian predentary extends farther rostrally and is directed more rostrodorsally to a sharp point. Among ceratopsids, centrosaurines (see *Styracosaurus* [e.g., AMNH 5372] and *Centrosaurus* [e.g., AMNH 5351]) typically have a much more vertically curved and dorsoventrally taller rostral tip in lateral view compared to the much flatter tip in chasmosaurine predentaries (see *Chasmosaurus* [e.g., ROM 843] and *Triceratops* [e.g., MOR 1110]), although this is not always the case, as *Pachyrhinosaurus*, a centrosaurine, also has a flatter predentary oral margin (TMP 1988.055.0161; TMP 1989.055.0030). As the dorsal oral margin extends caudally from the tip, it transitions into a mediolaterally-expanded surface on each side

(contacting with the premaxillae at occlusion) that widens to about three quarters of the rostrocaudal length, where it then is round into a caudodorsally projecting process. In chasmosaurines, the dorsal surface of the caudolateral process tends to be more transversely flattened whereas in centrosaurines the dorsal surface is usually oriented more dorsolaterally, although this is variable (Lehman, 1990; Mallon et al., 2014). In ventral view, there is an elongate, bilobate process extending caudally on the ventral aspect of the predentary that covers the ventral surface of the dentary symphysis. In a majority of ceratopsians, this ventral process extends much farther caudally than the caudolateral processes in lateral view. In leptoceratopsids, this ventral process is very deep dorsoventrally, in addition to being rostrocaudally elongate, and securely cradles the dentaries (see *Leptoceratops* [NMC 8889] and *Prenoceratops* [TCMI 2001.96.14]). In ceratopsids, the two lobes become relatively narrower and parallel to one another rostrocaudally rather than caudolaterally deflected relative to one another as in basal ceratopsians and basal ornithischians. There is also a narrow process that extends caudally from the internal oral surface of the predentary and just dorsal to the ventral process that enables it to secure the dentaries in ceratopsids. In lateral view, the rostrally-arched caudal margin of the predentary is placed between the dorsal caudolateral process and the ventral process.

FIGURE 7.20. Dorsal view of *Triceratops* predentary. Scale bar = 10 cm.

The morphology of the caudal aspect of most predentaries is also unique to the ceratopsian clade. In *Chaoyangosaurus*, *Yinlong*, and psittacosaurids, it is similar to the basal ornithischians condition, which bears a flatter caudal surface against which the dentary articulates on either side. The blunter and shallow caudolateral processes and ventral process in these taxa creates a limited surface area for the rostral aspect of the dentary. The predentary-dentary joint is fitted securely, although, due to the flatness of the predentary articulation, the predentary is not completely fastened to the narrow rostral ridge of the dentary. As such, this type of articulation would likely have accommodated a small amount of movement at the predentary-dentary articulation, as in *Lesothosaurus*

and basal ornithopods. Leptoceratopsids are unique in that, although the caudolateral process is much shorter than its deep ventral process, the caudolateral process fits inside what is functionally a slot in the dentary, creating a lock-and-key mechanism between the predentary and dentary (Varriale, pers. comm.). As ceratopsians evolved, however, the caudal surface connecting the caudolateral process and the ventral process on either side possesses a continuous embayment where the mediolaterally flattened dentary characteristic of most ceratopsians articulates and fits snugly. This embayment is concave enough, especially in the derived ceratopsids, that the dentary itself fits much more tightly, allowing for a much more sturdy predentary-dentary articulation on each side. Each caudal wing of the predentary envelops its corresponding dentary tightly, forming what is functionally a secondarily fused mandibular symphysis with a pointed beak in the middle. This 'secondary fusion' provides opportunities for forces to be potentially transmitted through the symphysis as the animal chews (Bell et al., 2009).

FIGURE 7.21. Ceratopsian predentaries. A, *Archaeoceratops* (IVPP V1114; photo courtesy of Frank Varriale); B, *Leptoceratops* (NMC 8889; photo courtesy of Frank Varriale); *Triceratops* (AMNH 972; ceratopsid); D, *Arrhinoceratops* (ROM 1439; predentary in caudal view showing indentations in caudolateral processes; photo courtesy of Frank Varriale). Abbreviations: clp, caudolateral process; d, dentary; p, predentary. Scale bar units in cm.

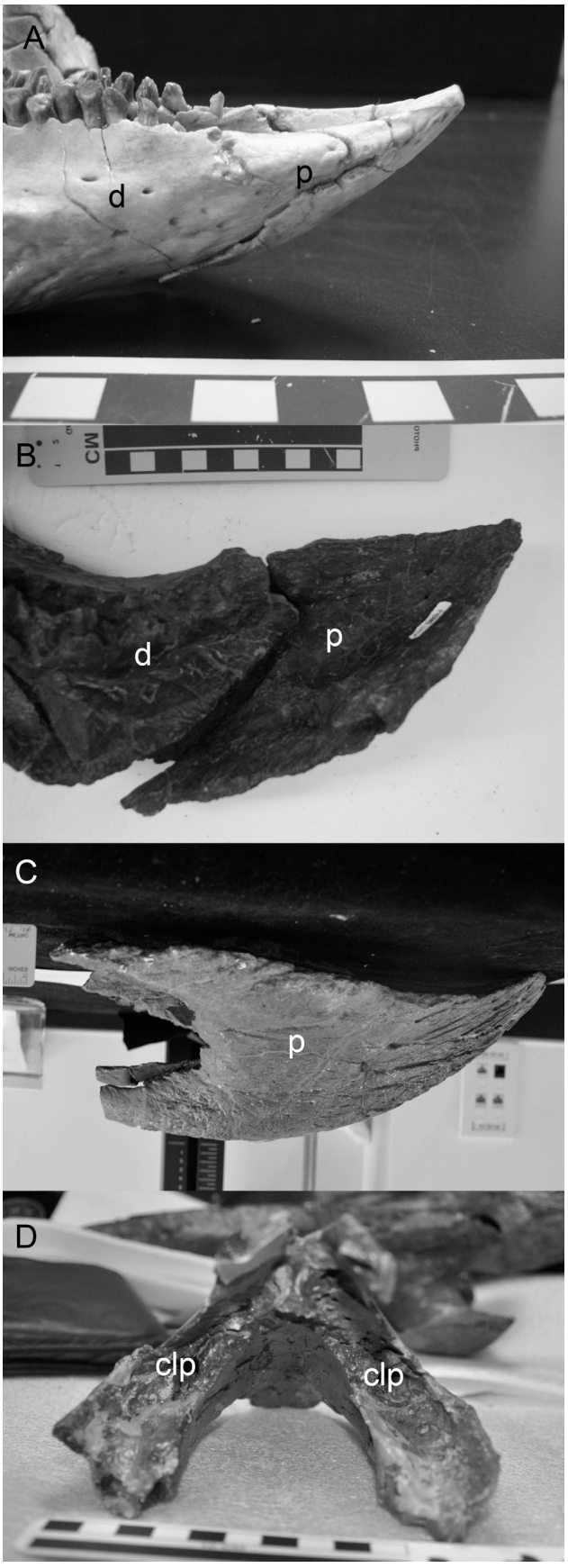
A
d
p
B
d
p
C
p
D
clp
clp

Dentary

Like that for all ornithischians, the dentary (Figs. 7.22; 7.23; 7.24; 7.25) is the largest element in the ceratopsian mandible. It articulates with the predentary and the opposite dentary rostrally, the splenial medially, and the surangular and angular caudally. It is generally elongate and elliptical rostrocaudally in most taxa, although in some cases, such as psittacosaurids and leptoceratopsids, it is much shorter in length and ventrally arched or u-shaped in lateral view. In more basal forms, such as *Chaoyangosaurus* (IGCAGS V3781), *Yinlong* (IVPP V14530), psittacosaurids (see *Psittacosaurus* [e.g., AMNH 6254]), leptoceratopsids (see *Leptoceratops* [e.g., NMC 8889] and *Prenoceratops* [TCMI 2001.96.14]), and protoceratopsids (see *Protoceratops* [e.g., AMNH 6438]), the rostral one-third of the dentary narrows at its rostral end, where it is blunt and rounded. Leptoceratopsids are unique in that, although the rostral margin is narrower, the rostral margin angles caudoventrally into a broad and triangular ventral margin where the enlarged and elongate predentary ventral processes articulate (see above), covering the dentary ventrally in a sturdy and locked positioning. In *Zuniceratops* (e.g., MSM P2224), the rostral margin is blunter and square, with a much shorter diastema than is usual in derived ceratopsids. The dentary in ceratopsids is broader and expanded as a round rostral margin in lateral view, the result of a mediolaterally compressed and elongate diastema along the rostral third of the dentary. The medial surface of the rostral dentary is generally flatter with just a shallowly concave, dish-like morphology.

FIGURE 7.22. *Chasmosaurus* (chasmosaurine ceratopsid) mandible (generalized). A, lateral view; B, medial view. Abbreviations: a, angular; ar, articular; cp, coronoid process of dentary; d, dentary; p, predentary; rap, retroarticular process; sa, surangular; sp, splenial. Scale bar = 15 cm.

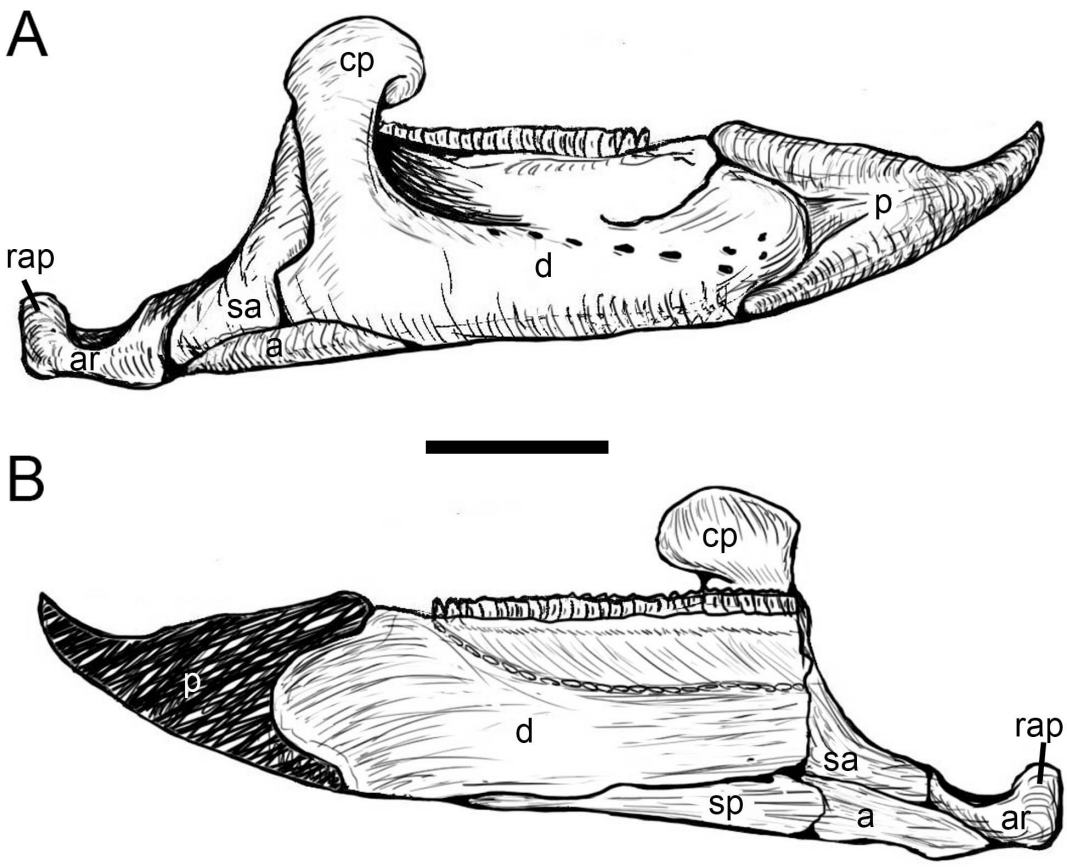

As mentioned above, the mediolaterally-compressed rostral margin fits into the shallow concavity of the caudal predentary of basal ceratopsians, as in other basal ornithischians, but in neoceratopsians, especially ceratopsids, the dentary fits into a dorsoventrally narrow slot that connects the caudolateral process and the ventral process on either side of the caudal predentary surface. This articulation secures the dentaries in a

tight symphysis with the predentary (see above for further description). The dentary also articulates with its partner slightly more caudally at the symphysis, although they do not fuse together. The rostral margin shows fine rugosities and ridges, suggesting rubbing against its counterpart in life during mastication. A series of foramina on the lateral surface of the rostral edge of the dentary suggest neurovasculature supplying the keratinous predentary sheath.

FIGURE 7.23. *Archaeoceratops* (IVPP V1114) mandible in dorsal view showing medially recurved tooth rows of dentaries. Photo courtesy of Frank Varriale. Scale bar units in cm.

The dentary tooth rows are at acute angles relative to one another and are closest with their counterpart at the mesial tip, coinciding with the maxillary dentition. The tooth row begins immediately caudal to the rostral expansion of the dentary on its dorsal margin. In all non-ceratopsid ceratopsians (except *Zuniceratops*) the tooth row is variably arched medially in dorsal view (Fig. 7.23), while in *Zuniceratops* (Fig. 7.24) and ceratopsids the tooth row is straighter (Fig. 7.25; see Dentition section for description of dentary tooth battery in ceratopsids). A buccal expansion immediately ventral to the mandibular tooth row creates a medially-inset tooth row, as is seen in the maxilla. The margin at which this buccal expansion from the tooth row meets the lateral surface of the mandible is a prominent sharp ridge that extends rostrocaudally. It probably accommodates the attachment region for soft tissue (i.e., fleshy cheeks [Galton, 1973]) along its lateral margin in life, although, again, some doubt has been expressed concerning this (Papp and Witmer, 1998). The caudal extent of the tooth row extends medial to the coronoid process part of its length and, in ceratopsids, extends even farther caudally than the coronoid process. See Dentition section below for a description of dental morphology.

FIGURE 7.24. *Zuniceratops* (MSM P3202) left dentary in lateral view, with shortened rostral diastema (relative to the longer diastema of ceratopsids). Photo courtesy of Frank Varriale. Scale bar units in cm.

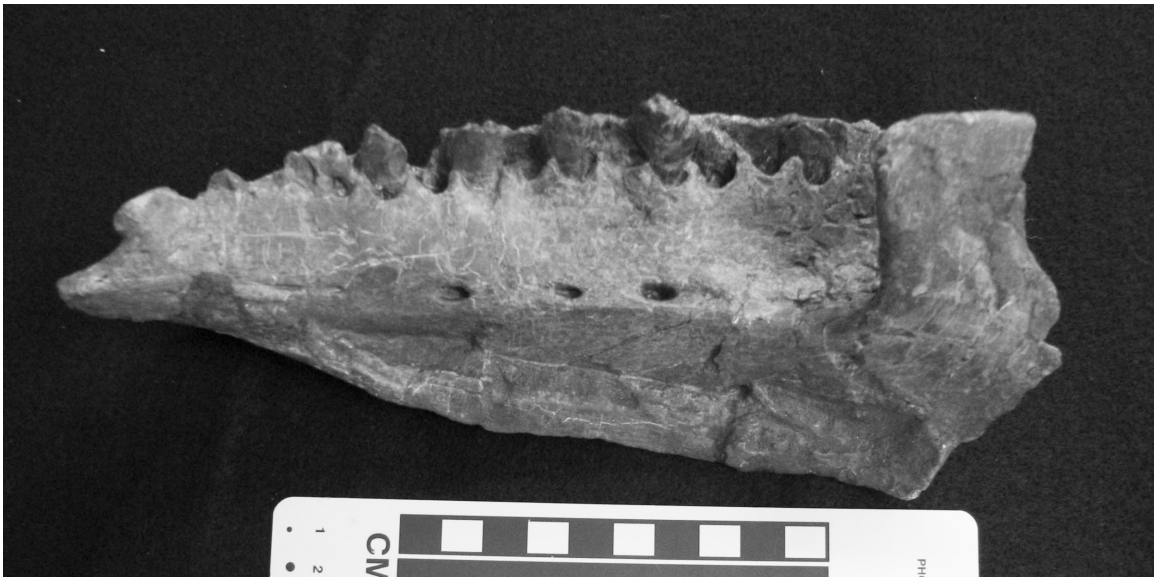

The coronoid process is elevated, relative to other more basal ornithischians. In all non-ceratopsid ceratopsians (except *Zuniceratops*), the coronoid process is broader and triangular in lateral view. In *Zuniceratops* and all ceratopsids, it is tall and broad with a cylindrical body and directed dorsally and slightly angled rostrally immediately above the level of the tooth row (Figs. 7.22; 7.25). As it extends dorsally, the coronoid process abruptly expands rostrocaudally in an oval to triangular morphology with a slightly convex lateral surface and a pointed apex at its dorsal-most margin where m. adductor mandibulae externus musculature had its rostral-most insertion (shown by rugose striations) before extending farther caudally along the coronoid process. The coronoid process in all ceratopsians is a caudal continuation of the lateral ridge of the buccal expansion beneath the tooth row described above. It is created rostrally by the dentary but also by the coronoid medially (in non-ceratopsids [except *Zuniceratops*]) and surangular caudally. Caudally, the dentary laterally overlaps the rostral margin of the surangular.

In caudal view, the mandibular canal is large and runs from immediately ventral to the caudal surface of the coronoid process to the ventral aspect of the dentary. It accommodated the inferior alveolar branch of the mandibular nerve (V_3) and served as part of the insertion for m. adductor mandibulae externus. The dental battery, especially in ceratopsids, arched medially and at its caudal margin medially creates a large portion of the mandibular canal. The surangular articulates medial to the lateral margin of the dentary coronoid to form the lateral margin of the mandibular canal. Ventral to the mandibular canal is a thin, slightly rounded surface for articulation with the angular. On the medial aspect of the dentary and ventral to the dental battery, the mandibular canal thins rostrally and is completely covered by the thin splenial.

FIGURE 7.25. *Centrosaurus* (ROM 767) dentaries and predentary. A, right lateral view; B, dorsal view. Photos courtesy of Frank Varriale. Scale bar units in cm.

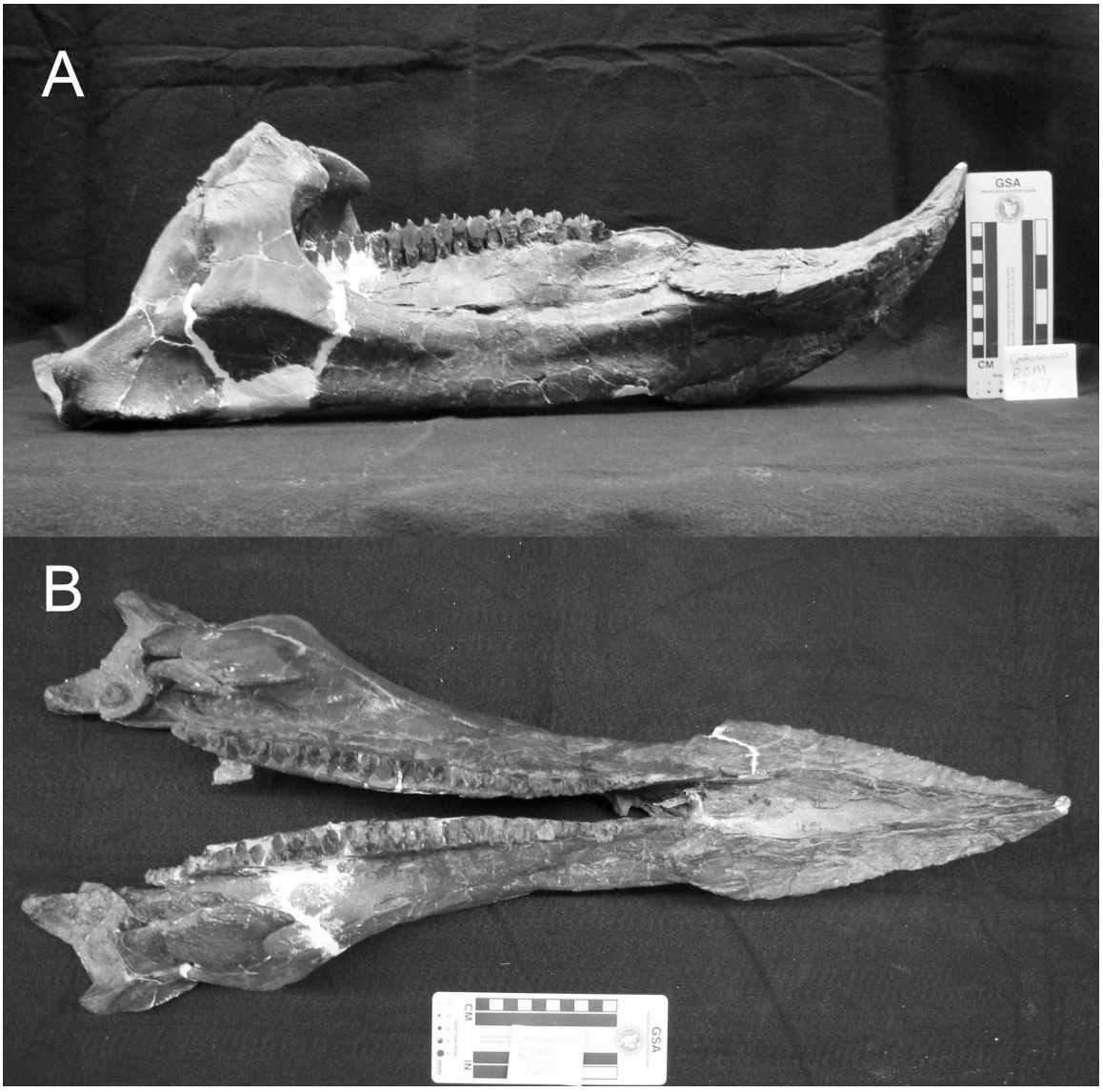

Coronoid

The coronoid is primitively present in ceratopsians, but absent in *Zuniceratops* and all Ceratopsidae, mainly due to the dorsal extension of the dentary coronoid process. It is visible on the medial aspect of the small and blunt apex of the coronoid eminence. The coronoid, with the surangular, creates the more caudal aspect of the coronoid eminence in non-ceratopsid ceratopsians, with the dentary articulating just rostral to them.

It also possesses a small process that articulates with the splenial and dentary ventrally.

Splenial

The splenial (Fig. 7.22) is a thin sheet of bone that lies along the medial aspect of the dentary ventral to the tooth row, covering the mandibular nerve (V_3), as it does in a majority of ornithischians. It is not fused to the dentary. In ceratopsians, the splenial is narrower rostrally than it is caudally and the caudal extension forms the lateral margin of a slit or foramen, which is the ventral aspect of the caudal entrance of the mandibular canal. This caudal extension also overlaps the caudoventrally-placed angular. It does not reach the symphysis rostrally.

Angular

The angular (Fig. 7.22) is relatively larger and more rostrocaudally elongate in *Chaoyangosaurus*, *Yinlong*, and psittacosaurids than it is in basal neoceratopsians and especially the derived ceratopsids. It articulates with the caudoventral aspect of the dentary and the ventral aspect of the surangular. In lateral view, its rostrodorsal margin creates the ventral margin of the external mandibular foramen of the lower jaw in more basal ceratopsians, bordered by the dentary rostrally and the surangular caudally. This foramen is absent in leptoceratopsids, protoceratopsids, and all ceratopsids. Internally, the angular has a ventrally concave, rostrocaudally elongate groove, creating the ventral surface of the mandibular fossa where m. adductor mandibulae posterior inserts in life. It contributes a process to the medial margin of the craniomandibular joint and the retroarticular process.

Prearticular

This elongate element articulates with the angular ventrally, surangular dorsally, splenial rostrally, and articular caudally (Fig. 7.22). It has a long, rostral projection in medial view that contributes to the ventromedial border of the mandibular canal. It possesses a process that ventrally contacts the articular.

Surangular

The irregularly-shaped and thin surangular forms the more caudal aspect of the coronoid process (Fig. 7.22). Due to the rostral elongation of the dentary and predentary in more derived ceratopsians, the surangular is smaller relative to the length of the mandible in ceratopsids than in other ceratopsians. In lateral view, it is rostrocaudally-elongate and rectangular in the basal *Chaoyangosaurus* (IGCAGS V3781), and triangular in *Yinlong* (IVPP V14530) and psittacosaurids, and tall, more symmetrically triangular in basal neoceratopsians (see Table 7.1 for specimens). In ceratopsids, the surangular is taller and thinner with a dorsal margin that extends caudoventrally. It creates the caudal-most aspect of the coronoid process, caudomedial to the cylindrical body of the coronoid process ventral to its apical rostrocaudal expansion. In non-ceratopsid ceratopsians, it also borders the coronoid bone, as well as the angular ventrally and the articular caudally, creating the lateral aspect of the craniomandibular joint. It extends farther caudally still to create the lateral margin of the retroarticular process.

Articular

The sinusoidal articular (Fig. 7.22; 7.26) extends caudally, with its dorsal surface forming a concave articulation for the ventral bicondylar quadrate. This articular surface is mediolaterally expanded and concave with triangular dorsally sloping lips formed on the medial and lateral margins by the angular and surangular, respectively. These lips help to restrict, but not completely preclude, transverse movement of the lower jaw during chewing cycles. The dorsal surface of the surangular is also rostrocaudally expanded into a circular morphology providing limited propalinal movement of the jaw. Its caudal-most extent creates a triangular projection directed caudally. This projection creates a majority of the retroarticular process, which was the insertion for m. depressor mandibulae as well as m. pterygoideus musculature.

FIGURE 7.26. Ceratopsid quadrate-mandibular articulation in caudal view.

Abbreviations: ar, articular surface; j, jugal; q, quadrate; qj, quadratojugal; rap, retroarticular process.

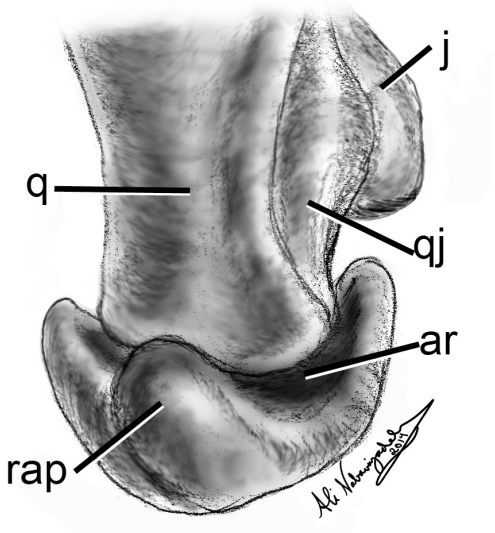

Dentition

Premaxillary dentition is only present in *Yinlong* (Fig. 7.27), basal neoceratopsians, and protoceratopsids. They are large (larger than the maxillary teeth), lacrimiform, and bulbous at the base of the crown in *Yinlong*, with the labial side of the crown showing vertical wear against the predentary (Varriale, 2011). They are much more cylindrical and peg-like in basal neoceratopsians (including protoceratopsids) and small in number (between two to four depending on the taxon). Neoceratopsian premaxillary teeth were likely not as crucial in feeding as in *Yinlong* because of a caudal transition in tooth use and therefore disappear in more derived taxa (Varriale, 2011).

FIGURE 7.27. *Yinlong* premaxillary tooth. (Left side; first tooth position.)

Maxillary dentition is similar to dentary dentition in ceratopsians, except the occlusal surface is on the lingual side instead of the buccal side, as it occludes with the buccal occlusal surface of dentary teeth in this orientation. Depending on the genus, the angle of the maxillary occlusal surface is oriented dorsomedial to ventrolateral from base

to apex. The teeth have a denticulate edge along the oral apical margin of the tooth crowns. More basal ceratopsians, such as *Yinlong* and *Archaeoceratops*, among others, have leaf-shaped teeth with a prominent buccal median apicobasal ridge and a less prominent lingual median ridge on the occlusal side. Derived ceratopsid tooth roots are distinctly bifurcated and the occlusal surface of ceratopsid teeth is much more vertical.

The dentition of the dentary is similar to that of the maxilla. The entire apical margin of the tooth crown is denticulate. In basal ceratopsians, such as psittacosaurids, the tooth crown is leaf-shaped and projects dorsally from the inset oral margin of the dentary. The lingual surface of the crown has a prominent ridge apicobasally and, in basal neoceratopsians, less prominent ridges on either side of the primary ridge are present. The buccal surface of the dentition also has a median apicobasal ridge; however, it is less pronounced due to the wear of the lingual surface of the maxillary tooth surface. The crowns in more basal ceratopsian teeth are slightly swollen at their base, with a cylindrical root (differing from the double-root in ceratopsids described below). The crown and single root in basal ceratopsians are at a steep angle relative to one another, resulting in an orthal occlusal pattern, which is also seen in dental microwear (Varriale, 2011). Psittacosaurid wear patterns termed “clinolineal”, consist of oblique, concave facets (Sereno et al., 2009; Varriale, 2011; Fig. 7.28).

FIGURE 7.28. *Psittacosaurus* dentary tooth.

Leptoceratopsids are a special case in which the occlusal plane on the buccal surface of the dentition is more buccally sloped at a right angle, where the maxillary dentition occludes and was directed more propalinally after an initially orthal chewing stroke (Ostrom, 1966; Varriale, 2011; Fig. 7.29) or possibly unilaterally transverse (Varriale, 2011). There is only one replacement tooth per tooth position in basal ceratopsians through protoceratopsids, but this is not the case in ceratopsids.

FIGURE 7.29. *Leptoceratops* right dentary teeth (note step-ladder-like occlusal surface morphology of tooth on left).

Ceratopsids, as well as their predecessor *Zuniceratops*, possess a dental battery, superficially similar to that in hadrosaurid ornithopods, in which up to 30 to 40 columns of 3 to 5 teeth are tightly packed across the rostrocaudal extent of the tooth row (Ostrom, 1966; Fig. 7.30). This dental battery creates a large, rostrocaudally elongate convexity along the medial surface of the dentary and an arched series of alveolar foramina is visible ventral to the tooth columns.

FIGURE 7.30. Ceratopsid (*Triceratops*) tooth battery.

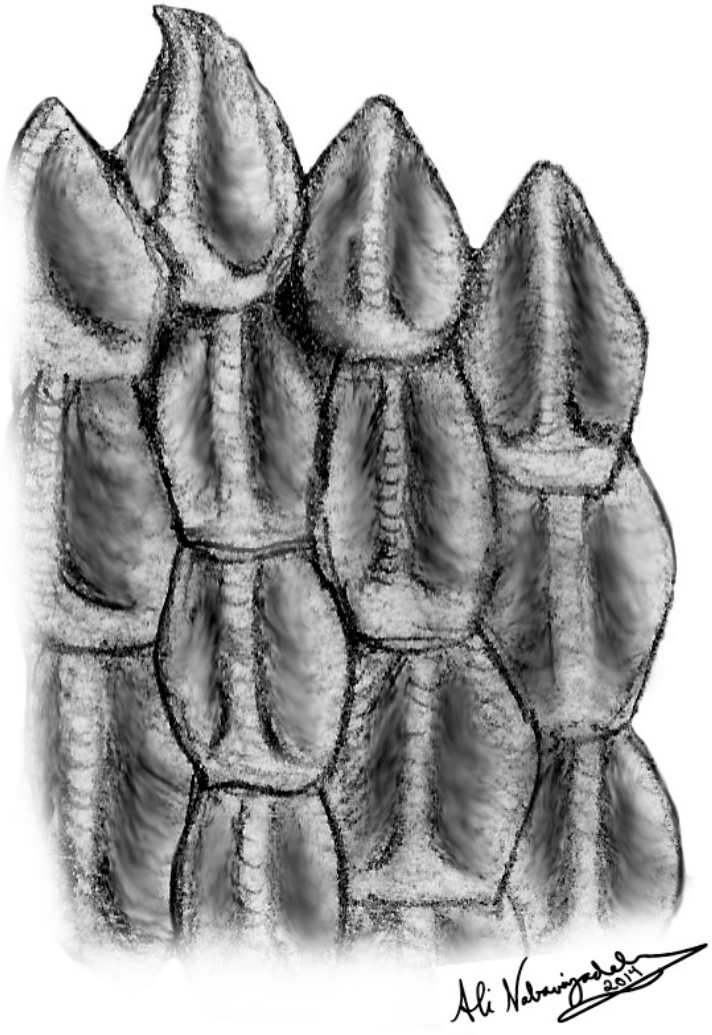

Ceratopsid tooth roots are different as well, in that they are split into two conical roots arranged buccolingually instead of a cylindrical root in more basal forms (Fig. 7.31). The buccal occlusal surface is vertical, creating an apicobasal plane against which the maxillary teeth occlude.

FIGURE 7.31. Ceratopsid tooth in side view, showing two roots.

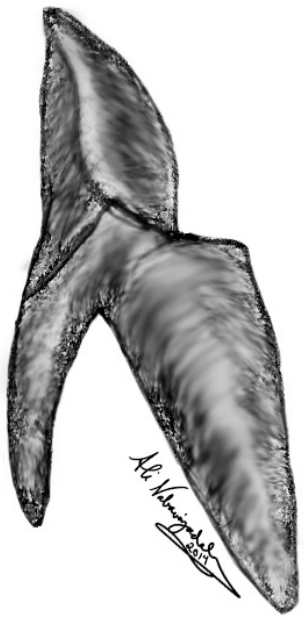

Dental microwear studies by Varriale (2011) have shown that derived ceratopsids have a multi-directional wear pattern in which there is frequent alternation between propalinal and orthal chewing strokes. Studies in ontogenetic trends have shown that the number of tooth positions increases as ceratopsians grow, as in other ornithischian clades (Lehman, 1989; Dodson et al., 2004), but tooth size also increases with it as well.

JAW MUSCULATURE

Placement of jaw musculature in marginocephalians has been the subject of only a few studies of presumed muscle scars as well as phylogenetic bracketing methodology (Haas, 1955; Ostrom, 1964, 1966; Maryańska & Osmólska, 1974; Sues and Galton, 1987; Holliday, 2009; Sereno et al., 2009). These descriptions were used as a baseline for inferring morphology and action of jaw musculature, generalized for all marginocephalians unless otherwise noted.

M. depressor mandibulae

M. depressor mandibulae (mDM; Fig. 7.32) was likely the primary muscle opening the jaws. According to Haas (1955) and Ostrom (1964), this muscle originated on the caudal surfaces of the paroccipital processes of the exoccipital-opisthotic complex on the caudal-most extent of the braincase. This morphology is more apparent in pachycephalosaurs and basal ceratopsians, but in the derived ceratopsids is more-or-less hidden in lateral view and fused to the ventral aspect of the parieto-squamosal frill. Sereno et al. (2009) noted a special case in psittacosaurids in which mDM may have originated in depressions on the caudodorsal aspect of the skull. The mDM extended ventrally to insert around the retroarticular process at the caudal-most region of the lower jaw. For the most part, this muscle is strongly acutely angled in marginocephalians when the jaw is closed, especially pachycephalosaurs and derived ceratopsoids, although it is variable between taxa.

M. adductor mandibulae posterior

The palinal motion of the jaw mechanism was likely accomplished by the enlarged m. adductor mandibulae posterior (mAMP; Fig. 7.32), which originated on the lateral surface of the rostrally-oriented pterygoid wing or rostral face of the quadrate body in all marginocephalians. It inserted rostroventrally into the mandibular canal of the mandibular adductor fossa, alongside the inferior alveolar nerve. This position/placement would make for a line of action for the muscle to contract and pull the jaw caudally. Such an action could have been useful for stripping vegetation against the dentition in that direction. As it is a large muscle, it likely produced considerable bite force in the caudal direction. There is no clear evolutionary trend in mAMP muscle orientation. Some basal ceratopsians, such as *Psittacosaurus*, have a very low angle, indicating a caudally focused palinal chewing stroke, whereas other basal ceratopsians, such as *Archaeoceratops*, exhibit a more caudodorsally oriented mAMP and, in turn, chewing stroke. Most ceratopsoids possess an extremely acute angle of mAMP orientation indicative of a strongly caudal chewing stroke. Although this is seen in dental microwear studies (Varriale, 2011), microwear also shows a more complex, multidirectional chewing style. The caudally oriented mAMP likely aided in the initial occlusion and slicing that was a major part of the overall feeding mechanism.

TABLE 7.2. Marginocephalian mAMP muscle vector angles.

Genus	Spec. #	mAMP(°)
Archaeoceratops	IVPP V 1114	46.56
Auroraceratops	IGCAGS 2004 VD001	36.6
Bagaceratops	GI SPS 100-528	30.62
Centrosaurus	USNM 8897	23.99
Chasmosaurus	ROM 839	26.9

Hongshanosaurus	IVPP V12617	36.33
Leptoceratops	NMC 8889	39.71
Liaoceratops	IVPP V12633	49.71
Pachycephalosaurus	Triebold Cast	31.46
Pachyrhinosaurus	TMP specimen (Display Skull)	29.48
Pentaceratops	OMNH 10165	28.47
Prenoceratops	TCMI 2001.96.14	43.07
Protoceratops	GI-SPS 100-522	33.24
Psittacosaurus	AMNH 6254	33.64
Stegoceras	UAVPL 2	29.87
Styracosaurus	AMNH 5372	28.58
Triceratops	ROM 55380	29.74
Yinlong	IVPP V14530	31.67
Zuniceratops	(Reconst. Cast)	32.02

M. pseudotemporalis

M. pseudotemporalis (Fig. 7.32) was almost certainly made of two bellies in marginocephalians: superficialis and profundus. Together, these muscles would have assisted in pulling the jaw closed during chewing cycles.

M. pseudotemporalis superficialis—According to Holliday (2009), m. pseudotemporalis superficialis (mPSTS) originated immediately caudal to the orbit on the laterosphenoid and extended rostroventrally to insert inside the medial mandibular fenestra in derived ceratopsids as well as on the margin of the dorsal apex of the coronoid eminence or process likely through a tendinous sheet in basal marginocephalians, indicated by distinct muscle scarring (Ostrom, 1964).

M. pseudotemporalis profundus—M. pseudotemporalis profundus (mPSTP) likely originated on the lateral surface of the braincase in basal marginocephalians, but is thought to have been absent in the derived ceratopsids, as these taxa have lost the epipterygoid evolutionarily (Holliday, 2009). Like mPSTS, it inserted onto the dorsal apex of the coronoid eminence and the rostral portion of the medial mandibular fenestra, likely through a tendinous sheet (Holliday, 2009).

FIGURE 7.32. Comparison of marginocephalian jaw musculature (m. pseudotemporalis, m. adductor mandibulae posterior, and m. depressor mandibulae). A, *Stegoceras* (pachycephalosaur); B, *Psittacosaurus* (basal ceratopsian); C, *Protoceratops* (basal neoceratopsians/protoceratopsid); D, *Triceratops* (ceratopsid). Abbreviations: mAMP, m. adductor mandibulae posterior; mDM, m. depressor mandibulae; mPST, m. pseudotemporalis. See Figs. 7.2 and 7.14 for scale bars.

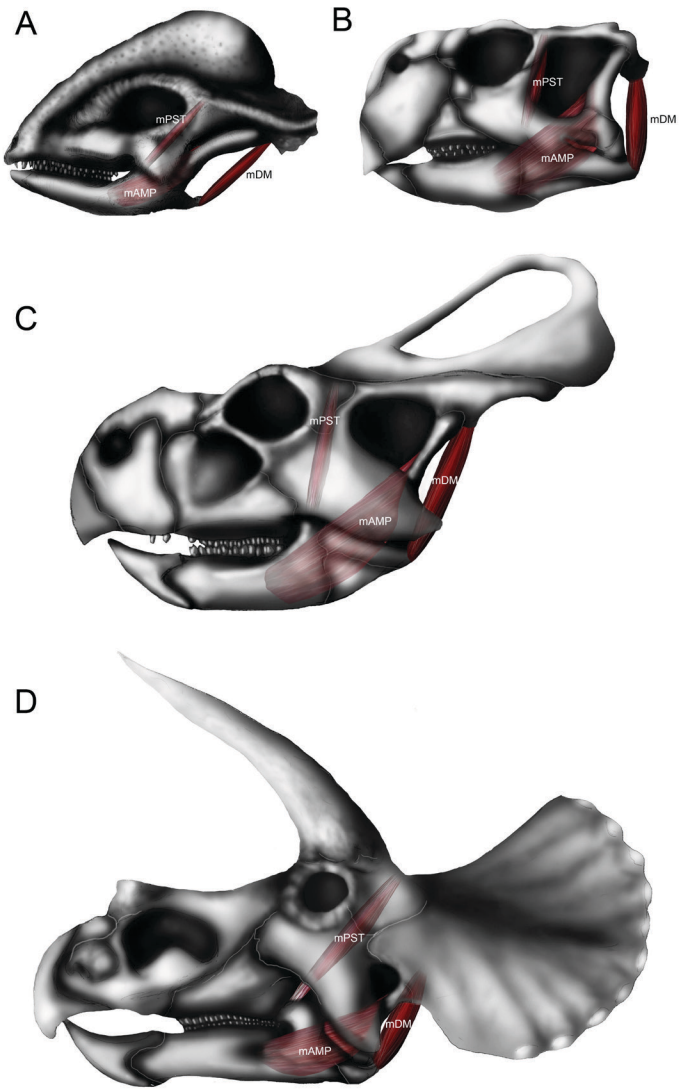

M. adductor mandibulae externus

The primary group of muscles acting to raise the lower jaw is the adductor mandibulae externus muscle group (Fig. 7.33), all of the muscles of which originated on the squamosal and temporal region and together might have functioned as a large fan of muscle (Haas, 1955; Ostrom, 1964; Sereno et al., 2009; Holliday, 2009).

M. adductor mandibulae externus superficialis—According to Holliday (2009), as seen in most other ornithischians, m. adductor mandibulae externus superficialis (mAMES) originated on the medial ridge of the supratemporal bar made of the postorbital and squamosal, as seen for example in extant lepidosaurs. Ostrom (1964) argued that, in ceratopsians with caudally extended frills, mAME (including superficialis, medialis, and profundus) originated on the dorsal surface of the parietosquamosal frill. Dodson (1996), however, disagreed with Ostrom's argument, because of the biomechanically disadvantageous nature of such a large muscle on a weak frill for a small jaw. Observations of specimens in the current study agree with Dodson's (1996) interpretation, especially given the vast diversity of frill orientations and shapes in more recently discovered taxa that would be unsuitable for and hinder any kind of large muscular contraction. M. adductor mandibulae externus superficialis expands along the more lateral portion of the dorsal rim of the coronoid process. Basal marginocephalians exhibit a shallow fossa along the dorsal surface of the surangular that likely demarcates the insertion of this muscle, as noted in *Protoceratops* by Haas (1955).

M. adductor mandibulae externus medialis—M. adductor mandibulae medialis (mAMEM) likely originated on the caudolateral surface of the supratemporal fossa just dorsal to the internal margin of the infratemporal fenestra. The mAMEM then coursed

rostroventrally to insert onto the medial surface of the dorsal ridge along the surangular portion of the coronoid process, just rostral to the insertion of mAMES. Exact demarcation of this muscle is unclear because, in many cases, mAMEM shares a muscle body with mAMEP (see below) and this insertion is mostly invisible.

M. adductor mandibulae externus profundus—M. adductor mandibulae externus profundus (mAMEP) likely originated on the lateral aspect of the parietal and squamosal parts of the skull roof, and covered the caudomedial wall of the supratemporal fenestra and the caudal portion of the sagittal crest in dorsal view (Ostrom, 1964; Holliday, 2009). This muscle likely inserted onto the caudodorsal apex of the coronoid process (Haas, 1955; Ostrom, 1964; Dodson, 1996; Holliday, 2009).

M. adductor mandibulae externus ventralis—Much like what was suggested for heterodontosaurids by Sereno (2012; see Chapter 4), m. adductor mandibulae externus ventralis (mAMEV; not figured) is a muscle included in reconstructions of *Psittacosaurus* by Sereno et al. (2009). Psittacosaurid jaws were compared to those that of a parrot, namely in having a muscle that originates at the ventral edge of the caudoventrally-oriented jugal process, wrapping around the lower jaw laterally and inserting onto ventral edge of the angular. Other authors, however, have not yet agreed as to whether this muscle truly existed in ornithischians.

MAME muscle vector angles—As is seen in Table 7.3, muscle fiber orientations and muscle fan sizes are quite variable among genera. Aside from the very extreme case of small acute mAME angle in the pachycephalosaurs *Pachycephalosaurus* and *Stegoceras*, many basal marginocephalians (mainly basal ceratopsians) possess a relatively higher angled mAME with a moderate muscle fiber span. There is an

evolutionary trend from mAMEP muscle vector angles in the vicinity of 50 degrees in basal neoceratopsians (i.e., *Aurorocerato*ps, *Archaeocerato*ps, and *Yinlong*) to much smaller angled mAME muscle vectors in the derived ceratopsids. The mAME muscle span is relatively stable throughout the clade, although orientation of the muscle fibers is variable. The caudally oriented mAME in derived ceratopsids is likely indicative of a caudally oriented power stroke, as is their caudally oriented mAMP. This caudal orientation of the muscles and quadrate leaves much less room for musculature to be present, although it could have spanned a large portion of the base of the frill. Still, there could have been an evolutionary trend in an increased recruitment of larger pterygoideus musculature to make up for the bite forces needed for feeding, as in the derived hadrosaurids (see Chapter 6). Further three-dimensional studies from CT scans are needed to make such an assertion, however.

TABLE 7.3. Marginocephalian mAME muscle vector angles.

Genus	**Spec. #**	**mAMEP(°) (Coronoid Apex)**	**mAMEM(°) (Coronoid Mid-height)**	**mAMES(°) (Coronoid Base)**
Archaeoceratops	IVPP V 1114	53.48	72.55	84.47
Auroraceratops	IGCAGS 2004 VD001	49.03	81.71	93.7
Bagaceratops	GI SPS 100-528	43.81	56.08	68.24
Centrosaurus	USNM 8897	40.2	56.92	67.77
Chasmosaurus	ROM 839	31.91	45.48	56.58
Hongshanosaurus	IVPP V12617	48.01	68.61	79.94
Leptoceratops	NMC 8889	45.15	68.31	79.06
Liaoceratops	IVPP V12633	56.63	76.31	85.52
Pachycephalosaurus	Triebold Cast	29.4	43.49	54.1
Pachyrhinosaurus	TMP specimen (Display Skull)	34.05	43.89	52.1
Pentaceratops	OMNH 10165	38.04	48.65	61.29

Prenoceratops	TCMI 2001.96.14	54.72	71.42	79.49
Protoceratops	GI-SPS 100-522	43.11	62.92	72.76
Psittacosaurus	AMNH 6254	46.8	72.09	86.14
Stegoceras	UALVP 2	30.49	41.28	47.23
Styracosaurus	AMNH 5372	43.81	52.99	59.23
Triceratops	ROM 55380	43.96	52.44	59.3
Yinlong	IVPP V14530	53.01	83.7	98.11
Zuniceratops	Reconst. Cast	49.8	68.2	78.4

FIGURE 7.33. Comparison of marginocephalian m. adductor mandibulae externus muscle complex morphology showing variations in muscle vector angles of m. adductor mandibulae externus profundus above horizontal. A, *Stegoceras* (pachycephalosaur); B, *Psittacosaurus* (basal ceratopsian); C, *Archaeoceratops* (basal neoceratopsian); D, *Leptoceratops* (basal ceratopsian/leptoceratopsid); E, *Protoceratops* (basal neoceratopsians/protoceratopsid); F, *Centrosaurus* (centrosaurine ceratopsid); G, *Triceratops* (chasmosaurine ceratopsid); H, *Chasmosaurus* (chasmosaurine ceratopsid). Note: angles listed are based on specimen data, not the illustration. See Figs. 7.2 and 7.14 for scale bars.

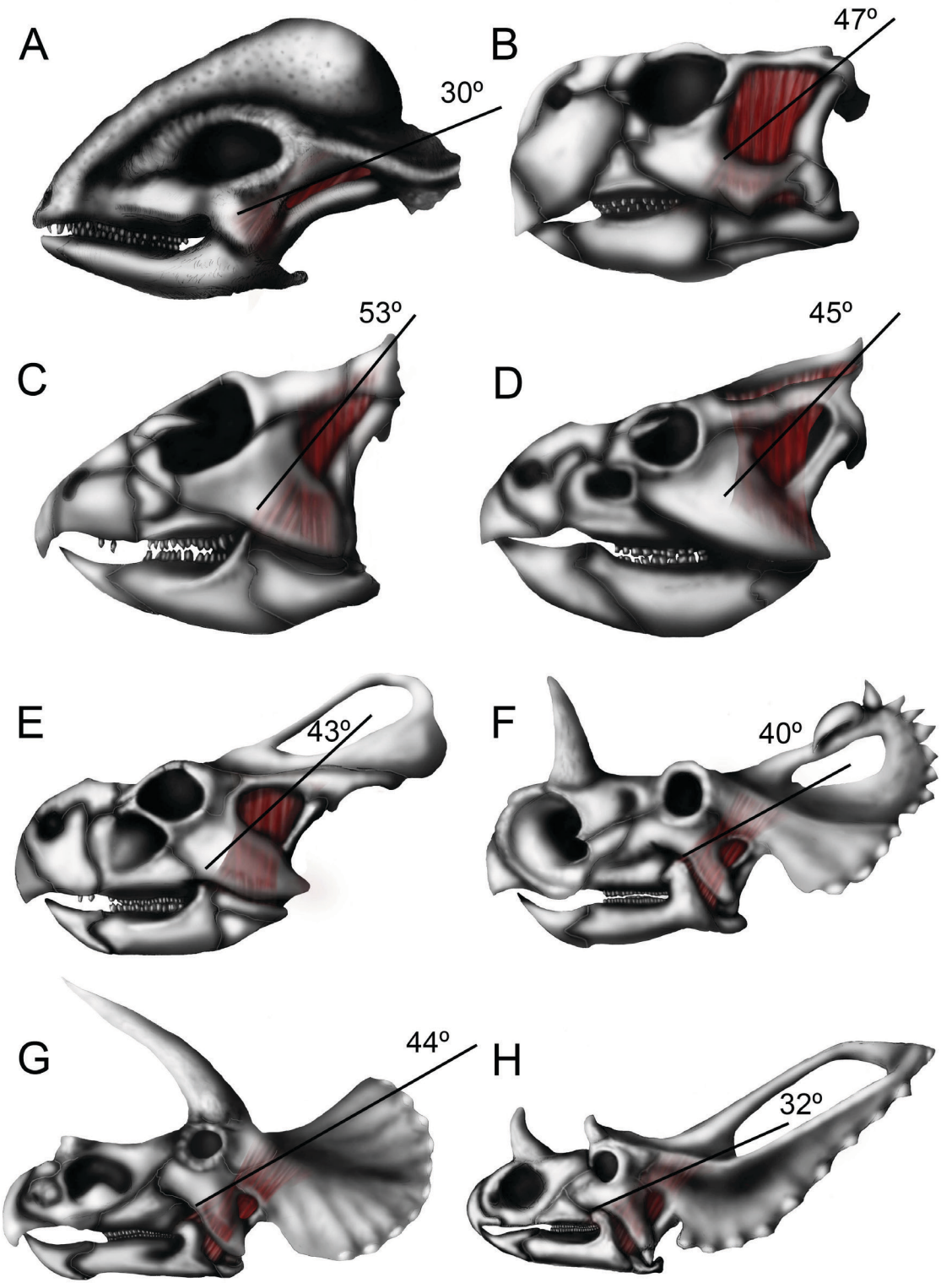
A
30º
B
47º
C
53º
D
45º
E
43º
F
40º
G
44º
H
32º

M. pterygoideus ventralis

M. pterygoideus ventralis (mPTV; Fig. 7.34) originated on the broad caudoventral surface of the pterygoid and on the ventral surface of the palate, indicated by a smooth surface on the on the ventral aspect of the pterygoid. The mPTV likely wrapped caudoventrally around the lateral aspect of the mandible and eventually inserted onto the ventrolateral aspect of the mandible and retroarticular process. However, exact insertion is unclear due to lack of muscle scarring on the outer surface of the bone (Haas, 1955; Ostrom, 1964; Holliday, 2009). The mPTV would have functioned in medial movement or restriction of the mandibular corpus. As stated above, this muscle might have been enlarged due to the reorientation of mAME musculature to expand, though further studies are necessary to make such an assertion.

M. pterygoideus dorsalis

M. pterygoideus dorsalis (mPTD; Fig. 7.34) likely originated on the dorsal aspect of the pterygoid and palatine, although these attachments are difficult to observe due to the smooth surface formed by the passages of the nasal cavity (Holliday, 2009). The mPTD wrapped caudoventrally around the medial aspect of the mandibular corpus. The insertion was likely on the medial aspect of the retroarticular process of the mandible. Its function, along with m. pterygoideus ventralis, plausibly suited the medial movement or restriction of the mandibular corpus on which is attached, depending on which side of the jaw was used in mastication (Ostrom, 1964; Holliday, 2009). Placed on opposite sides of the mandibular corpus, mPTD and mPTV would work well together in mediolateral movement or restriction of the mandibular corpus in general.

FIGURE 7.34. Comparison of marginocephalian m. pterygoideus ventralis (mPTV) and m. pterygoideus dorsalis (mPTD). A, B, *Stegoceras* (pachycephalosaur) (A, mPTV; B, mPTD); C, D, *Psittacosaurus* (basal ceratopsian) (C, mPTV; D, mPTD); E, F, *Protoceratops* (basal neoceratopsians/protoceratopsid) (E, mPTV; F, mPTD); G, H, *Triceratops* (ceratopsid) (G, mPTV; H, mPTD). See Figs. 7.2 and 7.14 for scale bars.

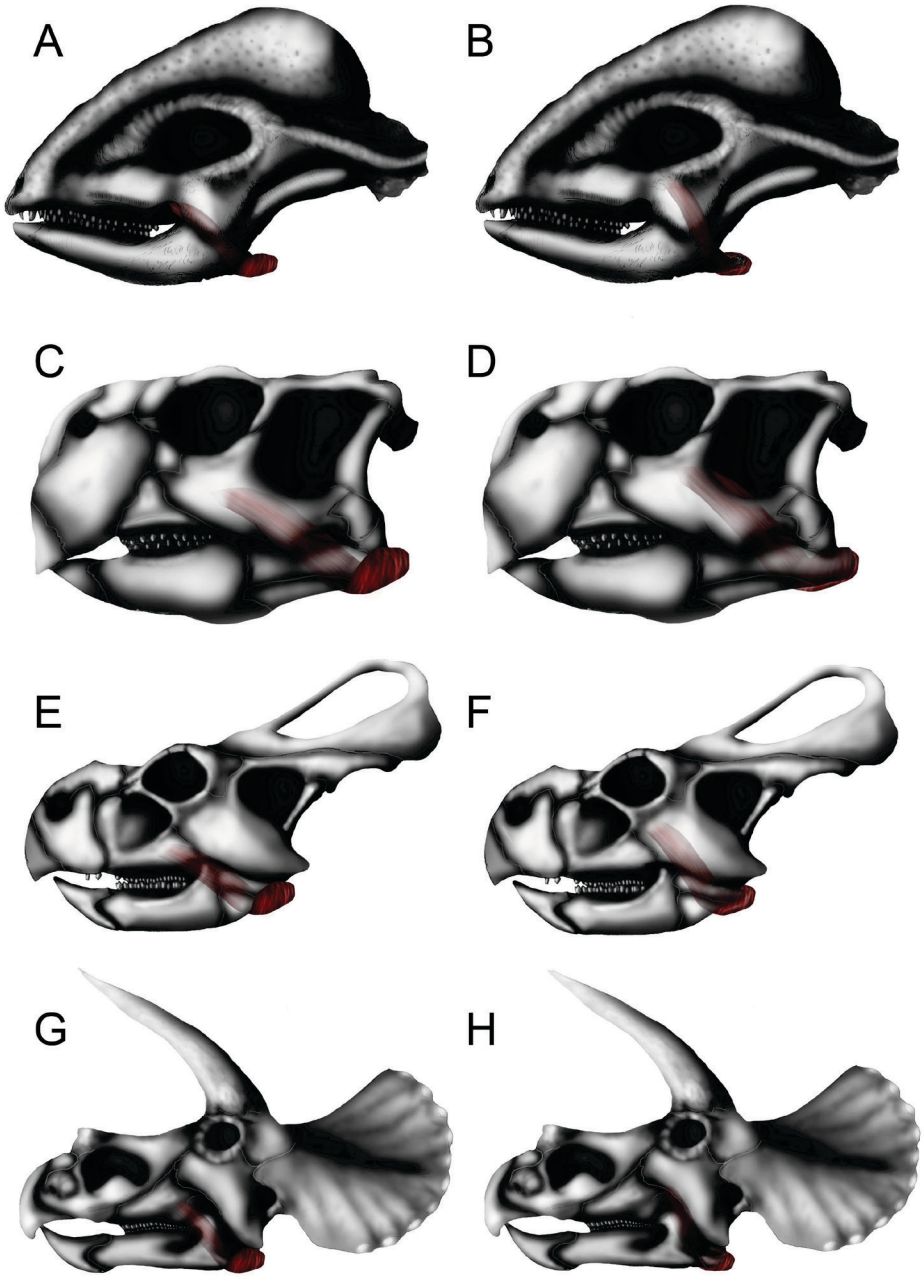

2D LEVER ARM ANALYSES

2D lever arm relative bite force (RBF) analysis was done on various marginocephalian genera and these were compared with each other as well as to the rest of Ornithischia (see Chapter 8). Below, the RBF results at the predentary as well as the rostral, middle, and caudal teeth are given (Table 7.4).

TABLE 7.4. Actual RBF values across marginocephalian tooth rows.

Genus	Spec. #/ Resource	Input Lever Angle in ° (mAMEP)	Predentary RBF	Rostral Tooth RBF	Middle Tooth RBF	Caudal Tooth RBF
Archaeoceratops	IVPP V 1114	53.48	0.361	0.522	0.672	0.935
Auroraceratops	IGCAGS 2004 VD001	49.03	0.388	0.545	0.687	0.938
Bagaceratops	GI SPS 100-528	43.81	0.346	0.469	0.597	0.822
Centrosaurus	USNM 8897	40.2	0.345	0.612	1.020	2.700
Chasmosaurus	ROM 839	31.91	0.364	0.615	0.956	1.881
Hongshanosaurus	IVPP V12617	48.01	0.362	0.453	0.546	0.694
Leptoceratops	NMC 8889	45.15	0.268	0.437	0.611	0.997
Liaoceratops	IVPP V12633	56.63	0.348	0.452	0.619	0.974
Pachycephalosaurus	Triebold Cast	29.4	0.262	0.323	0.494	0.870
Pachyrhinosaurus	TMP specimen (Display Skull)	34.05	0.320	0.550	0.831	1.688
Pentaceratops	OMNH 10165	38.04	0.275	0.496	0.864	2.636
Prenoceratops	TCMI 2001.96.14	54.72	0.481	0.681	0.832	1.029
Protoceratops	GI-SPS 100-522	43.11	0.335	0.466	0.611	0.870
Psittacosaurus	AMNH 6254	46.8	0.395	0.518	0.639	0.837
Stegoceras	UALVP 2	30.49	0.285	0.300	0.436	0.800
Styracosaurus	AMNH 5372	43.81	0.270	0.491	0.783	1.698
Triceratops	ROM 55380	43.96	0.319	0.508	0.805	1.758
Yinlong	IVPP V14530	53.01	0.419	0.471	0.603	0.840
Zuniceratops	(Reconstructed cast)	49.8	0.388	0.543	0.746	1.232

Mechanical Advantages Among Marginocephalian Jaws (with MANOVA Results)

There is a notable trend in the transition from a more evenly distributed RBF throughout the jaw in pachycephalosaurs and non-ceratopsid ceratopsians to a substantially stronger caudal RBF in ceratopsids. When comparing among more basal marginocephalians, pachycephalosaurs and non-ceratopsid ceratopsians show no significant difference in RBF value ($p = 0.074$; Fig 7.35). In most cases, this is because the jaw is relatively of the same shape, with a triangular coronoid eminence (or process), with a slightly heightened one in protoceratopsids and *Zuniceratops*. The rostral and middle RBFs in pachycephalosaurs are noticeably lower than in most basal ceratopsians, however they are roughly equal in caudal RBF.

FIGURE 7.35. Basal marginocephalian RBFs across the tooth row. Bite points are at the predentary (PD) tip as well as the rostral, middle, and caudal teeth.

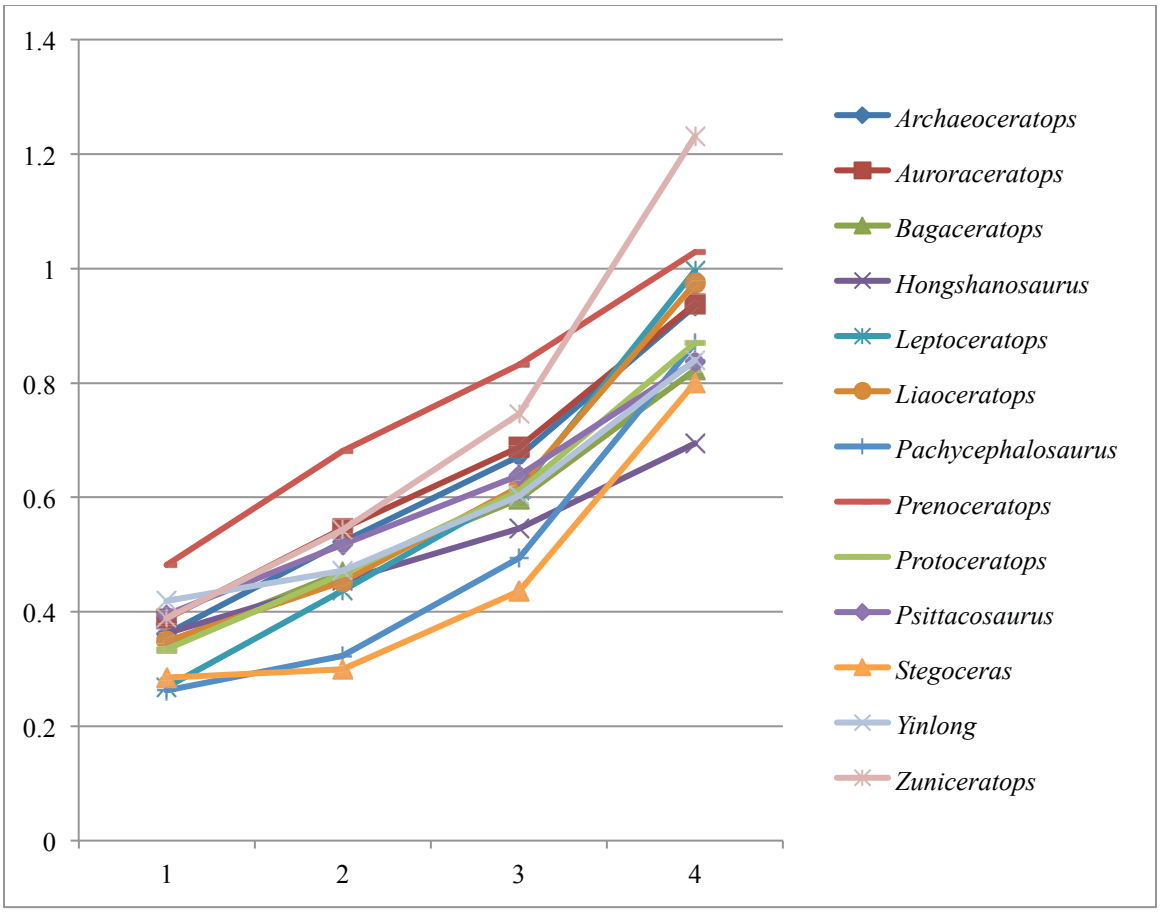

When comparing basal ceratopsians to the more advanced ceratopsids, however, there is clearly a strongly significant difference in RBF values across the tooth row, in which ceratopsids are typically higher in RBF caudally, yet noticeably much lower at the predentary ($p < 0.001$). The mechanical advantage in ceratopsids is obviously focused at the caudal aspect of the tooth row, as the tooth row is displaced caudally along the jaw line in ceratopsids compared to other ceratopsians. The heightened coronoid process also increases the mechanical advantage OF WHAT?(see Chapter 8). The two subclades within Ceratopsidae, Centrosaurinae and Chasmosaurinae, show no significant difference in RBF values across the tooth row ($p = 0.825$), again with very low predentary RBF values and a highly exaggerated increase in caudal tooth RBFs (Fig. 7.36). There is

variable overlap between the two groups in RBF values across the tooth row as well, suggesting that there is no great difference in jaw structure in these two subclades that would impact jaw mechanics in a large manner.

FIGURE 7.36. Ceratopsid RBFs across the tooth row compared to the basal ceratopsoid *Zuniceratops* (sister taxon to Ceratopsidae). Bite points are at the predentary (PD) tip as well as the rostral, middle, and caudal teeth.

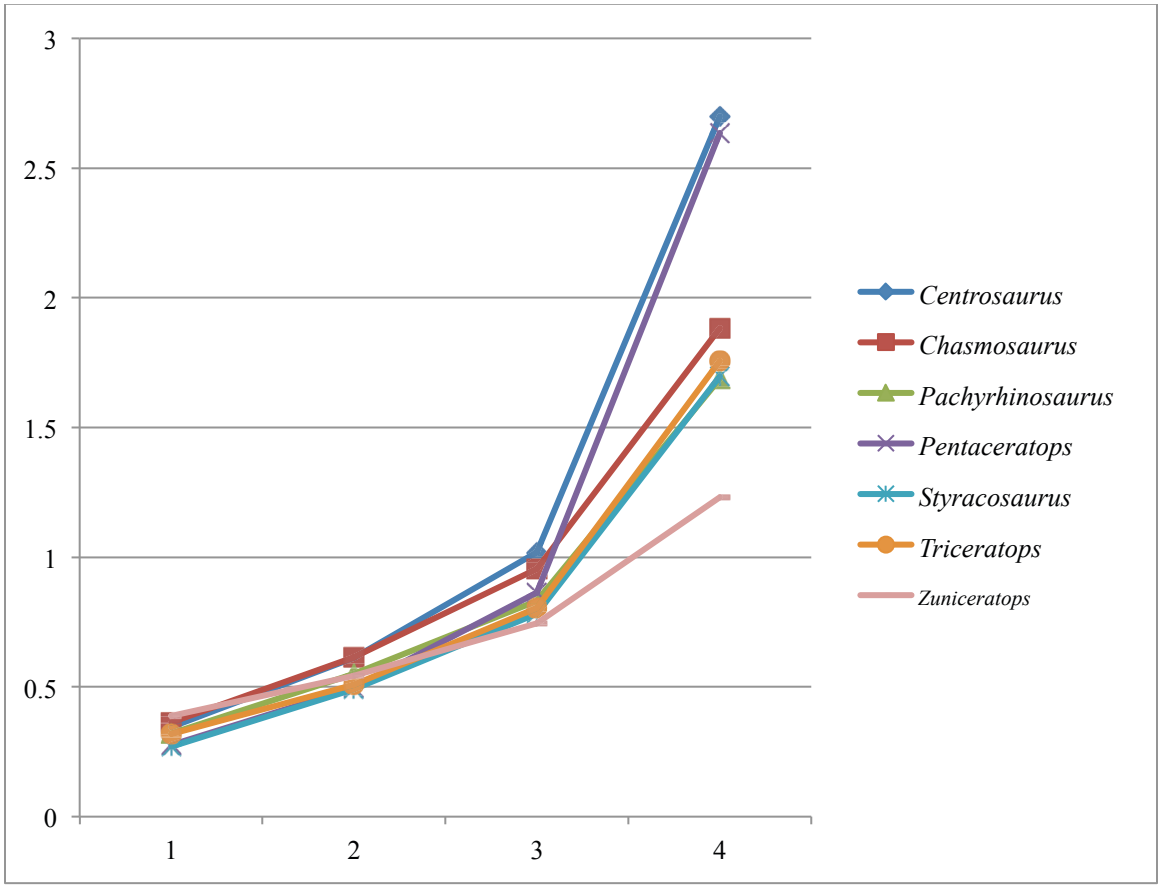

The phylogeny below (Fig. 7.37) visualizes the above results with optimized RBF values of the predentary and the caudal tooth compared to one another. Cooler colors show the lowest RBF values and warmer colors show gradually larger RBF values.

FIGURE 7.37. Phylogenetic mapping of RBFs across marginocephalian taxa, comparing predentary and caudal tooth RBF values. *Agilisaurus* is used as the outgroup taxon.

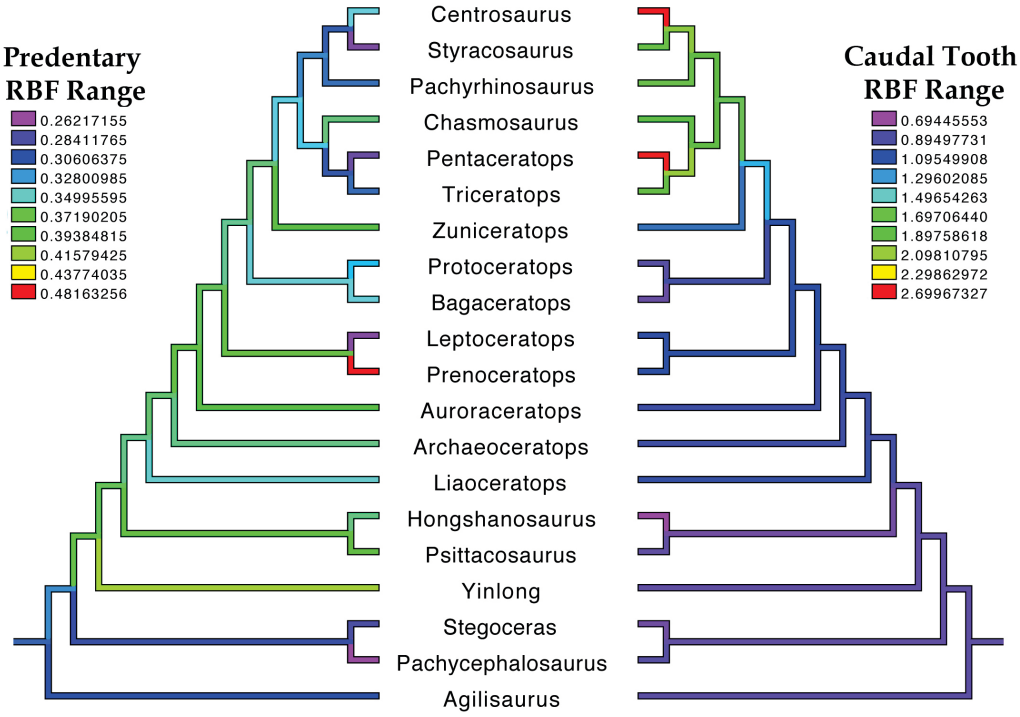

Perturbation analysis (Otten, 1983; 1985) results are shown below (Table 7.5) with RBF values with both the coronoid eminence removed and the jaw joint raised to the level of the maxillary tooth row:

TABLE 7.5. Hypothetical marginocephalian RBFs with coronoid process removed (left, black) and articular raised to level of the tooth row (right, white).

Genus	Spec. #	Input Lever Angle in ° (mAMEP)		Predentary RBF		Rostral Tooth RBF		Middle Tooth RBF		Caudal Tooth RBF	
Archaeoceratops	IVPP V 1114	59.29	53.48	0.292	0.318	0.422	0.460	0.543	0.595	0.755	0.834
Auroraceratops	IGCAGS 2004 VD001	54.92	49.03	0.336	0.305	0.472	0.435	0.595	0.556	0.812	0.775
Bagaceratops	GI SPS 100-528	49.93	43.81	0.287	0.293	0.390	0.401	0.497	0.513	0.684	0.713
Centrosaurus	USNM 8897	50.97	40.20	0.239	0.272	0.424	0.485	0.706	0.834	1.870	3.280
Chasmosaurus	ROM 839	39.52	31.91	0.240	0.272	0.406	0.477	0.631	0.787	1.242	1.499
Hongshanosaurus	IVPP V12617	52.75	48.01	0.322	0.295	0.403	0.371	0.486	0.447	0.618	0.566
Leptoceratops	NMC 8889	53.72	45.15	0.193	0.251	0.314	0.409	0.439	0.572	0.717	0.932
Liaoceratops	IVPP V12633	62.37	56.63	0.281	0.281	0.365	0.365	0.500	0.506	0.787	0.842
Pachycephalosaurus	Triebold Cast	32.14	29.40	0.234	0.132	0.288	0.162	0.440	0.246	0.775	0.503
Pachyrhinosaurus	TMP specimen (Display Skull)	43.46	34.05	0.207	0.228	0.355	0.410	0.535	0.636	1.088	1.485
Pentaceratops	OMNH 10165	46.17	38.04	0.200	0.235	0.360	0.418	0.628	0.741	1.917	3.076
Prenoceratops	TCMI 2001.96.14	64.37	54.72	0.364	0.410	0.515	0.583	0.630	0.712	0.778	0.914
Protoceratops	GI-SPS 100-522	50.61	43.11	0.264	0.320	0.369	0.449	0.483	0.585	0.687	0.849
Psittacosaurus	AMNH 6254	53.10	46.80	0.350	0.363	0.459	0.477	0.566	0.591	0.741	0.768
Stegoceras	UALVP 2	34.94	30.49	0.224	0.196	0.236	0.206	0.343	0.303	0.629	0.578
Styracosaurus	AMNH	49.54	43.81	0.197	0.213	0.359	0.387	0.572	0.637	1.241	1.875

	5372										
Triceratops	ROM 55380	49.68	43.96	0.245	0.242	0.391	0.390	0.619	0.629	1.351	1.705
Yinlong	IVPP V14530	57.55	53.01	0.380	0.405	0.428	0.456	0.548	0.580	0.762	0.815
Zuniceratops	(Reconstructed cast)	57.98	49.80	0.317	0.290	0.443	0.413	0.608	0.584	1.004	1.028

Results show that RBF values at all tooth positions in basal marginocephalian taxa are hypothetically lower if the jaw joint is raised to the level of the tooth row than it is if the coronoid was removed. This suggests that lowering the jaw joint ventrally has a larger influence on mechanical advantage than the coronoid, thereby retaining the basal condition seen in heterodontosaurids as well as thyreophorans (see Chapter 4 and 5). Also, note how removing the coronoid process increases the input muscle vector angle, as is expected. In the derived ceratopsids, however, due to the enlargement of the coronoid process, it is clear that the reverse is true. The evolved coronoid process takes over as a much more influential character in increased mechanical advantage. This is also seen in the derived hadrosaurids (see Chapter 7). See Chapter 8 for evolutionary implications.

Chapter 8: Discussion

Jaw mechanisms in ornithischian dinosaurs present an enormous spectrum of adaptations in feeding styles, not only among subclades, but across taxa within each subclade as well. This research implements detailed comparative analyses of mandibular shape, joint structure (both craniomandibular and intramandibular), tooth row curvature, tooth morphology and wear patterns, and origins, insertions, and orientation of inferred jaw musculature (both observed by the author and in the literature). Additionally, previous methods were used to find relative bite force across taxa, as they help aid in elucidating the evolutionary implications of the mechanical advantage of morphological traits of ornithischians. The culmination of these studies helps to develop a better understanding of the evolutionary paleoecology of ornithischian feeding mechanisms and their role in herbivory. The following is a comprehensive assessment of the evolution and functional significance of various osteological, arthrological, and myological traits examined in ornithischian jaws as well as evolutionary trends in mandibular mechanical advantage throughout the clade.

CRANIAL SHAPE

Cranial morphology in ornithischian dinosaurs is very diverse, with taxa presenting a plethora of shapes, sizes, and additional adornments, be it osteoderms in ankylosaurs, large narial crests in lambeosaurine hadrosaurids, or horns and frills in marginocephalians. Morphological variability of individual cranial elements suggests great plasticity in the way the skull of each taxon takes form. In many modern vertebrate taxa, plasticity in the way skulls are able to evolve depends on adaptations for feeding. An example of such an adaptation is the rostral elongation of the snout in extant large herbivorous ungulates aiding in both the procurement of vegetation as well as the chewing mechanisms involved with processing it (Smith and Savage, 1959; Greaves, 1978; Moore, 1981). Variability in terms of the shape of the snout itself is apparent depending on if the animal is a browser (for more generalized feeding) or a grazer (for more selective feeding**)** (Solounias et al., 1988; Solounias and Moelleken 1992; 1993).

Many of the basal-most genera of each ornithischian subclade possess small, triangular heads in lateral view. These taxa include heterodontosaurids, basal thyreophorans (i.e., *Lesothosaurus*), the basal cerapodan, *Agilisaurus*, basal ornithopods (i.e., *Hypsilophodon*), one of the most basal iguanodontians *Dryosaurus*, and basal marginocephalians (i.e., *Yinlong*). The triangular skull was likely a primitive adaptation for a specific orthal cropping mechanism for feeding on low-growing plants, although chewing mechanisms after the initial procurement of the vegetation are variable between taxa. As will be described below, relative bite force of many of these taxa seems to have been more or less mid-range, suggesting that triangular skull morphology was suitable for

animals of such small size, making for sufficient leverage in a tiny headed animal by bringing the bite point closer to the jaw joint. Bipedalism in these taxa seems to sometimes coincide with the consistent nature of such a skull shape in the basal-most genera of each of the major subclades, as they would have shared similar ecological backgrounds.

As many of the more derived genera in each clade evolved either facultative bipedalism (i.e., most iguanodontians) or quadrupedalism (i.e., stegosaurs, ankylosaurs, and most neoceratopsians) convergently, clade evolved its own novel cranial morphology to adapt to new ecological opportunities. Iguanodontians were typically much larger in size than more basal ornithopods and possessed relatively much more elongate rostra, although most juvenile iguanodontians possessed relatively much shorter rostra that lengthened as the animal aged (Kubota and Kobayashi, 2009). These juveniles likely had similar chewing styles and dietary preference to that of more basal ornithopods, as they are both more similar in both size and skull shape. The elongate rostrum in non-hadrosauroid iguanodontians was more rectangular in lateral view, yet more laterally compressed, which was likely ideal for a more selective feeding style (as is the case with other taxa with narrower snouts mentioned by Mallon and Anderson [2013]). Hadrosauroids also posses laterally compressed skulls, although the rostrum was considerably more dorsoventrally compressed and mediolaterally expanded at the end of the snout, forming the hadrosaurian “duck-bill” morphology. This expanded rostrum likely made it a more generalized feeder. Although iguanodontians possessed different tooth morphologies and likely different chewing styles, the elongation of the snout in these taxa likely served the same purposes of procurement of food in higher places (due

to their large size; Weishampel 1984b) as well as creating more opportunity for more complex jaw shapes and chewing behaviors (see below).

Stegosaurs also possessed relatively elongate and pointed snouts that may be a signal of selective feeding behaviors. Because they were quadrupedal animals that held their head close to the ground, it is almost certain that they fed on low-growing vegetation (Weishampel 1984b). With a small head on a large, thirty-foot-long body, animals such as *Stegosaurus* would have benefited from an elongate snout to be able to more easily select from a variety of vegetation sources. If its snout were small and triangular, as in basal ornithischians, it probably would not have been able to obtain as much food in one bite nor would it be able to process it as well, unless it had an elongate, highly maneuverable tongue. A similar strategy can be seen in nodosaurid ankylosaurs, which have a more pointed snout compared to the derived condition in ankylosaurid ankylosaurids. Ankylosaurids were conceivably more generalized browsers with a much more mediolaterally-broadened snout (Mallon and Anderson, 2013). Ankylosaurid skulls are much squarer in dorsal view, making for a much more rostrocaudally-shorter skull, which would potentially increasing leverage of the jaw musculature by bringing the bite point closer to the joint. Although this seems disadvantageous to the animal, due to its tremendous size, other mandibular features such as a mobile predentary-dentary symphysis and an exaggerated curved tooth row were likely much larger factors in feeding strategies (see below).

Among marginocephalians, pachycephalosaurs possess the primitive triangular skull morphology. Ceratopsians, however, diverge from this skull morphology with the addition of a caudally expanded parietal-squamosal complex, or “frill”. Although the

ceratopsian frill is mediolaterally expanded and the caudoventrally flaring jugals protrude laterally, the ceratopsian skull itself (rostral to the frill) is, for the most part, laterally compressed, so much so that the premaxillae are fused together at the rostral end. This fusion combined with a sharp pointed beak created a specialized mode of food procurement (Mallon and Anderson, 2013).

Various styles of cranial kinesis are largely used by fish, amphibians (Iordansky, 1990), reptiles (Frazzetta, 1962; Iordansky, 1990; 2011; Herrel et al., 2000), and birds (Bock, 1964; Zusi, 1984; Hoese and Westneat, 1996; Bout and Zweers, 2001) as an efficient mode of feeding. Most ornithischian subclades have been deemed akinetic due to the tight suturing of the quadrate and other cranial elements to the rest of the cranium itself (Weishampel and Norman, 1989; Barrett, 2001; Holliday and Witmer, 2008). In ornithopods, however, cranial kinesis has been considered a possible feeding mechanism; a pleurokinetic chewing model has been hypothesized (Weishampel, 1984; Norman and Weishampel; 1985; see Chapter 2). Although this hypothesis has recently been challenged (Rybczynski et al., 2008; Cuthbertson et al., 2012). For the purposes of this study, intracranial joints were not examined and, as such, no test for the pleurokinetic model is implemented because it is beyond the scope of this study. This study does, however, seek to infer other possible means of chewing in ornithopods as well as all other ornithischian groups with the assumption that the cranium is in fact relatively akinetic. These suggestions are mostly related to both intermandibular (i.e., at the mandibular symphysis) and the craniomandibular joints (see below).

BEAK SHAPE AND THE PREDENTARY BONE

The predentary bone does not exist in most other vertebrates, aside from convergences in a few fishes, some frogs, a few lizards, and some of the earliest ornithurine birds (De Beer, 1937; Baumel and Witmer, 1993; Schultze 1993; Trueb, 1993; Grande and Bemis, 1998; Adriaens and Verraes, 1998; Sheil, 1999; Yeh, 2002; Ferigolo and Langer, 2007; Zhou and Martin, 2011). All develop this element from a portion of the rostral tip of Meckel's cartilage known as the mentomeckelian cartilage (DeBeer, 1937). It is unknown, however, whether the predentary bone in ornithischians is also a derivative of the mentomeckelian cartilage rather than a derivative of the rostral end of Meckel's cartilage itself, but it is currently thought to be the most likely option (Ferigolo and Langer, 2007).

Regardless of its origin, the ornithischian predentary bone probably served in the feeding mechanisms throughout this clade. Selectivity and food procurement likely influenced much of the morphological diversity of ornithischian mandibular symphyses. Mallon and Anderson (2013) performed a quantitative analysis of beak shape in ornithischian taxa from the Dinosaur Park Formation of Alberta, Canada. This analysis included the ankylosaurid *Euoplocephalus*, the nodosaurid *Panoplosaurus*, and various genera of hadrosaurids and ceratopsids. Their findings suggest that the shape of the oral margin in these ornithischians is key in determining how generalized or selective a feeder the animal was in life, as has been found in extant mammals (see above; Solounias et al., 1988; Solounias and Moelleken 1992; 1993). They found that the nodosaurid, *Panoplosaurus*, has a much narrower, pointed snout, which probably signals that it was a

much more selective feeder than the more generalized feeding in the much wider snouted ankylosaurid *Euoplocephalus*. Using this reasoning, many hadrosaurids were probably much more generalized feeders than the much narrower snouted ceratopsids. Mallon and Anderson (2013) related these differences to the presence of niche partitioning and feeding preferences between taxa in the Dinosaur Park Formation, although they mentioned that not all of these animals coexisted temporally or spatially.

Predentary shape diversity throughout ornithischian taxa spanning all major subclades was investigated qualitatively in the current study, ranging from triangular, to rounded, to rectangular in dorsal view, depending on the taxon observed. The most basal heterodontosaurids exhibit a simple, cup-shaped predentary with a triangular rostral extremity that curves as it extends caudally on each side. This morphology is relatively more rostrally expanded in *Heterodontosaurus* and *Abrictosaurus* than it is in *Pegomastax*. This rounded triangular morphology is typical of many of the basal (and some derived) members of each major subclade as well. Among thyreophorans, *Lesothosaurus* and the stegosaurs *Huayangosaurus* and *Stegosaurus* exhibit a similar morphology, although stegosaurs are more rounded in dorsal view. Pointed to rounded predentaries are also seen in more basal members of Ornithopoda, with *Hypsilophodon*, *Thescelosaurus*, and *Dryosaurus* (among others) exhibiting more pointed predentaries and genera such as *Zalmoxes* and "*Kritosaurus*" having a much more rounded predentary. *Proa*, a more derived iguanodontian, also possesses a pointed predentary (with a bilobate ventral process), though this condition may be a secondarily derived feature (McDonald et al., 2012). The pointed predentary in thescelosaurids is much more rostrally elongate and pointed at its tip. In terms of feeding selectivity, elongation of the predentary and

beak probably helped to increase selectivity, in that the longer the predentary is for a given width, the more acute the angle of the predentary in dorsal view. The oral margin of the predentary is slightly beveled and capable of holding food while occluded with the premaxilla (or rostral in ceratopsians). In ornithischians with a pointed predentary, the larger the angle at the predentary tip, the more generalized a feeder it would have likely been with more surface area at the rostral margin to procure food (Mallon and Anderson, 2013).

Ceratopsian predentaries are, for the most part, triangular in dorsal view as well, with the exception of *Chaoyangosaurus* and psittacosaurids, which are round in dorsal view. The pointed nature of ceratopsian predentaries is likely tied to selectivity in feeding. However, they have a much broader and flatter oral margin, which extends caudally on both sides, thereby creating a larger surface area at occlusion. Additionally, among ceratopsids, chasmosaurines show a much flatter oral margin, while centrosaurines have a dorsally raised and narrow rostral tip of the predentary (with exceptions such as *Pachyrhinosaurus* [see Chapter 7]). This implies differences in either selectivity or food preference (or both) in these taxa. The vertical extension of the almost needle-like tip of the centrosaurine predentary likely made for a less sturdy occlusal contact at the rostral tip, although the slight breadth of the keratinous sheath may have accommodated this. Additionally, the ventral surface of the rostral bone was concave and perfectly fit for the predentary to be tucked underneath during occlusion. Because the predentary contacts both the rostral and premaxillae in most derived ceratopsids, this implies that the addition of more surface area at occlusion makes for a much more stable occlusion at the symphysis with much less long-axis rotation of the mandibular corpora in derived

ceratopsids (see below).

Many ornithischians have a square or rectangular predentary consisting of a transversely-widened oral margin. Ankylosaurs have a small predentary that is flat along the rostral end of the mandible. As mentioned above, in terms of skull shape, ankylosaurids are much more generalized feeders than nodosaurids, as their snouts are relatively wider (Mallon and Anderson, 2013). The small and thin predentaries in ankylosaurs (ankylosaurid and nodosaurid alike) come with the consequence, however, of not having a large surface area with which vegetation can be cropped at a time, as in iguanodontians or ceratopsids. The difference, however, is that ankylosaurs, especially ankylosaurids, have a substantial overbite, in which the premaxillae extend farther rostrally than the predentary does and also extend ventrally in a broad sheet of bone that overhangs the predentary (although the rhamphotheca might have accounted for some of thus gap in life). This overbite creates a cropping mechanism in which, during food ingestion, the premaxillae and predentary would strip the vegetation in opposite, ultimately cutting and holding it against the larger surface area of the upper palate. The food then would have been immediately pushed back to the sinusoidal tooth row characteristic of ankylosaurs (see Chapter 5), either by the animal lifting its head and letting the food fall into the tooth row or with the use of its tongue, assuming the tongue was a mobile muscle in ankylosaurs and ornithischians in general, which is unknown.

With the exception of dryosaurids, most iguanodontians (including all hadrosaurids) possess a rectangular rostral predentary edge as well. As stated above, non-hadrosauroid iguanodontians had a laterally compressed snout relative to their derived descendants, which is ideal for a more selective feeding strategy. The more derived

hadrosauroids, on the other hand, have a much more dorsoventrally compressed and mediolaterally expanded "duck-bill" snout, likely fit for more generalized feeding; although, more selectivity might have been possible had the animal tilted its head to the side to pluck vegetation. The broad expansion of the snout and flatter oral margin increase the surface area for the food to be initially cropped and allow muscle forces to be transmitted through the snout and predentary in a more dispersed manner, making it capable of withstanding higher forces. In hadrosauroids, especially, the lateral corner of the predentary and premaxillae are the only surface at which the elements actually occlude with each other, leaving a large, oval window in rostral view when the mouth was closed - although this was likely closed by the much more robust rhamphotheca on both the premaxillae and the predentary (Morris, 1970). Both the predentaries and premaxillae had prominent, triangular denticles protruding from the oral margin as well (a morphology likely reflected in the rhamphothecal sheath), which likely helped in gripping and stripping the vegetation more efficiently at food ingestion. These denticles were also likely exaggerated in size by the rhamphotheca surrounding them.

The keratinous rhamphotheca surrounding all ornithischian beaks might have had many functions. For purposes of nipping or cropping vegetation, it created even greater surface area at which the food is pressed against, allowing more plant material to be acquired at each given bite. Lautenschlager et al. (2013) recently conducted an FEA analysis reconstructing a keratinous rhamphotheca on the therizinosaur *Erlikosaurus*, a saurischian dinosaur distantly related to ornithischians. The study found that bite force stresses are dissipated with the addition of a keratinous rhamphotheca with a larger surface area, reducing the stress on any given point on the snout for more efficient

feeding. This dissipation of forces in the mandibular symphysis has also been studied in birds, which also possess a keratinous bill (Soons et al., 2012; Seki et al., 2012). It is therefore plausible to infer that ornithischians used a rhamphotheca for a similar purpose as well. Moreover, the premaxilla and predentary of ornithischians possess a large network of neurovasculature within them for rhamphothecal growth. The large network of neurovasculature suggests a possibility of neural receptors on the tips of their bills, creating a hypersensitive bill. An example is seen in a CT image of a *Euoplocephalus* predentary revealing many interconnected neurovasculature canals (see Chapter 5; Fig. 5.32), although whether or not this is solely for growth of the rhamphotheca or if its outer surface was actually touch-sensitive is difficult to infer.

PREDENTARY-DENTARY SYMPHYSEAL JOINT

Among extant amniotes, the mandibular symphysis plays a significant functional role during mastication (Lieberman and Crompton, 2000). The morphological properties of the mandibular symphysis have many implications in herbivores that chew isognathously (with both sides of the jaw occluding at the same time) versus anisognathously (chewing only on one side of the jaw at a time). It is the bridge across which forces acting on the mandible are transmitted bilaterally from the opposing side to apply force at the bite points in isognathous feeders. This symphyseal force transfer is especially important in the case of modern herbivores that orally process tough vegetation. Although mammals are not closely related to ornithischian dinosaurs, the biomechanical

implications of mammalian mandibular symphyses made in previous studies still apply in the fundamental biomechanics of ornithischian mandibular symphysis, aside from the predentary.

Previous studies in unfused reptilian mandibular symphyses are phylogenetically more relevant (such as studies in crocodilians [Porro et al., 2011], lizards [Herrel et al., 2000; Holliday et al., 2010], and *Sphenodon* [Jones et al., 2012]); however, they lack biomechanical comparisons to reptilian species with a completely fused mandibular symphysis. In modern herbivorous mammals, the mandibular symphysis may be fused or unfused (Greaves, 1978). In mammals with a fused mandibular symphysis (i.e., perissodactyls, elephants, camels, hippopotamuses), antagonistic muscle forces are transmitted through the symphysis, restricting bilateral axial rotation of each mandibular corpus, or individual side of the jaw (Greaves, 1978). In species with an unfused mandibular symphysis, including all ruminant artiodactyls (i.e., deer, cows, giraffe), the forces are not transmitted through the symphysis as efficiently as in species with a fused symphysis because of the dividing suture between the mandibular corpora. Consequently, medial torsion or rotation of the dentaries may be present during chewing (Greaves, 1978; Lieberman and Crompton, 2000; Hogue and Ravosa, 2001). The principles of an unfused symphysis during mastication apply to many different vertebrates, such as fishes, amphibians, and reptiles, in terms of providing mobility and deformation at the symphysis. The only other large clades of vertebrates besides mammals and earlier synapsids likely to have had the ability to chew tough vegetation were ornithischian dinosaurs, which also have the unique predentary bone at the mandibular symphysis.

As previously stated, the predentary bone is unusual as it is the only unpaired element in the ornithischian mandible (Weishampel, 2004). This bone remains unfused to the rest of the jaw throughout life and many aspects of the predentary, dentary, and postdentary in ornithischians support an interpretation of independent mobility of both dentaries with respect to the predentary bone. This is also supported by the variable rostrocaudal and mediolateral orientation of dental micro- and mesowear. Weishampel (1984), Crompton and Attridge (1986), Rybczynski and Vickaryous (2001), Bell et al. (2009), Norman et al. (2011), Cuthbertson et al. (2012), Sereno (2012), Ösi et al. (2014), and Nabavizadeh (*in press*) all hypothesized independent mobility of mandibular elements at the symphysis in various ornithischians. Due to its flexible articulation, the predentary likely acted as a single, central element allowing both dentaries articulating on either end to independently rotate mediolaterally or sometimes even dorsoventrally in relation to the predentary. This mobility would be to a smaller extent in heterodontosaurids, basal thyreophorans, stegosaurs, and basal cerapodans (including ornithopods and marginocephalians), but also to a larger extent in more derived iguanodontians and ankylosaurs (Fig. 8.1).

FIGURE 8.1. Rostral view of *Edmontosaurus* skull with premaxilla and predentary removed with arrows showing rotation of dentaries against maxillae. Line-drawing based on screen capture of surface scan in video from Rybczynski et al. (2008). Abbreviations: de, dentary; mx, maxilla.

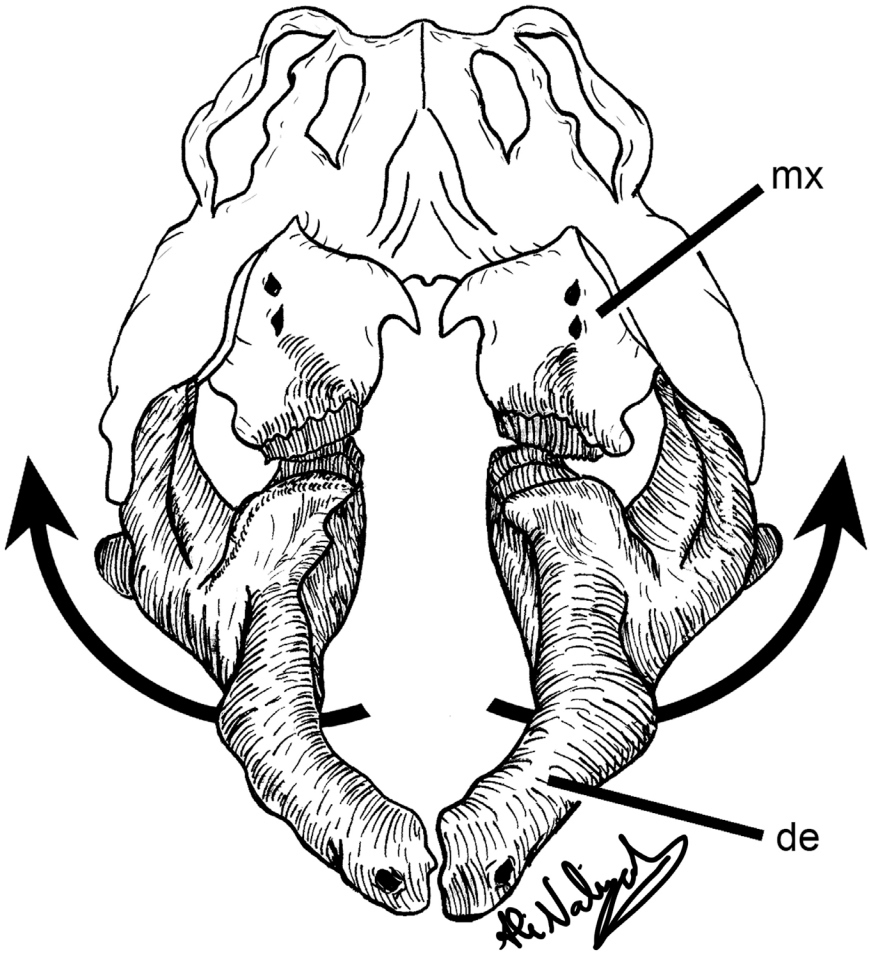

The dentary range of movement was restricted by the mediolateral width of the caudolaterally-oriented processes of the predentary. The volume of membranous or ligamentous material (a syndesmosis) assumed to be present that would have suspended the predentary from the dentaries would also play a role in restricting range of motion. For example, the rotational surfaces observed on the groove on the dorsal ridge of the dentary diastema also support mandibular rotation in hadrosauroids. The rugose and often tongue-and-groove edge of the rostral-most aspect of the dentary seen where it meets its

counterpart in most ornithischian dentaries observed (except in ceratopsids) suggests extensive rotational motion at this junction articulation. This long-axis rotation of the dentaries is analogous to the variably restricted long axis rotation seen in modern reptiles such as crocodilians (Porro et al., 2011), lizards (Herrel et al., 2000; Holliday et al., 2010), and *Sphenodon* (Jones et al., 2012) as well as in mammals such as ruminants with an unfused symphysis (Greaves, 1978; Hogue and Ravosa, 2001) and herbivorous marsupials (Crompton et al., 2010), although it is much more exaggerated. Early extinct ornithurine birds possessing predentaries may also have used kinesis of the dentaries against the predentary, although for differing mechanisms (Zhou and Martin, 2011).

There are other possible sources of mobility at the symphysis as well in addition to the likely presence of syndesmosis (membranous or ligamentous material). In the space between the dorsal and ventral processes of the predentary of many specimens (see Chapters 4-7 for predentary specimens), caudal to the rostral border, a number of small pits occur bilaterally where the symphysis articulates. These pits, although possibly suggestive of ligamentous attachment, might also indicate an attachment site for m. genioglossus, the main tongue muscle. If the attachment of m. genioglossus extends to the predentary, it might have acted in the control or independent movement of the predentary relative to the dentaries while the dentaries were in motion as well as the enabling the possibility of lingual feeding. This action is similar to that used by frogs to make of their mentomeckelian bone in tongue flipping (Regal and Gans, 1976). The potential of an autapomorphic synovial cavity at the predentary-dentary joint also cannot be ruled out, although such a joint is unheard of in vertebrate mandibular symphyses. Synovial joints are a made up of a pad of cartilage between bones surrounded by a cavity

of fluid, allowing much smoother mobility. There are no synovial cavities in the mandibular symphysis of extant reptiles and so the presence of a synovial cavity in ornithischians does not hold up to the expectations of the extant phylogenetic bracket (Holliday and Nesbitt, 2013). The slight possibility of an autapomorphic synovial mandibular symphysis in ornithischians cannot be completely precluded, however. If a synovial cavity did exist at this joint, it would provide even greater mobility at the symphysis than previously postulated. Further analysis of the morphology and histology of the symphyseal articular surfaces in ornithischians is necessary to seek the presence of calcified cartilage indicating a synovial cavity, however.

The subclade proving to be an exception to the mediolateral or dorsoventral rotation of the mandibular corpora in ornithischians is derived ceratopsians, including all ceratopsids (chasmosaurines and centrosaurines alike). Ceratopsid dentaries are nested within separate, bilateral slits on the caudolateral processes of the predentary (see Chapter 7). These caudal slits of the predentary envelop the flat, expanded rostral ends of each dentary, tightly securing them in place. This envelopment of the dentary ends creates what is functionally a secondarily fused mandibular symphysis, much like what is seen in mammals with a fused symphysis described above. Bilateral contraction of antagonistic muscles likely transmitted forces through the mandibular symphysis, restricting the bilateral axial rotation of each mandibular corpus seen in most other ornithischian clades, as is seen in large mammalian herbivores today with fused symphyses, such as horses, camels, and rhinoceroses.

The evolution of the dentary-dentary symphysis itself also plays a role in the method of kinesis at the predentary. Basal ornithischians, including heterodontosaurids as

well as the most basal taxa of Thyreophora, Ornithopoda, and Marginocephalia, all possess a dentary-dentary symphysis in which the rostral-most margin of the dentaries is mediolaterally flattened. The dorsoventrally-heightened rostral margins of the dentaries contact the predentary as well as its counterpart rostrally. Given that these taxa are relatively much smaller compared to many of their more derived descendants, rotation of each mandibular corpus around its long axis causes only a minimal degree of dorsoventral bending at the symphysis. Dorsoventral symphyseal bending consists of alternating separation and contact of the dorsal and ventral corners of the rostral margins of the dentaries. When the most dorsal corners of the dentary margins are in contact, the most ventral corners are separated and vise versa (Fig. 8.2).

FIGURE 8.2. Rostral view of *Edmontonia* mandibles (without predentary) showing how the derived condition of symphyseal processes of the dentaries contact one another allowing mediolateral rotation of the mandibular corpora with minimal dentary separation.

A convergent shift to the acquisition of a symphyseal process is seen in more derived forms, such as many iguanodontians and thyreophorans (especially ankylosaurs). In a symphyseal process, as the rostral portion of the dentary extends farther rostrally, the mandibular corpus curves medial or ventromedial as it reaches the symphysis, often creating a concave medial surface at this portion of the dentary. Hadrosaurids, especially, have a large diastema and a distinct ventrally curved symphysis, placing the predentary itself well ventral to the level of the tooth row. The ventromedial curving of the dentaries in these separate clades creates a morphology in which, instead of the basal condition with a dorsoventrally oriented dentary-dentary symphysis, it is a derived rostrocaudally-oriented symphyseal junction. The rostrocaudal symphysis makes it possible for mediolateral rotation of the dentaries around their long axes to occur because they each have rounded margins and can rotate against each other rather than an extreme case of dorsoventral bending as it would if the symphysis was dorsoventrally oriented. The convergent acquisition of this feature provides a good basis for inferring kinesis at the predentary-dentary contact in most larger-bodied ornithischians other than ceratopsids.

DENTITION AND TOOTH ROW MORPHOLOGY

The tooth row morphology and dentition in ornithischian dinosaurs go through many changes both between and among subclades. The premaxillary dentition is seen in heterodontosaurids as well the most basal members of Thyreophora (including basal stegosaurs, such as *Huayangosaurus*, and many nodosaurids [i.e., *Silvisaurus*, *Sauropelta*,

Tatankacephalus, *Pawpawsaurus*, *Gargoyleosaurus*, and *Struthiosaurus*; see Chapter 5]), basal Ornithopoda, and basal Marginocephalia (including all pachycephalosaurs as well as many basal ceratopsians). These premaxillary teeth are lacrimiform with a pointed apex, ideal for puncturing vegetation at ingestion. In some taxa, such as heterodontosaurids and pachycephalosaurs, the premaxillary teeth are variable in size along the oral margin, possibly influencing exact locations of the initial beak-bolus contact of the bite in each specific taxon. The premaxillary teeth are convergently lost in more derived taxa in each subclade. This evolutionary loss of premaxillary teeth could be linked to a shift in feeding strategies. One strategy would be the acquisition of an elongate diastema creating a relatively caudal positioning of the tooth row along the jaw, as in iguanodontians and ceratopsids. Alternatively, the loss of premaxillary teeth could be linked to developing a much broader oral margin of the rhamphotheca on the tip of the snout with a denticulate edge, as in many derived ornithischians, which would have helped crush plant material more easily at the initial bite.

Although much variation exists in tooth morphology, ornithischian maxillary and dentary teeth are primitively leaf-shaped with a number of sharp, triangular denticles around each apical ridge. A prominent median ridge that extends apicobasally along the enamel surface is present and some taxa even have one or two less prominent apicobasally-oriented ridges. These ridges create the larger denticles that reach the apex of the tooth, whereas the other smaller denticles are formed at the margin itself. The combination of all teeth working together creates a rostrocaudally elongate, serrated edge of the maxillary and dentary dentition at which the vegetation could have been cropped. Whether chewing is orthal or propalinal, a denticulate tooth margin is a good method for

processing food efficiently, as it makes its much more efficient in slicing the vegetation like the teeth of a saw blade. Hadrosauroids take the denticulate apical margin of the tooth row (or tooth battery in this case) a step farther and combine it with a flattened occlusal surface for a more specialized bolt-cutter method of chewing (described below).

Ceratopsids have a much more vertically-oriented occlusal surface at which the dentary and maxilla occlude side-by-side, yet microwear studies show much variation in chewing orientation. Varriale (2011) quantitatively analyzed the dental microwear of most species of ceratopsians (from basal forms to the derived ceratopsids) and documented the progression of orientations in jaw movements to test different previous hypotheses of ceratopsian jaw mechanisms. His analyses show that more orientations of jaw movements occur in derived clades than were previously hypothesized. He described an evolutionary, step-wise transformation in jaw movements throughout marginocephalian evolution, starting with an orthal power stroke in pachycephalosaurs and *Yinlong*, a clinolineal power stroke, in Chaoyangsauridae and Psittacosauridae, an isognathous motion combining an orthal and propalinal component together forming an inclined arc of dental microwear (Sereno et al., 2009), a palinal jaw motion in non-ceratopsid neoceratopsians (first seen in *Liaoceratops*), and finally a complex orthopalinal power stroke (mix of orthal shearing and palinal movements) in Ceratopsoidea. Both Varriale (2011) and Mallon and Anderson (2014) noted slight differences within ceratopsids as well, such as between centrosaurines and chasmosaurines, however the variation is too broad for any significant differences statistically.

The variable nature of tooth row morphology in ornithischians is another major

indicator of jaw mechanisms within the different subclades. In dorsal view, some tooth rows are straight (as in heterodontosaurids, *Lesothosaurus*, most iguanodontians, pachycephalosaurs, and ceratopsids), some are simply medially arched (as in *Scelidosaurus*, stegosaurs, basal ornithopods, and basal ceratopsians), and some are sinusoidal (as in ankylosaurs [see Chapter 5] and the unique case of the ornithopod *Ouranosaurus* [see Chapter 6]). In some cases, as in ankylosaurs, the maxillary tooth row is itself medially arched, while in many other ornithischians with a medially-arched dentary tooth row, the maxillary tooth row is relatively straight. For taxa with curved tooth rows, in many cases, the maxillary and dentary teeth do not simply match altogether during initial occlusion (Barrett, 2001; pers. observation). Ankylosaur jaws are one such case. When occluded, the dentary tooth row does not completely occlude with the maxillary tooth row. Many dentary teeth do not align with the maxilla due to the sinusoidal nature of the dentary tooth row. In ankylosaurs, the only way for all of the dentary teeth to be able to occlude with the maxillary teeth at some point during the chewing cycle is for the dentary to go through an extreme rotational movement to direct the lower tooth row to meet the upper jaw. Similar rotations were necessary for other ornithischians with curved tooth rows as well, as the more the tooth row is curved in a certain way, the more unlikely it is that it would be a means for simple orthal cropping without rotation of the mandibular corpora around their long axes.

The occurrence of curved tooth rows in many ornithischians matches well with the presence of a kinetic predentary-dentary joint. Mobility at the symphysis is necessary for rotation of the mandibular corpora to be possible, as stated above. It is can be inferred that this is a case where the two morphologies evolved hand-in-hand to serve the same

function. However, a curved tooth row is not present in all cases of mandibular rotation. Heterodontosaurids, for instance, had a relatively straight tooth row on each corpus, although the occlusal surfaces on their dentary teeth are tightly packed to form an elongate, flat occlusal surface. Tooth wear shows some degree of rotation and the predentary-dentary symphysis indicates this as well (Weishampel, 1984; Norman et al., 2011; Sereno, 2012).

Hadrosauroids are a special case because their tooth rows are straight, but, like heterodontosaurids, the occlusal surface is elongate and slightly concave with tightly-packed teeth. Hadrosauroids differ, however, in that they also have a large tooth battery, with many columns of teeth and are stacked dorsoventrally and curved together as a unit (see Chapter 6). This tooth row morphology, in addition to the stepladder tooth morphology of the occlusal surface (described in Chapter 6), is indicative of rotational movements of the jaw as well, as is also indicated by the rostrocaudal and mediolateral orientation of the tooth wear (Weishampel, 1984; Williams et al., 2009; Cuthbertson et al., 2012; Mallon and Anderson, 2014; see Chapter 6).

The hadrosauroid tooth wear mentioned above suggests a complex feeding mechanism (Fig. 8.3). Mesiodistal microwear in hadrosauroids indicates palinal movement and the more prominent labiolingual microwear suggests a mediolateral motion of each mandibular corpus. The step-ladder dental mesowear (see Chapter 6) shows a second medial rotation as well. Following occlusion, the two dentaries rocked caudally. The ventral ends likely swung laterally, causing the dorsal ends (i.e., the dental battery) to move medially and cut along the labial edge of the maxillary teeth to wear it down in a rounded fashion. This imitates, as stated before, a bolt-cutter motion in which

branches and conifer needles could be snapped apart and maneuvered into the oral cavity instead of letting them fall out. This bolt-cutter-like mechanism accounts for the occlusal surface of the dentary teeth facing labially rather than lingually (like many herbivorous mammals), making it difficult to push food already caught between the dentition into the oral cavity without an additional movement of the jaw in the opposite direction. After bringing the neck forward to obtain vegetation, hadrosauroids would have to have pulled their head back to strip the bark and leaves off of the branches. Correspondingly, hadrosauroids may have been able to drag the serrated edges of its dental battery along the branch as they sheared off the leaf-bearing bark into their mouths. The denticles along the edge of the premaxilla and predentary could have acted as additional cutting edges to push even more food into the mouth, assuming that the keratinous sheath covering them also possessed denticles; although, not all specimens have these denticles. This motion corresponds to the tooth wear along the edges of the serrations of the denticles on the top ridge of the dental batteries.

FIGURE 8.3. Proposed feeding mechanism (with coronal jaw cross-section illustrations based on Lambe (1920) with maxillae on top and dentaries on bottom). A, occlusion of dental batteries with simultaneous palinal motion in closing stroke; B, lateral view of hadrosauroid jaw stripping bark with palinal motion of the jaw; C, dorsal side of dentaries rotating medially in power stroke with maxillary teeth pressing against the dentary teeth maneuvering vegetation into the oral cavity along with possible tongue assistance; D, returning to resting position in opening stroke before repeating the process.

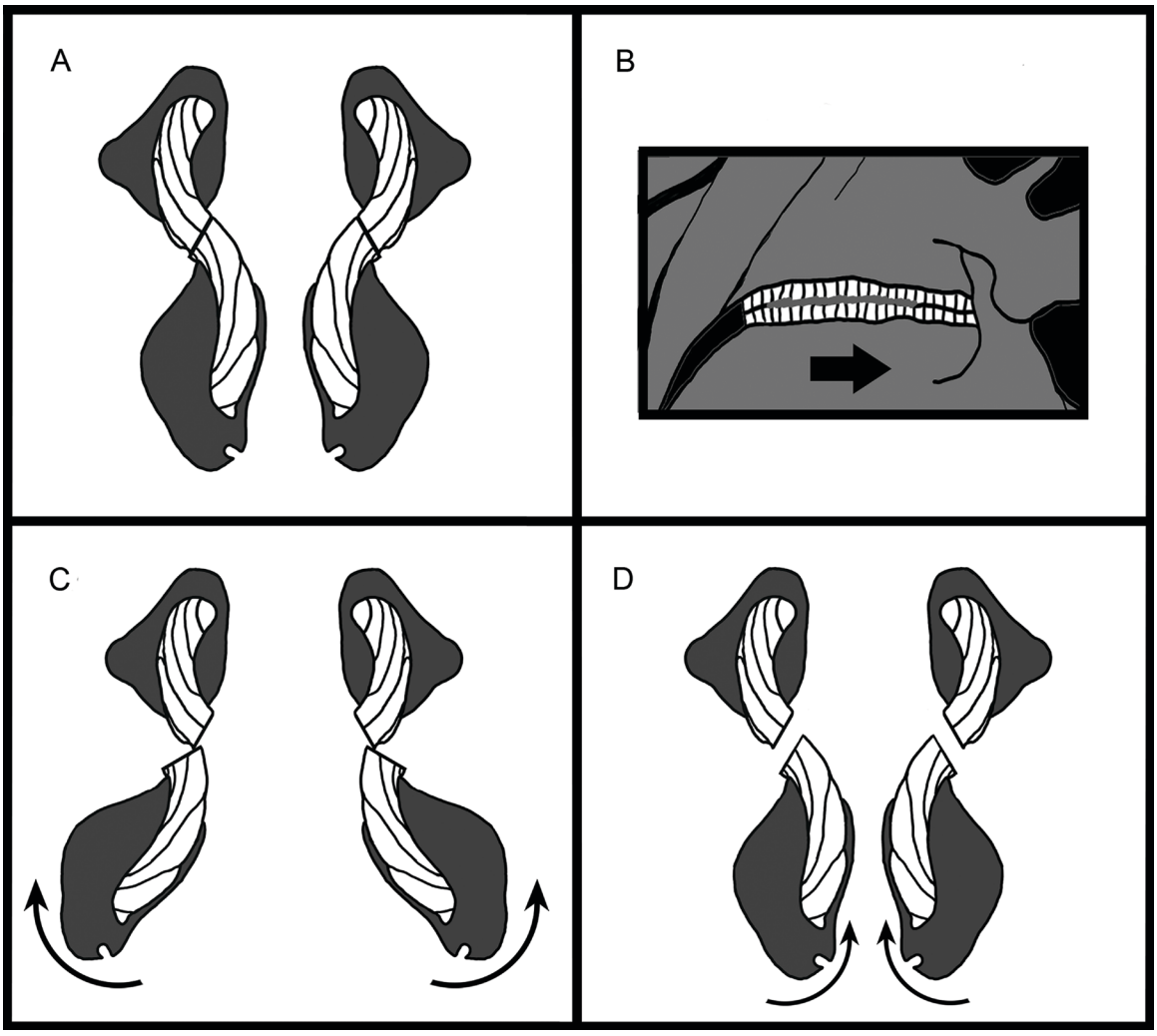

The rostrocaudally-cylindrical body shape of iguanodontian dentaries (hadrosauroids, especially) was allowed rotation of the corpora as well, as it would have limited deflection of the ventral aspect of the mandibles laterally because it would only be rotating around itself (see Fig. 8.1). As stated before, ceratopsid mandibles, although themselves complex with a dental battery of their own, likely did not mediolaterally rotate the mandibles because the predentary-dentary suture was more tightly articulated, as mentioned above (although relatively short-range rotations of the jaw were likely possible at the level of the tooth row itself. Although rotation of the mandibular corpora

is not required for this to occur, slight torsions of the mandibles likely could have assisted in multiple chewing stroke orientations, as observed by Varriale [2011]).

Diastemata in ornithischian mandibles are also common and often increase in relative size ontogenetically (Kubota and Kobayashi, 2009). They are seen in more derived taxa, especially ceratopsids and iguanodontians. Ankylosaurs and stegosaurs possess diastemata as well, although they are not as long. The tooth row in the basal stegosaur *Huayangosaurus* stretches the entirety of the jaw, from just caudal to the predentary to immediately rostral to the coronoid eminence. *Stegosaurus*, however, had a much shorter tooth row that was displaced rostrally and yet had a sheet-like dorsal projection along the oral margin, likely aiding in rostrally orthal food processing as a cutting edge. Ankylosaur diastemata do not stretch farther caudally than the caudal end of the symphyseal process itself. The ankylosaur tooth row begins abruptly when the jaw is oriented dorsally (see Chapter 5). The tooth rows in both ceratopsids and hadrosaurids are rostrocaudally straight, instead of the basal condition where tooth rows are at acute angles relative to one another. The straight tooth rows helped in the specialized jaw mechanisms used with the complex tooth batteries in hadrosaurids and ceratopsids. The tooth rows in ceratopsids and hadrosaurids also extend farther caudally and medial to the coronoid process, both elongating the tooth row and providing greater mechanical advantage, as is described below.

Although the tooth row and the predentary-dentary joint seem to be highly integrated evolutionarily, a number of other morphologies, such as the coronoid process and the jaw joint morphology, are also important to consider when deciphering ornithischian jaw mechanisms, as is described below.

CORONOID PROCESS

The coronoid process or eminence, located just caudal or lateral to the tooth row, is a protrusion of bone that extends dorsally from the body of the mandible, usually from the level of the tooth row. It is made primarily of the dentary rostrally followed by the surangular and coronoid bones just caudal to it. The lateral and medial surface of dorsal rim of the coronoid process is the attachment site for the m. adductor mandibulae externus musculature, originating at the squamosal and temporal region and inserting onto the coronoid process (Holliday, 2009). This muscle group is a large fan of muscle that, when contracted, manipulates the jaws in various ways depending on the feeding strategy. The coronoid region (not to be confused with the coronoid bone) extends much farther dorsally as a prominent process in iguanodontians and ceratopsids relative to all other ornithischian taxa. The coronoid process of iguanodontians and ceratopsids possesses more of a cylindrical base before becoming rostrocaudally expanded and mediolaterally compressed at its apex for further insertion of the adductor musculature. In other more basal members of their respective subclades, as well as in heterodontosaurids and thyreophorans, the coronoid region is not nearly as elevated and is more of a mediolaterally-compressed sheet of bone with a rounded dorsal rim.

The extent to which the coronoid process rises above the level of the tooth row is variable among ornithischian taxa, both within and among subclades. The taller the coronoid process of an individual taxon is, the more acute-angled orientation of the vector of the adductor musculature becomes, depending on the dorsoventral height of the cranium. For instance, the coronoid process in non-hadrosauroid iguanodontians, such as

Iguanodon, is relatively shorter than the coronoid process of the more derived hadrosauroids. A shorter coronoid creates a larger angle at which the adductor musculature attaches to the mandible in non-hadrosauroid iguanodontians, creating more of a vertical pull of the lower jaw. The smaller angle of the muscle vector in hadrosauroids indicates a more caudally-oriented vector. The transition from a shorter coronoid to a taller one in multiple ornithischian clades is indicative of a convergence toward better mechanical advantage. The farther rostrally-displaced from the jaw joint the coronoid process is, the more advantageous the jaw lever system also is, as it helps in increasing lever arm length. Hadrosauroids and ceratopsids take this a step further with by possessing a rostrally-angled coronoid process, displacing the apex of the muscle attachment more rostrally itself. See Lever Arm and Perturbation Analyses sections below for more detailed descriptions

The coronoid process also has implications for mediolateral rotation of the mandibular corpora. The smaller coronoid eminence of most ornithischians would have provided considerable freedom for the dorsal rim of the mandibles to be rotated medially. In much larger taxa, however, such as in hadrosauroids, the coronoid is recurved medially at its apex. This medially recurved coronoid process allows medial dentary rotation to occur as well, as it permitted the dentary to sweep ventromedial to the ventral edge of the jugal while rotating, rather than pressing against it. Lever arm length in the mediolateral direction also increases, thereby providing a greater mechanical advantage in this respect, although this remains to be quantified. Although ceratopsids have a tall coronoid process, it does not curve medially as much; this is likely related to their more securely articulated predentary-dentary suture precluding much mediolateral rotation of the jaw that is seen in

most other ornithischians.

M. adductor mandibulae externus could have acted in both raising and medially rotating the lower jaw in all ornithischian taxa, as the muscles were directed ventrolaterally. When the muscles contracted, they would have pulled the coronoid process caudodorsally as well as medially rotating it. For further description of the effect of the muscle as well as quantification of mechanical advantage of coronoid morphology in lateral view, see the Comparative Myology and Lever Arms Analyses sections below.

CRANIOMANDIBULAR JOINT MORPHOLOGY

For the most part, ornithischians are known to possess a craniomandibular jaw joint that is ventrally displaced from the level of the tooth row (Weishampel, 2004). An exception is a derived condition in some basal ceratopsians, where the jaw joint is near the level of the tooth row (Tanoue et al., 2009); however, this condition secondarily reverts to a lowered jaw joint in more derived ceratopsians. Craniomandibular joint morphology is crucial in understanding what movements of the jaw occurred during mastication. The morphology of this synovial joint as well as the synovial capsule plays a crucial role in determining the range of movement of a given jaw.

Since the synovial cavity is not preserved in the fossil record, a perfectly accurate quantitative prediction of range of movement cannot be assessed with great confidence, although this could be predicted somewhat with assumptions made in computer modeling. In observing the osteology itself, however, all ornithischians share a dish-like or bowl-

like morphology of the glenoid surface, with raised edges along the their outer rims, except for the case in psittacosaurs, where the glenoid surface is flat. The ventral head shape of the quadrate also indicates what types of movements were allowed at this joint, which is why they require more detailed descriptions with three-dimensional shape analyses of the condyles. In many ornithischians, the distal condyles are bicondylar, except in many hadrosaurids, which have just one spherical condyle. The rounded nature of these condyles permitted a large range of movement of the mandibular corpus, whether it is orthal, transverse, or propalinal motion of the jaw. Mediolateral rotation of the mandibular corpora would also have been permitted with such rounded quadrate condyles.

Heterodontosaurids and ceratopsids had a bicondylar head with the lateral condyle displaced farther ventrally than the medial condyle, whereas in most stegosaurs and ankylosaurs the medial condyle is displaced ventrally. In many other taxa, such as non-hadrosauroids and basal thyreophorans, the condyles are more or less even in height. Either way, the mediolaterally elongate nature of a bicondylar quadrate is ideal as a hinge joint, rotating around a transverse axis. The single spherical condyle in hadrosaurids indicates a greater range of movement in multiple directions. Given the complexity of hadrosauroid mandibles, it is stronger evidence of mediolateral rotation of the mandibular corpora.

Any given chewing style is partially dependent on which of these conditions a taxon might have had (see below). The spherical ventral end of the quadrate, whether it is a single condyle or two, articulating with the broadened, shallow, bowl-shaped basin of the surangular and articular suggests a great deal of mediolateral rotation of the mandibular corpus at the craniomandibular joint in most taxa (although less so in

ceratopsids, as their quadrate head is exceptionally elongate mediolaterally). The fact that the ventral end of the quadrate does not occupy the entire rostrocaudal length of the articular surface in many taxa also provides potential for propalinal motion as well in many cases (see below). The overall cylindrical, mediolaterally-curved long-axis of the mandible suggests long axis rotation, and the postdentary elements, including the glenoid, would not be affected as they act as a continuation of the overall shape of the mandibular corpus and, therefore, the mandibular corpus acted as one large unit.

COMPARATIVE MYOLOGY

Jaw muscle reconstruction has long been used to infer ornithischian dinosaur feeding mechanisms. Previous studies in dinosaur jaw musculature have used comparative methodology, largely extant phylogenetic bracketing methods (Witmer, 1995), to qualitatively compare muscle origins and insertions in a select few ornithischian genera (Ostrom, 1961; Weishampel, 1984; Holliday, 2009; Norman et al., 2011; etc.). The current study uses criteria from previous jaw muscle studies, as well as more in-depth case-by-case analyses, to reconstruct each muscle associated with the jaw apparatus in a large diversity of ornithischian taxa spanning all subclades. Additionally, vectors of the primary musculature involved with initial jaw occlusion, namely the adductor mandibulae externus complex (mAME) as well as m. adductor mandibulae posterior (mAMP), were measured. Below is a comparative summary of jaw musculature spanning all subclades with an account on their main influence in jaw mechanisms.

M. depressor mandibulae (mDM)

Although a large driving force in opening the lower jaw is gravity, mDM (Fig. 8.4) is the major muscle that is actually physically acted to depress the jaw. It is functionally the reptilian equivalent of the digastric musculature in mammals, although attachment sites are different. It is consistent throughout the entirety of Ornithischia in terms of origins and insertions. The distal tips of the paroccipital processes of the exoccipitals are accepted as being the origin of mDM (Holliday, 2009). Sereno et al. (2009) and Sereno (2012) speculated that in heterodontosaurids and psittacosaurids, respectively, the origin of mDM might have been on the caudodorsal aspect of the cranium itself rather than the paroccipital processes due to the presence of depressions in the skull. If this is true, then it could have been a transition to a more stable origin with larger surface area to provide more force. This larger surface area also would have permitted the muscle to be relatively larger as well for more force.

The mDM inserted on and around the dorsal aspect of the retroarticular process at the caudal-most extent of the lower jaw. Muscle contraction raised the retroarticular processes dorsally at a small arc angle, thereby causing the rostral region of the mandible to be pulled ventrally at a much greater arc angle due to the caudally-positioned craniomandibular hinge joint. Contraction of mDM would have also contributed to gape size, depending on the height of the caudal region of the skull. Taxa with a much more angled mDM, such as ankylosaurs, basal ornithopods, lambeosaurines, pachycephalosaurs, and ceratopsids, possibly could have had a wider gape when opening their mouths due to the angle of contraction. The caudal pull of the muscle might have

produced enough pull in the caudal direction to open the mouth wider, although this is purely speculatory.

M. adductor mandibulae posterior (mAMP)

Palinal (caudal) jaw movement is the main function of mAMP (Fig. 8.4). When teeth are in occlusion, mAMP produces the caudal grinding of plant material. It also likely helped in jaw elevation. In all ornithischians, the muscle originated on the lateral surface of the pterygoid wing of the quadrate. The pterygoid is dorsoventrally expanded so that that muscle would have good support for pulling the mandible in its direction. Due to its origin, mAMP is itself located within the bounds of the cranium and therefore hidden in lateral view.

The insertion of mAMP is located within and around the medial mandibular fossa, with a large area on which the muscle could expand and attach. The mAMP was a large muscle. The large, round insertion site creates stability for the movement of the mandibular corpus. Given that the angle of the muscle from the horizontal plane is variable, it is safe to infer that the higher the angle of the muscle, the more likely it is that it was used more in jaw elevation than in caudal movement of the lower jaw. This is seen in *Huayangosaurus*, various ankylosaurs, some basal ceratopsians (i.e., *Archaeoceratops* and *Liaoceratops*), and some saurolophine hadrosaurids (see Chapters 4-7). The opposite holds true if the dorsoventral angle of the muscle was smaller: the jaw would have acted in a caudal movement of the mandible. This is seen in cases such as some ankylosaurs, *Stegosaurus*, many lambeosaurines, pachycephalosaurs, and ceratopsids. In either case,

mAMP was an essential adductor muscle for caudodorsal movement of the jaw during the initial chewing stroke.

M. pseudotemporalis

MPST (Fig. 8.4) (in many cases divided into two bodies—superficialis and profundus) is another muscle (or pair of muscles depending on the taxon) that assists in elevating the jaw to occlusion, albeit to a lesser extent than mAME. It originates inside the skull along the lateral surface of the braincase just caudal to the orbital region. The mPST extends ventrally to insert onto the rostral-most apex of the coronoid process. In many cases, it also inserts as far down as the mandibular fenestra for even more leverage. This muscle likely acted to stabilize the jaw at the chewing stroke, restricting extreme caudal movement of the jaw caused by the mAME muscle mass. The combination of the mAME mass as well as mPST creates a majority of the muscle force at occlusion.

FIGURE 8.4. *Panoplosaurus* skull with jaw musculature (from left to right: mPST, mAMP, and mDM).

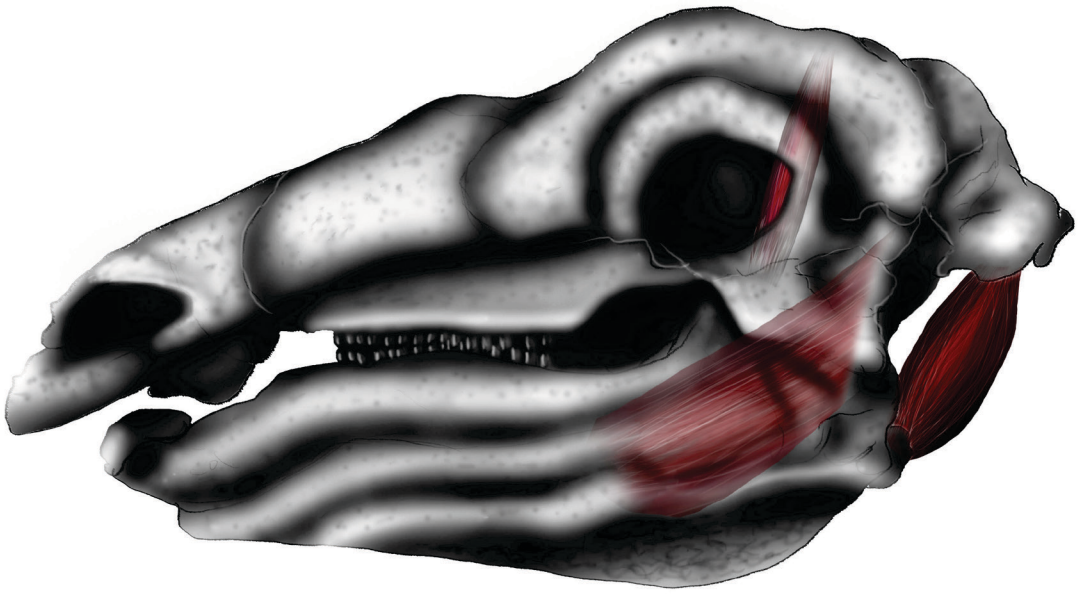

M. adductor mandibulae externus (mAME) and m. pseudotemporalis (mPST)

The main musculature involved with elevating the mandible and providing a majority of the bite force at occlusion is that of mAME (Fig. 8.5) (divided into three muscle bodies—superficialis, medialis, and profundus). The method and orientation at which these muscles contract indicates what movements of the jaw are possible, whether it be long-axis rotation, transverse movements, or propalinal movements.

FIGURE 8.5. *Triceratops* skull exhibiting mAME muscle complex.

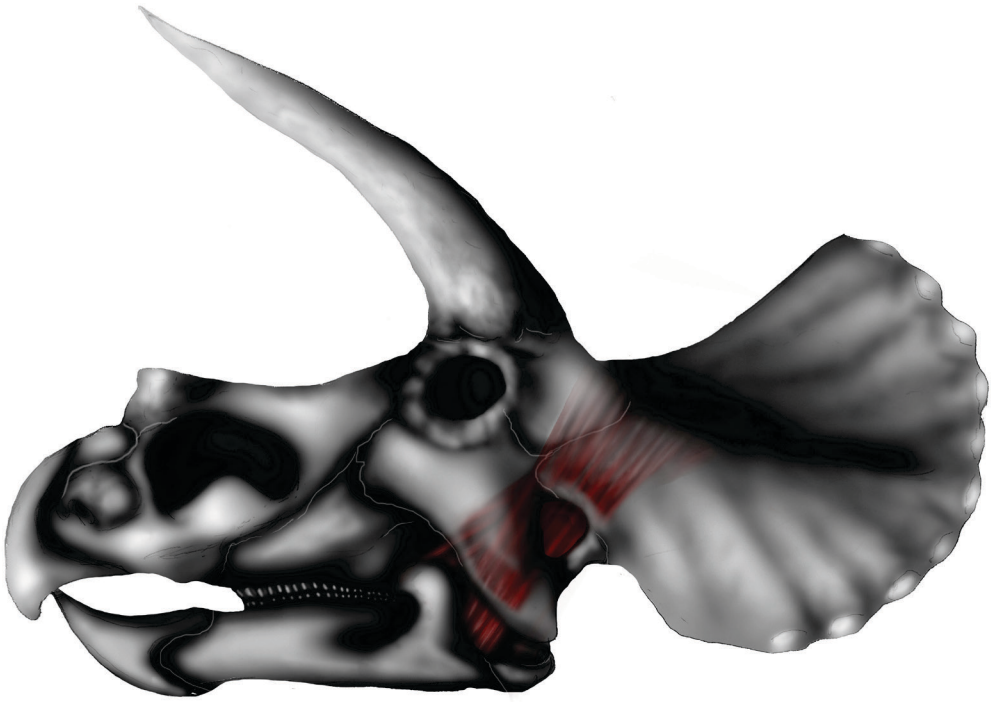

In dorsal view, the origins of all three mAME muscle bodies are externally visible in taxa possessing an open supratemporal and infratemporal fenestra. The mAMES originates on the medial surface of the supratemporal bar, mAMEM originates at the caudolateral margin of the supratemporal fenestra, and mAMEP originates on its caudomedial margin. In some cases, such as heterodontosaurids and ornithopods, the mAMES fibers extend onto depressions on the lateral surface of the supratemporal bar as well, giving additional force to the bite. Some of the fibers of all three muscle bellies likely blended together, as seen in many crocodilians and birds (Holliday and Witmer, 2007; Holliday, 2009), and acted as one large fan of muscles that extends rostroventrally

just medial to the infratemporal fenestra. This conjoined muscle acts as a single unit to elevate the lower jaw at the dorsal margin of the coronoid process. As mentioned before, coronoid processes range from dorsoventrally short to relatively tall (see above). Taxa with short coronoid processes tend to have a larger surface area on which mAME inserts to pull the jaw more vertically. However, for taxa with a tall coronoid process, such as ceratopsids and iguanodontians, the muscle vector is oriented more caudally because the insertion area is now dorsoventrally-oriented rather than rostrocaudally (see below for further description). Due to the ventrolaterally-angled nature of mAME in caudal view, this muscle also contributed greatly to the mediolateral rotation of the mandibular corpora around their long axes, as the vector of pull and the medially curved nature of the coronoid process suggested the jaw would rotate around its rostrocaudal axis.

The infratemporal fenestra is variable in size and shape, both within and among subclades, and is mostly a window allowing muscle bulging to occur during contraction of adductor musculature, namely mAME. A much narrower infratemporal fenestra, seen in taxa such as nodosaurids and some hadrosaurids like *Parasaurolophus* and *Edmontosaurus* consequently have a much smaller space in which mAME was able to fit; therefore, the muscle was probably smaller. This smaller muscle space suggests a possible trade-off in muscle size and usage with the pterygoideus musculature. It makes room for cranial adornments or a more caudal positioning of the orbit, among other reasons. A narrow infratemporal fenestra also correlates with a more caudodorsally-oriented (rather than just dorsally-oriented) muscle vector and a more caudally angled quadrate bone. Caudally angled muscle vectors indicate a more caudodorsally palinal tooth movement rather than just vertically orthal.

Results of mAME (as well as mAMP) vectors (see Chapters 4-7) show general trends from a mid-range caudodorsal orientation in basal ornithischians and most armored thyreophorans to a decrease in vector angles indicating more caudally oriented jaw movements found convergently in other taxa (e.g., derived thyreophorans, basal ornithopods, lambeosaurines, pachycephalosaurs, and derived ceratopsids). Some exceptions do occur, however, where mAME vector angles increase to improve mechanical advantage, such as in many saurolophine hadrosaurids, although this is in sync with other morphological features that create an effect, such as the dorsoventral deepening of the skull. The extensive variation in muscle vectors, both between and among subclades, however, suggests variable feeding mechanisms among genera and shows that feeding mechanisms of an entire subclade should not be based only on a few taxa, as has been previously done (Ostrom, 1964; 1966; Tanoue, et al., 2009).

In many cases, mostly lambeosaurines, some saurolophines (i.e., *Edmontosaurus*; Prieto-Marquez, 2010), and ceratopsids, there is substantially less room for mAME musculature to be present within the skull due to the evolutionary reorientation of skull elements, among other things. This decrease in space for musculature could have led to the evolutionary recruitment of enlarged pterygoideus musculature to accommodate for the decreased mAME bite force. With CT scan data, this assertion can be further analyzed in future studies, with volumetric data of the adductor chamber as well as the size of pterygoid bone attachment sites.

M. pterygoideus ventralis (mPTV) and dorsalis (mPTD)

The mPTV (Fig. 8.6) and mPTD are large muscle masses that originate on the ventral and dorsal surfaces of the pterygoid, respectively, as well as surrounding elements. The pterygoids are especially larger in more derived taxa, such as hadrosaurids and ceratopsids. Both mPTV and mPTD extend caudoventrally to insert onto either side of the retroarticular process caudal to the craniomandibular glenoid. These two muscles, in addition to mDM, create a large cluster of muscle insertions on the retroarticular process, thereby determining the extent of its elongate morphology.

The sizes of both mPTD and mPTV were probably variable depending on the jaw mechanism as well as the shape of the skull itself. As mentioned above, these muscles could have greatly enlarged when mAME had less space within the cranium, thereby acting as a functional alternative to mAME. However, size of these muscles is difficult to discern due to the open nature of the space ventral to the skull through which the muscles passed to reach their insertions. Both muscles likely contracted in tandem to either move or even restrict the jaw in whatever way necessary depending on the feeding mechanism used by each taxon. These functions include occlusion (for which it still contributes a fair amount), mediolateral translation, restriction, or even long-axis rotation of the jaw. Restriction of the jaw would have occurred by both muscles contracting simultaneously and pulling the jaw in either direction, possibly stabilizing the joint against disarticulation during powerful caudal bites.

FIGURE 8.6. *Heterodontosaurus* skull exhibiting mPTV.

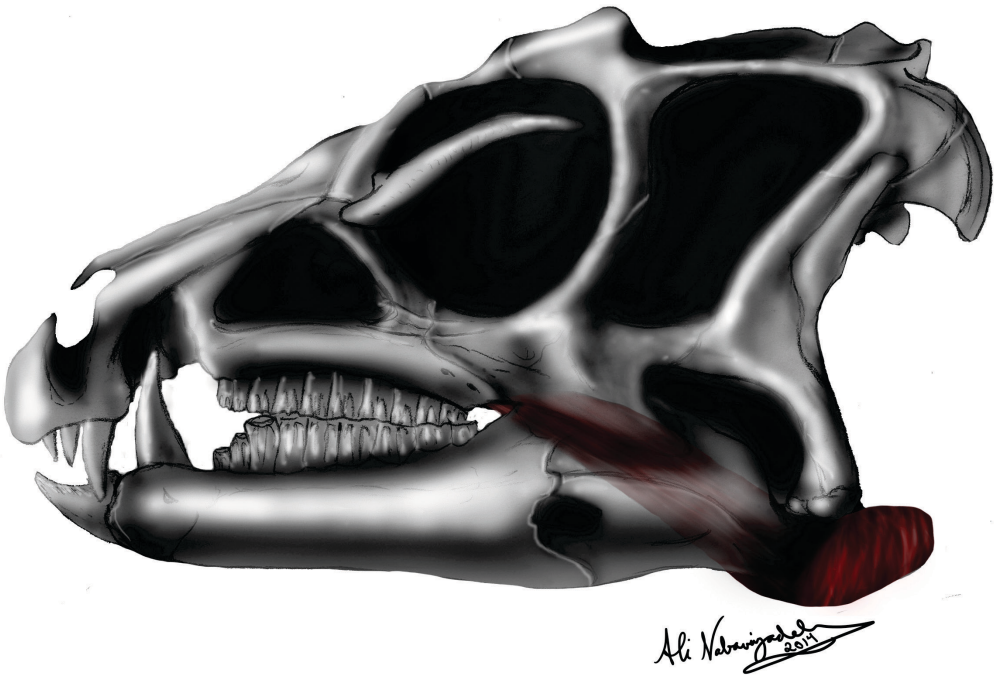

LEVER ARM ANALYSES

Relative Bite Forces (RBFs)

A number of previous studies have addressed cranial musculoskeletal function in terms of RBFs (Ostrom, 1964; 1966; Tanoue et al., 2009; Mallon and Anderson, *in press*). As indicated above, ornithischians have considerable diversity in jaw structure, especially among subclades, but also among genera within a given subclade. These morphologies

greatly influence mechanical advantage of the jaw at occlusion. Examples of morphologies influencing mechanical advantage consist of, but are not limited to: a ventrally offset craniomandibular joint relative to the level of the tooth row, a dorsally-heightened coronoid process or eminence, a tooth row displaced caudally along the jaw, and a more caudal angle of m. adductor mandibulae externus. Any combination of these morphologies has a major impact on how well a given jaw apparatus performs mechanically.

In this study, relative muscle forces within ornithischian subclades, as well as among these clades, were calculated using 2D lever arm methods. Such lever arm mechanics independently estimate relative adductor muscle force for one side of the mandible, focusing on the effect of jaw shape and muscle angle difference on bite forces throughout the jaw. It should also be emphasized that, since there are no data of actual muscle cross-sectional area in the fossil record, these results are based on a consistent muscle pull unit of 1 throughout all genera, making this a shape-based study only and discounting the effect of size. As expected, relative bite force is greatest at bite points nearest the jaw joint, or fulcrum, in all genera. The farther the bite point is from the fulcrum, the longer the output lever becomes relative to the input lever length, which is the moment arm perpendicular to the muscle vector. Major instances of overlap occur, however, in the bite point positions in which there was a greater mechanical advantage.

FIGURE 8.7. RBF value averages for each subclade across the tooth row.

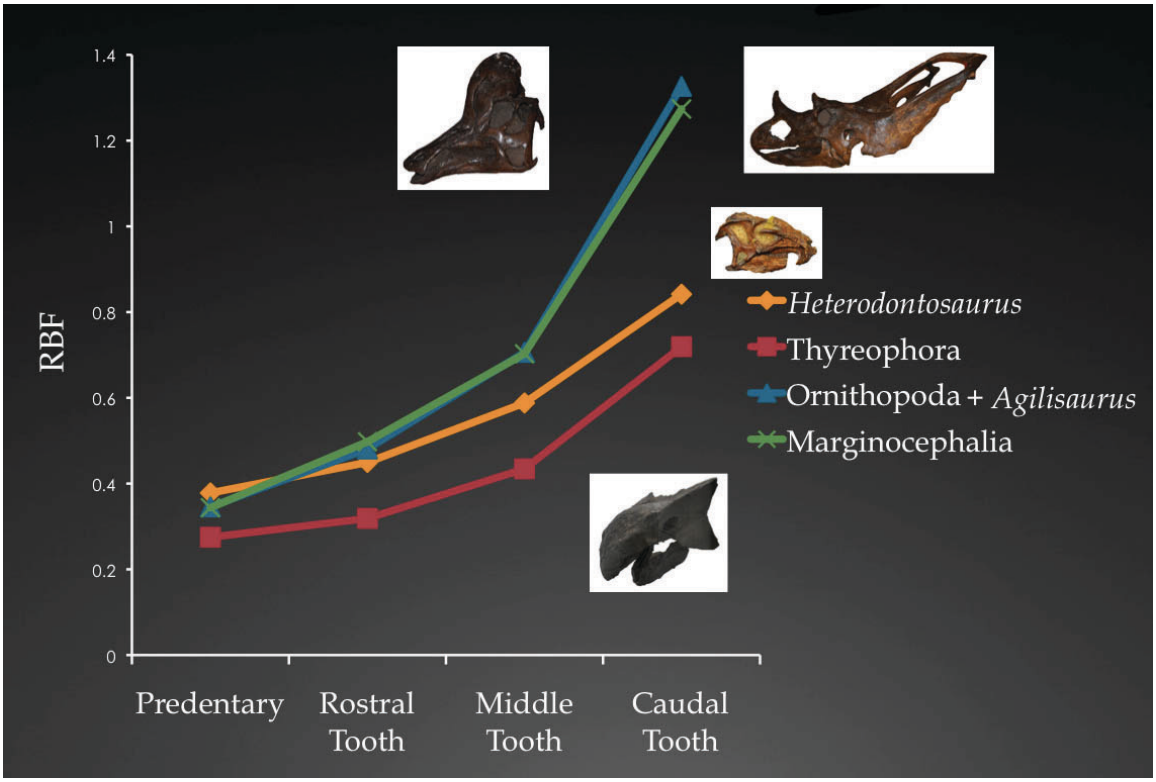

All taxa in this study showed the expected incremental trend from lower RBFs at the predentary to a much higher RBF at the caudal tooth (Fig. 8.7). As indicated in Chapters 5-7, notable trends are seen in increased mechanical advantage within each major clade (i.e., Thyreophora, Ornithopoda, and Marginocephalia) (Fig. 8.8). Thyreophorans, altogether, had much lower RBF values across the tooth row compared to other groups. Thyreophora and Ornithopoda are significantly different in terms or RBF ($p = 0.001$) as well are Thyreophora and Marginocephalia ($p < 0.001$), with Thyreophora clearly showing lower RBF values than both other groups.

The trends within Thyreophora are interesting in themselves. Basal thyreophorans, stegosaurs, and ankylosaurs do not show significant differences from each other in terms

of different RBF values. Within each of these clades, however, taxa show much more notable differences in RBF values. See Chapter 5 for a more in-depth examination of these trends.

The more interesting evolutionary trend, however, lies in the relationship between Ornithopoda and Marginocephalia. At a broad scale, Ornithopoda and Marginocephalia, sister clades that, together, form the clade known as Cerapoda, show no significant difference in RBF values throughout the tooth row ($p = 0.082$). When focusing on a smaller scale, looking at only the basal members of each clade, basal ornithopods and basal marginocephalians show no significant difference either ($p = 0.441$). The same also holds true for the derived members of each clade, with hadrosaurids (derived ornithopods) and ceratopsids (derived marginocephalians) showing no significant difference in RBF values relative to one another ($p = 0.085$). However, as was noted in Chapters 6 and 7, a significant difference is seen in RBF values between hadrosaurids and basal ornithopods (+ *Dryosaurus* and *Camptosaurus*; $p < 0.001$) as well as between hadrosaurids and non-hadrosaurid iguanodontians ($p = 0.001$). This is also true within Marginocephalia, with more basal marginocephalians and the derived ceratopsids having significantly different RBF values across the tooth row. Since groups within both Ornithopoda and Marginocephalia show significant differences (see Chapter 6 and 7), and since hadrosaurids and ceratopsids show no significant difference in RBF values (a result also seen in Mallon and Anderson [*in press*]), an obvious phylogenetic signal in convergent increased mechanical advantage exists in bite forces of both hadrosaurids and ceratopsids. See Chapters 6 and 7 for a more in-depth examination of evolutionary trends in RBFs within these subclades.

FIGURE 8.8. Phylogenetic mapping of RBFs in taxa across Ornithischia as a whole, comparing predentary and caudal tooth RBF values.

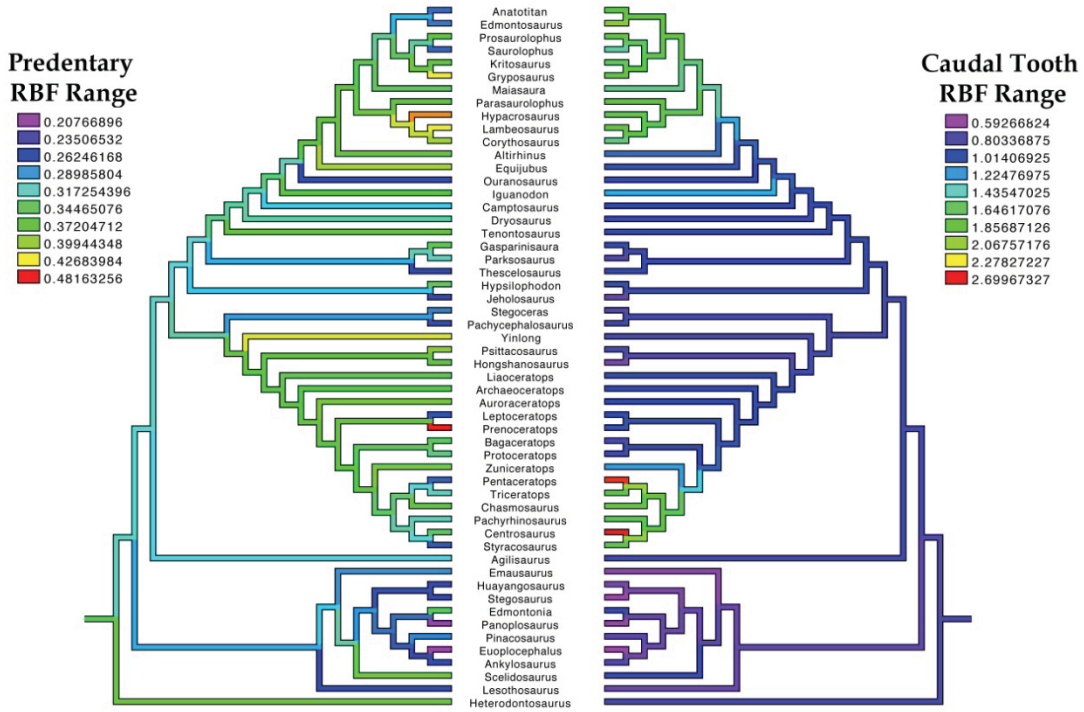

The most obvious explanation for this convergent increase in mean mechanical advantage in hadrosaurids and ceratopsids is exaggerated increase in RBF value at the caudal-most tooth in all members of these clades. This extreme caudal increase of bite force in both hadrosaurids and ceratopsids is, as noted in Chapter 2, due to a transition from a normally third class lever, with the resistant bite point placed rostral to the input adductor force, to a second class lever, with the resistant bite point placed caudal to the input adductor force (Ostrom, 1964; 1966). This transition is due to the fact that hadrosaurids and ceratopsids have both a caudal displacement of the tooth row itself and a tooth row that extends even farther caudally medial to the coronoid process, where the

main mAME is inserted, creating a much shorter output lever arm thereby increasing the RBF value.

It is important to note, however, that, although increased mechanical advantage in both hadrosaurids and ceratopsids is convergent, this convergence is achieved in slightly different ways as well, namely differences in orientation of the adductor muscle angle. Within Ornithopoda, adductor vector orientation significantly increases in time (in successively derived genera) in many cases ($p = 0.048$) whereas among ceratopsians, adductor angle significantly decreases in most cases ($p = 0.001$). This difference in muscle vector orientations shows that a culmination of various jaw morphologies lead to convergently increased mechanical advantage in all of these taxa, with a different combination of characters for hadrosaurids and ceratopsids.

Perturbation Analyses

Perturbation analyses (Otten, 1983; 1985) constructing hypothetical jaw morphologies with coronoid processes removed as well as the jaw joint raised to the level of the tooth row were also performed to explore the effect of these jaw morphologies on the mandibular mechanical advantages for each taxon. In all taxa, both having a coronoid process and the lowered jaw joint increase moment arm length and therefore increase the mechanical advantage of the jaw apparatus.

When examining results in Chapters 4-7, in more basal ornithischian taxa, lowering the jaw joint increased mechanical advantage to a higher degree than the presence of a coronoid eminence. However, throughout the evolutionary transition to derived genera within each subclade, the presence of a more prominent coronoid process

was far more influential in increasing mechanical advantage than lowering the jaw joint, a trend unseen in previous studies (Fig. 8.9). The convergent acquisition of a much more heightened coronoid process in hadrosaurids and ceratopsids clearly influence increased mechanical advantage more than the lowering of the articular jaw joint. In this context, one possible reason for the evolution of a coronoid process is that perhaps the jaw joint is already as low as it can be lowered and still be useful in chewing. Therefore, to increase RBF for larger and tougher foods, the coronoid process is raised to lengthen the moment arm even farther for greater mechanical advantage. These analyses elucidate overall evolutionary trends in mandibular mechanical advantages across ornithischian taxa and show that these dinosaurs evolved more complex feeding apparatuses within different clades in morphologically convergent ways. See Chapters 4-7 for more in-depth examination of perturbation analyses of hypothetical jaw morphologies within each clade.

FIGURE 8.9. Results of perturbation analyses showing whether the mechanical advantage of RBF in each taxon is more dependent on a lowered articular or a coronoid process (subclades from top to bottom: Heterodontosauridae, Thyreophora, Ornithopoda, Marginocephalia).

Lowered Articular	Coronoid Eminence / Process
Heterodontosaurus (.169)	NONE
Ankylosaurus, Edmontonia, Emausaurus, Euoplocephalus, Huayangosaurus, Lesothosaurus, Panoplosaurus, Pinacosaurus, Scelidosaurus, Stegosaurus	NONE
*(Agilisaurus), **Altirhinus**, Camptosaurus, Equijubus, Gasparinisaura, Dryosaurus, Hypsilophodon, Jeholosaurus, **Iguanodon**, Ouranosaurus, Parksosaurus, Tenontosaurus*	*Anatotitan, Corythosaurus, Edmontosaurus, Gryposaurus, Hypacrosaurus, Kritosaurus, Lambeosaurus, Maisaura, Parasaurolophus, Prosaurolophus, Saurolophus, **Thescelosaurus***
*Auroraceratops, Hongshanosaurus, Pachycephalosaurus, Stegoceras, **Zuniceratops***	*Archaeoceratops, Bagaceratops, Centrosaurus, Chasmosaurus, Leptoceratops, Liaoceratops, Pachyrhinosaurus, Pentaceratops, Prenoceratops, Protoceratops, Psittacosaurus, Styracosaurus, Triceratops, **Yinlong***

PALEOECOLOGICAL SIGNIFICANCE AND CONCLUSIONS

Evolutionary trends in ornithischian jaw apparatuses were influenced by both phylogeny and environment. In many respects, ornithischian jaws and those of extant mammalian herbivores show similarities in morphological adaptations to environmental conditions of feeding. Various jaw morphologies are important for specific modes of feeding or for processing certain plant material. All megaherbivores, whether dinosaurian or mammalian, either retain primitive morphology of or modify the mandibular symphysis to either allow or restrict movements at this junction or even allow or resist

bite forces to transfer through this junction. Megaherbivores also tend to evolve a coronoid process for jaw muscle insertion used in elevation of the jaw. Positioning of the craniomandibular joint offset from the level of the tooth row, whether higher than the tooth row in extant mammalian megaherbivores (Smith and Savage, 1959) or lower than the tooth row in most ornithischian dinosaurs (Weishampel, 2004) and sauropodomorphs (Galton, 1985), creates occlusion in which all teeth occlude simultaneously (Smith and Savage, 1959). This would only happen, however, if the distance between the joint and the upper tooth row is equal to the distance between the joint and the lower tooth row (Greaves, 1980).

It should be noted, however, that exceptions do exist, such as the scissor-like tooth occlusion in the heterodontosaurid *Tianyulong* (Zheng et al., 2009). Basal ornithischians, such as heterodontosaurids, basal thyreophorans, and basal cerapodans such as *Agilisaurus* (ZDM 6011), have such variable dentition that the possibility of omnivory should not be precluded as possible lifestyles for these animals. *Agilisaurus*, for instance, has premaxillary teeth that are pointed and caudally recurved, making it suited for capture of small prey. Heterodontosaurids have a large caniniform tooth that could signal an omnivorous lifestyle as well, although their diet was likely primarily vegetation given the flat occlusal surface of their more caudal dentition. Still, a transition from omnivory within basal Ornithischia needs to be explored in greater detail to understand fully the significance of the complex derived dentition adapted for processing plant material in hadrosaurids and ceratopsids.

Cranial and snout shape played a large role in determining ornithischian feeding strategies and food preferences. As stated above, a wider, more robust snout and skull, as

seen in ankylosaurids and hadrosaurids, signal a much more generalized browsing feeding behavior whereas a narrower snout tip, as seen in basal ornithischians, stegosaurs, nodosaurids, and ceratopsids, signals a relatively more selective feeding behavior. This is not to say, however, that all generalized and all selective feeders were eating the same plant material. Plants possess many defenses against herbivorous feeding, whether they are extrinsic structural defenses or intrinsic (such as silica phytoliths, toxins, etc.), and are variably stiff and tough in their material properties (Weishampel 1984; Lucas, 2004; Mallon and Anderson, *in press*). The stiffer or tougher a plant may be, the better suited a herbivore needs to become to orally process it, whether it be better mechanical advantage and higher bite force with large tooth batteries, as in hadrosaurids and ceratopsids, or the possession of a modified tooth row, as in ankylosaurs, for instance, with curved, sinusoidal tooth rows. Some basal ornithischians, especially some basal thyreophorans and ceratopsians, possess a medially-curved tooth row, which is unseen in modern herbivores. Tanoue et al. (2009) suggested, with lever arm mechanics analyses, that these curved tooth rows were meant to increase the mechanical advantage at a more medially placed bite point in basal ceratopsian taxa, since it makes for a slightly shorter output lever arm length. This increased mechanical advantage was likely tied with the ability to maneuver the mandibular corpus around its long axis and move the jaw at the predentary-dentary joint on each side of the jaw independently to allow all teeth to occlude a given point in the chewing stroke. This motion creates considerable freedom of mobility in the entire mandible and indicates more complex chewing mechanisms involved in feeding mechanics rather than solely mechanical advantage.

Many morphological aspects of the predentary-dentary junction as well as

postdentary elements and dental microwear support the presence of independent kinesis of the paired dentary bones relative to the predentary in many ornithischians. The predentary served as a point for simultaneous mediolateral rotation of the paired dentaries, with the adductor musculature pulling the dentaries correspondingly (Weishampel, 1984; Crompton and Attridge, 1986; Rybczynski and Vickaryous, 2001; Bell et al., 2009; Norman et al., 2011; Cuthbertson et al., 2012; Sereno, 2012; Ösi et al., 2014; Nabavizadeh, *in press*). Various other mandibular features also suggest a rotating surface and range of movement with membranous or ligamentous material at the predentary-dentary junction, thus allowing medial rotation of both dentary bones. Muscular or synovial mobility of the predentary-dentary joint are also possible alternatives to a membranous or ligamentous attachment, but this requires further testing. Independent rotation of the mandibular corpora would maneuver the vegetation into the oral cavity independently on both sides (i.e., work both sides of the jaw simultaneously rather than one side at a time as in most herbivores). Flexible predentary-dentary articulations are most prevalent within Ornithopoda, with hadrosaurids showing the most potential for mobility at this joint. Thyreophorans also possess a mobile predentary bone, although not to the extent of hadrosaurids. Stegosaur predentaries have bifurcating processes similar to basal ornithopods and *Lesothosaurus* (Galton and Upchurch, 2004). Ankylosaur predentaries possess the most indeterminate articulation of all, with their predentaries shaped roughly like a cylindrical body with a flattened surface on the caudoventral side that merely rested on the dentaries (Rybczynski and Vickaryous, 2001; Vickaryous et al., 2004). More derived ceratopsians, with parrot-like beaks, seem to be the only case where the predentary locks into the dentaries by means of a slit in the predentary (Dodson et al.,

2004); however, phylogenetically this is a derived feature within Ornithischia. Due to the extensiveness of loose predentary-dentary articulation in a large variety of ornithischian dinosaurs, it can be inferred that the predentary evolved as a key element in feeding mechanisms of ornithischians and could give insight into paleoecology throughout ornithischian evolution.

Along with a mobile predentary-dentary joint and curved tooth rows, the possession of an elevated coronoid process and lowered articular jaw joint has a large effect on jaw mechanisms in ornithischian dinosaurs, mainly in terms of increased mechanical advantage. A lowered articular jaw joint and heightened coronoid process can increase moment arm length and, in many cases, a coronoid process can also direct adductor musculature more caudally, all are beneficial to mechanical advantage. These are trends seen in all ornithischians in general, but are especially accentuated in hadrosaurids and ceratopsids, as mentioned above.

The effect of position and orientation of jaw musculature is also key in understanding ornithischian jaw structure and mechanics and must be taken into account when examining the jaw apparatus as a whole. Although musculature is not preserved in the fossil record, muscle scars and the Extant Phylogenetic Bracketing method have given much insight into the diversity of ornithischian jaw mechanisms. A more caudal origin of adductor musculature (mainly the mAME complex as well as mAMP) suggests a more caudal chewing stroke, which is many times corroborated with dental microwear studies, as suggested by Varriale (2011). Pterygoideus musculature was large and sometimes likely replaced the mAME muscle complex in terms of bite force exerted while feeding, given that some ornithischian adductor chambers were reduced in size due

to caudal displacement of the orbit relative to the skull length (as seen in many lambeosaurines, such as *Parasaurolophus*, and even some hadrosaurines, such as *Edmontosaurus*). Further analysis of adductor chamber size, however, is needed to explore this in further detail.

It is important to note, also, that larger skulls and adductor chambers correlate with larger jaw musculature and, in turn, produce larger actual bite force (Kiltie, 1982; Herrel et al., 2001, 2002; Meers, 2002; van der Meij and Bout, 2008; Verwaijen et al., 2002; Erickson et al., 2012). An example of differences in muscle size is seen in ceratopsids versus hadrosaurids. Although ceratopsids and hadrosaurids share results in RBF values and mechanical advantage, it is safe to assume that ceratopsids produced a higher actual bite force than hadrosaurids (Mallon and Anderson, *in press*), which means that contemporaneous taxa likely ate different types of angiosperms and conifers accordingly. This was not necessarily a problem, however, because of the differences in feeding height affecting what foods each clade could or could not eat (Mallon and Anderson, 2013).

The combination of all of the aforementioned adaptations explains the plethora of jaw mechanisms seen throughout Ornithischia. Herbivory in the Mesozoic was dominated by a majority of dinosaur species (citation), large and small, and the impact that herbivores such as ornithischians had on the environment was tremendous. Investigation of the array of jaw mechanisms in ornithischian dinosaurs continues and will benefit from quantitative analyses of three-dimensional skull modeling, multi-body dynamics, and finite element analyses (among others). Furthermore, these analyses need to be focused in a functional as well as a phylogenetic context, whereby multiple taxa of

a given subclade are tested to examine the evolutionary trends in feeding styles. Many of the characters influencing jaw mechanics mentioned in this study are in need of incorporation into phylogenetic analyses so as to create a much clearer understanding of their evolutionary patterns. It is important to examine each taxon individually to truly explore evolutionary patterns of jaw morphologies to help elucidate the significance of the diversity in ornithischian jaw evolution and, ultimately, its implications on the 140-million-year success of the clade.

Bibliography

Abramoff, M. D., P. J. Magalhaes, and S. J. Ram. 2004. Image processing with ImageJ. Biophotonics International 11(7):36–42.

Adriaens D, and W. Verraes. 1998. Ontogeny of the osteocranium in the African catfish, *Clarias gariepinus* (Burchell, 1822) (Siluriformes: Clariidae): ossification sequence as a response to functional demands. Journal of Morphology 235:183–237.

Bakker, R. T. 1986. The dinosaur heresies: new theories unlocking the mystery of the dinosaurs and their extinction. New York: Morrow.

Barrett, P. M. 1998. Herbivory in the non-avian Dinosauria. Ph.D. dissertation, University of Cambridge. 308 pp.

Barrett, P. M. 2000. Prosauropod dinosaurs and iguanas: Speculations on the diets of extinct reptiles. In: Sues, H.-D. (ed.). Evolution of Herbivory in Terrestrial Vertebrates: Perspectives from the Fossil Record. Cambridge University Press, Cambridge. Cambridge. Pp. 42–78.

Barrett, P. M. 2001. Tooth wear and possible jaw action of *Scelidosaurus harrisonii* Owen and a review of feeding mechanisms in other thyreophoran dinosaurs. In:

K. Carpenter (ed.), The Armored Dinosaurs. Bloomington: Indiana University Press. Pp. 25 – 52.

Barrett, P. M. 2005. The diet of ostrich dinosaurs (Theropoda: Ornithomimosauria). Palaeontology, 48(2):347-358.

Barrett, P. M., R. J. Butler, W. Xiao-Lin, and X. Xing. 2009. Cranial anatomy of the iguanodontoid ornithopod *Jinzhousaurus yangi* from the Lower Cretaceous Yixian Formation of China. Acta Palaeontologica Polonica, 54(1):35-48.

Barrett, P. M., and P. Upchurch. 1994. Feeding mechanisms of *Diplodocus.*In: Lockley, M. G., Santos, V. F. dos, Meyer, C. A., and Hunt, A. (eds.). Aspects of Sauropod Paleobiology. Gaia 10:195–204.

Bates, K. T., and P. L. Falkingham. "Estimating maximum bite performance in *Tyrannosaurus rex* using multi-body dynamics." *Biology letters* 8.4 (2012):660-664.

Baumel, J. J., and L. M. Witmer. 1993. Osteologia. In: Baumel, J. J., editor. Handbook of Avian Anatomy: Nomina Anatomica Avium. Cambridge: Publications of the Nuttall Ornithological Club. Pp. 45–132.

Bell, P. B., E. Snively, and L. Shychoski. 2009. A comparison of the jaw mechanics in

hadrosaurid and ceratopsid dinosaurs using finite element analysis. Anatomical Record 292:1338–1351.

Benton, M. J. 1985. Classification and phylogeny of the diapsid reptiles. Zoological Journal of Linnean Society London 84:97–164.

Berman, D. S., and J. S. McIntosh. 1986. Description of the lower jaw of *Stegosaurus* (Reptilia, Ornithischia). Annals of Carnegie Museum, 55:29–40.

Bock, W. J. 1964. Kinetics of the avian skull. Journal of Morphology, 114(1):1-41.

Bonaparte, J. F. 1976. *Pisanosaurus mertii* Casamiquela and the origin of the Ornithischia. Journal of Paleontology 50:808–820.

Bout, R. G., and G. A. Zweers. 2001. The role of cranial kinesis in birds. Comparative Biochemistry and Physiology Part A: Molecular & Integrative Physiology, 131(1):197-205.

Boyd, C. A., C. M. Brown, R. D. Scheetz, and J. A. Clarke. 2009. Taxonomic revision of the basal neornithischian taxa *Thescelosaurus* and *Bugenasaura*. Journal of Vertebrate Paleontology 29(3):758-770.

Busbey, A. B. 1980. Form and function of the feeding apparatus of *Alligator mississippiensis*. Journal of Morphology 202(1):99-127.

Butler, R. J., J. Liyong, C. Jun, and P. Godefroit, P. 2011. The postcranial osteology and phylogenetic position of the small ornithischian dinosaur *Changchunsaurus parvus* from the Quantou Formation (Cretaceous: Aptian–Cenomanian) of Jilin Province, north-eastern China. Palaeontology, 54(3):667-683.

Butler, R. J., L. B. Porro, P. M. Galton, and L. M. Chiappe. 2012. Anatomy and cranial functional morphology of the small-bodied dinosaur *Fruitadens haagarorum* from the Upper Jurassic of the USA. PloS One, *7*(4):e31556.

Butler, R. J., P. Upchurch, and D. B. Norman. 2008. The phylogeny of the ornithischian dinosaurs. Journal of Systematic Palaeontology 6:1–40.

Calvo, J. 1994. Jaw mechanics in sauropod dinosaurs. In: Lockley, M. G., Santos, V. F. dos, Meyer, C. A., and Hunt, A. (eds.). Aspects of Sauropod Paleobiology. Gaia 10:183–194.

Carpenter, K. 2001. Skull of the polacanthid ankylosaur *Hylaeosaurus armatus* Mantell, 1833, from the Lower Cretaceous of England. In: Carpenter, K. (ed.). The Armored Dinosaurs. Indiana University Press, Bloomington. Pp. 169–172.

Carpenter, K., J. I. Kirkland, D. Burge, and J. Bird. 2001. Disarticulated skull of a new primitive ankylosaurid from the Lower Cretaceous of eastern Utah. In: Carpenter, K. (ed.). The Armored Dinosaurs. Indiana University Press, Bloomington. Pp. 211–238.

Colbert, E. H. 1981. A primitive ornithischian dinosaur from the Kayenta Formation of Arizona Bulletin of the Museum of Northern Arizona 53:1–61.

Coombs, W. P., Jr. 1971. The Ankylosauria. Ph.D. dissertation, Columbia University, New York. 487 pp.

Coombs, W. P. 1978. The families of the ornithischian dinosaur Order Ankylosauria. Palaeontology 21:143–170.

Coombs, W. P., Jr., and T. Maryańska. 1990. Ankylosauria. In: Weishampel, D. B., Dodson, P., and Osmólska, H. (eds.). The Dinosauria. University of California Press, Berkeley. Pp. 456–483.

Chinnery, B. J., and J. R. Horner. 2007. A new basal neoceratopsian dinosaur linking North America and Asian taxa. Journal of Vertebrate Paleontology 27:625-641.

Cooper, M. R. 1981. The prosauropod dinosaur *Massospondylus carinatus* Owen from Zimbabwe: its biology, mode of life and phylogenetic significance. Occasional

Papers of the National Museums and Monuments, series b, v. 6, part 10:689-840.

Cooper, M. R. 1985. A revision of the ornithischian dinosaur *Kangnasaurus coetzeei* Haughton, with a classification of the Ornithischia. Annals of the South African Museum 95:281–317.

Crompton, A. W., and J. Attridge. 1986. Masticatory apparatus of the larger herbivores during Late Triassic and Early Jurassic times; pp. 223–236 in K. Padian (ed.), The Beginning of the Age of Dinosaurs: Faunal Change Across the Triassic-Jurassic Boundary. Cambridge University Press, London, England.

Crompton, A. W., T. Owerkowicz, and J. Skinner. 2010. Masticatory motor pattern in koala (*Phascolarctos cinereus*): a comparison of jaw movements in marsupial and placental herbivores. Journal of Experimental Zoology 313A:564–578.

Cuthbertson, R. S., A. Tirabasso, N. Rybczynski, and R. B. Holmes. 2012. Kinetic limitations of intracranial joints in *Brachylophosaurus canadensis* and *Edmontosaurus regalis* (Dinosauria: Hadrosauridae), and their implications for the chewing mechanics of hadrosaurids. The Anatomical Record 295:968-979.

Czerkas, S. 1999. The beaked jaw of stegosaurs and their implications for other ornithischians. In: Gillette, D. D. (ed.). Vertebrate Paleontology in Utah. Miscellaneous Publications of Utah Geological Survey 99–1:143–150.

Davis, D. D. 1955. Masticatory apparatus in the spectacled bear *Tremarctos ornatus*. Fieldiana: Zoology 37:25-46.

De Beer, G. R. 1937. The development of the vertebrate skull. Oxford: Oxford University Press.

DeMar, R., and H. R. Barghusen. 1972. Mechanics and the evolution of the synapsid jaw. Evolution 26:622-637.

Dodson, Peter. 1996. The horned dinosaurs: A natural history. Princeton University Press.

Dodson, P., C. A. Forster, and S. D. Sampson. 2004. Ceratopsidae. In: D. B. Weishampel, P. Dodson, and H. Osmólska (eds.), The Dinosauria, Second edition. University of California Press, Berkeley, California. Pp. 494–513.

Dong, Z. 2002. A new armored dinosaur (Ankylosauria) from Beipao Basin, Liaoning Province, Northeastern China. Vert. PalAs. 40:276–285.

Dong Z., X. Li, S. Zhou, and Y. Zhang. 1977. [On the stegosaurian remains from Zigong (Tzekung), Szechuan Province]. Vert. PalAs. 15:307–312. (In Chinese with English summary.)

Dong Z., S. Zhou, and Y. Zhang. 1983. [The dinosaurian remains from Sichuan Basin, China]. Palaeontol. Sinica, n.s. C, 23:1–145. (In Chinese with English summary.)

Eaton, T. H., Jr. 1960. A new armored dinosaur from the Cretaceous of Kansas. Univ. Kansas Paleontological Contributions 25:1–24.

Erickson, G. M., P. M. Gignac, S. J. Steppan, A. K. Lappin, K. A. Vliet, J. D. Brueggen, B. D. Inouye, D. Kledzik, and G. J. Webb. 2012. Insights into the ecology and evolutionary success of crocodilians revealed through bite-force and tooth-pressure experimentation. PloS one, 7(3):e31781.

Erickson, G. M., B.A. Krick, M. Hamilton, G. R. Bourne, M. A. Norell, E. Lilleodden, and W. G. Sawyer. 2012. Complex dental structure and wear biomechanics in hadrosaurid dinosaurs. Science, 338(6103):98-101.

Erickson, G. M., S. D. Van Kirk, J. Su, M. E. Levenston, W. E. Caler, and D. R. Carter. 1996. Bite-force estimation for *Tyrannosaurus rex* from tooth-marked bones. Nature, 382(6593):706-708.

Evans, D. C. 2010. Cranial anatomy and systematics of *Hypacrosaurus altispinus*, and a comparative analysis of skull growth in lambeosaurine hadrosaurids (Dinosauria: Ornithischia). Zoological Journal of the Linnean Society 159:398-434.

Evans, D. C., R. K. Schott, D. W. Larson, C. M. Brown, and M. J. Ryan. 2013. The oldest North American pachycephalosaurid and the hidden diversity of small-bodied ornithischian dinosaurs. Nature communications, 4:1828.

Fairman, J., A. Nabavizadeh, and D. Weishampel. 2013. Early sauropodomorph jaw apparatus anatomy: a comparative study with iguanian lizards. Society of Vertebrate Paleontology Program and Abstracts Book:124A.

Ferigolo, J., and M. Langer. 2007. A Late Triassic dinosauriform from south Brazil and the origin of the ornithischian predentary bone. Historical Biology 19:23-33.

Fiorillo, A. R. 1998. Dental microwear patterns of the sauropod dinosaurs *Camarasaurus* and *Diplodocus:* Evidence for resource partitioning in the Late Jurassic of North America. Historical Biology 13:1–16.

Forster, C. A.. 1996. New information on the skull of *Triceratops.* Journal of Vertebrate Paleontology 16:246–258.

Frazzetta, T. H. 1962. A functional consideration of cranial kinesis in lizards. Journal of Morphology, 111(3):287-319.

Galton, P. M. 1973. The cheeks of ornithischian dinosaurs. Lethaia 6:67–89.

Galton, P. M. 1974. The ornithischian dinosaur *Hypsilophodon* from the Wealdon of the Isle of Wight. Bulletin of the British Museum (Natural History) Geology 25:1–152.

Galton, P. M. 1978. Fabrosauridae, the basal family of ornithischian dinosaurs (Reptilia: Ornithopoda). Paläontology Z. 52:138–159.

Galton, P. M. 1983. The cranial anatomy of *Dryosaurus*, a hypsilophodontid dinosaur from the upper Jurassic of North America and East Africa, with a review of hypsilophodontids from the Upper Jurassic of North America. Geologica et Palaeontologica 17:207-243.

Galton, P. M. 1985. Diet of prosauropod dinosaurs from the late Triassic and early Jurassic. Lethaia, v. 18:105-123.

Galton, P. M. 1986. Herbivorous adaptations of Late Triassic and Early Jurassic dinosaurs. In: The Beginning of the Age of Dinosaurs, Padian, Kevin, ed. Cambridge University Press: pp. 205-221.

Galton, P. M., and W. A. Coombs, Jr. 1981. *Paranthodon africanus* (Broom), a stegosaurian dinosaur from the Lower Cretaceous of South Africa. Géobios 14:299–309.

Galton, P. M., and P. Upchurch. 2004. Stegosauria. In: D. B. Weishampel, P. Dodson, and H. Osmólska (eds.), The Dinosauria, Second edition. University of California Press, Berkeley, California. Pp. 343–362.

Gilmore, C. W. 1914. Osteology of the armored dinosaurs in the United States National Museum, with special reference to the genus *Stegosaurus.* Bulletin of the U.S. National Museum 89:1–136.

Gilmore, C. W. 1924. On *Troodon validus,* an ornithopodous dinosaur from the Belly River Cretaceous of Alberta, Canada. Bulletin of the Department of Geology University of Alberta 1:1–143.

Goodwin, M. B., and J. R. Horner. 2004. Cranial histology of pachycephalosaurs (Ornithischia: Marginocephalia) reveals transitory structures inconsistent with head-butting behavior. Paleobiology 30(2):253-267.

Greaves, W. S. 1978. The jaw lever system in ungulates: a new model. Journal of Zoology in London 184:271–285.

Greaves, W. S. 1980. The mammalian jaw mechanism – the high glenoid cavity. The American Naturalist 116(3):432-440.

Grande, L., and W. E. Bemis. 1998. A comprehensive phylogenetic study of amiid fishes (Amiidae) based on comparative skeletal anatomy. An empirical search for interconnected patterns of natural history. Society of Vertebrate Paleontology Memoir 4:1–690.

Haas, G. 1955. The jaw musculature in Protoceratops and in other ceratopsians. American Museum Novitates 1729:1-24.

Haas, G. 1963. A proposed reconstruction of the jaw musculature of *Diplodocus.* Annals of the Carnegie Museum 36:139–157.

Haas, G. 1969. On the jaw muscles of ankylosaurs. American Museum Novitates 2399:1-11.

Hatcher, J. B., O. C. Marsh, and R. S. Lull. 1907. The Ceratopsia. U.S. Geological Survey Monograph 49:1–300.

Haubold, H. 1990. Ein neuer Dinosaurier (Ornithischia, Thyreophora) aus dem unteren Jura des nördlichen Mitteleuropa. Rev. Paléobiol. 9:149–177.

Hennig, E. 1935. Ein Dentale von *Kentrurosaurus aethiopicus* Hennig [A dentary of *Kentrurosaurus aethiopcius* Hennig]. Palaeontographica. Supplement 7 Part II (in German):311–312.

Herrel, A., P. Aerts, and F. De Vree. 2000. Cranial kinesis in geckoes: functional implications. The Journal of Experimental Biology 203:1415-1423.

Herrel, A., E. de Grauw, and J. A. Lemos-Espinal. 2001. Head shape and bite performance in xenosaurid lizards. Journal of Experimental Zoology 290:101–107.

Herrel, A., J. C. O'Reilly, and A. M. Richmond. 2002. Evolution of bite performance in turtles. Journal of Evolutionary Biology 15:1083–1094.

Hoese, W. J., and M. W. Westneat. 1996. Biomechanics of cranial kinesis in birds: Testing linkage models in the white-throated sparrow (*Zonotrichia albicollis*). Journal of Morphology, 227(3):305-320.

Hofer, H. 1950 Zur Morphologie der Kiefermuskulatur der VoÅNgel. Zoologische Jahrbücher, Abteilung für Anatomie und Ontogenie der Tiere 70:427–556.

Hogue, A. S., and M. J. Ravosa. 2001. Transverse masticatory movements, occlusal orientation, and symphyseal fusion in selenodont artiodactyls. Journal of Morphology 249:221–241.

Holland, W. 1924. The skull of *Diplodocus.* Mem. Carnegie Mus. 9:379–403.

Holliday, C. M. 2009. New insights into dinosaur jaw muscle anatomy. The Anatomical Record 292:1246-1265.

Holliday, C. M., and L. M. Witmer. 2007. Archosaur adductor chamber evolution: integration of musculoskeletal and topological criteria in jaw muscle homology. Journal of Morphology 268:457-484.

Holliday, C. M., and L. M. Witmer. 2008. Cranial kinesis in dinosaurs: intracranial joints, protractor muscles, and their significance for cranial evolution and function in diapsids. Journal of Vertebrate Paleontology 28:1073–1088.

Holliday, C. M., N. M. Gardner, S. M. Paesani, M. Douthitt, and J. L. Ratliff. 2010. Microanatomy of the mandibular symphysis in lizards: patterns in fiber orientation and Meckel's Cartilage and their significance in cranial evolution. The Anatomical Record 293:1350-1359.

Holtz Jr., T. R., D. L. Brinkman, and C. L. Chandler. 1998. Denticle morphometrics and a possibly omnivorous feeding habit for the theropod dinosaur *Troodon*. Gaia, 15:159-166.

Hopson, J. A. 1980. Tooth function and replacement in early Mesozoic ornithischian dinosaurs: implications for aestivation. Lethaia 13:93–105.

Horner, J. R. 1992. Cranial morphology of *Prosaurolophus* (Ornithischia: Hadrosauridae) with descriptions of two new hadrosaurid species and an evaluation of hadrosaurid phylogenetic relationships. Museum of the Rockies Occasional Paper 2:1–119.

Horner, J. R., D. B. Weishampel, and C. A. Forster. 2004. Hadrosauridae. In: D. B. Weishampel, P. Dodson, and H. Osmólska (eds.), The Dinosauria (Second Edition). University of California Press, Berkeley, California. Pp. 438–463.

Hopson, J. A. 1950. The origin of the mammalian middle ear. American Zoologist 6:437-450.

Hou L. 1977. [A new primitive Pachycephalosauria from Anhui, China]. Vert. PalAs. 15: 198–202. (In Chinese with English summary.)

Iordansky, N. N. 1964. The jaw muscles of the crocodiles and some relating structures of the crocodilian skull. Anatomischer Anzeiger, 115:256-280.

Iordansky, N. N. 1990. Evolution of Complex Adaptations: Jaw Apparatus of the Amphibians and Reptiles. Academia Nauk CCCP, Moscow:3-310.

Iordansky, N. N. 2011. Jaw muscles of the crocodiles: structure, synonymy, and some implications on homology and functions. Russian Journal of

Herpetology, 7(1):41-50.

Ji Q., Currie, P. J., Norell, M. A., and Ji S.-A. 1998. Two feathered dinosaurs from northeastern China. Nature 393:753–761.

Jones, M. E. H., P. O'Higgins, M. J. Fagan, S. E. Evans, and N. Curtis. 2012. Shearing mechanics and the influence of a flexible symphysis during oral food processing in *Sphenodon* (Lepidosauria: Rhynchocephalia). The Anatomical Record 295:1075-1091.

Kilbourne, B., and K. Carpenter. 2005. Redescription of *Gargoyleosaurus parkpinorum*, a polacanthid ankylosaur from the Upper Jurassic of Albany County, Wyoming. Neues Jahrb Geol Palaontol Abh, 237:111-160.

Kiltie, R. A. 1982. Bite force as a basis for niche differentiation between rain forest peccaries (*Tayassu tajacu* and *T. pecari*). Biotropica 14:188–195.

Kirkland, J. I. 1998. A polacanthine ankylosaur (Ornithischia: Dinosauria) from the Early Cretaceous (Barremian) of eastern Utah. In: Lucas, S. G., Kirkland, J. I., and Estep, J. W. (eds.). Lower and Middle Cretaceous Ecosystems. New Mexico Museum Natural History Science Bulletin 14:271–281.

Klein, N., K. Remes, C. T. Gee, and P. M. Sander. (Eds.). 2011. Biology of the sauropod

dinosaurs: understanding the life of giants. Indiana University Press.

Kripp, D., von 1933. Die Kaubewegung und Lebensweise von *Edmontosaurus* spec. auf Grund der mechanisch-konstruktiven Analyse. Palaeobiologica 5:409–422.

Kubota, K., and Y. Kobayashi. 2009. Evolution of dentary diastema in iguanodontian dinosaurs. Acta Geologica Sinica-English Edition, 83(1):39-45.

Lakjer, T. 1926. Die Trigeminus-versorgte kaumuskulatur der sauropsiden. Kopenhagen: Auf Kosten der Carlsbergstiftung. 126 pp.

Lambe, L. M. 1919. Description of a new genus and species *(Panoplosaurus mirus)* of armored dinosaur from the Belly River Beds of Alberta. Transactions of the Royal Society Canada, ser. 3, 13:39–50.

Lambe, L. M. 1920. The hadrosaur *Edmontosaurus* from the Upper Cretaceous of Alberta. Canadian Geological Survey Memoir 120:1–79.

Lautenschlager, S. 2013. Cranial myology and bite force performance of *Erlikosaurus andrewsi*: A novel approach for digital muscle reconstructions. Journal of anatomy, 222(2):260-272.

Lautenschlager, S., L. M. Witmer, P. Altangerel, and E. J. Rayfield. 2013. Edentulism,

beaks, and biomechanical innovations in the evolution of theropod dinosaurs. Proceedings of the National Academy of Sciences, 110(51):20657-20662.

Lee, Y.-N. 1996. A new nodosaurid ankylosaur (Dinosauria: Ornithischia) from the Paw Paw Formation (late Albian) of Texas. Journal of Vertebrate Paleontology 16: 232–345.

Lehman, T. M. 1989. *Chasmosaurus mariscalensis,* sp. nov., a new ceratopsian dinosaur from Texas. Journal of Vertebrate Paleontology 9:137–162.

Lieberman, D. E., and A. W. Crompton. 2000. Why fuse the mandibular symphysis? A comparative analysis. American Journal of Physical Anthropology 112:517–540.

Lucas, P. W. 2004. Dental Functional Morphology: How Teeth Work. Cambridge University Press, Cambridge, UK, 355 pp.

Lull, R. S. 1908. The cranial musculature and the origin of the frill in the ceratopsian dinosaurs. American Journal of Science, ser. 4, 25: 387–399.

Lull, R. S. 1933. A revision of the Ceratopsia or horned dinosaurs. Memoirs of Peabody Museum of Natural History 3 (3):1–175.

Lull, R. S., and N. E. Wright. 1942. Hadrosaurian dinosaurs of North America.

Geological Society of America Special Paper 40:1–242.

Maidment, S. C. 2010. Stegosauria: a historical review of the body fossil record and phylogenetic relationships. Swiss Journal of Geosciences, 103(2):199-210.

Maidment, S. C. R., D. B. Norman, P. M. Barrett, and P. Upchurch. 2007. Systematics and phylogeny of Stegosauria (Dinosauria: Ornithischia). Journal of Systematic Palaeontology 6:367-407.

Makovicky, P. J., and M. A. Norell. 2006. *Yamaceratops dorngobiensis*, a new primitive ceratopsian (Dinosauria: Ornithischia) from the Cretaceous of Mongolia. American Museum Novitates:1-42.

Mallon, J. C., and J. S. Anderson. *In press*. Jaw mechanics and the evolutionary palaeoecology of the megaherbivorous dinosaurs from the Dinosaur Park Formation (Upper Campanian) of Alberta, Canada. Journal of Vertebrate Paleontology.

Mallon, J. C., and J. S. Anderson. 2013. Skull ecomorphology of megaherbivorous dinosaurs from the Dinosaur Park Formation (upper Campanian) of Alberta, Canada. PloS One 8(7): e67182. doi:10.1371/journal.pone.0067182.

Mallon, J. C., and J. S. Anderson. 2014. Implications of beak morphology for the

evolutionary palaeoecology of the megaherbivorous dinosaurs from the Dinosaur Park Formation (upper Campanian) of Alberta, Canada. Palaeogeography, Palaeoclimatology, Palaeoecology 394:29-41.

Mallon, J. C., D. C. Evans, M. J. Ryan, and J. S. Anderson. 2013. Feeding height stratification among the herbivorous dinosaurs from the Dinosaur Park Formation (upper Campanian) of Alberta, Canada. BMC Ecology 13:14.

Marsh, O. C. 1893. The skull and brain of *Claosaurus*. American Journal of Science (Series 3) 55:83–86.

Maryańska, T. 1977. Ankylosauridae (Dinosauria) from Mongolia. Palaeontol. Polonica 37:85–151.

Maryańska, T., and H. Osmólska. 1974. Pachycephalosauria, a new suborder of ornithischian dinosaurs. Palaeontologica Polonica 30:45–102.

Maryańska, T., R. E. Chapman, and D. B. Weishampel. 2004. Pachycephalosauria In: D. B. Weishampel, P. Dodson, and H. Osmólska (eds.), The Dinosauria, Second edition. University of California Press, Berkeley, California. Pp. 464–477.

Mateus, O., S. C. Maidment, and N. A. Christiansen. 2009. A new long-necked 'sauropod-mimic'stegosaur and the evolution of the plated dinosaurs. Proceedings

of the Royal Society B: Biological Sciences, 276(1663):1815-1821.

Mazzetta, G. V., Cisilino, A. P., Blanco, R. E., & Calvo, N. (2009). Cranial mechanics and functional interpretation of the horned carnivorous dinosaur *Carnotaurus sastrei*. Journal of Vertebrate Paleontology, 29(3):822-830.

McDonald, A. T. 2012. Phylogeny of basal iguanodonts: an update. PloS One. 7(5):1-5.

McDonald, A. T., E. Espilez, L. Mampel, J. I. Kirkland, and L. Alcala. 2012. An unusual new basal iguanodont (Dinosauria: Ornithopoda) from the Lower Cretaceous of Teruel, Spain. Zootaxa, 3595:61-76.

Meers, M. B. 2002. Maximum bite force and prey size of *Tyrannosaurus rex* and their relationships to the inference of feeding behaviour. Historical Biology 16:1–12.

Miles, C. A., and C. J. Miles. 2009. Skull of *Minotaurasaurus ramachandrani*, a new Cretaceous ankylosaur from the Gobi Desert. Current Science (00113891), 96(1).

Molnar, R. E. 1996. Preliminary report of a new ankylosaur from the Early Cretaceous of Queensland, Australia. In: Novas, F. E., and Molnar, R. E. (eds.). Proceedings of the Gondwanan Dinosaur Symposium. Mem. Queensland Mus. 39:653–668.

Moore, W. 1981. The mammalian skull. Biological structure and function. Cambridge

University Press, Cambridge.

Morris, W. J. 1970. Hadrosaurian dinosaur bills – morphology and function. Contributions in Science, Los Angeles County Museum of Natural History 193:1–14.

Nabavizadeh, A. *In press*. Hadrosauroid jaw mechanics and the functional significance of the predentary bone. In: The Hadrosaurs: Proceedings of the International Hadrosaur Symposium (D. Evans and D. Eberth, eds), Indiana University Press, Bloomington.

Nabavizadeh, A. 2011. Thyreophoran Jaw Mechanics and the Functional Significance of the Predentary Bone. Society of Vertebrate Paleontology Program and Abstracts Book: 164A.

Nopsca, F. B. 1900. Dinosaurierreste aus Siebenbergen. I. Schadel von *Limnosaurus transsyvanicus* nov. gen. et spec. Denkschr Akad Wiss Wien 68:555–591.

Nopcsa, F. B. 1928. Dinosaurierreste aus Siebenbürgen. IV. Die Wirbelsäule von *Rhabdodon* und *Orthomerus.* Palaeontol. Hungarica 1:273–304.

Norman, D. B. 1984. On the cranial morphology and evolution of ornithopod dinosaurs. Symposium of the Zoological Society in London 52:521–547.

Norman, D. B. 1986. On the anatomy of *Iguanodon atherfieldensis* (Ornithischia: Ornithopoda). Bulletin de L'Institut Royal des Sciences Naturelles de Belgique, Sciences de la Terre 56:281–372.

Norman, D. B. 1998. On Asian ornithopods (Dinosauria: Ornithischia). 3. A new species of iguanodontid dinosaur. Zoological Journal of the Linnean Society London 122:291–348.

Norman, D. B. 2002. On Asian ornithopods (Dinosauria: Ornithischia). 4. Redescription of *Probactrosaurus gobiensis* Rozhdestvensky 1966. Zoological Journal of the Linnean Society London 136:113–144.

Norman, D. B. 2004. Basal Iguanodontia. In: D. B. Weishampel, P. Dodson, and H. Osmólska (eds.), The Dinosauria, Second edition. University of California Press, Berkeley, California. Pp. 413–437.

Norman, D. B., and D. B. Weishampel. 1985. Ornithopod feeding mechanisms: their bearing on the evolution of herbivory. American Naturalist 126:151–164.

Norman, D. B., and D. B. Weishampel. 1991. Feeding mechanisms in some small herbivorous dinosaurs: Processes and patterns. In: Rayner, J. M. V., and Wootton, R. J. (eds.). Biomechanics and Evolution. Cambridge University Press,

Cambridge. Pp. 161–181.

Norman, D. B., A. W. Crompton, R. J. Butler, L. B. Porro, and A. J. Charig. 2011. The lower Jurassic ornithischian dinosaur *Heterodontosaurus tucki* Crompton & Charig, 1962: cranial anatomy, functional morphology, taxonomy, and relationships. Zoological Journal of the Linnean Society 163:182–276.

Norman, D. B., L. M. Witmer, and D. B. Weishampel. 2004. Basal Ornithischia. In: D. B. Weishampel, P. Dodson, and H. Osmólska (eds.), The Dinosauria, Second edition. University of California Press, Berkeley, California. Pp. 325–334.

Olson, E. C. 1961. Jaw mechanisms: rhipidistians, amphibians, reptiles. American Zoology 1:205-215.

Ösi, A., P. M. Barrett, T. Földes, and R. Tokai. 2014. Wear Pattern, Dental Function, and Jaw Mechanism in the Late Cretaceous Ankylosaur *Hungarosaurus*. The Anatomical Record 297:1165-1180.

Ostrom, J. H. 1961. Cranial morphology of the hadrosaurian dinosaurs of North America. Bulletin of the American Museum of Natural History 122:39–186.

Ostrom, J. H. 1964. A functional analysis of jaw mechanics in the dinosaur *Triceratops*.

Postilla 88:1-35.

Ostrom, J. H. 1966. Functional morphology and evolution of the ceratopsian dinosaurs. Evolution 20:290–308.

Otten, E. 1983. The jaw mechanism during growth of a generalized Haplochromis species: H. elegans Trewavas 1933 (Pisces, Cichlidae). Netherlands Journal of Zoology 33:55-98.

Otten, E. 1985. Proportions of the jaw mechanism of cichlid fishes: Changes and their meaning. In: G. A. Zweers and P. Dullemeijer (eds.), Architecture in Living Structure, Dordrecht, The Netherlands: Martinus Nijhoff / Dr. W. Junk 'L Publishers. Pp. 207-217.

Pang, Q., and Cheng Z. 1998. A new ankylosaur of the Late Cretaceous Tianzhen, Shanxi. Progr. Nat. Sci. 8:326–334.

Papp, M. J., and L. Witmer. 1998. Cheeks, beaks, or freaks: A critical appraisal of buccal soft-tissue anatomy in ornithischian dinosaurs. Journal of Vertebrate Paleontology 18 (suppl.):69A.

Parsons, W. L., and K. M. Parsons. 2009. A new ankylosaur (Dinosauria: Ankylosauria) from the lower Cretaceous Cloverly formation of central Montana. Canadian

Journal of Earth Sciences, 46(10):721-738.

Perle, A., T. Maryañska, and H. Osmólska. 1982. *Goyocephale lattimorei* gen. et sp. n., a new flat-headed pachycephalosaur (Ornithischia, Dinosauria) from the Upper Cretaceous of Mongolia. Acta Palaeontologica Polonica, 27(1-4):115-127.

Pol, D., O. W. Rauhut, and M. Becerra. 2011. A Middle Jurassic heterodontosaurid dinosaur from Patagonia and the evolution of heterodontosaurids. Naturwissenschaften, 98(5):369-379.

Porro, L. B. 2007. Feeding and jaw mechanisms in *Heterodontosaurus tucki* using finite element analysis. Journal of Vertebrate Paleontology 27(3, Supplement):131A.

Porro, L. B., C. M. Holliday, F. Anapol, L. C. Ontiveros, L. T. Ontiveros, and C. F. Ross. 2011. Free body analysis, beam mechanics, and finite element modeling of the mandible of *Alligator mississippiensis*. Journal of Morphology 272:910-937.

Prieto-Marquez, A. 2010. Global phylogeny of hadrosauridae (Dinosauria: Ornithopoda) using parsimony and Bayesian methods. Zoological Journal of the Linnean Society 159:435-502.

Prieto-Márquez, A., and M. A. Norell. 2010. Anatomy and relationships of *Gilmoreosaurus mongoliensis* (Dinosauria: Hadrosauroidea) from the Late

Cretaceous of Central Asia. American Museum Novitates, (3694):1-49.

Rayfield, E. J. 2004. Cranial mechanics and feeding in *Tyrannosaurus rex*. Proceedings of the Royal Society of London. Series B: Biological Sciences, 271(1547):1451-1459.

Rayfield, E. J. 2005a. Using finite-element analysis to investigate suture morphology: A case study using large carnivorous dinosaurs. The Anatomical Record Part A: Discoveries in Molecular, Cellular, and Evolutionary Biology, 283(2):349-365.

Rayfield, E. J. 2005b. Aspects of comparative cranial mechanics in the theropod dinosaurs *Coelophysis*, *Allosaurus* and *Tyrannosaurus*. Zoological Journal of the Linnean Society, 144(3):309-316.

Rayfield, E. J., A. C. Milner, V. B. Xuan, and P. G. Young. 2007. Functional morphology of spinosaur 'crocodile-mimic'dinosaurs. Journal of Vertebrate Paleontology, 27(4):892-901.

Rayfield, E. J., D. B. Norman, C. B. Horner, J. R. Horner, P. M. Smith, J. J. Thomason, and P. Upchurch. 2001. Cranial design and function in a large theropod dinosaur. Nature 409:1033–1037.

Reichel, M. 2010. A model for the bite mechanics in the herbivorous dinosaur *Stegosaurus* (Ornithischia, Stegosauridae). Swiss Journal of Geosciences, 103(2):235-240.

Regal, P. J., and C. Gans. 1976. Functional aspects of the evolution of frog tongues. Evolution 30:718-734.

Russell, L. S. 1940. *Edmontonia rugosidens* (Gilmore), an armored dinosaur from the Belly River Series of Alberta. University of Toronto Stud. Geol. Ser. 43:3–28.

Rybczynski, N., and M. K. Vickaryous. 2001. Evidence of complex jaw movement in the Late Cretaceous ankylosaurid *Euoplocephalus tutus* (Dinosauria: Thyreophora); pp. 299–317 in K. Carpenter (ed.), The Armored Dinosaurs. Indiana University Press, Bloomington, Indiana.

Rybczynski, N., A. Tirabasso, P. Bloskie, R. Cuthbertson, and C. Holliday. 2008. A three-dimensional animation model of *Edmontosaurus* (Hadrosauridae) for testing chewing hypotheses. Palaeontologica Electronica 11(9A).

Sampson, S. D. and M. A. Loewen. 2010. Unraveling a radiation: a review of the diversity, stratigraphic distribution, biogeography, and evolution of horned dinosaurs (Ornithischia: Ceratopsidae). In: M. J. Ryan, B. Chinnery-Allgeier, and D. A. Eberth (eds.), New Perspectives on Horned Dinosaurs: the Royal Tyrell

Museum Ceratopsian Symposium. Indiana University Press, Bloomington, Indiana. Pp. 405-427.

Sampson, S. D., M. A. Loewen, A. A. Farke, E. M. Roberts, C. A. Forster, J. A. Smith, A. L. Titus. 2010. New horned dinosaurs from Utah provide evidence for intracontinental dinosaur endemism. PloS One 5 (9):e12292.

Sampson, S. D., E. K. Lund, M. A. Loewen, A. A. Farke, and K. E. Clayton. 2013. A remarkable short-snouted horned dinosaur from the Late Cretaceous (late Campanian) of southern Laramidia. Proceedings of the Royal Society B: Biological Sciences, 280(1766).

Schultze, H-P. 1993. Patterns of diversity in the skulls of jawed fishes. In: J. Hanken and B. K. Hall (eds.), The Skull, Volume 2: Patterns of Structural and Systematic Diversity. Chicago: Chicago University Press. Pp. 189–254.

Schumacher, H-C. 1973. The head muscles and hyolaryngeal skeleton of turtles and crocodilians. In: C. Gans and T. S. Parsons (eds.), The Biology of the Reptilia, Volume 4: Morphology D. London: Academic Press. Pp. 109-199.

Seki, Y., M. Mackey, and M. A. Meyers. 2012. Structure and micro-computed tomography based finite element modeling of Toucan beak. Journal of Mechanical Behavior of Biomedical Materials 9:1–8.

Sereno, P. C. 1986. Phylogeny of the bird-hipped dinosaurs (Order Ornithischia). National Geographic Research 2:234-256.

Sereno, P. C. 1987. The ornithischian dinosaur *Psittacosaurus* from the Lower Cretaceous of Asia and the relationships of the Ceratopsia. Ph.D. dissertation, Columbia University, New York. 554 pp.

Sereno, P. C. 1991. *Lesothosaurus*, "fabrosaurids," and the early evolution of Ornithischia. Journal of Vertebrate Paleontology 11:168–97.

Sereno, P. C. 2012. Taxonomy, morphology, masticatory function, and phylogeny of heterodontosaurid dinosaurs. ZooKeys 226:1-225.

Sereno, P. C., and Dong Z. 1992. The skull of the basal stegosaur *Huayangosaurus taibaii* and a cladistic analysis of Stegosauria. Journal of Vertebrate Paleontology 12:318–343.

Sereno, P. C., Z. Xijin, and T. Lin. 2009. A new psittacosaur from Inner Mongolia and the parrot-like structure and function of the psittacosaur skull. Proceedings of the Royal Society B 277:199–209.

Sheil, C. A. 1999. Osteology and skeletal development of *Pyxicephalus adspersus*

(Anura: Ranidae: Ranidae). Journal of Morphology 240:49–75.

Sinclair, A. G., and R. M. Alexander. 1987. Estimates of forces exerted by the jaw muscles of some reptiles. Journal of Zoology 213:107-115.

Smith, D. 1992. The type specimen of *Oviraptor philoceratops,* a theropod dinosaur from the Upper Cretaceous of Mongolia. N. Jb. Geol. Paläontol. Abhandl. 186:365–388.

Smith, J. M., and R. J. G. Savage. 1959. The mechanics of mammalian jaws. School Science Review 40:289-301.

Snively, E., J. R. Cotton, R. Ridgely, and L. M. Witmer. 2013. Multibody dynamics model of head and neck function in *Allosaurus* (Dinosauria, Theropoda). Palaeontologia Electronica, 16.

Snively, E., and A. P. Russell. 2007. Functional variation of neck muscles and their relation to feeding style in Tyrannosauridae and other large theropod dinosaurs. The Anatomical Record, 290(8):934-957.

Solounias, N., M. F. Teaford, and A. Walker. 1988. Interpreting the diet of extinct ruminants: the case of a non-browsing giraffid. Paleobiology 14:287–300.

Solounias, N., and S. Moelleken. 1992. Dietary adaptations of two goat ancestors and

evolutionary considerations. Geobios 25:797-809.

Solounias, N., and S. Moelleken. 1993. Tooth microwear and premaxillary shape of an archaic antelope. Lethaia 26:261-268.

Soons, J., P. Lava, D. Debruyne, and J. Dirckx. 2012. Full-field optical deformation measurement in biomechanics: Digital speckle pattern interferometry and 3D digital image correlation applied to bird beaks. Journal of the mechanical behavior of biomedical materials, 14:186-191.

Starck, D., and A. Barnikol. 1954. Beitrage zur Morphologie der Trigeminusmuskulatur der Vogel (besonders der Accipitres, Cathartidae, Striges und Anseres. Gegenbaurs Morphologisches Jahrbuch 94:1–64.

Sues, H.-D. 1980. Anatomy and relationships of a new hypsilophodontid dinosaur from the Lower Cretaceous of North America. Palaeontographica (A) 169:51–72.

Sues, H.-D., and P. M. Galton. 1987. Anatomy and classification of the North American Pachycephalosauria (Dinosauria: Omithischia). Palaeontographica Abt. A 198:1–40.

Tait, J., and B. Brown. 1928. How the Ceratopsia carried and used their head. Transactions of the Royal Society Canada 22:13–23.

Taquet, P. 1976. Ostéologie d'*Ouranosaurus nigeriensis*, Iguanodontide du Crétacé Inférieur du Niger. Géologie et Paléontologie du Gisement de Gadoufaoua (Aptien du Niger), Chapitre 3:57–168.

Tanoue, K., B. S. Grandstaff, H. You, and P. Dodson. 2009. Jaw mechanics in basal Ceratopsia (Ornithischia, Dinosauria). Anatomical Record 292:1352–1369.

Tanoue, K., H. You, and P. Dodson. 2010. Mandibular Anatomy in Basal Ceratopsia. In: M. J. Ryan, B. Chinnery-Allgeier, and D. A. Eberth (eds.), New Perspectives on Horned Dinosaurs: the Royal Tyrell Museum Ceratopsian Symposium. Indiana University Press, Bloomington, Indiana. Pp. 234-250.

Thompson, R. S., J. C. Parish, S. C. R. Maidment, and P. M. Barrett. 2012. Phylogeny of the ankylosaurian dinosaurs (Ornithischia: Thyreophora). Journal of Systematic Palaeontology 10:301-312.

Thulborn, R. A. 1971. Tooth wear and jaw action in the Triassic ornithischian dinosaur *Fabrosaurus*. Journal of Zoology in London 164:165–179.

Thulborn, R. A. 1974. A new heterodontosaurid dinosaur (Reptilia: Ornithischia) from the Upper Triassic Red Beds of Lesotho. Zoological Journal of the Linnean Society London 55:151–175.

Thulborn, R. A. 1978. Aestivation among ornithopod dinosaurs of the African Trias. Lethaia 11:185–198.

Trueb, L. 1993. Patterns of cranial diversity among the Lissamphibia. In: J. Hanken and B. K. Hall (eds.), The Skull, Volume 2: Patterns of Structural and Systematic Diversity. Chicago: Chicago University Press. Pp. 255–343.

Tumanova, T. A. 1983. [The first ankylosaur from the Lower Cretaceous of Mongolia]. Trudy Sovm. Sov.-Mong. Paleontol. Eksped. 24:110–120. (In Russian with English summary.)

Tumanova, T. A. 1985. Skull morphology of the ankylosaur *Shamosaurus scutatus* from the Lower Cretaceous of Mongolia. In: Taquet, P., and Sudre, C. (eds.). Les Dinosaures de la Chine à la France. Muséum d'Histoire Naturelle de Toulouse, France et Muséum d'Histoire Naturelle, Chongqing. Pp. 73–79.

Tumanova, T. A. 1993. [Concerning a new armored dinosaur from the southeastern Gobi]. Paleontol. Zh. 27 (2):92–98. (In Russian with English summary.)

Upchurch, P., and P. M. Barrett. 2000. The evolution of sauropod feeding mechanisms. In: Sues, H.-D. (ed.). Evolution of Herbivory in Terrestrial Vertebrates: Perspectives from the Fossil Record. Cambridge University Press, Cambridge. Pp.

79–122.

Upchurch, P., P. M. Barrett, and P. Dodson. 2004. Sauropoda. In: D. B. Weishampel, P. Dodson, and H. Osmólska (eds.), The Dinosauria, Second edition. University of California Press, Berkeley, California. Pp. 259–322.

van der Meij, M. A. A., and R. G. Bout. 2008. The relationship between shape of the skull and bite force in finches. Journal of Experimental Biology 211:1668–1680.

Varriale, F. 2004. Dental microwear in *Triceratops* and *Chasmosaurus* and its implication

for jaw mechanics in Ceratopsidae. Journal of Vertebrate Paleontology 24:124A–125A.

Varriale, F. J. 2011. Dental microwear and the evolution of mastication in ceratopsian dinosaurs. Doctoral Dissertation. Johns Hopkins University School of Medicine, Baltimore, Maryland.

Versluys, J. 1910. Streptostylie bei Dinosauriern nebst Bemerkungen uber die Verwandtschaft der Vogel und Dinosaurier. Zoologische Jahrbucher Abteilung fur Anatomie und Ontogenie der Tiere 30:175–260.

Versluys, J. 1912. Das Streptostylie-Problem und die Bewegung im Schadel bei

Sauropsida. Zoologische Jahrbucher Abteilung fur Systemik (Okologie) Geographie und Biologie der Tiere (Supplement) 15:545–716.

Versluys, J. 1923. Der Schadel des Skeletts von *Trachodon annectus* im Senckenberg-Museum. Abhandlungen Herausgegeben von der Senckenbergischen Naturforschenden Gesellschaft. 38:1–19.

Verwaijen, D., R. Van Damme, and A. Herrel. 2002. Relationships between head size, bite force, prey handling efficiency and diet in two sympatric lacertid lizards. Functional Ecology16:842–850.

Vickaryous, M. K., and A. P. Russell. 2003. A redescription of the skull of *Euoplocephalus tutus* (Archosauria: Ornithischia): A foundation for comparative and systematic studies of ankylosaurian dinosaurs. Zoological Journal of the Linnean Society London 137:157–186.

Vickaryous, M. K., T. Maryańska, and D. B. Weishampel. 2004. Ankylosauria. In: D. B. Weishampel, P. Dodson, and H. Osmólska (eds.), The Dinosauria, Second edition. University of California Press, Berkeley, California. Pp. 363–392.

Vickaryous, M. K., A. P. Russell, P. J. Currie, and X.-J Zhao. 2001. A new ankylosaurid (Dinosauria: Ankylosauria) from the Lower Cretaceous of China,

with comments on ankylosaurian relationships. In: Currie, P. J. (ed.). Results from the Sino-Canadian Dinosaur Project. Part 3. Canadian Journal of Earth Sciences 38:1767–1780.

Weishampel, D. B. 1983. Hadrosaurid jaw mechanics. Acta Palaeontologica Polonica 28: 271–280.

Weishampel, D. B. 1984a. Evolution of jaw mechanisms in ornithopod dinosaurs. Advances in Anatomy Embryology and Cell Biology 87:1–109.

Weishampel, D. B. 1984b. Interactions between Mesozoic plants and vertebrates: Fructifications and seed predation. N. Jb. Geol. Paläontol. Abhandl. 167:224–250.

Weishampel, D. B. 2004. Ornithischia. In: D. B. Weishampel, P. Dodson, and H. Osmólska (eds.), The Dinosauria, Second edition. University of California Press, Berkeley, California. Pp. 323–324.

Weishampel, D. B., and D. B. Norman. 1989. Vertebrate herbivory in the Mesozoic; jaws, plants, and evolutionary metrics. Geological Society of America Special Paper 238:87-100.

Weishampel, D. B., and C. M. Jianu. 2011. Transylvanian dinosaurs. JHU Press, Baltimore.

Weishampel, D. B., C.-M. Jianu, Z. Csiki, and D. B. Norman. 2003. Osteology and phylogeny of *Zalmoxes* (n.g.), an unusual euornithopod dinosaur from the latest Cretaceous of Romania. Journal of Systematic Palaeontology 1:1-56.

White, T. E. 1958. The braincase of *Camarasaurus lentus* (Marsh). Journal of Paleontology 32:477–494.

Whitlock, J. A. 2011. Inferences of diplodocoid (Sauropoda: Dinosauria) feeding behavior from snout shape and microwear analyses. PloS One, 6(4):e18304.

Williams, S. H., C. J. Vinyard, C. E. Wall, and W. L. Hylander. 2007. Masticatory motor patterns in ungulates: a quantitative assessment of jaw-muscle coordination in goats, alpacas and horses. Journal of Experimental Zoology Part A: Ecological Genetics and Physiology 307:226–240.

Williams, S. H., C. E. Wall, C. J. Vinyard, C. E. Wall, and W. L. Hylander. 2008. Symphyseal fusion in selenodont artiodactyls: New insights from in vivo and comparative data. In: M. J. Vinyard, M. R. Ravosa, and C. E. Wall (eds.), Primate Craniofacial Function and Biology. Springer Science + Business Media. Pp. 39-61.

Williams, V. S., P. M. Barrett, and M. A. Purnell. 2009. Quantitative analysis of dental

microwear in hadrosaurid dinosaurs, and the implications for hypotheses of jaw mechanics and feeding. Proceedings of the National Academy of Sciences 106:11194–11199.

Winkler, D. A., P. A. Murry, and L. L. Jacobs. 1997. A new species of *Tenontosaurus* (Dinosauria: Ornithopoda) from the Early Cretaceous of Texas. Journal of Vertebrate Paleontology 17(2):330-348.

Witmer, L. M. 1995. The extant phylogenetic bracket and the importance of reconstructing soft tissues in fossils. In: J. J. Thomason (ed.), Functional Morphology in Vertebrate Paleontology. Cambridge University Press, New York. Pp. 19 – 33.

Witmer, L. M., and R. C. Ridgely. 2008. The paranasal air sinuses of predatory and armored dinosaurs (Archosauria: Theropoda and Ankylosauria) and their contribution to cephalic structure. The Anatomical Record, 291(11):1362-1388.

Xu, X., Q. Tan, J. Wang, X. Zhao, and L. Tan. 2007. A gigantic bird-like dinosaur from the Late Cretaceous of China. Nature, 447(7146):844-847.

Yates, A. M. 2010. A revision of the problematic sauropodomorph dinosaurs from Manchester, Connecticut and the status of *Anchisaurus* Marsh. Palaeontology, 53(4):739-752.

Yeh, J. 2002. The evolution of development: two portraits of skull ossification in pipoid frogs. Evolution 56:2484–2498.

You, H., and P. Dodson. 2004. Basal Ceratopsia. In: D. B. Weishampel, P. Dodson, and H. Osmólska (eds.), The Dinosauria, Second edition. University of California Press, Berkeley, California. Pp. 478–493.

You, H., D. Li, Q. Ji, M. C. Lamanna, and P. Dodson. 2005. On a new genus of basal neoceratopsian dinosaur from the Early Cretaceous of Gansu Province, China. Acta Geologica Sinica, 79(5):593-597.

Young, C. C. 1959. On a new Stegosauria from Szechuan, China. Vert. PalAs. 3:1–8.

Young, M. T., E. J. Rayfield, C. M. Holliday, L. M. Witmer, D. J. Button, P. Upchurch, and P. M. Barrett. 2012. Cranial biomechanics of *Diplodocus* (Dinosauria, Sauropoda): testing hypotheses of feeding behaviour in an extinct megaherbivore. Naturwissenschaften 99:637–643.

Zanno, L. E., D. D. Gillette, L. B. Albright, and A. L. Titus. 2009. A new North American therizinosaurid and the role of herbivory in 'predatory'dinosaur evolution. Proceedings of the Royal Society B: Biological Sciences, 276(1672):3505-3511.

Zanno, L. E., and P. J. Makovicky. 2011. Herbivorous ecomorphology and specialization patterns in theropod dinosaur evolution. Proceedings of the National Academy of Sciences, 108(1):232-237.

Zheng, X. T., H. L. You, X. Xu, and Z. M. Dong. 2009. An Early Cretaceous heterodontosaurid dinosaur with filamentous integumentary structures. Nature, 458(7236):333-336.

Zhou, Z., and L. D. Martin. 2011. Distribution of the predentary bone in Mesozoic ornithurine birds. Journal of Systematic Palaeontology 9:25–31.

Zusi, R. L. 1984. A functional and evolutionary analysis of rhynchokinesis in birds. Smithsonian Contributions to Zoology 395:1–40.

Zusi, R. L. 1993. Patterns of diversity in the avian skull. In: J. Hanken and B. K. Hall (eds.), The Skull, Volume 2: Patterns of Structural and Systematic Diversity. Chicago: Chicago University Press. Pp. 391 – 437.

CURRICULUM VITAE

Ali Nabavizadeh

Center for Functional Anatomy and Evolution
Johns Hopkins University School of Medicine
1830 E. Monument St., Rm. 306
Baltimore, MD 21205
Email: alinabav@gmail.com

PERSONAL INFORMATION

- Birth Date: 01/14/1987
- Birth Place: Defiance, Ohio
- Citizenship: USA
- Languages spoken: English, Farsi, some Spanish

EDUCATION

- **Ph.D. Functional Anatomy and Evolution**
  - Johns Hopkins University School of Medicine
  - Fall 2009 – Summer 2014 (expected)
  - **Dissertation Title:** *Diversity, Functional Morphology, and Evolution of the Jaw Apparatus in Ornithischian Dinosaurs* (Advisor: David B. Weishampel)
- **B.S. Ecology and Evolutionary Biology with Honors**
  - University of Kansas, Lawrence, KS
  - Fall 2005–Spring 2009
  - **Biology Honors Thesis Title:** *Functional Analysis of the Predentary-Dentary Bone Articulation in Duck-Billed Dinosaurs and its Role in Feeding* (Advisor: Larry D. Martin)

TEACHING EXPERIENCE

2012 - 2013 Medical Gross Anatomy Teaching Assistant (sub) and Tutor – Johns Hopkins University School of Medicine

2011 Medical Gross Anatomy Teaching Assistant – Johns Hopkins University School of Medicine

2010 - 2011 Summer Institute in Anatomy Teaching Assistant – Johns Hopkins University School of Medicine – Summer 2010 and 2011.

2011 Dinosaurs Course Teaching Assistant – some lecture – Johns Hopkins University

PUBLICATIONS

Articles:

- **Nabavizadeh, A.** *In press*. Hadrosauroid jaw mechanics and the functional

significance of the predentary bone. *In* The Hadrosaurs: Proceedings of the International Hadrosaur Symposium (D. Evans and D. Eberth, eds), Indiana University Press, Bloomington.

Conference Abstracts:

- **Nabavizadeh, A.** 2014. Jaw muscle reconstruction and vector analysis in ornithischian dinosaurs. *American Association of Anatomists Meeting*. (Platform Talk)
- **Nabavizadeh, A.** 2013. Jaw mechanics in ornithischian dinosaurs and the evolutionary relationship between morphology and bite force. *Society of Vertebrate Paleontology Program and Abstracts Book*: 182A-183A. (Platform Talk)
- Fairman, J., **A. Nabavizadeh**, and D. Weishampel. 2013. Early sauropodomorph jaw apparatus anatomy: a comparative study with iguanian lizards. *Society of Vertebrate Paleontology Program and Abstracts Book*: 124A. (Poster)
- **Nabavizadeh, A.** 2013. How the elephant got its trunk: evolutionary implications from long and short jaws in proboscideans. *Annual Meeting of the Society for Cenozoic Research (TerQua) Abstract Book*. (Platform Talk)
- **Nabavizadeh, A.** 2012. Jaw mechanics over proboscidean evolution. *Society of Vertebrate Paleontology Program and Abstracts Book*: 148A. (Poster)
- Weishampel, D.B., C.E. Sartin, and **A. Nabavizadeh.** 2012. Hadrosaurids from the 'lost continent' of Appalachia. *Society of Vertebrate Paleontology Program and Abstracts Book*: 192A. (Platform Talk)
- **Nabavizadeh, A.** 2011. Thyreophoran jaw mechanics and the functional significance of the predentary bone. *Society of Vertebrate Paleontology Program and Abstracts Book*: 164A. (Platform Talk)
- **Nabavizadeh, A.** 2011. The functional significance of the predentary bone in ornithopod jaw mechanisms. *Hadrosaur Symposium Abstract Volume*: 108-112. (Platform Talk)
- **Nabavizadeh, A.** 2010. New functional significance of the predentary bone in hadrosauroid mastication. *Society of Vertebrate Paleontology Program and Abstracts book*:138A. (Poster)
- **Nabavizadeh, A.** 2009. A possible key to the success of ornithischian dinosaurs. *Transactions of the Kansas Academy of Science* 112(1/2). (Platform Talk)
- **Nabavizadeh, A.,** L.D. Martin, and D.A. Burnham. 2008. Do defensive structures in *Triceratops* prove predatory behavior in *Tyrannosaurus*? *Transactions of the Kansas Academy of Science* 111(1/2). (Platform Talk)
- **Nabavizadeh, A.** 2007. Preliminary observations of a *Pentaceratops* specimen. *Transactions of the Kansas Academy of Science* 110(3/4). (Platform Talk)

LECTURES / EDUCATIONAL OUTREACH

2014 **"Evolutionary Trends in the Jaw Apparatus of Herbivorous Dinosaurs"** – 3rd Annual Northeast Regional Vertebrate Evolution Symposium.

2014 **"Kids and Dinosaurs"** – Ignite Hopkins Event – Johns Hopkins School of Medicine, Baltimore, MD

2013, 2011 **JHMI Science Day (2013, 2011)** – Taught Baltimore area elementary school children about comparative anatomy and fossils.

2013 **"Evolutionary Trends in Ornithischian Jaw Mechanics"** – Geobiology Symposium – Smithsonian Museum of Natural History, Washington, D.C.

2012 **"The Evolution of Jaw Mechanisms in Herbivorous Dinosaurs"** – Guest speaker in Comparative Pathobiology Department at Johns Hopkins School of Medicine, Baltimore, MD.

2011 **"A Dinosaur Paleontologist in a Medical Student's World"** – Ignite Hopkins Event – Johns Hopkins School of Medicine, Baltimore, MD

2011 **"New Functional Significance of the Predentary Bone in Hadrosauroid Mastication"** – Geobiology Symposium 2011 – University of Pennsylvania, Philadelphia, PA

2010 **"Rhinoceros Chewing Orientation**: **Dental Microwear and the Mandibular Symphysis"** – Research rotation talk, Johns Hopkins University School of Medicine, Baltimore, MD

2010 **"Feeding Biomechanics of Duck-Billed and Other Plant Eating Dinosaurs: A New Perspective"** – Science Fiction Convention, Hunt Valley, MD

2009 - 2013 **Lectures about dinosaurs for elementary schools** - Baltimore, MD

2009 **"Functional Analysis of the Predentary-Dentary Bone Articulation in Duck-Billed Dinosaurs and its Role in Feeding"** – Senior honors thesis talk, University of Kansas, Lawrence, KS

2009 "**Triceratops and Kin: A Field Guide to Ceratopsian Dinosaurs**"— Kansas City Gem and Mineral Show and the Gem and Mineral Society in Topeka, KS

PROFESSIONAL AND ACADEMIC AFFILIATIONS

- American Association of Anatomists— 2013—Present
- Society of Vertebrate Paleontology— 2008–Present
- Kansas Academy of Science— 2006-2009
- Undergraduate Research Assistant— 2007–2009

AWARDS, HONORS, AND SCHOLARSHIPS

- **National Science Foundation (NSF) Graduate Research Fellowship – $30,000 per year** for three years of living expenses for graduate school, plus an additional $10,000 per year for three years to my department.
- **American Association of Anatomists Meeting Travel Grant – $250**
- **Hadrosaur Symposium Travel Grant – $300**
- **University of Kansas Research Grant – $2,000**
- **OAS Scholarship from the University of Kansas**
- **University of Kansas Honor Roll**

OTHER LEADERSHIP AND MUSEUM POSITIONS

2011 - Present	**Musical Director and Founder** of the Johns Hopkins University School of Medicine Graduate Student Association a cappella singing group, **The CentriFugues**.
2007 – 2009	**Fossil Preparation Volunteer Coordinator** at the University of Kansas Museum of Natural History.
2007 – 2008	**Collections Assistant -** Department of Invertebrate Paleontology at the University of Kansas